THE PENNSYLVANIA STATE UNIVERSITY
Department of Mineral Engineering

Geomechanics Section

MICROSEISMIC MONITORING OF A LONGWALL COAL MINE
VOLUME I — MICROSEISMIC FIELD STUDIES

Prepared for
UNITED STATES DEPARTMENT OF THE INTERIOR
BUREAU OF MINES

Bureau of Mines Open File Report 30(1)-80

by
H. Reginald Hardy, Jr.
Gary L. Mowrey
Edward J. Kimble, Jr.

FINAL REPORT
on
Grant No. G0144013

August 31, 1978

COLLEGE OF EARTH AND MINERAL SCIENCES
University Park, Pennsylvania

DISCLAIMER NOTICE

The views and conclusions contained in this document are those of the authors and should not be interpreted as necessarily representing the official policies or recommendations of the Interior Department's Bureau of Mines or of the U.S. Government.

50272-101

REPORT DOCUMENTATION PAGE	1. REPORT NO. BuMines OFR 30(1)-80	2.	3. Recipient's Accession No. PB 80 163392

4. Title and Subtitle
Microseismic Monitoring of a Longwall Coal Mine Volume I--Microseismic Field Studies

5. Report Date
August 31, 1978

6.

7. Author(s)
H. Reginald Hardy, Jr., Gary L. Mowrey, and Edward J. Kimble, Jr.

8. Performing Organization Rept. No.

9. Performing Organization Name and Address
Department of Mineral Engineering
Pennsylvania State University
University Park, PA 16802

10. Project/Task/Work Unit No.

11. Contract(C) or Grant(G) No.
(C)
(G) Go144013

12. Sponsoring Organization Name and Address
Office of the Director--Minerals Health and Safety Technology
Bureau of Mines
U.S. Department of the Interior
Washington, DC 20241

13. Type of Report & Period Covered
University grant, 10/1/73-6/30/77

14.

15. Supplementary Notes
Approved by the Director, Bureau of Mines, for placement on open file, March 27, 1980.

16. Abstract (Limit: 200 words)

This report is volume I of a three-volume report on the microseismic monitoring of longwall coal mines. Volume I deals mostly with the detailed aspects of the microseismic field study; however, brief references are made to other secondary studies described in volumes II and III. During the field study, a mobile microseismic monitoring facility and associated transducers were employed to detect and record microseismic activity above a longwall panel at Greenwich Collieries, Barnesboro, Pa. The fundamental objectives of the study were (1) to evaluate the feasibility of detecting microseismic activity originating from longwall mining operations using an approximately planar, near-surface, geophone array installed above the longwall and (2) to attempt to locate the sources of the various microseismic events. The investigation proved, that using the techniques developed, it is possible to detect microseismic events at depths of more than 400 ft and at horizontal distances in excess of 800 ft from the source. The majority of the events had frequencies on the order of 10 to 100 Hz, and particle velocities of 50 to 300 μips. When a suitable velocity model was utilized, most of the events located were computed to be within ±100 ft vertically of the coal seam and ±50 ft horizontally of the longwall face. The results of the overall research project suggest that additional research should be undertaken in a number of associated areas.

17. Document Analysis a. Descriptors
Coal mines
Microseismic activity
Mine safety
Longwall

b. Identifiers/Open-Ended Terms

c. COSATI Field/Group 08I

18. Availability Statement	19. Security Class (This Report)	21. No. of Pages
Unlimited release by NTIS.	20. Security Class (This Page)	22. Price

DO NOT PRINT THESE INSTRUCTIONS AS A PAGE IN A REPORT

INSTRUCTIONS

Optional Form 272, Report Documentation Page is based on Guidelines for Format and Production of Scientific and Technical Reports ANSI Z39.18–1974 available from American National Standards Institute, 1430 Broadway, New York, New York 10018. Each separately bound report—for example, each volume in a multivolume set—shall have its unique Report Documentation Page.

1. Report Number. Each individually bound report shall carry a unique alphanumeric designation assigned by the performing organization or provided by the sponsoring organization in accordance with American National Standard ANSI Z39.23–1974, Technical Report Number (STRN). For registration of report code, contact NTIS Report Number Clearinghouse, Springfield, VA 22161. Use uppercase letters, Arabic numerals, slashes, and hyphens only, as in the following examples: FASEB/NS–75/87 and EPA/RD–75/09.
2. Leave blank.
3. Recipient's Accession Number. Reserved for use by each report recipient.
4. Title and Subtitle. Title should indicate clearly and briefly the subject coverage of the report, subordinate subtitle to the main title. When a report is prepared in more than one volume, repeat the primary title, add volume number and include subtitle for the specific volume.
5. Report Date. Each report shall carry a date indicating at least month and year. Indicate the basis on which it was selected (e.g. date of issue, date of approval, date of preparation, date published).
6. Sponsoring Agency Code. Leave blank.
7. Author(s). Give name(s) in conventional order (e.g., John R. Doe, or J. Robert Doe). List author's affiliation if it differs from the performing organization.
8. Performing Organization Report Number. Insert if performing organization wishes to assign this number.
9. Performing Organization Name and Mailing Address. Give name, street, city, state, and ZIP code. List no more than two levels of an organizational hierarchy. Display the name of the organization exactly as it should appear in Government indexes such as Government Reports Announcements & Index (GRA & I).
10. Project/Task/Work Unit Number. Use the project, task and work unit numbers under which the report was prepared.
11. Contract/Grant Number. Insert contract or grant number under which report was prepared.
12. Sponsoring Agency Name and Mailing Address. Include ZIP code. Cite main sponsors.
13. Type of Report and Period Covered. State interim, final, etc., and, if applicable, inclusive dates.
14. Performing Organization Code. Leave blank.
15. Supplementary Notes. Enter information not included elsewhere but useful, such as: Prepared in cooperation with . . . Translation of . . . Presented at conference of . . . To be published in . . . When a report is revised, include a statement whether the new report supersedes or supplements the older report.
16. Abstract. Include a brief (200 words or less) factual summary of the most significant information contained in the report. If the report contains a significant bibliography or literature survey, mention it here.
17. Document Analysis. (a). Descriptors. Select from the Thesaurus of Engineering and Scientific Terms the proper authorized terms that identify the major concept of the research and are sufficiently specific and precise to be used as index entries for cataloging.

    (b). Identifiers and Open-Ended Terms. Use identifiers for project names, code names, equipment designators, etc. Use open ended terms written in descriptor form for those subjects for which no descriptor exists.

    (c). COSATI Field/Group. Field and Group assignments are to be taken from the 1964 COSATI Subject Category List. Since the majority of documents are multidisciplinary in nature, the primary Field/Group assignment(s) will be the specific discipline area of human endeavor, or type of physical object. The application(s) will be cross-referenced with secondary Field/Group assignments that will follow the primary posting(s).
18. Distribution Statement. Denote public releasability, for example "Release unlimited", or limitation for reasons other than security. Cite any availability to the public, with address, order number and price, if known.
19. & 20. Security Classification. Enter U.S. Security Classification in accordance with U.S. Security Regulations (i.e., UNCLASSIFIED).
21. Number of pages. Insert the total number of pages, including introductory pages, but excluding distribution list, if any.
22. Price. Enter price in paper copy (PC) and/or microfiche (MF) if known.

☆ U.S. GPO: 1977-0-241-530 0461

FOREWORD

The following report was prepared by The Pennsylvania State University under USBM Contract No. G0144013. The contract was initiated under the USBM Coal Mine Health and Safety Program. It was administered under the technical direction of DMRC, with Mr. F. W. Leighton acting as the technical project officer. Mr. J. A. Herickes was the contract administrator for the Bureau of Mines.

This report is Volume I of a three volume final report dealing with the microseismic monitoring of a longwall coal mine. Portions of the material presented in this volume forms the basis of an M.S. thesis in Mining Engineering by one of the authors (Mowrey). The research presented in Volume I includes a detailed description of the primary phase of the overall project including a brief review of the microseismic field monitoring techniques utilized, details of the field site and transducer installation procedures, data collection and analysis techniques, and detailed field results. Volume I also includes a brief summary of the material presented in Volume II--"Determination of Seismic Velocity with Application to Microseismic Field Studies," and Volume III--"Field Study of Mine Subsidence," and concludes with a general discussion of the accomplishments of the overall project.

This project could not have been possible without the continuous assistance provided by the administrative and technical staff of the Greenwich Collieries. The authors wish also to express their appreciation to Mineral Engineering Department staff and graduate students for their assistance in carrying out the field and laboratory aspects of this study. Detailed acknowledgements are included later in this report.

TABLE OF CONTENTS

TABLE OF CONTENTS (Continued)

TABLE OF CONTENTS (Continued)

TABLE OF CONTENTS (Continued)

TABLE OF CONTENTS (Continued)

LIST OF TABLES

LIST OF TABLES (Continued)

LIST OF FIGURES

LIST OF FIGURES (Continued)

LIST OF FIGURES (Continued)

LIST OF FIGURES (Continued)

LIST OF FIGURES (Continued)

LIST OF FIGURES (Continued)

NOMENCLATURE

The nomenclature presented here is used in general throughout this thesis unless otherwise indicated. A number of symbols, not included here, are used only occasionally and are defined locally in the text where they occur.

a = acceleration (feet per second per second)

A = post-amplifier

a-c = alternating-current

A/D = analog-to-digital conversion

BNC = bayonet lock, constant impedance connector

BP = break point

C = electrical capacitance (farads)

CR = cable reel

CRO = oscilloscope

CRT = cathode ray tube

d = distance (feet)

D/A = digital-to-analog conversion

dB = decibel

d-c = direct-current

epm = events per minute

F = filter

fps = feet per second

ft = feet

Hz = Hertz (cycles per second)

NOMENCLATURE (Continued)

ID = identification number

I/O = input/output

ips = inches per second

J = electrical connector

JB = junction box

ms = milliseconds

mV = millivolts

N = total number of microseismic events

PA = preamplifier

PS = power supply

P(x,y,z) = general point in Cartesian coordinates

R = electrical resistance (ohms)

RA = radio receiver

RC = resistive-capacitive network

RTL = reference time line

s = seconds

S/N = signal-to-noise ratio

SRG = source-to-reference geophone

t = time (seconds)

T = transducer

t_i = microseismic arrival times (seconds)

t_o = microseismic origin time (seconds)

UV = ultraviolet

v = velocity (feet per second)

V = volts

NOMENCLATURE (Continued)

Vac = alternating-current voltage (volts)

Vdc = direct-current voltage (volts)

x,y,z = Cartesian coordinates

x_i, y_i, z_i = microseismic event origin coordinates

μips = microinches per second

I. INTRODUCTION

1. General

Visible and sometimes audible indications of excessive underground rock pressure such as cracks, fracturing, squeezes on chocks, and the like are familiar to mining engineers. Such indications often precede rock failure and may be used as a warning; nevertheless, they do not provide an adequate means of evaluating the existing pressure conditions in a mine. The need for a better method of determining the areas of excessive stress and potential instability as a means of improving both the safety and the economic operation of the mine is readily apparent. Microseismic techniques appear to be one of the most promising methods for the study of the stability of such structures.

Geomechanical and mining engineers generally agree that during the process of rock deformation and failure small-scale seismic vibrations are generated in the rock. These transient vibrations propagate through the rock structure and may be detected at a considerable distance from the failed rock by employing suitable electronic monitoring equipment. Such seismic vibrations are referred to as microseismic activity. Other terms that researchers use to describe these vibrations are rock noise, seismo-acoustic activity, subaudible noise, and acoustic emission. Until recently, few microseismic studies have been conducted in coal mines, especially in North America; however, open-pits and underground hard rock mines have been monitored microseismically during the 1960's and 1970's with an increasing degree of success.

Monitoring such activity should prove to be invaluable in the detection and location of unstable roof conditions and overstressed pillars caused by both development and production work. According to Scott (1971), during the years 1969 and 1970, nearly 50 percent of the fatal accidents in United States bituminous coal mines occurred due to roof falls; falls of face, rib, or pillar; and coal bumps or rock bursts. The employment of microseismic techniques should reflect in increasing the safety for miners and in decreasing the cost for mining operations and down-time. Using microseismic techniques, it should be possible to evaluate quantitatively such factors as the effect of mining rate on the stability of the mine structure; the efficiency of caving operations; and the quality of the roof, ribs, and floor.

Mine safety has always been a prime concern of the U.S. Bureau of Mines, and over the years much of their in-house research has been directed towards reduction of accidents and health hazards associated with the mining industry. As a consequence of the 1969 Coal Mine Health and Safety Bill, additional funds became available to the U.S. Bureau of Mines for support of outside research at industrial and educational institutions. The studies presented in this report are part of a comprehensive microseismic investigation undertaken by The Pennsylvania State University on behalf of the U.S. Bureau of Mines during the period 1970-1978. The research undertaken during this period involved two specific projects. The earlier one (1970-1974) involved the development of the necessary monitoring facilities and field techniques, and the completion of detailed preliminary field trials. The current project (1974-1978) utilized the facilities and expertise developed in the

earlier study to investigate in detail the microseismic activity associated with an active longwall coal mine.

2. Brief Review of Earlier Project

The general scope of this project (Grant G0101743) was the investigation of microseismic techniques relative to coal mine safety. During the period June 15, 1970 to March 31, 1974, mobile microseismic monitoring facilities were developed and field studies were undertaken to investigate the feasibility of using microseismic techniques to locate potential zones of instability around coal mine workings. Field studies associated with this project were undertaken at the North Mine of the Greenwich Colliery in central Pennsylvania. Basically, these studies involved monitoring the microseismic activity generated by a working mine using surface transducers located in shallow boreholes positioned over the active areas of the mine. This study was unique in the fact that measurements were made from the surface rather than underground. Such an approach provides several advantages, including the fact that there are no electrical limitations on the monitoring system, and that the study in no way interferes with normal mine operations.

A detailed final report (Hardy, 1974) covering these studies was prepared early in 1974, in which the following conclusions were listed:

(1) The feasibility of monitoring underground strata instability using microseismic transducers installed in surface locations was positively verified.

(2) The mobile microseismic monitoring facility designed specifically for these studies proved to be most successful. Field measurements using this facility were developed into a relatively simple, routine operation.

(3) Field techniques and in particular those associated with transducer installation underwent a considerable metamorphism during the project. Final transducer installation techniques appeared to be optimum.

(4) Microseismic measurements were made at an active coal mine site for a period of over one year. During this time detailed studies were conducted over a previously mined development area, and two active longwall wall sections (A-2 and west B-4). Positive microseismic signals were obtained for both longwall sites, however, few signals of positive microseismic origin were detected over the development area.

(5) In the case of the second of the two longwall studies (west B-4 site), it was observed that the character of the microseismic data observed on surface depended on the operating conditions of the associated longwall. For example, under poor conditions (unsatisfactory roof failure behind the support system and resulting bad floor conditions), microseismic signals were not received at all locations in the transducer array, and the frequency content of the signals were relatively high. In contrast, under good longwall conditions microseismic signals were of lower frequency content and were generally received on all transducers in the array.

(6) Preliminary studies at a third Greenwich longwall site (east B-4 site) were a complete success. Detailed studies at this site were planned to be undertaken during a later USBM sponsored research project (Grant G0144103).

(7) More sonpisticated computer techniques for signal recognition and analysis are required to make efficient use of observed microseismic data. This is due in part to the fact that the mechanical instabilities associated with normal mining operations (e.g. longwall) are considerably smaller than those associated with major instabilities, such as rock or coal bursts, for which major analysis efforts have been concentrated in recent years.

(8) A number of factors were still found to limit the usefulness of microseismic techniques in efficiently evaluating the stability of geologic structures such as underground coal mines, namely:

(i) Difficulty in separating small microseismic signals from ambient background noise.

(ii) Inability in most geologic structures to obtain an equivalent unloaded condition in order to evaluate local background noise.

(iii) Large dimensions of most geologic structures and resulting attenuation (usually highly frequency dependent) of microseismic signals with distance from their source.

(iv) Electrical and mechanical difficulties in instrumenting such structures.

(v) Difficulty in source location due to lack of information on propagation velocities, and the normally anisotropic velocity characteristics of geologic materials.

In general the results of the initial study provided further evidence of the usefulness of microseismic techniques in strata control and associated mine safety monitoring, and on the basis of this evidence a second microseismic research study (current project) was initiated in late 1973.

3. Brief Review of Current Project

The current USBM project (Grant G0144013) was initiated October 1, 1973 and involved specifically the use of microseismic techniques as a means of monitoring the structural stability of an active longwall coal mine. As noted in the previous section, an earlier project, completed in September 1973, involved the development of a mobile microseismic monitoring facility, the investigation of associated field techniques, and completion of a number of preliminary field studies. The current project utilized the equipment and techniques developed in this earlier project to study longwall stability in detail.

Field studies, development of data processing techniques, data analysis, and report preparation associated with this project have been underway during the period October 1, 1973 to September 31, 1978. During the period three different aspects of the problem were investigated, and the final report associated with this project consists therefore of three volumes, namely:

Volume I -- Microseismic Field Studies

Volume II -- Determination of Seismic Velocity

Volume III -- Field Study of Mine Subsidence

Due to the extensive field data involved in this project and the fact that each of the three different aspects of the study was associated with graduate student thesis research, completion of the project involved considerably more time than was originally anticipated. This is particularly true of the research included in Volume I. Although the majority of the field data associated with Volume I was collected following the original project schedule, suitable techniques for analysis of this data required more than 24 months of additional part time effort by the associated graduate student then was originally anticipated. The additional time for this work was agreed to by the USBM project TPO (Leighton) who felt that such efforts would result in a much more meaningful final report. The graduate student originally financially supported by the USBM grant (Mowrey) was willing to undertake the additional effort at no cost due to his personal interest in the subject.

It should be noted here that material associated with the primary aspects of the overall study are contained in Volume I of the final report. Volumes II and III contain material of somewhat secondary importance. In order to put the various phases of the overall project in perspective, a brief review of each will be included here prior to considering the primary aspects of the study (microseismic field studies) in depth.

Microseismic field studies

Volume I of the final report (present volume) deals for the most part with the detailed aspects of the microseismic field study. During this investigation, a suitable mobile microseismic monitoring facility was employed to detect and record microseismic activity above a longwall panel (east B-4 site) at Greenwich Colleries, Barnesboro, Pennsylvania. Using the Greenwich field site, various techniques were investigated to determine the most suitable one for detecting microseismic events embedded in ambient background noise and to locate the source of the detected microseismic events.

The fundamental objectives of this investigation were (1) to evaluate the feasibility of detecting microseismic activity originating from longwall mining operations using an approximately planar geophone array installed from surface above the longwall and (2) to attempt to locate the source of the various detected microseismic events.

An array of geophones buried at depths of 10 to 25 ft from surface was positioned approximately 430 ft above the active area of the longwall panel. These geophones were employed to sense any microseismic activity (rock noises) occurring. A mobile microseismic monitoring facility was used to amplify, filter, and record the data obtained. Source locations for the 150 largest microseismic events were computed, using a least-square travel-time-difference method. Isotropic, anisotropic, and unique wave propagation velocity models were considered when evaluating the source locations.

This investigation has proven that the monitoring system was capable of detecting microseismic events at depths of more than 400 ft and at horizontal distances in excess of 800 ft from the source. The

majority of events, which resembled decaying sinusoidal transient waveforms, had frequencies on the order of 10 to 100 Hz, and particle velocities of 50 to 300 μips. When the unique velocity model was utilized, most of the events located were computed to be ±100 ft vertically of the coal seam and ±50 ft horizontally of the longwall face.

Determination of seismic velocity

The research presented in Volume II of the final report is concerned with the evaluation of field techniques for obtaining seismic velocity data required for computing microseismic source locations. The report describes the evaluation of a number of different field techniques and the seismic velocity data obtained at the Greenwich mine site where the microseismic studies, described in Volume I of the final report, were carried out. Three different methods were employed to evaluate seismic velocities, namely; surface refraction, down-hole, and transmission. In all cases the seismic sources were either located on surface (mechanical impact) or near-surface (explosive charges).

It was found that a mechanical energy source could be conveniently utilized to determine shallow velocities and make bedrock-regolith interface depth determinations. For deeper velocity determinations, suitable explosive charge sources were required. In general, refraction data did not always plot in a linear manner and some subjective interpretation was necessary. The down-hole method was found to be useful for incremental vertical velocity evaluation, however, the transmission method provided the most consistent average vertical velocity data. At the Greenwich site, seismic velocities were found to be anisotropic with values ranging from 9,551 to 10,739 ft per second depending on direction.

Field study of mine subsidence

The research presented in Volume III of the final report was undertaken as part of the overall microseismic project in an effort to relate, if possible, observed microseismic activity with surface subsidence. Field measurements of subsidence carried out at the Greenwich mine site are described. Comparative analysis of actual field results with data obtained using empirical and finite element techniques was undertaken. Comparison of field results with published National Coal Board data revealed marked differences. The influence of stronger rock beds overlying the coal seam in the current study was assumed to be the main cause. Use of the general Gaussian profile resulted in a satisfactory fit to the field data provided the value of the maximum field subsidence was used in the analysis. In general, when low tensile strengths were assumed for the associated rocks, finite element techniques gave results which compared well with the observed field data. The study also indicated that at shallow depths there is a marked difference in subsidence over dip and rise sides of the coal-face, maximum subsidence being shifted more towards the dip side. Finally, time-dependent deformations were shown to be insignificant shortly after mining operations ceased.

4. Outline of Final Report--Volume I

As indicated earlier in this chapter, the purpose of Volume I of the final report is to provide a brief overall review of the current project as well as a related earlier project, and to describe in detail the recent microseismic field studies. The latter is dealt with in Chapters II to VIII and includes a review of a number of the recent

microseismic research studies underway at Penn State and elsewhere; a brief description of the microseismic monitoring system employed in the present study; details of the field site; a review of the experimental techniques and data analysis methods employed; typical experimental results obtained from the field site; and a discussion as to the overall success of the study.

A general discussion of the overall accomplishments of the current project is included in Chapter IV along with suggested future research in the microseismic area. Finally, a series of Appendices (A to J), providing detailed information on various aspects of the study, are included.

II. REVIEW OF RELATED MICROSEISMIC LABORATORY AND FIELD STUDIES

1. Introduction

For workers concerned with the mechanical behavior of geologic materials (rock mechanics), the phenomenon of microseismic activity provides a novel method of investigating material deformation and failure. Numerous disciplines including those of mining engineering, civil engineering, geophysics, non-destructive testing engineering, and others have successfully incorporated such microseismic techniques to predict or detect impending failure of rock, to locate instabilities, and to determine the effectiveness of supporting systems in mines, highways, rock and soil slopes, and dams.

The origin of microseismic activity is not yet well understood, but most researchers agree that it appears to be related to deformation and failure processes which are accompanied by a sudden release of strain energy. For geologic materials, being basically polycrystalline structures, such activity may originate at a microlevel as a result of dislocations, or at the macrolevel by movement of grains, twinning, or fractures initiating and propagating through and between grains. As strain energy is released whenever any of these processes occur, it is assumed that an elastic stress wave is produced which travels radially outward from the point of origin within the material to the boundaries where it may be observed as a rock noise. As an example, Figure 1 shows a simplified method of detecting and recording microseismic

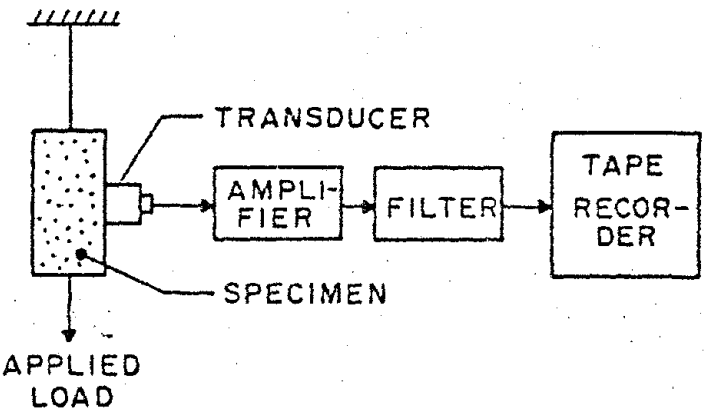

(A) Basic Experimental Arrangement for Detecting and Recording Microseismic Activity

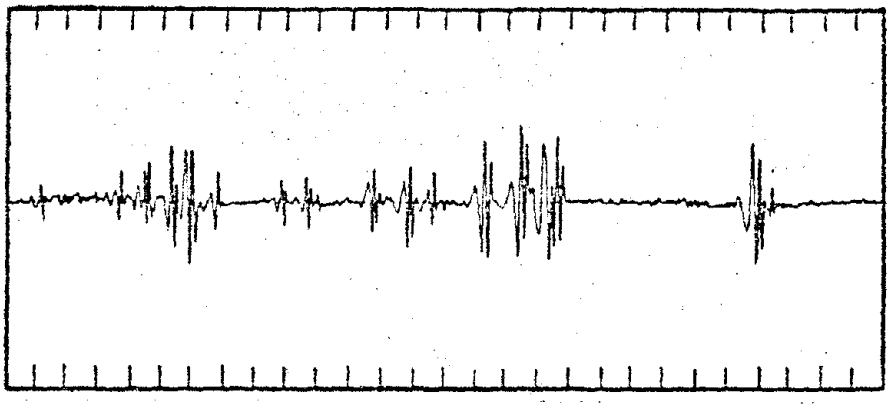

(B) Example of Typical Microseismic Data (Each Division Represents 6 ms)

Figure 1. Basic Laboratory Method for Recording Microseismic Activity and Typical Data (After Hardy, 1972).

activity for a rock specimen subjected to tensile stresses, and typical microseismic data from such a test.

Laboratory studies have been conducted primarily to confirm results obtained in field studies, although a few studies have been carried out to investigate the basic deformation and failure behavior of rocks loaded in compression, tension, and flexure. Such investigations have considered frequency spectra, amplitude, energy, and the number of rock noises produced by such known loading conditions. Since this thesis is concerned mainly with the field aspects of microseismic activity, the reader is referred to a recent paper by Hardy (1972) for further details on laboratory research in this area.

Obert, Duvall, Hodgson, and others in North America have investigated field microseismic methods associated with mine design and rock burst prevention beginning in the late 1930's. European and Asian research began near the end of the 1940's. A detailed discussion of the field aspects will be considered in the next section.

2. Field Studies

Field studies involving microseismic techniques were initiated by Obert (1941) and Obert and Duvall (1942, 1945) during the late 1930's and early 1940's. They noted that as underground structures became highly loaded, the rate of microseismic activity increased greatly. After failure of the structure either by natural or artificial means and equilibrium was re-established, the rate of microseismic activity decreased. Such conclusions, i.e., that the microseismic noise rate was a factor indicative of the degree of a structure's instability,

formulated the basis of the majority of microseismic field studies conducted thereafter.

2.1 Hard rock mines

United States and Canadian government agencies in the late 1930's and early 1940's initiated microseismic studies related to underground hard rock mining. At approximately the same time, European and Asian researchers also became involved in similar studies. Problems related to higher stresses at deeper mining depths and the unpredictability of rock bursts gave scientists reason to conduct such investigations. Not until the 1960's did the microseismic equipment and techniques become more sophisticated and more advanced than those originally employed by Obert and Duvall. For example, Cook (1963) of South Africa refined the basic microseismic monitoring system by using eight transducers and a 16-channel tape recorder. Each transducer was connected to two channels, whose sensitivities differed by a factor of 30. His monitoring system had an essentially flat frequency response of 15 to 300 Hz in order to cover adequately the frequency bandwidth of the microseismic events. The major microseismic energy was found to be in the 20 to 50 Hz region. By denotating two to three pounds of explosive at known locations within the mine and by measuring the arrival times at each transducer, Cook was able to determine the velocity of propagation to an accuracy of ±5 percent. He estimated that with such velocity measurements his source locations could be determined to within ±10 ft.

Microseismic monitoring systems developed by Blake (1971), Blake and Duvall (1969), and Leighton and Steblay (1977) had a flat frequency response in the range of 20 to 10,000 Hz, as they noted that there were

normally many high-frequency components present in a microseismic event. These systems were much wider in frequency bandwidth than that of Cook's.

The transducers used by these researchers were commercially available piezoelectric accelerometers. Holes were drilled in various underground locations, and the transducers were cemented in these holes. Each transducer was connected to a preamplifier which was also cemented in the same hole. A cable then linked the preamplifier to a post amplifier, whose output was connected to one input channel of a seven-channel FM magnetic tape recorder located in a permissible area. Provided that at least five transducers detected a particular event, a source location could be determined. Travel time differences were determined by playing back the data recorded on the tape recorder onto a multichannel oscillograph (visicorder) and physically measuring the time differences from the hardcopy output of the oscillograph. Velocity of propagation data were obtained from blasts which occurred at known locations. Leighton and Blake (1970) estimated that their location techniques were accurate to within ±10 ft. They believed that a wide frequency bandwidth system would give much more quantitative information about the behavior of a rock structure than the more typical narrow band system.

In the block caving mine at Climax, Colorado, researchers Oudenhoven and Tipton (1973) utilized a planar array of seven accelerometers located above the block of ore being caved to monitor any microseismic activity during caving. Evaluated source locations were believed to be accurate to ±20 ft.

2.2 Coal mines

Few microseismic investigations have been carried out in North American coal mines because (1) most coal mines are fairly shallow (less than 700 ft deep) and consequently are not subjected to high-stresses and (2) strict Federal and State mining laws limit the use of electrical and electronic equipment in such mines. Nevertheless, two coal mine microseismic projects are currently being conducted in the United States. The first is Leighton and Steblay's (1977) microseismic monitoring of a rock-burst-prone Rocky Mountain coal mine south of Denver, Colorado. Here, geophones (velocity sensitive transducers) are employed in various sections of the mine to detect areas of impending instability and to forecast rock bursts. The basic monitoring system is located outside the mine. The frequency bandwidth utilized is narrowband (90 to 180 Hz) to minimize unwanted noises of other frequencies and thus increase the sensitivity of the system over the frequencies of interest. The second study is the subject of this thesis.

European coal mines are generally much deeper (2,000 ft) and therefore are subject to higher stress conditions and to frequent occurrences of coal bumps if conditions are favorable. Underground coal mine microseismic studies are underway in Poland (Neyman, Czecowka, and Zuberek, 1972), Czechoslovakia (Stas, 1971), and Russia (Antsyferov, 1966). In West Germany an extensive investigation of coal bumps in a coal mine in the southern Ruhr Valley has begun (Cete, 1975) using a three-station array consisting of 2 Hz, three-dimensional, displacement transducers located on the surface.

2.3 Surface-mining applications

Broadbent and Armstrong (1968) discuss the design, installation, and problems of microseismic monitoring equipment for slope stability studies in open-pit mining. At Boron, California, Paulsen, Kistler, and Thomas (1967) employed microseismic equipment to monitor slope stability and plotted microseismic activity against time to delineate the stability of the pit. A normal amount of background microseismic activity occurred at all times and this background noise level was termed ambient noise. An increase in the microseismic activity indicated the possibility of a potential slope instability. A decrease suggested that stabilization was occurring. An accelerating rate of microseismic activity indicated that the slope was approaching imminent failure.

A recent microseismic study at Kennecott's Kimbley pit near Ruth, Nevada was undertaken while the pit slope was steepened from 45° to 60° (Wisecarver et al., 1969). The 60° slope was considered stable, but the microseismic monitoring was considered to be a beneficial safety measure and to be a possible correlation tool to relate microseismic activity to slope angle. Transducers were installed in the pit wall itself and also inside two adits driven into the pit wall. Monitoring measurements were carried out only between shifts and on weekends as the normal mining operations generated too much ambient noise for the microseismic system. The microseismic rate was found to be erratic as the slope was being steepened, but tended to correlate with temporary stress concentrations occurring during mining. The microseismic rate decreased to a low-value after the 60° slope was completed, which appeared to suggest that the new slope was stable.

2.4 Other applications

Hydrofracturing, the process of injecting fluids under pressure into low-permeability strata with the intent of fracturing these strata and increasing their permeability, is generally used to stimulate poorly producing oil or gas wells. Apart from standard surface monitoring of injection pressure, rate, volume, core drilling, formation testing, or viewing an image of the fractured zone by way of a borehole television, very little is known regarding the processes, types, and extents of fractures. Overbey and Pasini (Hardy, 1975) are currently employing microseismic techniques to locate and to determine the direction of such hydrofractures.

In the area of natural gas engineering, Hardy and Khair (1973) have utilized microseismic activity associated with underground natural gas storage reservoirs to determine possible areas of instability. Continued studies in this area are presently underway at an underground gas storage site in central Michigan (Hardy, 1976).

In the civil engineering area, tunnels have been monitored microseismically by researchers such as Crandell (1955) and Beard (1962) in order to evaluate their stability. Furthermore, structures such as dams, reservoirs, landslide areas, and highway cuts have had the microseismic method applied as a safety tool to measure their stability. For example, Goodman and Blake (1964, 1966) correlated microseismic activity rate with slope stability. They found that microseismic events could be located only if the landslide was comprised of competent rock. Landslides of less competent rock attenuated high-frequency microseismic activity beyond 100 ft and also had a wide range of

propagation velocities, thereby making source location in such cases extremely inaccurate.

III. MICROSEISMIC MONITORING SYSTEM

1. General

Figure 2 shows a block diagram illustrating a very basic single-channel microseismic monitoring system. Any microseismic signals sensed by the transducer (T) (accelerometer, velocity gage or geophone, or displacement gage) transforms these mechanical signals into electrical signals which are coupled to a preamplifier (PA). This preamplifier amplifies the weak transducer signals and also provides a very high-input impedance (1,000 MΩ) and a low-output impedance for maximum voltage transfer between the transducer and the main electronic system. Generally the cable connecting the preamplifier to the transducer is made as short as practical (typically 5 to 30 ft) to minimize the susceptibility to external electrical noises and transients being inductively coupled to the input of the preamplifier. Signals from the preamplifier are connected to the post-amplifier by a multiconductor shielded cable which ranges from 100 to 1,000 ft in length. The post-amplifier amplifies the signals from the preamplifier, and its output is coupled to an active analog filter (F). The purpose of the filter is to reject all signals below a given frequency as well as all signals above another given frequency. All signals lying between these two frequency limits are passed unaltered through the filter and are finally recorded on an analog magnetic tape. Signals can also be visually observed using an oscilloscope. Hard copies (permanent visual records)

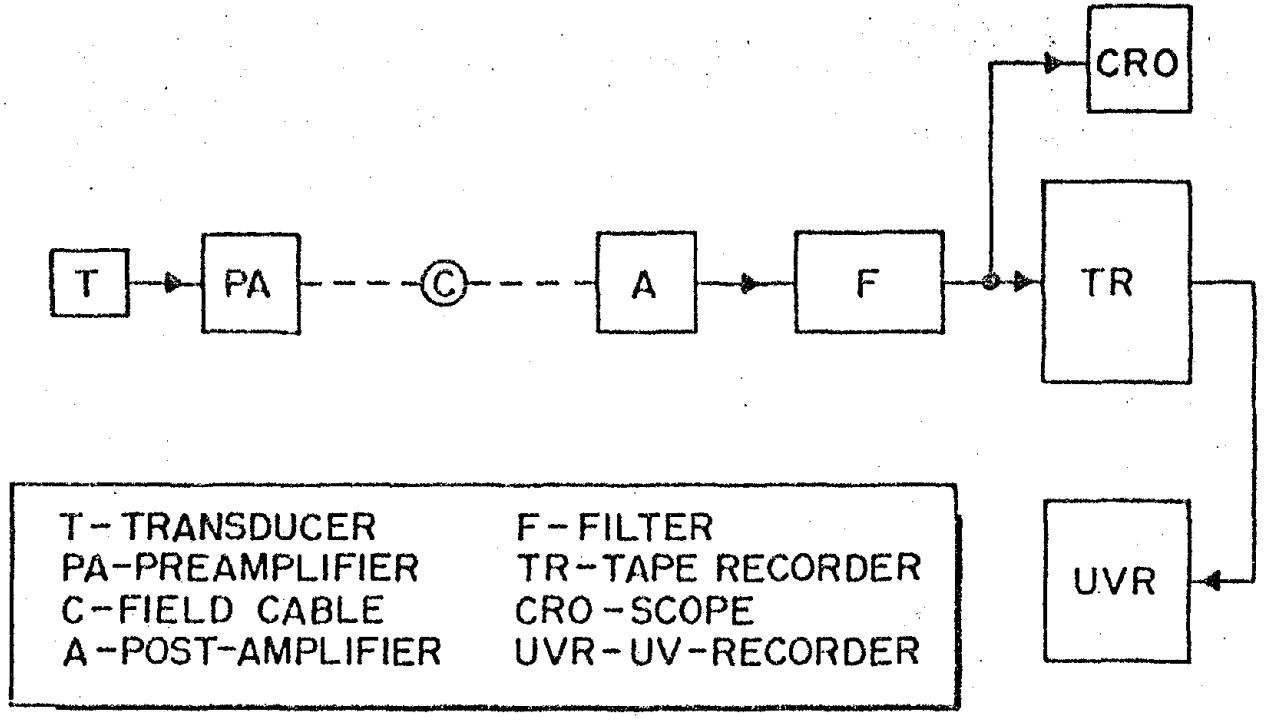

Figure 2. Block Diagram of a Simplified Microseismic Monitoring System.

of the signals can be obtained using an ultraviolet recorder (visicorder or oscillograph).

A mobile multichannel monitoring system for use in a number of field projects was developed at The Pennsylvania State University. A block diagram of the system is shown in Figure 3. The basic system allows for monitoring and recording the outputs of up to seven transducers although the tape recorder is capable of recording as many as 14-channels of data simultaneously. For flexibility input and ouput connections for the tape recorder and filters, output connections for the post-amplifiers and input connections for the driver amplifiers (used in conjunction with the visicorder) are located on a patch panel. Such an arrangement conveniently allows the user to monitor the system at various points and also to modify easily the configuration of each channel as desired.

In addition to acquiring data, the monitoring system has the capability of playing back data either during or after recording. An oscilloscope may be used to observe the recorded data. If a hard copy is desired, the inputs of the visicorder may be connected to the outputs of the tape recorder through a set of visicorder driver amplifiers. The monitoring system can be powered from 110 Vac, 60 Hz (supplied by a motor generator or by commercial power lines) or from a 28 Vdc battery supply.

The microseismic monitoring system was located within a rack unit designed to fit inside a Dodge B-300 series van. Vibration isolating mounts connected the rack unit to an aluminum base which in turn was bolted directly to the frame of the van. Consequently, the monitoring system could be easily transported to any site accessible to the van.

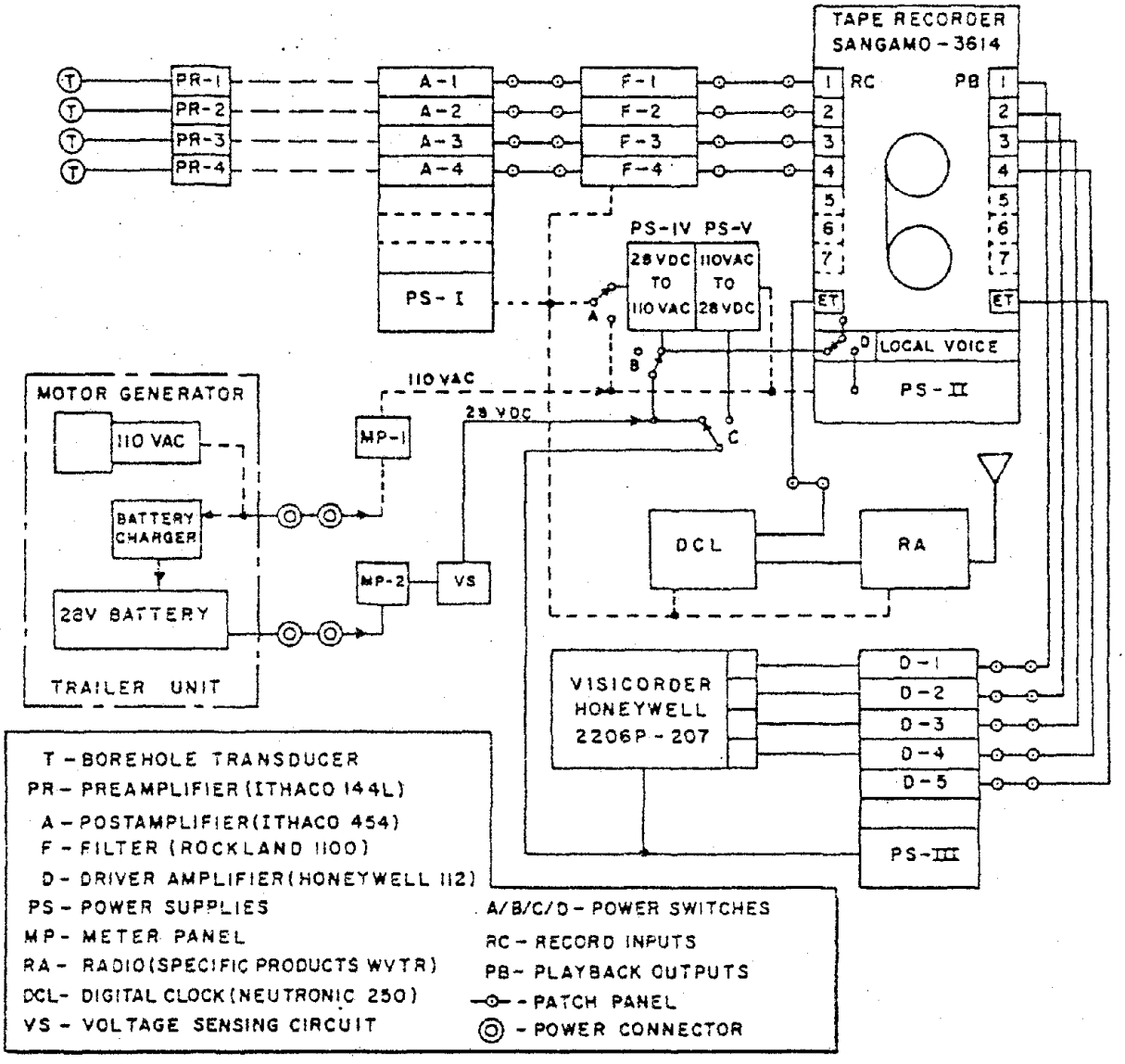

Figure 3. Block Diagram of the Basic Monitoring System in the Penn State Mobile Microseismic Facility (After Hardy, 1974).

Figure 4 shows the front view of the rack mounted system. The Dodge van and associated trailer is shown in Figure 5.

Advantages of the mobile microseismic monitoring system developed at The Pennsylvania State University include:

(1) mobility,

(2) ease in monitoring microseismic activity at above ground locations,

(3) broadband frequency response,

(4) high-sensitivity,

(5) high-signal-to-noise ratio,

(6) wide electronic configuration flexibility, and

(7) self-contained power.

Details of the mobile microseismic monitoring system used in this current study have been described in recent papers by Hardy and Kimble (1972) and Hardy (1974). For clarity however, certain aspects of the system will be briefly discussed in the following sections.

2. Transducers

A transducer is a device which converts a physical quantity into a proportional electrical signal. Stress waves generated by mechanical instabilities travel through the associated geologic media and can be detected by measuring the associated displacement, velocity, or acceleration. All three parameters, displacement, velocity, and acceleration, are related by the mathematical equation

$$a = dv/dt = d^2s/dt^2 \qquad \text{(Eq. 1)}$$

where a is acceleration, v is velocity, s is displacement, and t is

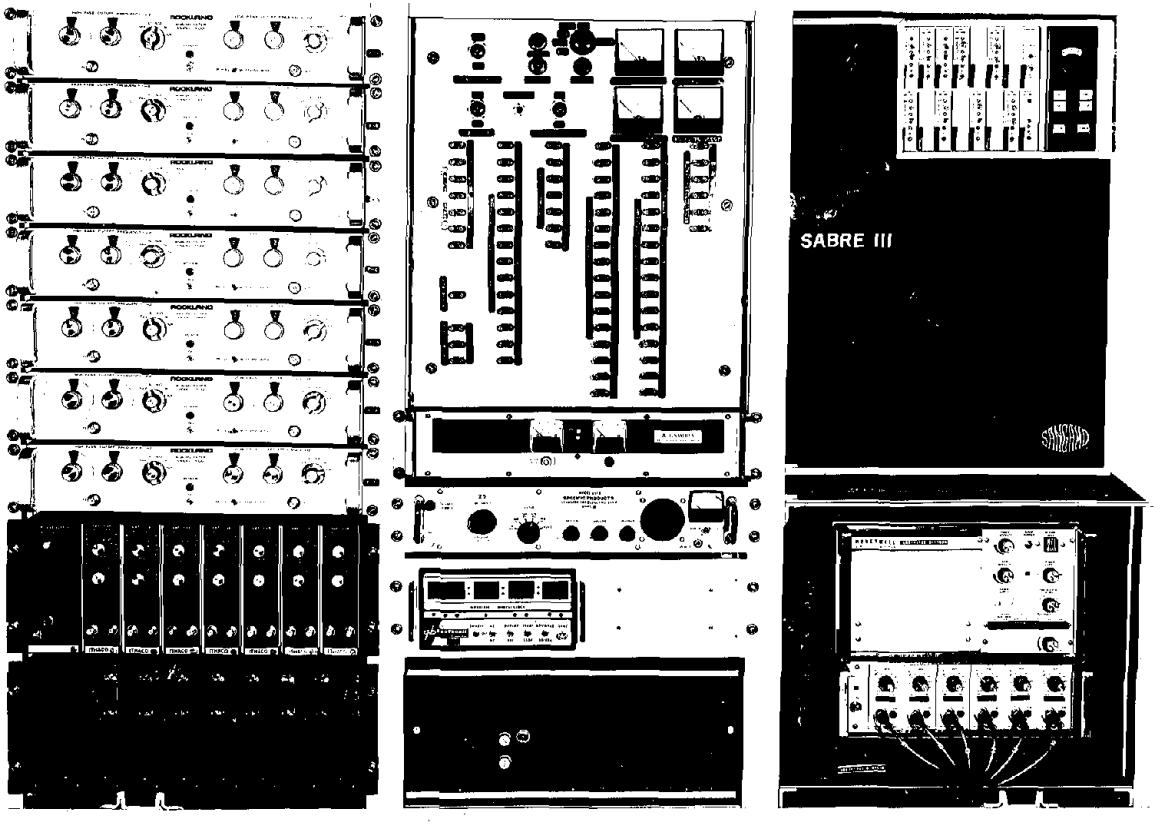

Figure 4. Front View of Basic Monitoring System in Microseismic Monitoring Facility (After Hardy, 1974). [The left rack contains at top, seven filter units, and at bottom, two sets of post-amplifiers. The middle rack contains at top, the power switching and monitoring facilities and the signal patch panel; below this is power supply PS-V, the radio, digital clock, and power supply PS-II. The right rack contains at top, the tape recorder; and below, the UV-recorder and driver amplifiers.]

Dr. H. Reginald Hardy, Jr.
Professor and Chairman,
Geomechanics Section

Figure 5. View of Completed Mobile Microseismic Monitoring Facility Ready for Field Use.

Dr. H. Reginald Hardy, Jr.
Professor and Chairman,
Geomechanics Section

time. Hard-wired electronic circuits, digital computation, or manual computation may be used to convert from one quantity to another.

For transducers located near the origin of the microseismic activity (e.g., 0 to 50 ft), typical signal frequencies would be on the order of 500 Hz to 50 KHz depending upon such parameters as the hardness, density and competency of the geologic media, and upon the distance the stress waves must transverse. Here, accelerometers would be the most suitable due to their high frequency response characteristics.

For monitoring activity at distances of 50 to 2,000 ft, a geophone or seismometer would be the appropriate device, provided the major frequencies involved were in the range of 5 to 500 Hz. Transducers employed to monitor activity at distances of more than 2,000 ft should probably be either a displacement gage or a very low-resonant frequency seismometer since very few microseismic signals would contain frequencies greater than 10 Hz at such distances.

Geophones have been utilized as transducers in the majority of the field studies described in this report. A geophone is a velocity type gage. Its construction consists of a light movable wire coil suspended by a spring in a permanent magnetic field. When the geophone is moved or jarred, the suspended coil remains in its original stationary position for an instant due to its inertia. Magnetic lines of flux are then cut because of the small relative movement between the magnet and the coil. The coil then begins to move in response to the geophone motion but is influenced by its own weight, freedom of motion, and the damping characteristic of the spring. Again, magnetic lines of flux are cut by the coil. As a result, a varying voltage is generated by

the coil which is proportional to the relative motion or velocity between the coil and the magnet.

For the field studies discussed, Geospace model GSC-11D geophones with marsh waterproof cases were successfully employed as shown in Figure 6. Typical output response is given as 0.6 to 0.8 V per inch per second, with a mechanical resonance of 14 Hz. Figure 6 also shows a typical response curve for the 14 Hz type geophone used in the current study.

3. Amplifiers

Amplifiers are used to amplify voltage, current, or power, and they can serve as impedance matchers. The mobile microseismic monitoring facility utilized two types of amplifiers, namely preamplifiers and post-amplifiers.

The preamplifier is used to amplify the very-weak voltages originating from the geophone. To obtain a maximum voltage transfer from the geophone to the preamplifier, the amplifier's input impedance should be very high, in this case 1,000 MΩ. The gain of the amplifier used is fixed at 40 dB (voltage gain of 100). In particular, the Ithaco model 144L preamplifier is used due to its very low-noise characteristics, low-distortion, high-stability, and ruggedness.

Ithaco model 454 post-amplifiers are employed to provide a further stage of amplification. These amplifiers have variable gains of from -10 dB to 90 dB in 1 dB steps. To achieve a maximum voltage transfer between the preamplifier, field cable, and post-amplifier, the impedances are purposely mismatched (i.e., preamplifier output of 50 Ω and post-amplifier input of 1 MΩ). Low-noise, low-distortion, and

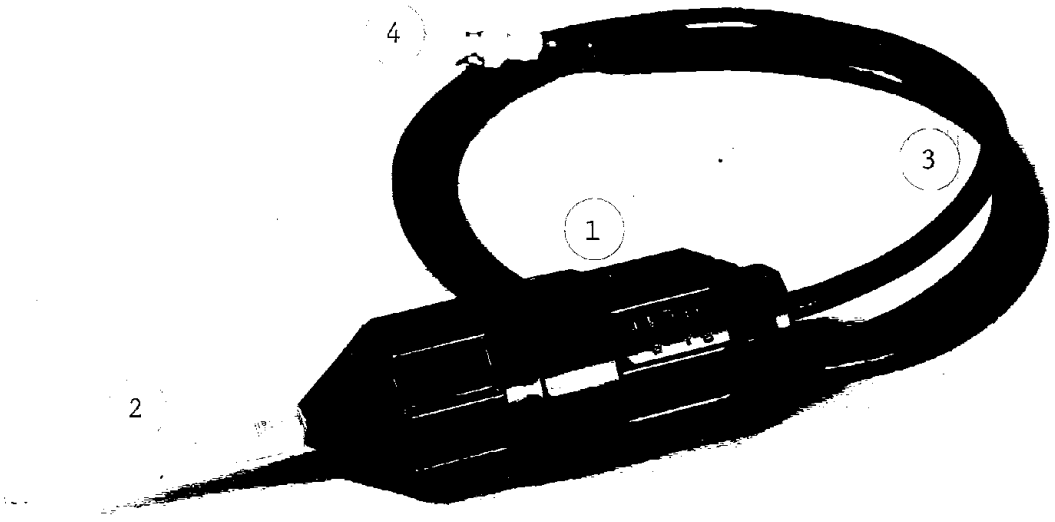

(A) Typical Geophone (1--geophone in marsh case, 2--installation spike, 3--waterproof cable, 4--BNC connector)

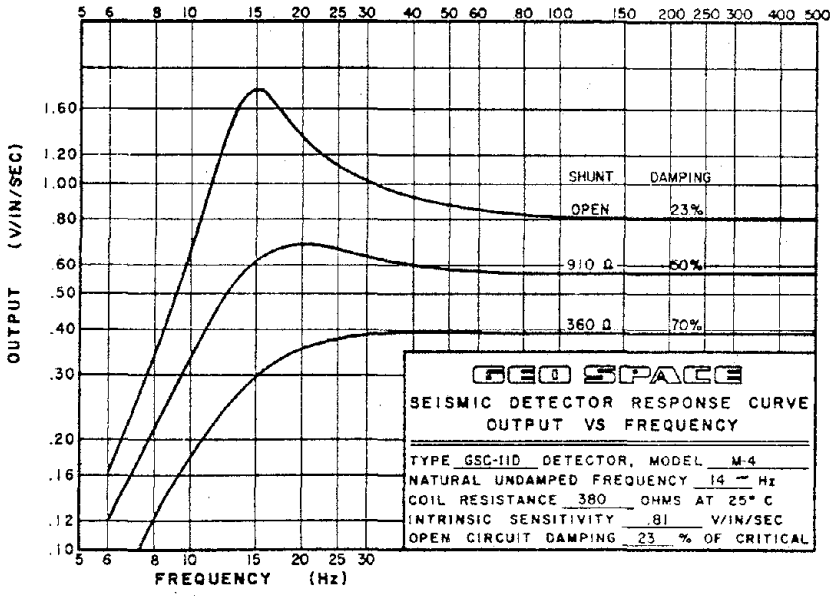

(B) Typical Geophone Response Curve

Figure 6. Details of Geophone Used in Current Study.

Dr. H. Reginald Hardy, Jr.
Professor and Chairman,
Geomechanics Section

high-stability characteristics are considered vital to successful microseismic monitoring.

4. Filters

One of the most annoying problems encountered when dealing with weak signals which have been amplified many thousands of times is that of noise. Thermal and electrical noises can originate at the geophone, the preamplifier, and the associated connecting cable and junction box. These noises are then amplified along with the desired signals as much as 80 to 90 dB (10,000 to 30,000 gain). The preamplifier and the field cables connecting the preamplifier to the post-amplifier are also susceptible to external and internal noises, but such noise would only be amplified by the post-amplifier, approximately 40 to 50 dB (100 to 300 gain). The post-amplifier is not immune to noise, but there is little or no amplification of post-amplifier noise, and hence, it is normally neglected.

Filters attenuate certain frequency bands, while allowing other frequencies to pass. Undesirable noise exists over the entire frequency spectrum. Since much of the frequency spectrum is of little use in terms of extracting meaningful data, provided the frequencies containing the desired information can be isolated, it is possible to selectively reject or attenuate all those frequencies lying below or above the range (or bandwidth) of interest. Filters can be placed between the geophone and preamplifier, between the preamplifier and the post-amplifier, or between the post-amplifier and the tape recorder. Filtering can thus remove unwanted noise from the data, provided the noise does not have the same frequency components as the desired data.

Generally, additional amplification can then be used because the noise, which is attenuated, can no longer saturate the amplifiers. For the microseismic facility used in the current study, a passive resistor-capacitor (RC) filter circuit was incorporated in a junction box connecting the geophone to the preamplifier. This filter was designed to attenuate frequencies greater than 1,000 Hz. An active operational amplifier filter circuit (Rockland Model 1100) was also placed between each post-amplifier and the associated tape recorder input to attenuate the high frequencies further.

5. Tape Recorder

Since microseismic events are transient in nature, they cannot be conveniently observed on an oscilloscope if any analysis is to be performed. Some form of temporary or permanent storage is needed such as a tape recorder, disk, cards, or paper tape. Time and monetary considerations recommended that a frequency modulated (FM) analog multichannel instrumentation tape recorder be utilized, since analog storage is relatively cheap and the associated circuitry simple and straightforward. The Sangamo Sabre III recorder was selected for the microseismic monitoring system. It has the capability of recording at seven speeds (from 1-7/8 ips to 120 ips); however, only three FM playback speeds (1-7/8, 15, and 60 ips) are currently available, due to fund limitations.

6. Junction Boxes and Field Cable

In order to couple the geophone to the preamplifier, a special junction box is required, referred to as JB-A. This junction box contains a shunt resistor to flatten the geophone frequency response

which normally peaks around the mechanical resonance and to reduce electrical noise, and a passive, low-pass, RC filter (3 dB down at 1,000 Hz) to attenuate frequencies above 1,000 Hz. Figure 7 shows a schematic diagram of the junction box circuit.

A second junction box (JB-B) is used to connect the preamplifier output to the input of the field cable. There are no conditioning circuits in JB-B as its sole purpose is to couple the preamplifier to the field cable.

The field cable used to connect JB-A to the monitoring facility is composed of three twisted pairs of 22 AWG wire, each pair being individually shielded, with the shields being insulated from each other. Both the use of twisted pairs and the shielding, aids in reducing the cable's susceptibility to external electrical noise. The basic wiring arrangement from the transducer to the monitoring facility is illustrated in Figure 8.

7. System Sensitivity

The lower amplitude sensing limit of the microseismic monitoring facility is the front-end thermal noise of the geophone and the preamplifier. This can be measured by shorting the input of the preamplifier and determining the amount of noise present at the output of the system. Dividing the noise developed at the output by the total system gain gives the background electrical noise of the system. The inherent noise of the geophone itself may also be a limiting factor; however, this is difficult to obtain since it requires that the geophone or its movable coil be completely motionless. These noise values are

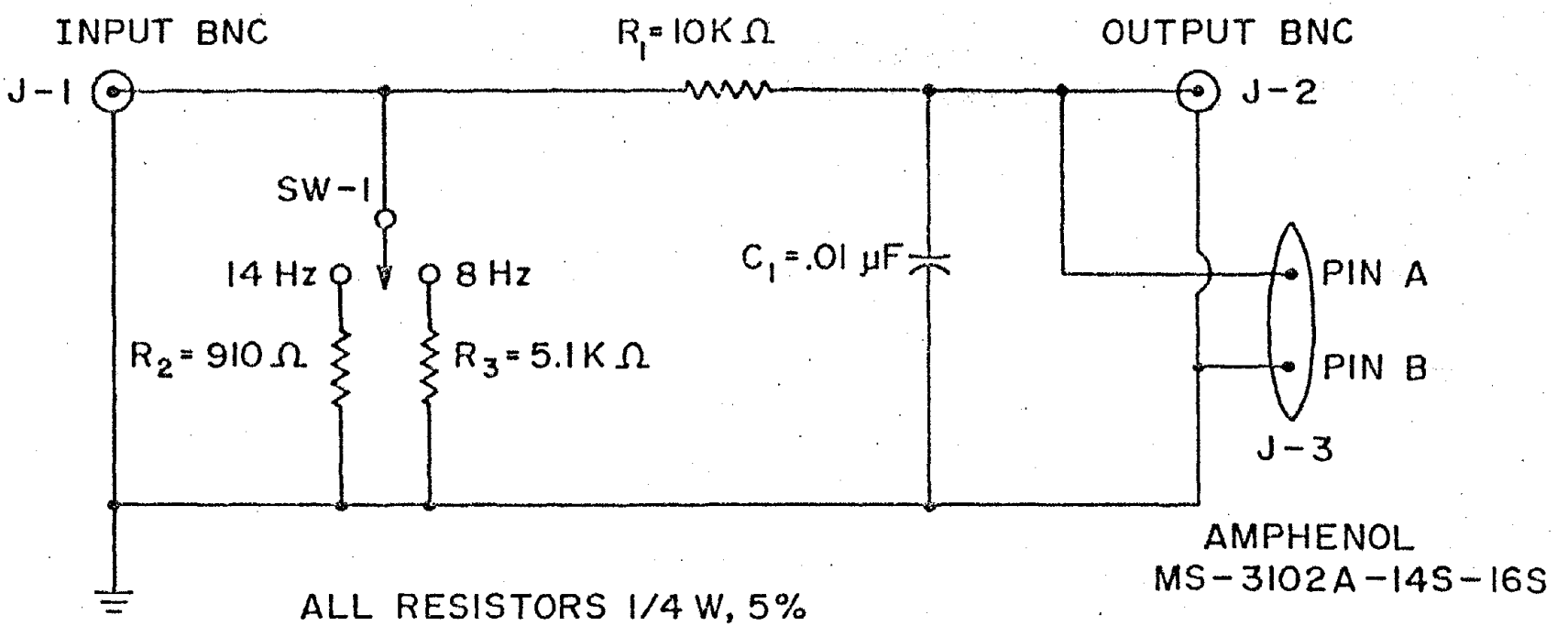

Figure 7. Simplified Diagram of Junction Box Type JB-A (After Hardy, 1974).

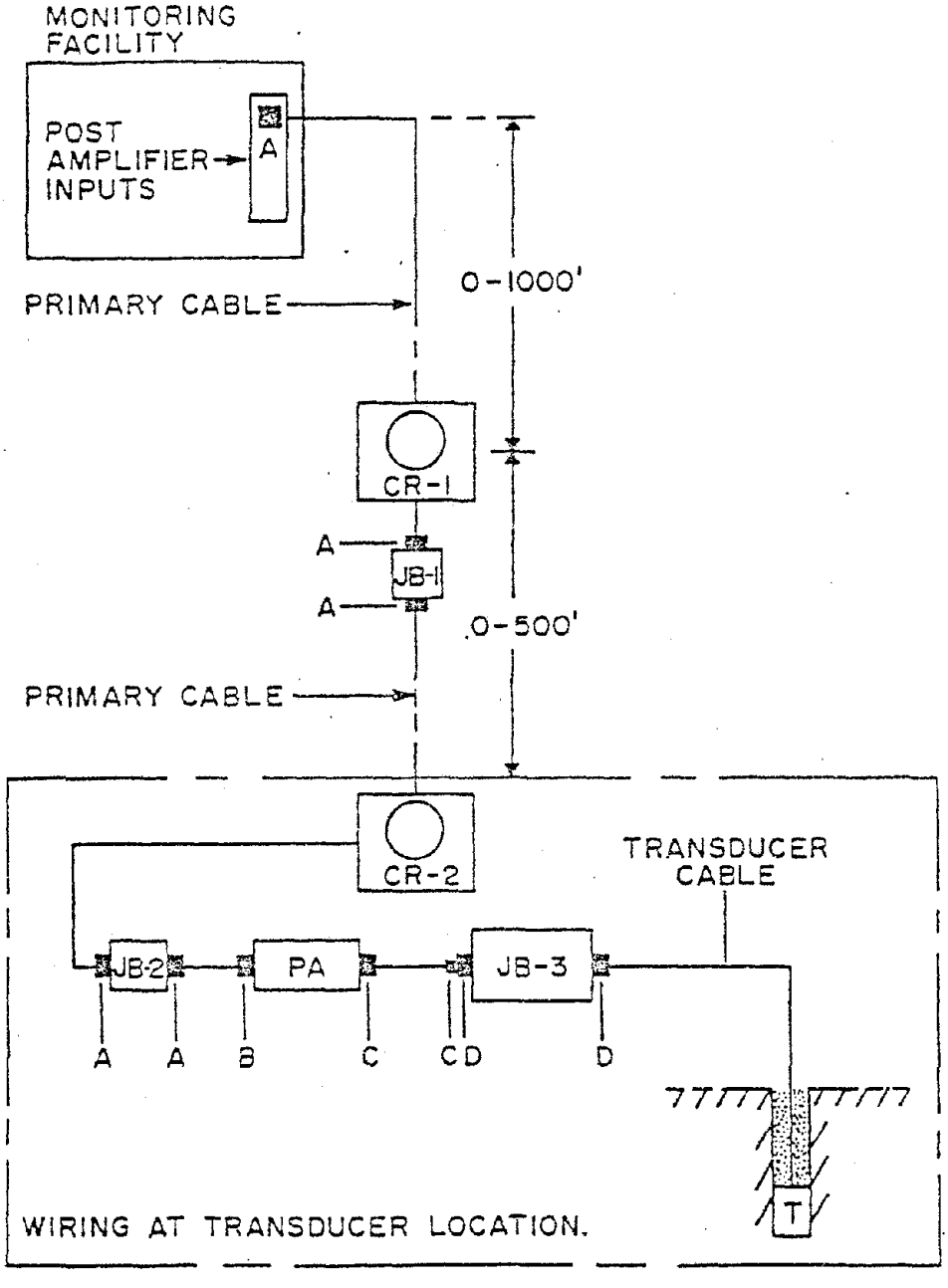

Figure 8. Typical Field Wiring Arrangement [where T, JB, PA, and CR designate transducer, junction box, preamplifier and cable reel respectively].

considered to constitute the background electrical noise level of the system.

Mechanical background noise levels must be determined at the field site under study. Noise generated by wind, rain, frost, traffic, heavy machinery, earth tremors, and other natural and man-made phenomena all constitute background mechanical noise which could well overshadow true microseismic events of smaller amplitude.

In order for microseismic events to be observed without utilizing special analytical techniques, such events must generally have at least the same amplitude as the associated combined electrical and mechanical background noise levels. Furthermore, the frequency sensing limit of the microseismic system is dependent on the combined frequency response of the geophone and the monitoring facility. For events to be detected, their frequency spectrum must lie within the frequency limits of the overall monitoring system.

The actual intrinsic rms noise of the microseismic monitoring system has been measured to be 8.9×10^{-9} V/$\sqrt{\text{Hz}}$, for a frequency bandpass of 10 to 250 Hz, a total system gain of 126 dB, and with the preamplifier input shunted with a 910 Ω resistor to simulate the geophone impedance (Hardy, 1974). For the geophones used in this study, the minimum equivalent rms ground motion that could be detected has been calculated to be 1.5×10^{-8} in./s/$\sqrt{\text{Hz}}$. These values have been obtained under optimum laboratory conditions; in actual field conditions, a somewhat higher noise value would be anticipated due to the factors mentioned in the previous paragraphs.

8. Calculation of Equivalent Ground Motion

The procedure for relating the voltage generated at the output of a geophone to ground motion is as follows.

(1) Measure the amplitude (A) of the event (or background noise level) in inches on the visicorder paper.

(2) Convert the amplitude A to an equivalent voltage by considering that the visicorder has a sensitivity of 1 in. = 1 V at 0 dB gain of the visicorder driver amplifiers. Divide A by the gain of the monitoring system (preamplifier, postamplifier, filter, tape recorder, and visicorder driver amplifier). Thus the voltage output of the geophone may be computed by

$$V = A/(10 \exp dB/20) \qquad \text{(Eq. 2)}$$

where V is the geophone voltage output, A is the event amplitude in inches, and dB is the total system gain.

(3) Convert V into a particle velocity by utilizing the transducer sensitivity. For example, the sensitivity for the 14 Hz geophones employed in the current longwall studies is approximately 0.58 V = 1 ips particle velocity. Therefore,

$$PV = V/0.58 \qquad \text{(Eq. 3)}$$

where PV is the particle velocity, and 0.58 is the geophone sensitivity for frequencies above 12 Hz.

9. Signal-to-Noise Improvements

Signal-to-noise ratio (S/N) is the ratio of the amplitude of a desired signal at any time to the amplitude of the background noise at

the same time. A number of techniques may be employed to increase the signal-to-noise ratio for microseismic events. Firstly, geophones may be placed nearer the source of microseismic activity by burying them deeper. This means that the stress waves would then travel shorter distances, and travel in more competent formations rather than in soil and unconsolidated media. Furthermore, since surface waves are continually being detected by geophones buried near the surface, more deeply buried geophones have soil cover to attenuate such waves.

Secondly, frequency bandpass filtering can effectively improve the S/N by eliminating noises which lie outside the frequency band of the desired signals. The narrower the bandpass, the greater the S/N. Filters can be either active or passive. Analog filtering may be employed at the output of the geophone, the input to the preamplifier, the input to the post-amplifier, and/or the input to the tape recorder. A filter with low-noise characteristics is essential if the signal, after passing through the filter, is to be further amplified. Passive filters have much less internal noise than active filters, although active filters have much sharper slopes at the edge of the bandpass frequencies.

Thirdly, the S/N can be improved, often dramatically, by eliminating periodic noises such as 60 Hz, using notch filters (filters designed to reject one specific frequency). Such filters can be employed at any stage in the system, in the same manner as the regular bandpass filters.

Finally, the use of geophone subarrays (several small arrays arranged within the main array) can be used to improve the S/N of a

microseismic monitoring system by summing the signals received from each geophone in the subarray. Random noises can best be minimized using this method. This technique is rather sophisticated and was not utilized in the current study.

IV. FIELD SITE DETAILS

1. Introduction

Since 1970, the Rock Mechanics Laboratory of The Pennsylvania State University has been carrying out microseismic studies related to coal mine safety. To date these studies have been confined to the study of microseismic activity associated with longwall coal mine operations. Figure 9 illustrates the basic experimental arrangement employed.

The mine selected for these studies was Greenwich Collieries, at Barnesboro, Pennsylvania. Greenwich Collieries consists of a North and a South mine, and during the period 1970 to 1978, four main sites were investigated at the North mine, as illustrated in Figure 10, namely the A-2 site, the air return shaft site, the I(A,B,C) West B-4 site, and the I(D) East B-4 longwall site. This current study will be concerned with the tests conducted at the I(D) East B-4 site. Preliminary data from the other three sites have already been briefly discussed in a recent U.S. Bureau of Mines (USBM) report (Hardy, 1974). Subsequent study of the data from the other three sites indicated that it was not of sufficient quality to merit additional analysis. In order to put the studies at the I(D) East B-4 site in proper context, a brief outline of the general Greenwich mine site has been included here along with details of the mining operations and the associated roof control conditions experienced in the North mine.

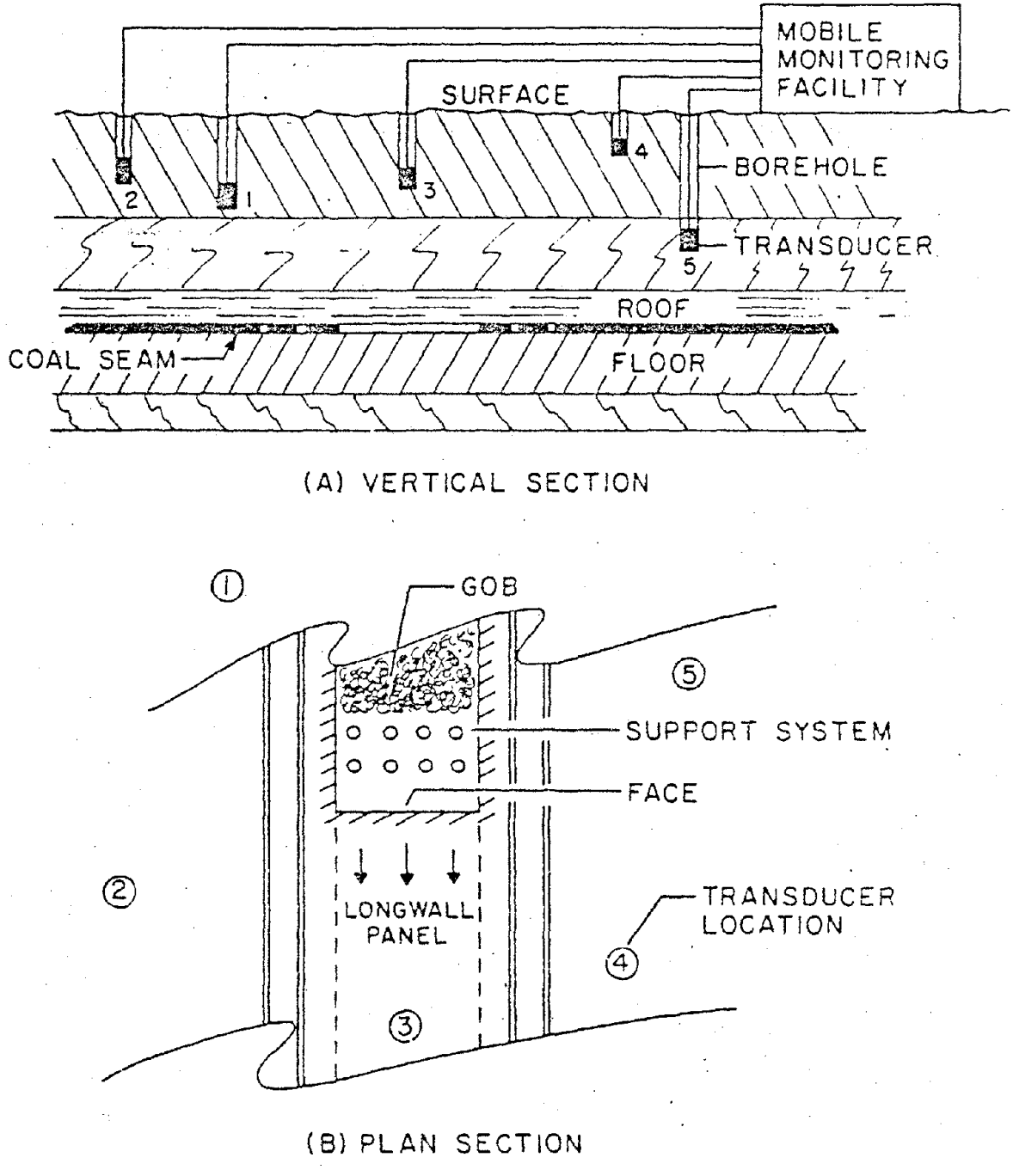

Figure 9. Basic Experimental Arrangement for Microseismic Study (After Hardy, 1974).

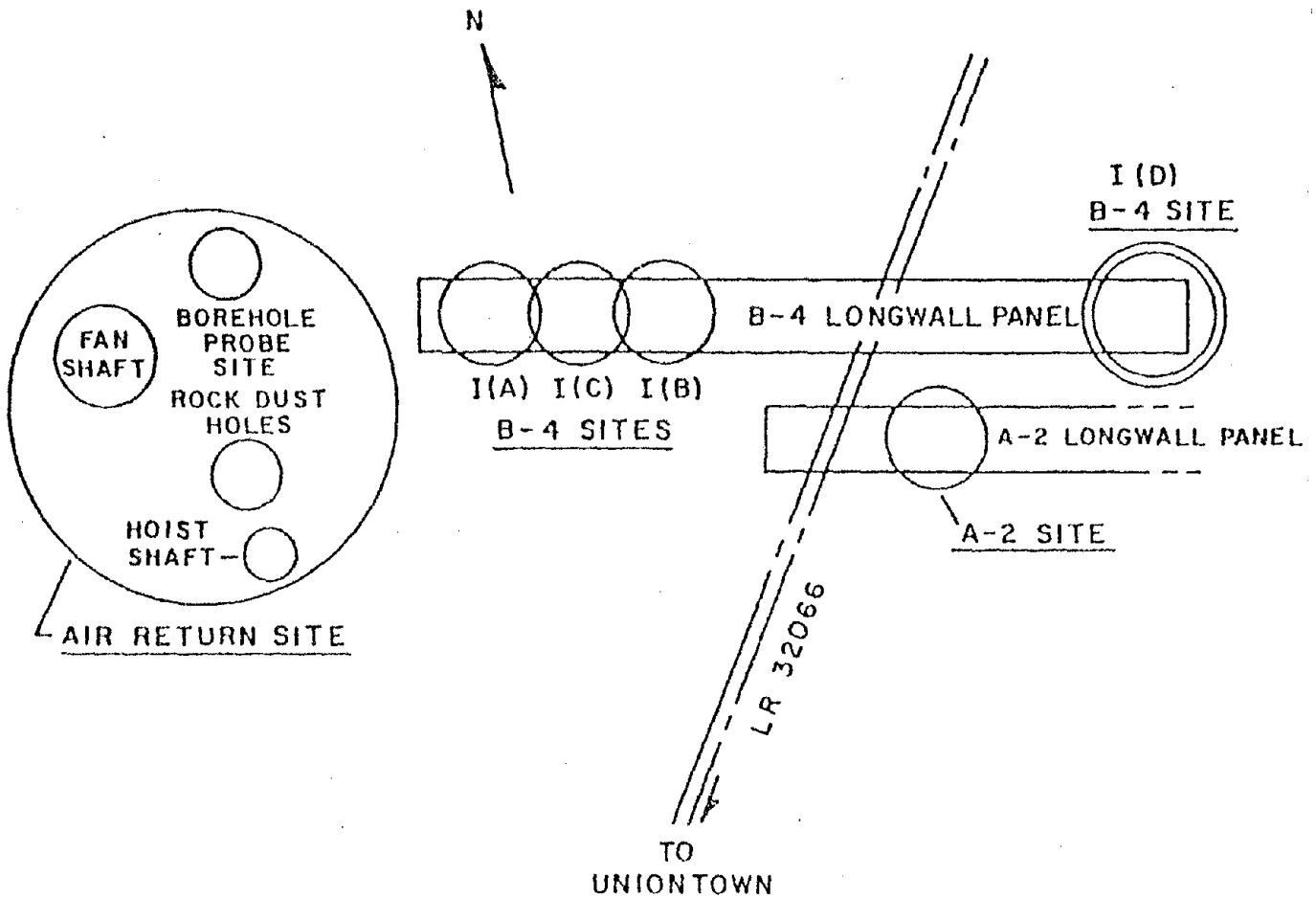

Figure 10. Approximate Locations of Microseismic Test Sites at Greenwich North Mine Study Area (After Hardy, 1974).

2. Field Site Selection

Early in 1971, project personnel visited several coal mines in Central Pennsylvania in search of a suitable site for monitoring microseismic activity. The choice of the site was based on a number of factors, including easy surface access above the coal mine, minimal interference with mining operations, and the mine management's desire to cooperate with the project personnel. Greenwich Collieries, located near Barnesboro, Pennsylvania, was selected for the microseismic field study. The general location in relation to the University Park campus of The Pennsylvania State University is shown in Figure 11.

Yonkoske (1972) has described the Greenwich area, and portions of his description are given below. Greenwich Collieries is located on the eastern part of the Appalachian Plateau in Central Pennsylvania. Situated slightly west of Uniontown, the mine is at an outcrop of the Freeport "D" seam.

Primary drainage of this area is provided by the west branch of the Susquehanna River which flows to the north. Structurally, the relief between anticlines and synclines in this area is approximately 500 to 700 ft. The mine dips at 3-1/2 degrees to the northwest down a syncline having a slightly plunging axis in the northeast direction.

Stratigraphically, the Appalachian Plateau lies above the Devonian, Mississippian, Pennsylvanian, and Permian beds. The Pennsylvanian sedimentations are typically cyclic in nature and are described by Weller (1930). With the aid of information from boreholes previously drilled in the South mine of Greenwich Collieries, Jones (1972) found the strata to consist of "alternating and laterally discontinuous shales, siltstones, sandstones, and coal." Such strata overlying the

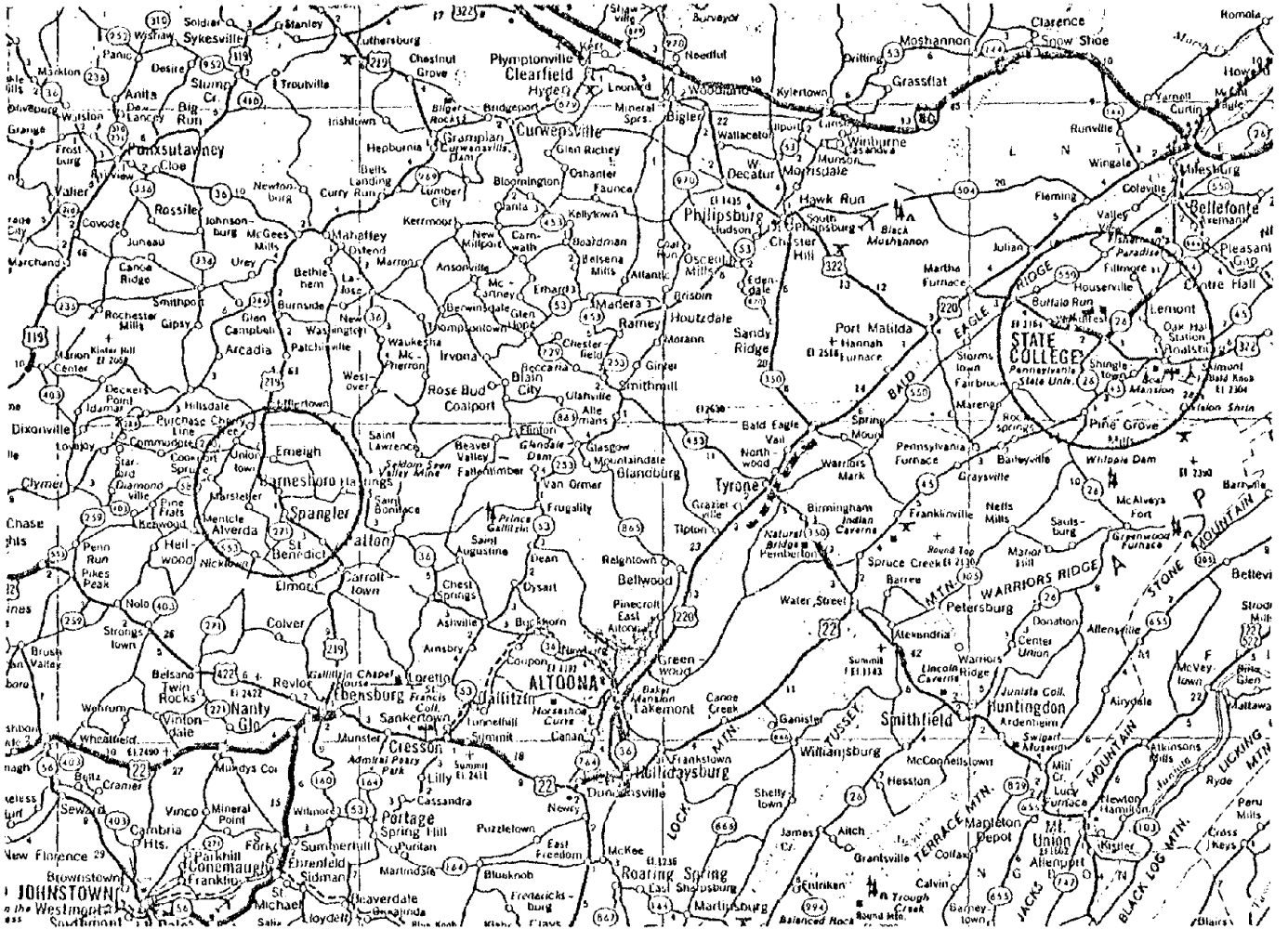

Figure 11. Map Showing General Location of Greenwich Colliery at Barnesboro. [The Pennsylvania State University is located at State College.]

coal seam would most probably be very heterogeneous, anisotropic, and geologically complex.

3. Greenwich Mine

3.1 General

Greenwich Collieries, a wholly owned subsidiary of Pennsylvania Power and Light Company, consists of two mines (the North, or No. 1 mine, and the South, or No. 2 mine) in the lower Freeport coal seam (locally known as the "D" seam). The mines are located north of Barnesboro, Pennsylvania, in Indiana County. The seam thickness averages about 42 in. laying under an average of 430 ft of cover. Both mines are drift mines, having an average coal seam dip of 4 percent.

Room and pillar areas and several longwall panels are being worked at Greenwich. Typically, the entries are 20 ft in width, the pillars are 60 ft by 90 ft, and the longwall panels are 450 ft wide by 5,000 ft in length.

Daily production of clean coal approximates 11,000 tons, with about 23 percent reject (Trevorrow, 1975). Conveyor belts transport the coal out of the mines to a central screening point, after which it is transferred to a preparation plant. The resultant clean coal is transported some 4,400 ft to a stockpile and load-out area by way of an overland conveyor. Unit trains receive the clean coal and transport the coal to the Montour generating plant in Montour County.

Twenty-five continuous miners and three longwall production shifts are in operation daily in each mine. For both development and the continuously mined sections, the output production of the mines is

approximately 150 tons per shift. For the longwall production, the output is projected to average 600 tons per shift.

3.2 Rock conditions

The floor or bottom rock consists generally of 6 in. of soft fire clay (Trevorrow, 1975), with a harder shale (uniaxial compressive strength of 8,000 psi), having a thickness of from 12 to 18 in., lying below the fire clay. Beneath this lies an extremely hard rock which varies from a sandy shale to sandstone. Compressive tests conducted at The Pennsylvania State University on this rock indicated that its strength ranged from 18,000 to 31,000 psi.

The roof or top rock above the coal seam may be classified in two parts, namely the immediate roof and the upper roof. A moderately strong shale (uniaxial compressive strength of 8,000 psi) constitutes the immediate roof, which typically has a thickness of 20 to 30 in. On top of the immediate roof is the upper roof consisting of a dark gray slaty shale which is estimated by the mine personnel to be 10 ft or more in thickness. This shale has a compressive strength of about 15,000 psi. The coal seam itself is comprised of coal ranked as Class II high-volatile "A" bituminous coal. The BTU rating is about 125,000. Analysis of the coal reveals the following: volatiles = 22.8 percent, fixed carbon = 56.2 percent, ash = 16.3 percent, moisture = 4.6 percent, and sulfur = 0.9 percent.

3.3 Equipment employed

Development section -- Lee Norse oscillating-head miner LN-26H and the Lee Norse fixed-head miner LN-265HH are the two types of

continuous miners used. The mine is slowly converting oscillating-head miners to fixed-head miners. The shuttle cars are four-ton capacity National Mine Car flexcars, typically carrying 2-1/2 tons. The belt feeder is a Stammler, and the belt system is manufactured by Airdox. A Fletcher LTDO provides roof-bolting capability of from 42 to 84 in. Generally roof bolts are placed in a 4 ft by 4 ft pattern. Roughly 30 percent of the roof bolts installed are resin bolts (Beck and Khair, 1974).

Longwall section -- The shearer used is a single-drum Eickoff Model No. EW 170, with ranging arm. The Eickoff is distributed by Joy Manufacturing Company and has a rating of 230 horsepower, consuming 170 kilowatts of electrical power. The roof supporters are four-leg Gullick Dobson (Wigan) supports, consisting of a 300-ton lower stage and a 500-ton upper stage. These double-telescopic supports are also described as hinged canopies. When the supports are fully extended, a maximum yield load of 300 tons is available. Once half the available leg travel is utilized, a maximum load of 500 tons may be obtained. As much as 32 tons can be applied at the tips. The supports are 45 in. wide and are 173 in. from the tip of the face to the back. Usually the supports are spaced at 4 to 5 ft intervals (Beck and Khair, 1974).

3.4 Roof control in the longwall area

Hydraulically-powered chocks at the face are utilized to support the immediate roof for protection of the mining personnel and the shearer. Once the shocks advance the immediate roof generally caves and becomes part of a well-fragmented gob. Much of the caving fragments range from 2 to 12 in. in length, being of a lenticular and slabby

geometry. Massive slabs of immediate roof as much as 20 ft in length, 5 ft in width, and 20 to 30 in. thick, occasionally fall. Resting on the gob is the sagging, massive upper roof as shown in Figure 12. Whittaker (1974) observed the upper roof is generally unbroken along the entire longwall face, which is quite unusual for normal caving of longwall mining operations, and that typically the height of caving ranges from one to three times the extracted seam height. The strength of the upper roof allows adequate spanning of the face to the gob. The weight of the upper roof aids in consolidating the fragmented immediate roof, which in turn acts as an effective abutment behind the chocks.

When the chocks are fully extended, a maximum of 300 tons of yielding support is available and is utilized. Unfortunately, this value generally permits excessive roof convergence. Difficulties are then encountered in roof control, by the time the 500-ton load is applied (Whittaker, 1974).

Because the roof convergence is often excessive, several problems arise, namely the following.

(1) The roof frequently fractures between the face and the chocks. Sizable blocks of rock then slip slightly downward, effectively prohibiting or hindering the passage of the shearer or the advancement of the chocks, as illustrated in Figure 13.

(2) At times the rear legs of some of the chocks contract fully ("close solid"). To remove the chocks, blasting is required.

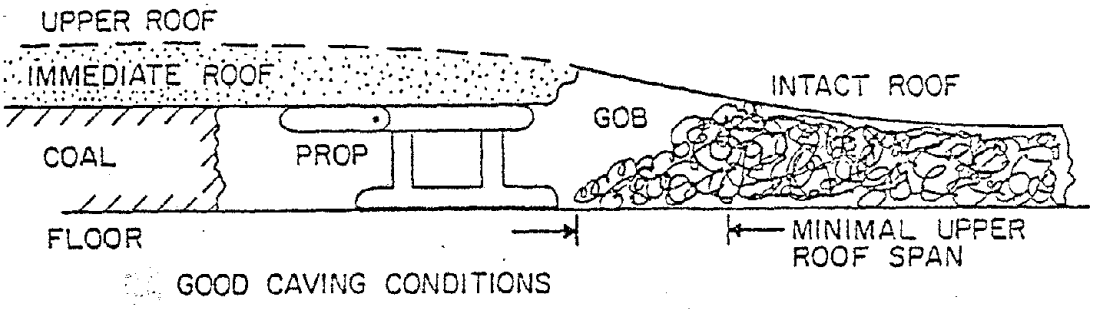

Figure 12. Normal Caving of B Seam.

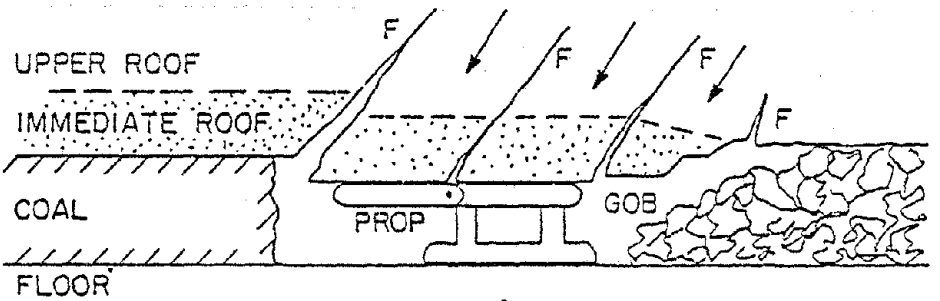

Figure 13. Roof Breaks Between Props and Coal Face.

(3) Sometimes the shearer becomes stuck due to the roof converging just behind the face. Blasting is generally employed to free the shearer and/or to make a sufficient clearance for the shearer to pass.

(4) Excessive scoring of seals and abnormal flexing of hoses permits hydraulic fluid to lead from the chocks which prevents the supports from obtaining maximum effectiveness. The fluid wets the mine floor, which is sensitive to water, thereby magnifying strata control problems.

Whittaker (1974) visited the B-6 longwall at Greenwich Collieries in August of 1974; on this occasion he heard rumbling sounds, similar to thunder, originating from the roof. For new longwalls these noises are typical until proper caving exists, which generally does not occur until after the longwall advances a distance equal to its width. Such rock noises are generated by the fracturing of beds in the upper roof as illustrated in Figure 14.

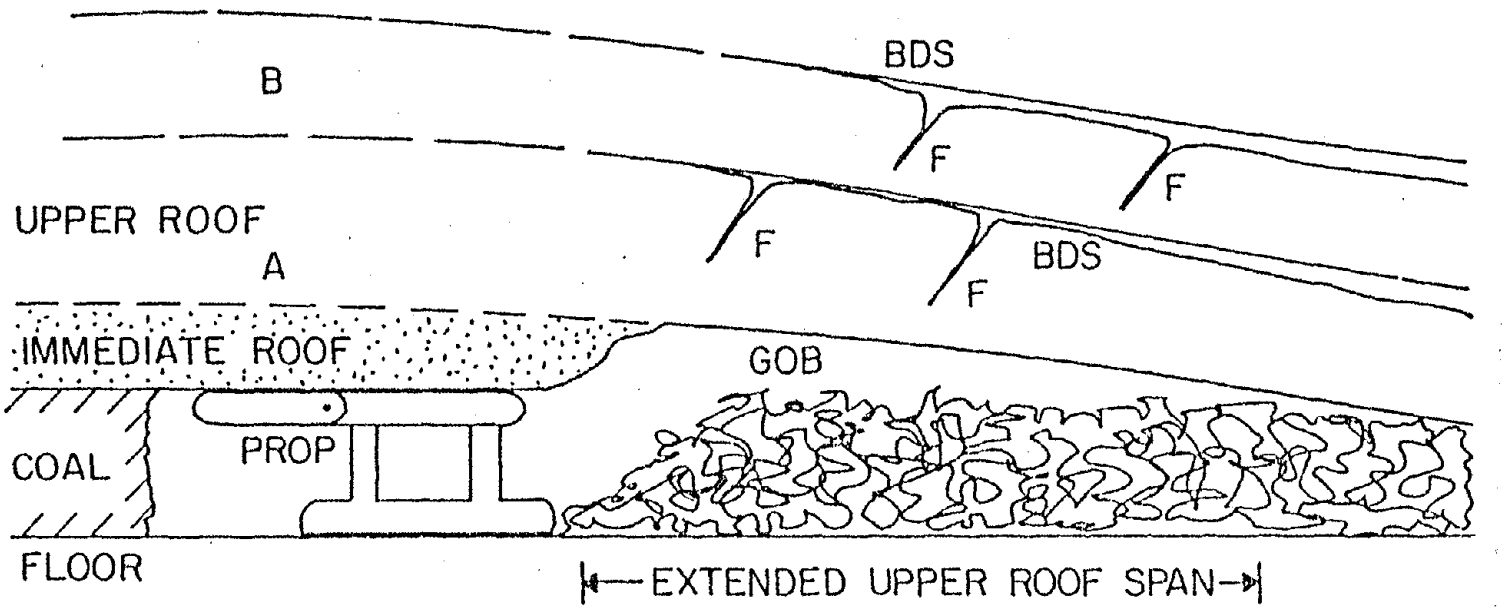

Figure 14. Bed Separation and Bed Fracture in the Upper Roof of a Longwall (After Whittaker, 1974).

V. FIELD PROCEDURES

1. General

To investigate the feasibility of using microseismic techniques to detect and locate potential zones of instability around a longwall, a study involving a number of field monitoring sessions are conducted over a longwall mining operation. An array of 15 transducers (geophones) mounted in shallow boreholes at depths of from 10 to 25 ft was installed above the active area of the longwall to detect any microseismic activity being generated in the proximity of the array. During each field session, a monitoring facility (described earlier) amplified, filtered, and recorded the activity sensed by the transducers. Following each field trip, the recorded microseismic data was played back on visicorder paper, which was then examined for true microseismic events. These events were analyzed in more detail as described later in this report. In this chapter details of the more important field procedures will be discussed.

2. Geophone Installation

In general there are three techniques used to install the geophones. They include (1) surface-mounted, (2) shallow-burial, and (3) deep-burial. These are illustrated in Figure 15.

In the initial longwall studies the spiked tip of a geophone was vertically wedged securely in the ground at the surface. The A-2 longwall study utilized this surface-mounted technique exclusively due to

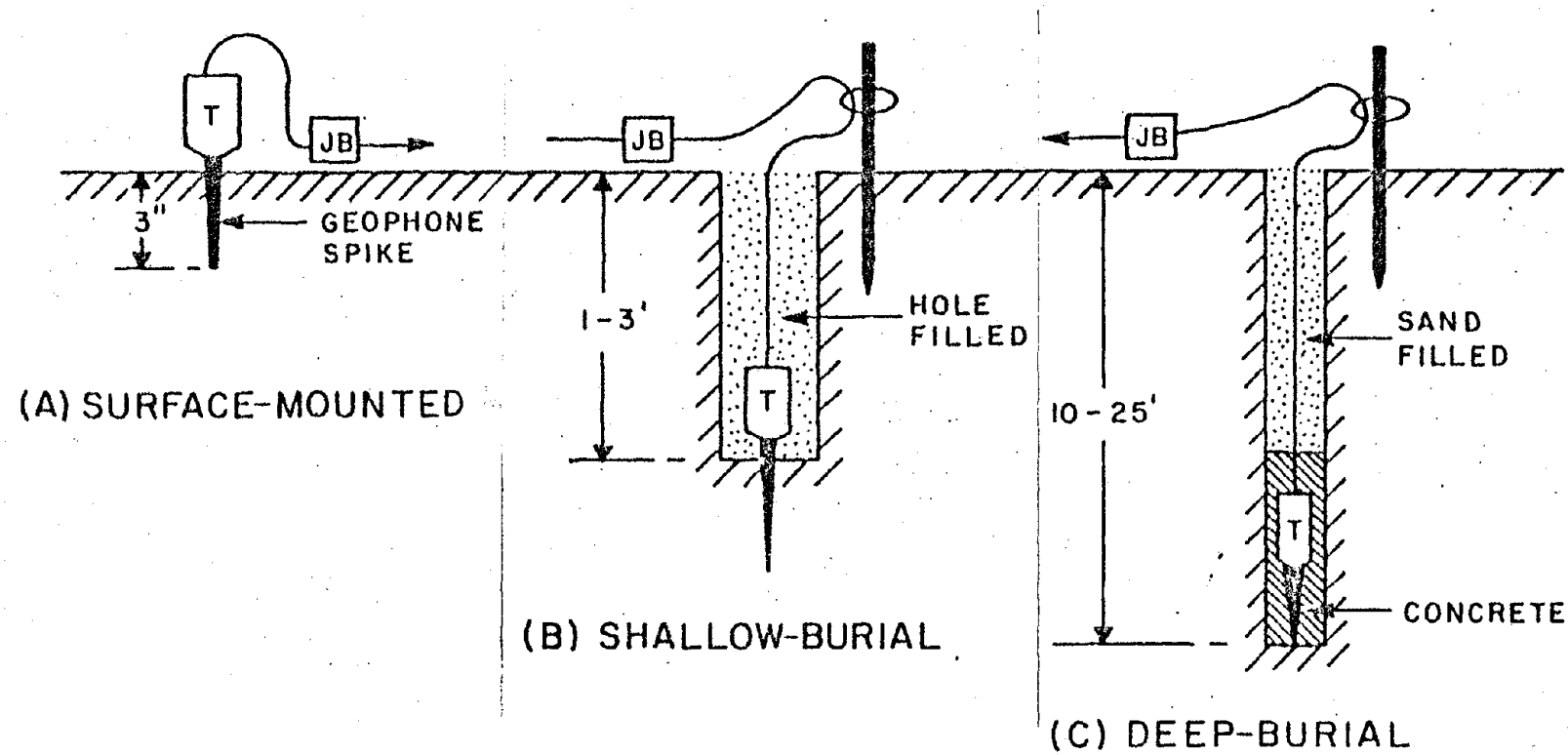

Figure 15. Typical Types of Transducer Installations.

the ease and simplicity of the installation. Drawbacks for the surface-mounted technique include poor acoustical coupling between the ground and the geophone, and high-susceptibility to surface noises such as wind, rain, and vehicular traffic.

If more isolation from surface noises and an improvement in the acoustic coupling is desired at a very minimal cost, the shallow-burial technique is worth considering. Here a post-hole digger (hand-operated) is employed to dig a hole roughly 6 in. in diameter and 2 to 3 ft in depth, provided rocks and bedrock are not encountered. Barring problems such as rocky soil, holes can be dug in 10 to 20 minutes. A digging bar is useful whenever rocks are encountered and must be broken. Once the hole is at the desired depth, a geophone is vertically mounted, spike downward, in the soil at the bottom of the hole. The soil removed from the hole is then carefully and firmly repacked around the geophone using the flat end of the digging bar. The remainder of the hole is similarly repacked. At all times care must be exercised in protecting the geophone and the associated cable from damage. A steel rod, fence post, pipe, or wooden stake is inserted about 6 to 12 in. away from the geophone hole to act as a support for the geophone cable. For ease in locating the geophone holes on subsequent field trips, a strip of red surveyor's ribbon is connected to the top of the stake. The geophone cable is secured to the stake with electrical tape, and a plastic bag is utilized to protect the BNC connector, at the end of the cable, from moisture and weather. The end of the BNC connector should be positioned facing toward the ground to prevent moisture from accumulating inside. The open end of the plastic bag likewise should face toward the ground

with the end left slightly open to permit air to circulate and dry any moisture that might enter.

The most satisfactory method for installing geophones is the deep-burial technique. This requires a small drilling rig with a 3- or 4-in. auger. A hole is augered to a depth of 12 in. or so into bedrock which, for the Greenwich site, is usually 10 to 20 ft below surface. As soon as the auger is removed from the hole, a geophone, with 6 to 12 in. of heavy steel washers placed on top to help the geophone to be positioned vertically, is lowered to the bottom of the hole. Approximately one-half cubic foot of concrete is then poured down the hole while the geophone cable is held taut. Stakes or posts are next driven in the ground 6 to 12 in. from the hole, and the remainder of procedure is the same as discussed in the previous paragraph. After the concrete has had time to set (typically several days), fine sand is poured into the hole, until it is filled, to prevent possible hazards to people in the area, and to prevent it becoming a drain for surface water. Should the hole be drilled more than several hours before a geophone is to be installed, it is advisable to case the hole with plastic sewer pipe or other available casing to prevent the hole from deteriorating prior to geophone installation.

Surface-mounted or shallow-burial geophones are subjected to a variety of mechanical and electrical surface noises. For example, mechanical noises include wind, rain, vehicular traffic, trees, people, and animals. Also, the unconsolidated soil having been packed around the geophones produces noises by shifting and settling with time and changing weather conditions (e.g., freezing, thawing, rain saturation, and dehydration). Electrical noises are generated by heavy electrical

machinery (motors and generators), power lines, radio transmitters, corrosion control systems (cathodic protectors), electrical storms, and electrical fences.

The waveforms of events detected by the surface-mounted or shallow-burial geophones are generally quite distorted. Microseismic events originating underground are attenuated in amplitude with increasing distance between the source and geophone in even a simple homogeneous, isotropic, continuous, elastic formation. The higher frequency components present in the waveforms are also more highly attenuated with distance than the lower frequency components. In actual field conditions most formation are heterogeneous, anisotropic, and discontinuous, all of which distort the waveforms further. Another factor which influences the amplitudes of the waveforms is the acoustic impedance of the formation. The consolidated formations beneath the top soil have much higher acoustic impedances than soil. Because of this impedance mismatch, these formations will tend to retain any vibrations coming from within or beneath them. Consequently, relatively little energy will be released into the soil. Furthermore, the soil, being an insulating or acoustically poor conductor, rapidly attenuates whatever energy propagates through it.

During one field trip to the I(D) East B-4 longwall site (May 10, 1975), a study was conducted to investigate the effect of geophone installation depth on signal characteristics. Three geophones were previously installed at one location (N-9, see Figure 23) at depths of 20 ft (deep-burial), 3 ft (shallow-burial geophone), and on surface (surface-mounted geophone).

The following results were obtained.

(1) Signals from the surface-mounted geophone exhibited the highest amount of background noise. Much of this noise was on the order of 1,000 Hz and was moderately large in amplitude, possibly due to the wind blowing during the monitoring session. Similar frequencies, but smaller amplitudes, were found for the shallow-burial geophone, which suggests that the top soil is an effective acoustic filter.

(2) All three geophones were found to respond to large underground or surface noises.

(3) Generally, if the surface of the ground was impacted with a steel digging bar, the observed signals were highest in frequency on the surface geophone and lowest on the deep geophone. Also, the signal amplitudes were greatest on the surface-mounted geophone and smallest on the deep-burial geophone.

(4) The surface-mounted geophone always appeared to exhibit the largest amplitude for both surface and underground events.

Reviewing then, the advantages of a deep-burial geophone over a shallow-burial or surface-mounted geophone include:

(1) higher signal-to-noise ratio, due to the high attenuation of signals originating from surface;

(2) more accurate arrival times for surface locations, due to reduced background noise.

On the other hand, the advantages of a shallow-burial or surface-mounted geophone over a deep-burial geophone include:

(1) much easier and less costly to install;

(2) greater sensitivity to surface noises, thereby providing good correlation with events occurring at surface, e.g., aircraft, vehicles, animals, and people.

3. Pre-Field-Trip Procedures

Proper preparation for microseismic field trips is extremely important. When preparing for a field trip, one must first determine what supplies are to be taken. Items to be procured include reels of magnetic tape, boxes of visicorder paper, junction boxes, cables adaptors, preamplifiers, cable reels, tool box, walkie talkies, gasoline container, oscilloscope, multimeter, spare parts, and expendable supplies. Prior to a field trip the tape recorder must be cleaned, the microseismic monitoring system tested for proper functioning, and the walkie talkie batteries charged. The instrument van should be emptied and swept out, then packed with the above items, which are arranged so as to minimize damage to the equipment rack in the event of a sudden emergency stop. The trailer, containing the motor generator, power cables, and large tools is connected to the van just prior to departure. Climatic conditions indicate whether items such as rainsuits, heaters, and the like are needed.

4. Field Site Procedures

Upon arrival at the field site, project personnel first unload the van and the trailer. The motor generator is started and the electronic equipment is warmed up while personnel unwind field cables. The geophones (usually permanently installed) are then connected to the field cables through various junction boxes and amplifiers. Equipment

settings are selected (post-amplifier gains, filter frequency bandwidths), and each channel is then monitored using an oscilloscope. A magnetic tape is mounted on the recorder, and a 50 Hz, 1 V peak-to-peak triangular waveform, from a signal generator, is connected to one channel of the tape recorder as a reference signal. Next, to provide a suitable mechanical signal to insure each geophone channel is operating satisfactorily, one person walks past each geophone station, while a second person monitors the response of the associated channel using the oscilloscope.

At this time, the tape recorder is started to initiate data recording, the equipment settings are again checked, and the time and tape footage are noted on the field data log. During the microseismic monitoring period all observable events (vehicles, aircraft, people, weather, etc.) are documented in the field log, along with all equipment setting changes and tape footages.

At the end of the monitoring period, personnel retrieve all junction boxes and preamplifiers, and rewind the field cables on their respective wheels. The magnetic tape is then rewound and labeled, after which time the motor generator is shut down. The van is then repacked in the same manner as described in the previous section.

5. Post-Field-Trip Procedures

Generally on the day following a field trip, the van is unloaded and cleaned. The field equipment is then set up to playback the recorded data. In this mode the tape recorder outputs are connected to the analog filters which in turn are connected through driver amplifiers to the visicorder. Appropriate filter bandwidths and driver amplifier

gains are employed. Data is played back on the tape recorder at a speed of at least four times that of the original recording speed, and the visicorder paper drive is set at a slow speed (typically 0.4 ips). A hard copy of the entire microseismic field monitoring session can thus be obtained in a condensed form for immediate perusal. Typically more than three hours of data can be hardcopied on one roll of visicorder paper 100 ft long. This provides sufficient resolution to select potential microseismic events. All potential events are then replayed at a slow tape speed (usually 1-7/8 ips) and are hardcopied at a medium or high visicorder paper drive speed (usually 4 to 80 ips) for later detailed analysis.

VI. DATA ANALYSIS PROCEDURES

1. General

Two methods have been employed to analyze microseismic data, namely (1) manual analysis and (2) computer analysis. Manual analysis, in general, consists of hardcopying the microseismic data from magnetic tape to visicorder paper and evaluating quantities such as event activity rate, frequency content, amplitude, duration, and arrival times by hand, or playing the data back through a number of hardwired analysis units such as a frequency analyzer or event counter to obtain specific microseismic parameters. Computer analysis, in contrast, consists of digitizing selected portions of microseismic data directly from the magnetic tapes and then mathematically processing these digitized portions using suitable computer programs.

2. Manual Analysis

Manual analysis constitutes the major portion of the data analysis performed during this study. Figure 16 illustrates the editing and manual analysis procedures employed. Data reduction through selective editing is accomplished by playing back the field tapes at an intermediate tape speed and by running the visicorder at a slow speed. Possible events of interest are noted, and these events are expanded by playing the data on a slow tape speed and a high visicorder speed. Crude frequency analysis can be made by replaying the event at several narrow bandwidth filter settings and noting the amplitude of the event

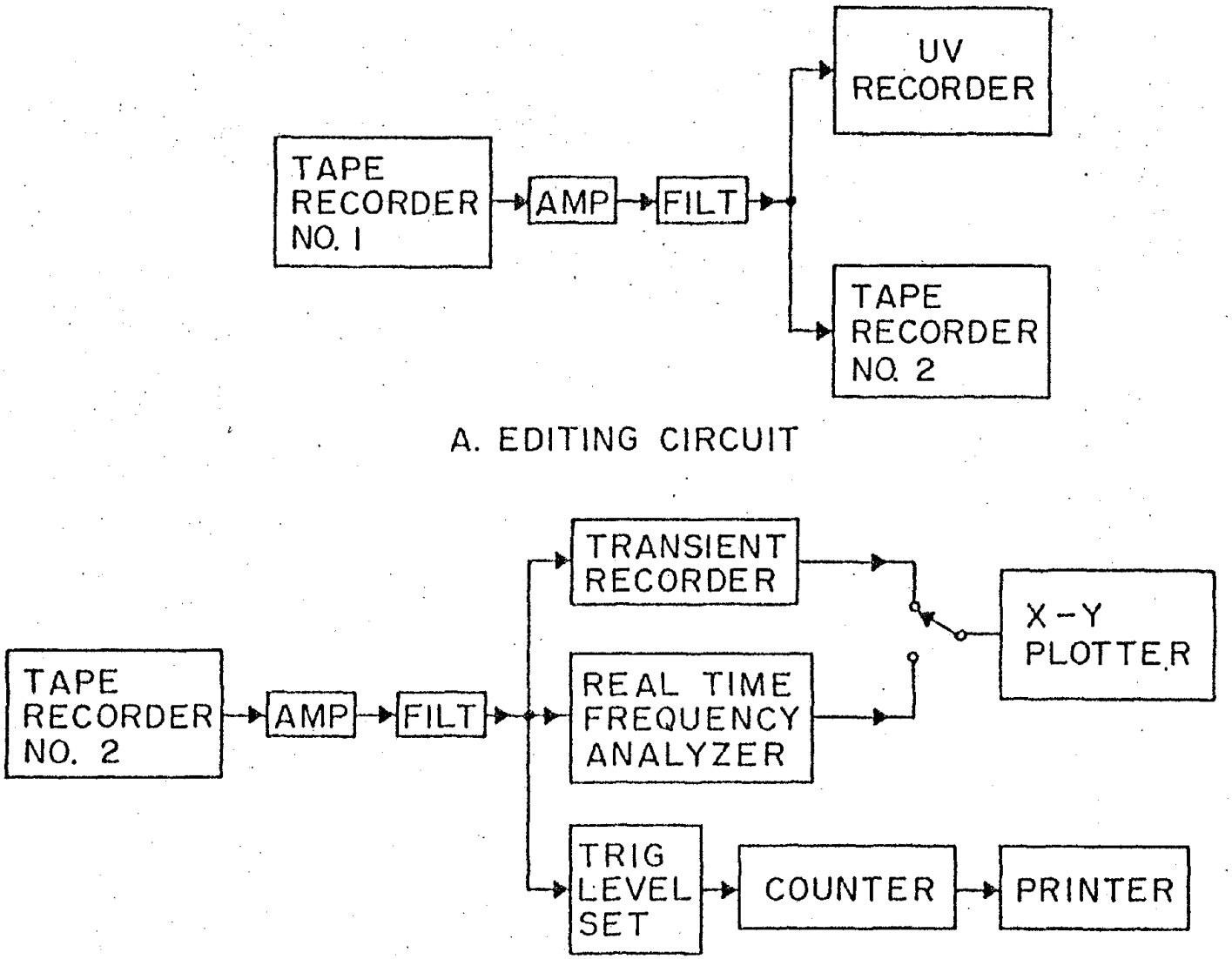

Figure 16. Block Diagrams of the Editing and Manual Analysis Systems.

at each filter setting, or by measuring the time for one complete cycle of the signal and taking its reciprocal to obtain frequency. Arrival times, phases, and durations of the events may likewise be obtained from the oscillograms by visual inspection.

If more than just a hardcopy output of the data is desired, a second, portable recorder is employed to record selected sections of the data onto a second tape. This portable recorder may then be transported to a laboratory or a computer facility for further analysis. In the laboratory, a transient recorder, a real time frequency analyzer, and digital counter and printer are available for data analysis. The transient recorder is an analog-to-digital converter having a digital memory, with a pretrigger mode which enables one to capture a complete event and display it on an oscilloscope for perusal or record it using an associated X-Y plotter. The real-time frequency analyzer may be used to determine the frequency components present in individual events and in ambient background data. The digital counter and associated printer may be used to obtain event activity rate (number of events above a selected amplitude per unit time). All three instruments mentioned have the common disadvantages that only one signal channel may be analyzed at a time. Multichannel analysis is therefore very time consuming with such equipment.

3. Computer Analysis

The method best suited for data processing and analysis is a computer based system. One of the authors (Mowrey, 1977) has written several computer programs utilizing the Hybrid Computer Facility of The Pennsylvania State University. These are designed to digitize

rapidly and accurately several channels of analog data, store the digital data on tape, perform mathematical operations upon the digitized data, and display the data on a digital display or oscilloscope. Figure 17 shows a simplified block diagram of the Hybrid Computer Facility, and a brief description of the associated computer programs developed by the writer are given in a paper entitled "Computerized Data Processing Programs for Use with a Multichannel Analog Microseismic Data Acquisition System" (Mowrey, 1975). The basic format of the digitized data is designed to be compatible with an available set of hybrid computer data analysis programs called DATNL developed at The Pennsylvania State University by Kellmel, Fortune, and Vosenilek (1974).

The hybrid computer programs have not been utilized extensively as yet due to

(1) the limited availability of the hybrid computer facility,

(2) the problem of timesharing the hybrid computer during digitization of analog signals,

(3) the time consumed in properly wiring the analog portion of the hybrid computer, and

(4) the relative difficulty in transferring the microseismic field data to the hybrid computer facility.

To alleviate these problems, which have thus far limited the amount of data processed, one of the authors (Mowrey) has been developing a minicomputer system which would essentially incorporate the above programs and would also be completely dedicated for the acquisition, data reduction, processing, and digital storage of microseismic data. With a suitable telephone interface, the minicomputer system will be

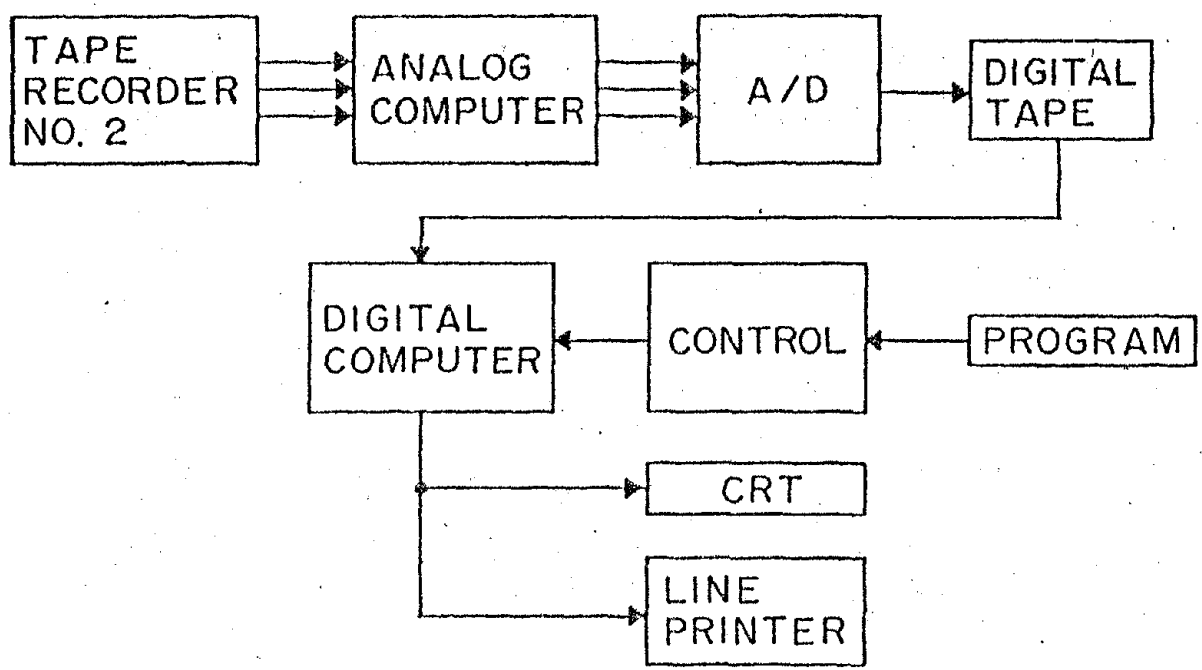

Figure 17. Hybrid Computer System Block Diagram.

connected to the IBM 370/168 digital computer of The Pennsylvania State University to permit additional storage, more complex computerized data analyses, and utilization of associated line-printers, magnetic tape drives, disks, and other periferal devices linked to the digital computer facility.

In contrast to hybrid computer analysis techniques, which are still in the development stage, digital computer analysis has been used extensively in the current study for the computation of microseismic source locations. Details of the techniques and associated digital computer programs are presented in the section entitled "Source Location" later in this chapter.

4. Recognition of True Microseismic Events

When carrying out microseismic monitoring of a geologic structure as complex as a mine, a wide variety of signals is often observed. Only a limited number of these signals are true microseismic events.

4.1 Criteria for a microseismic event

Four basic criteria have been used in this investigation for delineating true microseismic events, namely the following.

(1) The event must be above a certain amplitude level (above the ambient background noise).

(2) The event must lie within a certain frequency range.

(3) The event must exist for a certain duration of time.

(4) The event, as detected by a number of geophones, must exhibit coincidence in the following manner:

(a) at least three geophones in the array must detect the event within a specific time window and

(b) not more than three geophones should detect the event simultaneously.

Although computer techniques have been under investigation by the authors for automated recognition of true events, they have not as yet been sufficiently developed. Consequently, only manual techniques have been used in the current study.

4.2 Typical waveforms observed

During the recent longwall microseismic studies, some 15 general types of signal waveforms have been observed as illustrated in Figure 18. In this section the character and probable source of the various types of signals are discussed.

True microseismic events are nearly always characterized by signals of type -9 and -10. These resemble rapidly decaying transients in most instances. Events having high energies and being at large distances from the transducer often show an increase in amplitude before decaying, as the P, S, and Rayleigh waves (which have different propagation velocities) sequentially reach the geophone.

Electrical spikes or transients caused by system noises generally appear as a type -1 waveform. Two or more such transients occurring nearly simultaneously would appear as a type -2. Basically these are high amplitude, high frequency waveforms having a short duration. In contrast, if a person walks by a geophone site a series of increasing amplitude transients occur, followed by a series of decreasing amplitude transients, denoted as type -3.

"Rumblings" appear as blossoming and slowly decaying background noises with duration which may vary from a few seconds to as much as an

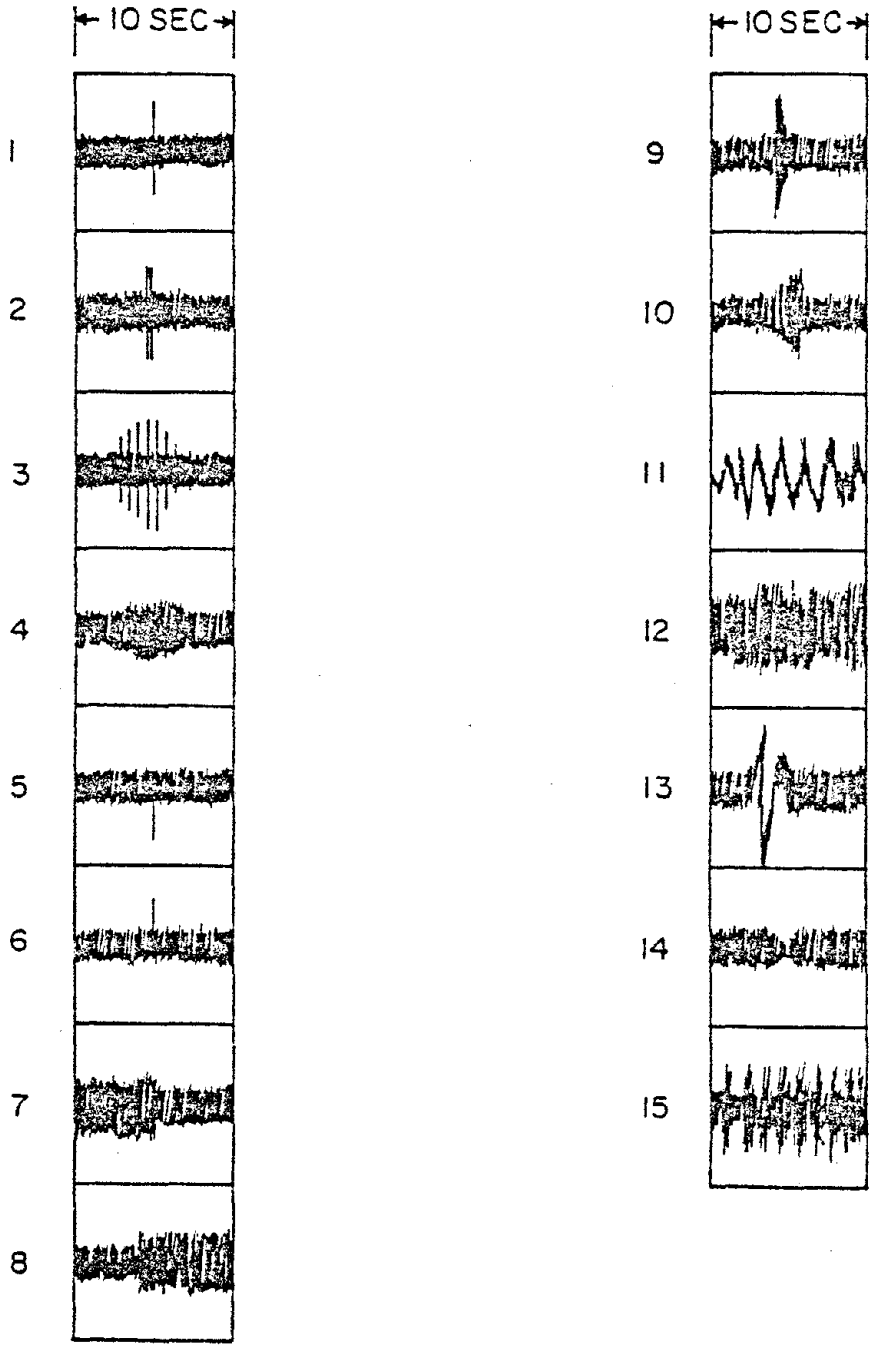

Figure 18. Typical Types of Waveforms Observed.

hour or more. The source of these "rumblings" are as yet uncertain, but they are currently believed to be related to distant noise sources which have generated surface waves (e.g., mining machinery, such as the shearer cutting rocks harder than coal, or electrical noises within the ground or air). The type -4 waveform is characteristic of a typical "rumbling." Types -12 and -15 are related closely to type -4 except that the frequency of vibration is lower. Type -15 appears to represent a series of closely spaced single events. The source of these events has not been established.

Signals with waveforms of type -5 and -6 are generally observed only once and cannot be repeated at the same type footage. These are apparently due to a problem of poor tape tracking caused by dirty recording or playback tape recorder heads. Cleanliness of the heads and tape usually minimize the occurrence of this type of signal.

Whenever the ambient background noise level abruptly decreases (type -7) or abruptly increases (type -8), electrical ground currents are suspected to be the cause. High-voltage and high-current machinery being switched on or off can quickly alter electrical ground currents and may be the cause of such signals.

The Microdot connectors, used between the geophone and the pre-amplifier, are often a source of trouble. A damaged or intermittant Microdot connector typically develops a signal having a type -11 waveform. Basically this signal is a high-amplitude, low-frequency random noise.

A signal waveform of the type -13, which exhibits a high-amplitude, low-frequency, decaying oscillation, is usually observed whenever the

hoist (mine elevator) is in operation. The operation of other heavy mining equipment is also found to generate such waveforms.

Occasionally, the general ambient background noise level appears to decrease for one or two seconds and then return to its original level as illustrated by the type -14 waveform. The reason for this behavior is unknown, but it is believed to be related to tape recorder tracking problems in the recording or playback modes rather than to actual changes in the background noise level.

5. Microseismic Source Location

5.1 General

The ability to locate the source of microseismic events is important when it is necessary to delineate areas of instability within rock structures and to evaluate the success of measures taken to stabilize such regions. Mapping progressive regions of instability and stress buildup becomes possible when source location techniques are employed.

The location of unstable regions in a geologic structure can be determined by several methods. A probing technique (Obert, 1941) has been employed which consists of moving a transducer to different locations in the structure, amplifying the received signals, monitoring the resulting signals with a set of headphones, and listening for the locations with the greatest amplitude and/or highest frequencies. This method is rather simple, but it provides one with a practical, although crude, means to locate the approximate source of observed microseismic events. Disadvantages are as follows.

(1) The risk of danger becomes increasingly higher as the region emitting the events is approached.

(2) The events may not be detected if the transducer is too far removed from the emission source.

(3) The accuracy of this method becomes poor if the events are occurring deep within a massive structure.

A second simple source location method involves the comparison of the signal amplitudes observed at a number of geophones, as a result of a single event. The geophone whose signal amplitude is the largest is then assumed to be nearest the microseismic source. This method provides only a very approximate source location and is dependent upon having one geophone relatively near to the source compared to the other geophones. The assumption that all waves are attenuated equally in all directions with increasing distance from the source must also be made for this method to work. Comparing the amplitudes of several geophones with their corresponding coordinates, one can better approximate the source location using this method.

A third technique, probably the most objective and accurate method of source location, is that of measuring relative microseismic arrival times at various geophones whose coordinates are known, and employing these arrival times in a set of equations to mathematically solve for the source location. This is generally known as the travel-time-difference method.

5.2 Details of travel-time-difference method

The fundamental problem in this source location method is to obtain the x, y, and z coordinates required to fix the source point (P_0) of the microseismic event in three-dimensional space (i.e., obtain a

hypocenter location for the source). Figure 19 illustrates an example for a five-geophone array surrounding the source.

The most direct approach is to use Flinn's method (1960) by considering the standard distance equation:

$$d_i = [(x_i - x)^2 + (y_i - y)^2 + (z_i - z)^2]^{1/2} \qquad \text{(Eq. 7)}$$

where d_i is the distance from the source to the i^{th} geophone: z, y, z are the unknown source coordinates; and x_i, y_i, z_i are the i^{th} geophone coordinates. To solve for x, y, and z, it is necessary to reduce equation (7) to three linearly independent equations in three unknowns.

The distance d_i from the source to i^{th} geophone can also be expressed by:

$$d_i = v_i(t_i - t) \qquad \text{(Eq. 8)}$$

where v_i is the wave velocity of a ray from the source to the i^{th} geophone; t_i is the arrival time (the time required for the wave to travel from the source to the i^{th} geophone); and t is the time when the event occurred, generally assumed to be 0 ms.

The right hand sides of equations (7) and (8) can then be equated as shown in equation (9).

$$[(x_i - x)^2 + (y_i - y)^2 + (z_i - z)^2]^{1/2} = v_i(t_i - t) \qquad \text{(Eq. 9)}$$

Provided v_i and t_i are known, data from three geophone stations are required to uniquely solve for x, y, and z. In practice, however, v_i and t_i are both unknown quantities as well. In some cases a mean value for v_i can be obtained from prior velocity measurements (e.g.,

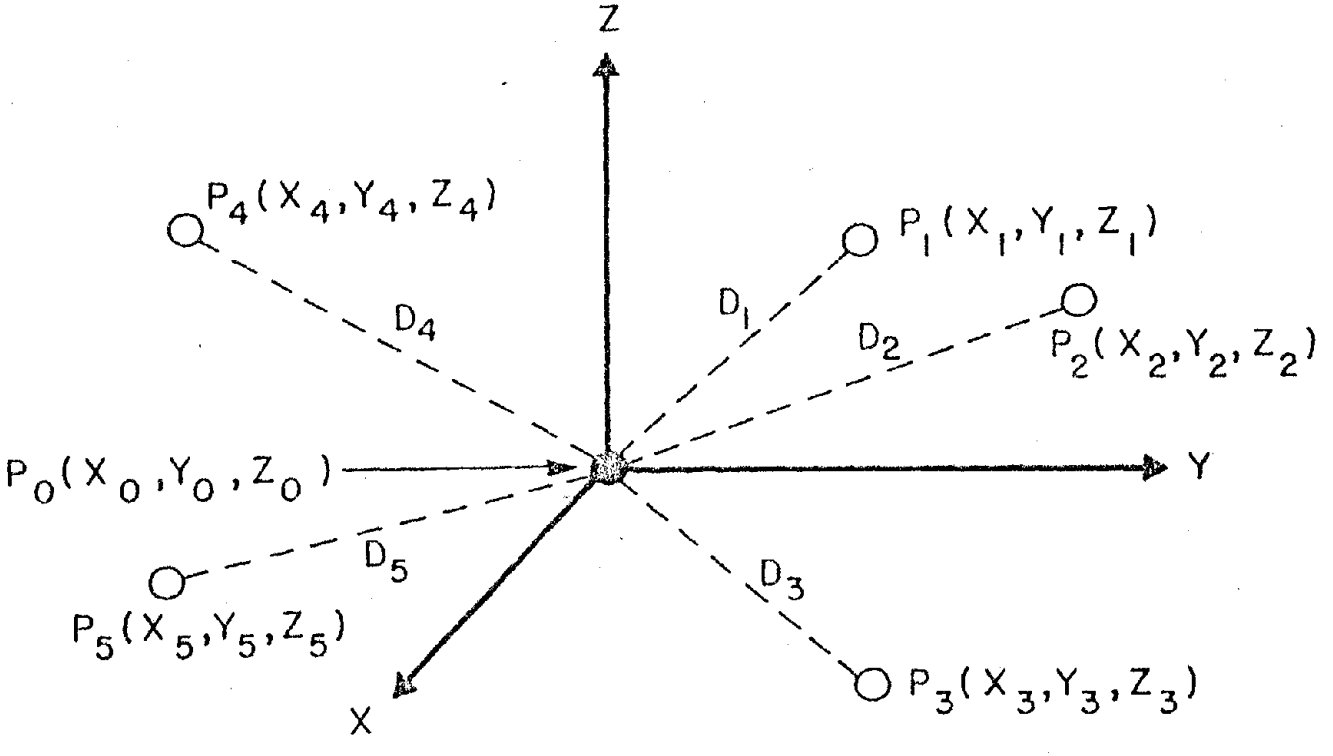

Figure 19. Geophone Array Geometry and Location of Observed Microseismic Event. (P_1 through P_5 are the Geophone Locations and P_0 is the True Source Location of the Detected Event.)

seismic surveys or sonic logging of suitably located boreholes); however, this is frequently not practical.

Continuing with the analysis, equation (9) is squared to obtain

$$(x_i - x)^2 + (y_i - y)^2 + (z_i - z)^2 = v_i^2(t_i - t)^2 \qquad \text{(Eq. 10)}$$

The errors of the first approximation x_o, y_o, z_o, and t_o are

$$\Delta x = x - x_o \qquad \text{(Eq. 11a)}$$

$$\Delta y = y - y_o \qquad \text{(Eq. 11b)}$$

$$\Delta z = z - z_o \qquad \text{(Eq. 11c)}$$

$$\Delta t = t - t_o \qquad \text{(Eq. 11d)}$$

Substituting equations (11) into equation (10) and neglecting all the squares of the errors, equation (12) is obtained.

$$(x_i - x_o)\,\Delta x + (y_i - y_o)\,\Delta y + (z_i - z_o)\,\Delta z - v_i^2(t_i - t_o)\,\Delta t = R_i \qquad \text{(Eq. 12)}$$

where

$$R_i = 1/2\,[(x_i - x_o)^2 + (y_i - y_o)^2 + (z_i - z_o)^2 - v_i^2(t_i - t_o)^2] \qquad \text{(Eq. 13)}$$

This results in n equations for the four errors of Δx, Δy, Δz, and Δt, and provided that n is greater than four, the problem is overdetermined.

One method to solve these n equations to obtain a best average solution is by way of least squares in which a set of deltas (errors) are determined which minimize the sum of the squares of the station residuals.

Equation (12) can be expressed in its matrix notation form as

$$A \Delta = B \qquad \text{(Eq. 14)}$$

where Δ is a column vector with components (Δx, Δy, Δz, Δt), B is a row vector with components (R_1, R_2, R_3, . . . R_n), and the matrix A is as follows:

$$A = \begin{vmatrix} x_1 - x_o & y_1 - y_o & z_1 - z_o & -v_1^2(t_1 - t_o) \\ x_2 - x_o & y_2 - y_o & z_2 - z_o & -v_2^2(t_2 - t_o) \\ x_3 - x_o & y_3 - y_o & z_3 - z_o & -v_3^2(t_3 - t_o) \\ x_n - x_o & y_n - y_o & z_n - z_o & -v_n^2(t_n - t_o) \end{vmatrix} \qquad \text{(Eq. 15)}$$

The vector B can be readily solved, but due to the high relative measurement errors involved, particularly in the arrival times, the solution obtained will not be well behaved.

To overcome this problem, equation (14) may be premultiplied by A's transpose, namely A^t

giving $$C \Delta = D \qquad \text{(Eq. 16a)}$$

where $$C = A^t A \qquad \text{(Eq. 16b)}$$

and $$D = A^t B \qquad \text{(Eq. 16c)}$$

where matrix C is a positive definite symmetric 4 x 4 matrix. Multiplying the inverse of matrix C on both sides of equation (16a), the

solution becomes

$$\Delta = C^{-1} D = (A^t A)^{-1} A^t B \qquad \text{(Eq. 17)}$$

which will be well behaved and will be the best solution when using the method of least squares.

The Δ matrix is solved by Gauss elimination. This Δ matrix is then added to x_o, y_o, z_o, and t_o to obtain a better approximation solution. The process is repeated until a convergence criterion is reached. In some cases the convergence criterion is too small and the solution will not converge to the selected tolerance. For these cases a maximum number of iterations is employed to terminate the process.

A computer program, which is based on the foregoing method, was available (Harding, 1970; Harding and Rothman, 1974), and this was modified for the current microseismic study. Details on this program are given in Appendix B.

5.3 Conditions required for application of the travel-time-difference method

This section is concerned with the conditions necessary for locating the source of underground microseismic events detected by a number of geophones arranged in a planar array. In general, the event must meet the following conditions.

(1) The first arrivals must be direct waves (P-waves).

(2) Suitable first arrivals must be observed by at least five geophones.

(3) The P-wave velocity from the source of each geophone must be known.

This method requires that the location (x, y, z) of each geophone station be accurately known. An initial guess for the source location must be provided, although the solution is usually insensitive to the initial guess. The geologic media through which the microseismic signal passes is generally considered to be homogeneous and continuous. The velocity model employed however may be isotropic, anisotropic, or unique. The unique velocity model assumes that each geophone location has associated with it a unique velocity. This velocity is determined by placing a seismic source (e.g., a blast) at a known location underground, computing the difference between this source and each geophone, measuring the total travel-time from the source to each geophone, and dividing the total distance by the total travel-time to obtain an associated velocity value for each geophone. This model, although difficult to justify theoretically, has been used successfully by other workers (Blake, Leighton, and Duvall, 1974).

5.4 A method for approximating unique velocities

Provided that a geophone array whose coordinates are known, a blast having known coordinates, and the relative travel-times of n geophones are available, an approximate unique velocity value can be established for each geophone (Blake, Leighton, and Duvall, 1974).

The vector distances "d_i" between the blast and each geophone location are computed as follows:

$$d_i = [(x_i - x_o)^2 + (y_i - y_o)^2 + (z_i - z_o)^2]^{1/2} \qquad \text{(Eq. 18)}$$

where d_i is the distance from the blast location to the i^{th} geophone;

x, y, z are the i^{th} geophone coordinates; and x_o, y_o, and z_o are the blast location coordinates.

The geophone having the smallest travel-time is referred to as the reference geophone and has the subscript "r." The reference distance "d_r" is subtracted from each geophone distance to obtain distance differences "Δd_i" as shown

$$\Delta d_i = d_i - d_r \qquad \text{(Eq. 19)}$$

The reference travel-time "t_r" is also subtracted from each geophone travel-time "t_i" to obtain time differences "Δt_i" as shown

$$\Delta t_i = t_i - t_r \qquad \text{(Eq. 20)}$$

An initial velocity approximation "v_{ai}" for each geophone is then obtained by dividing the distance differences "Δd_i" by their corresponding travel-time differences, namely:

$$v_{ai} = \Delta d_i / \Delta t_i \qquad \text{(Eq. 21)}$$

A blast-to-reference geophone (SRG) travel-time "t_{bi}" is next computed for each geophone. This "t_{bi}" is determined by dividing the total distance "d_i" between each geophone and blast by the initial velocity approximation "v_{ai}" and then subtracting the time differences "t_i" from this result as follows:

$$t_{bi} = (d_i / v_{ai}) - \Delta t_i \qquad \text{(Eq. 22)}$$

All the SRG travel-times "t_{bi}" are next summed to obtain:

$$t_s = \sum_{i=1}^{m} t_{bi} \qquad \text{(Eq. 23)}$$

where m is the number of geophones excluding the reference geophone. The average SRG travel-time "t_a" is computed by dividing the sum of the SRG travel-time "t_s" by the number of geophones, excluding the reference geophone, as follows:

$$t_a = t_s/m \qquad \text{(Eq. 24)}$$

Finally, the compensated velocity "v_{ci}" is calculated by dividing the distance "d_i" from the blast to each geophone by the average SRG travel-time "t_a" and the time difference "Δt_i" of each geophone.

$$v_{ci} = d_i/(t_a + \Delta t_i) \qquad \text{(Eq. 25)}$$

Ideally "t_a" is as small as possible for best results which implies that the reference geophone should be as near the blast as possible. Moreover, these compensated velocities are valid only in the general region of the blast.

5.5 Determining estimated arrival times

The absolute or total travel-time of any stress wave to propagate from its source to a given geophone station can be roughly estimated by following the steps listed below. Total travel-times are estimated only to make the arrival time data appear realistic. These times are used in the travel-time-difference method to obtain source locations, although the method actually requires only the travel-time differences.

To estimate total travel-times, the following steps must be carried out.

(1) The geologic medium is assumed to be homogeneous, elastic, and continuous.

(2) A 10,000 fps isotropic wave propagation velocity value is assumed unless a better velocity value for the field site is known.

(3) The general area where the source is believed to originate is estimated.

(4) The three-dimensional vector distance between the estimated source location, and the nearest geophone (referred to as the reference geophone) is calculated.

(5) The vector distance obtained in step (4) is divided by the propagation velocity given in step (1) to obtain the total travel-time for the reference geophone.

(6) The nearest time line to the "break point" (BP) of the reference geophone is found on the oscillogram, as illustrated by Figure 20. BP, the point at which the microseismic signal is first detected, may be observed by noting an amplitude, frequency, and/or phase change in the microseismic signals. The nearest time line is defined as the reference time line (RTL) and is assigned the total travel-time value as computed in step (5).

(7) The BP's associated with the other geophones are then measured with respect to the RTL determined in step (6). These BP's may be measured by using an engineer's scale or by using a digitization routine in conjunction with the Hewlett Packard 9810 calculator, digitization board, and digitization module as shown in Figure 21. The value of the RTL is added to the value of the BP time to obtain the total travel-time for the event to propagate to a particular geophone. In

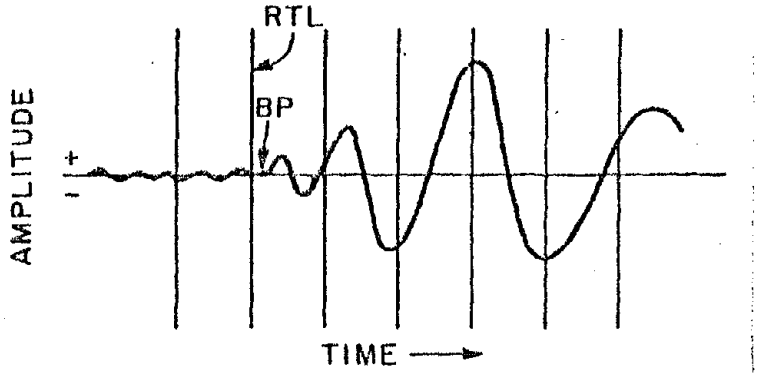

(a) BP Occurring After the RTL

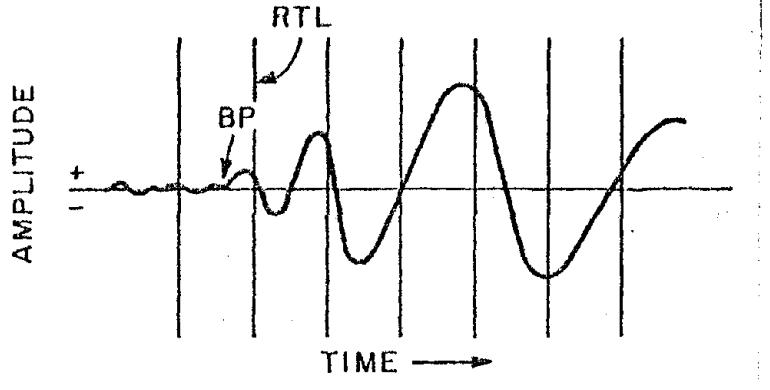

(b) BP Occurring Prior to the RTL

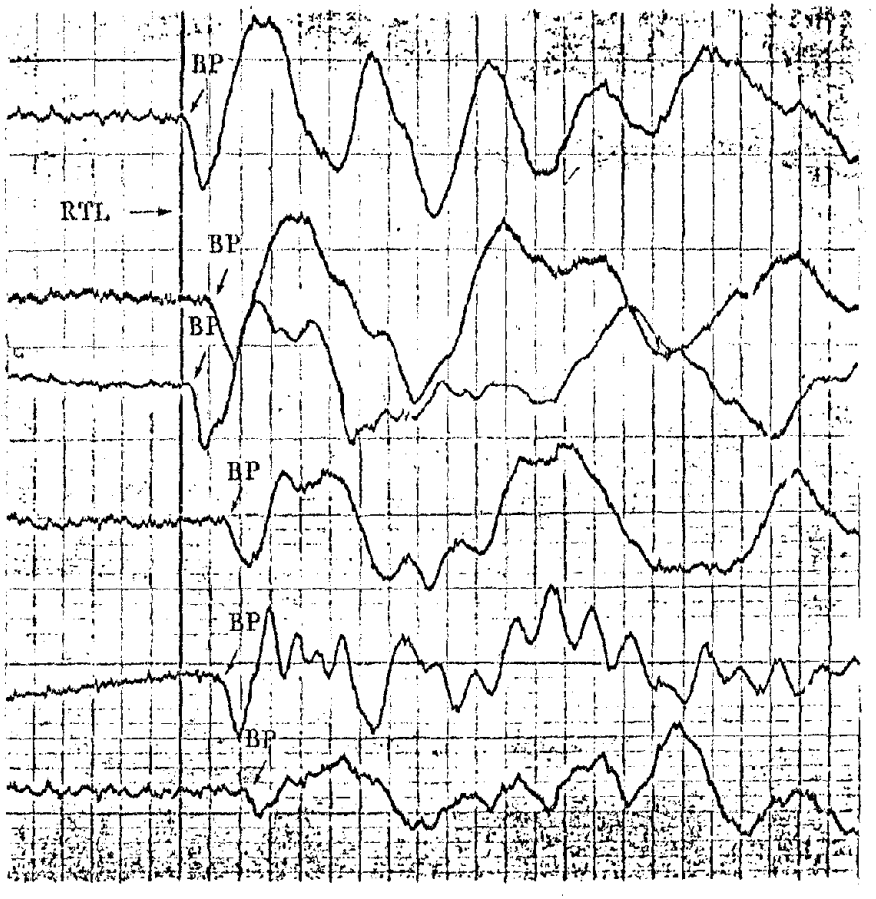

(c) Actual Microseismic Signal Showing BP's Occurring After the RTL

Figure 20. Typical Microseismic Signal Showing Break Points (BP) and Reference Time Lines (RTL).

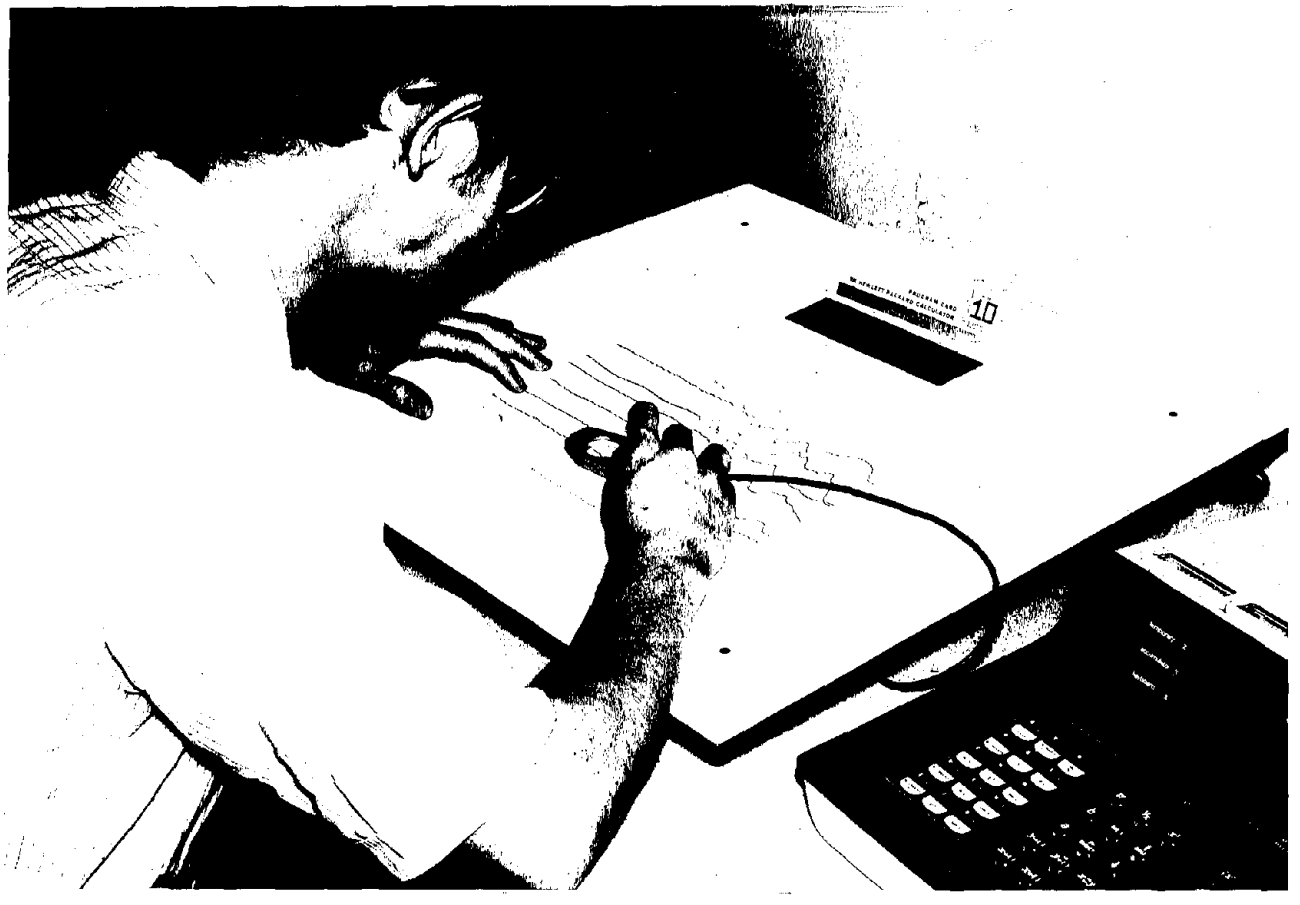

Figure 21. Measuring Break Points Using a Calculator and Digitization Board.

Dr. H. Reginald Hardy, Jr.
Professor and Chairman,
Geomechanics Section

these cases where the BP occurs before the RTL, the BP time is considered negative and consequently the total travel-time will be less than the reference travel-time.

5.6 Source location errors

Errors in source location arise from a number of factors including:

(1) accuracy of the velocity model utilized,

(2) ability to time and read arrival times,

(3) transducer array geometry,

(4) array size,

(5) errors in transducer location survey,

(6) location of the source relative to the array, and

(7) depth of the source.

Velocity -- Seismic velocity is dependent upon many factors including rock type, porosity, and density of the rock matrix, temperature, pressure, stress levels in the rock (e.g., velocity increases with increasing depth), density of the fluid in the pores of the rock, and the dispersive properties of the rock itself (e.g., each frequency component in a seismic wave travels at its own velocity). Velocity, furthermore, may not necessarily be the same in all directions. Moreover, for a longwall coal mining operation, there appears to be at least three regions having different velocity characteristics, namely:

(1) the gob or fractured region behind the longwall face,

(2) the immediate region around and above the longwall face, and

(3) the virgin region ahead of the longwall face.

Since the longwall operation is a dynamic process as the longwall face progresses, the three velocity region follow it. Hence, as the array

of geophones remains fixed, the rather complex three-dimensional dynamic velocity model associated with the structure under study is continually changing its characteristics as the coal is being mined.

Some means of obtaining an appropriate velocity value for each geophone station is needed to construct such a velocity model. Most researchers believe that underground blasts occurring at known locations and times should provide the best velocity data. Such blasts should be monitored as often as economically possible. Velocities obtained should be compared with those from previous blasts at or near the same location. It should be noted that in the often complex strata associated with a mining situation, the actual seismic propagation paths are unknown, but for computational purposes these are assumed to be the most direct paths between the source and the associated geophones.

Arrival time -- The ability to determine accurately arrival times is governed by the signal-to-noise ratio, the frequency of the waveform, and the timing system (i.e., the accuracy of the tape recording and playback speeds, the visicorder speed, and the timing lines generated by the visicorder). At times, either the signals are of such a low-frequency that the actual "first break" is spread out over several milliseconds, or the noise levels are so high that the first arrival is obscured on one or more geophones. As mentioned earlier, high-frequency noises can be minimized by using a filter. Additionally, human judgment is invaluable in discerning signal from noise.

Transducer array geometry and size -- The effect of array geometry and location of the event relative to the array are discussed in detail in Appendix C. Each array has its own error boundaries and,

consequently, every array under consideration should be analyzed before using in the field. Generally, as the source moves away from the center of the array, the source location error increases. In a like manner, as the depth of the event increases, the location error increases (assuming a planar array on surface). The size of the array influences the location error as follows.

(1) Source locations are very accurate for a small array provided that they originate within the boundaries of the array.

(2) Source locations are less accurate for a large array, but a greater area may be monitored.

Transducer location survey -- In the present study, it is felt that the transducer locations were accurate to within ±5 ft in the horizontal directions since the surveyed array was correlated with an aerial photographed map encompassing the same area. Geophone elevation data were obtained from the depth of the geophones in the hole and the hole collar elevation. Hole depths were estimated from the associated driller's log and verified by the amount of geophone cable remaining outside the installation hole. Surface elevations were determined by using a monument to tie the localized elevation survey to a mine map of the general area. It is the authors' opinion that all transducer location errors were negligible with respect to other sources of errors mentioned earlier.

6. Event Activity Rate

In order to quantify the rate of occurrence of microseismic events, a parameter termed the event activity rate was evaluated. The basic method for establishing this rate was to count the number of detected

microseismic events occurring within each span of 100 ft of recording tape (approximately 5 minutes and 20 s). For a specific signal to be considered a countable event, the following criteria had to be satisfied.

(1) At least four geophones had to detect the signal within a certain time interval. For this longwall study, a time interval of 100 ms was considered adequate.

(2) The signal had to resemble a decaying sinusoidal wave of at least two cycles in duration. This requirement provided a means for elimination of most electrical transients.

(3) Signals with near simultaneous detection (within 1 ms) on four or more geophones were rejected, since each behavior was characteristic of purely electrical disturbances.

Once a specific signal was considered an event, three categories of such events were established based on signal amplitude, namely:

(1) level-1 events: events having less than a 2:1 signal-to-noise ratio (S/N),

(2) level-2 events: events having a S/N of between 2:1 and 5:1, and

(3) level-3 events: events having a S/N greater than 5:1.

For a specific event, certain geophones were found to have higher S/N's than others. Consequently, an average S/N for all the geophones detecting the event was employed. The number of events observed in each of the three levels of amplitude were then plotted in histogram form as shown on Figure 22, along with the total number of events (sum of the level-1, level-2, and level-3 events) per unit time. In Figure 22, it is noted that the largest number of events detected were those of the level-1 type, followed by the level-2 and level-3 events, respectively.

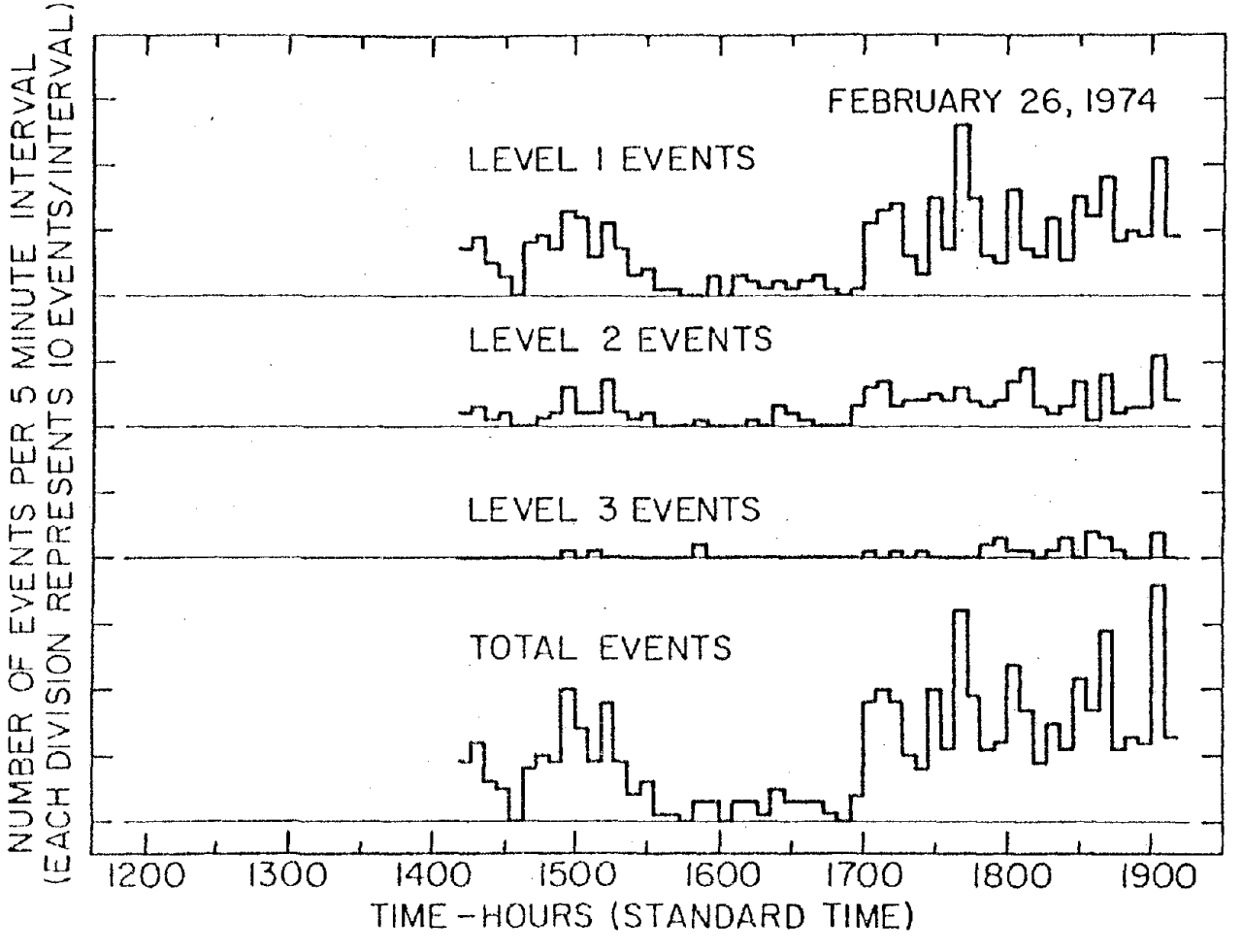

Figure 22. Typical Event Activity Rate Histogram.

VII. RESULTS

1. General

During the East B-4 longwall study a total of 17 field trips were made to this site in order to monitor microseismic activity. This site was instrumented with an array of 15 deep burial geophones in the Fall of 1973. Figure 23 shows an expanded view of the East B-4 site, with the 15 geophone locations (N-1 through N-15) and the coal seam elevations (1,320 ft to 1,340 ft above sea level). These locations were established on October 16, 1973. Appendix A lists the coordinates of the transducer locations. Commercial augering of the holes at these locations was performed on October 22 and 23, 1973 by the Tinney Drilling Company. Geophones were installed and grouted in place immediately after each hole was drilled. On October 26, 1973, after the grout was thoroughly set, the open section of each borehole was completely filled with sand to minimize the accumulation of ground water.

Microseismic monitoring of the longwall was initiated on November 28, 1973 and was completed on August 21, 1974. A graphical record of East B-4 longwall face advance during this period is shown in Figure 24. A good rate of advance can be observed from January to the end of February, at which time the mine became plagued with bad roof conditions and periods of work stoppage until the middle of July. Mining of the longwall panel was finally completed on July 25, 1974.

Measurements made during the 17 field trips to the East B-4 longwall site served three objectives:

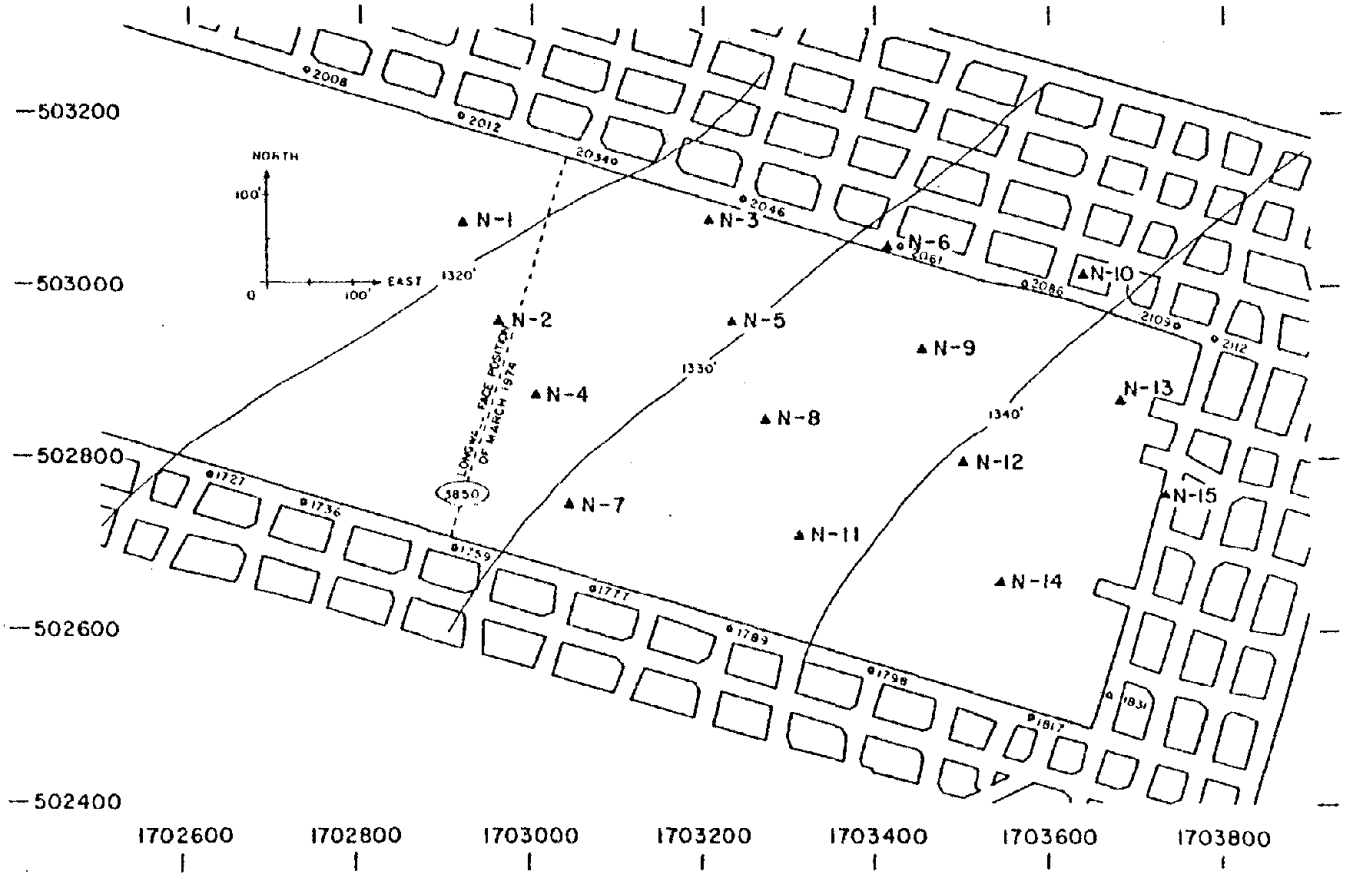

Figure 23. East B-4 Longwall Site Showing Geophone Stations and Surface Elevations.

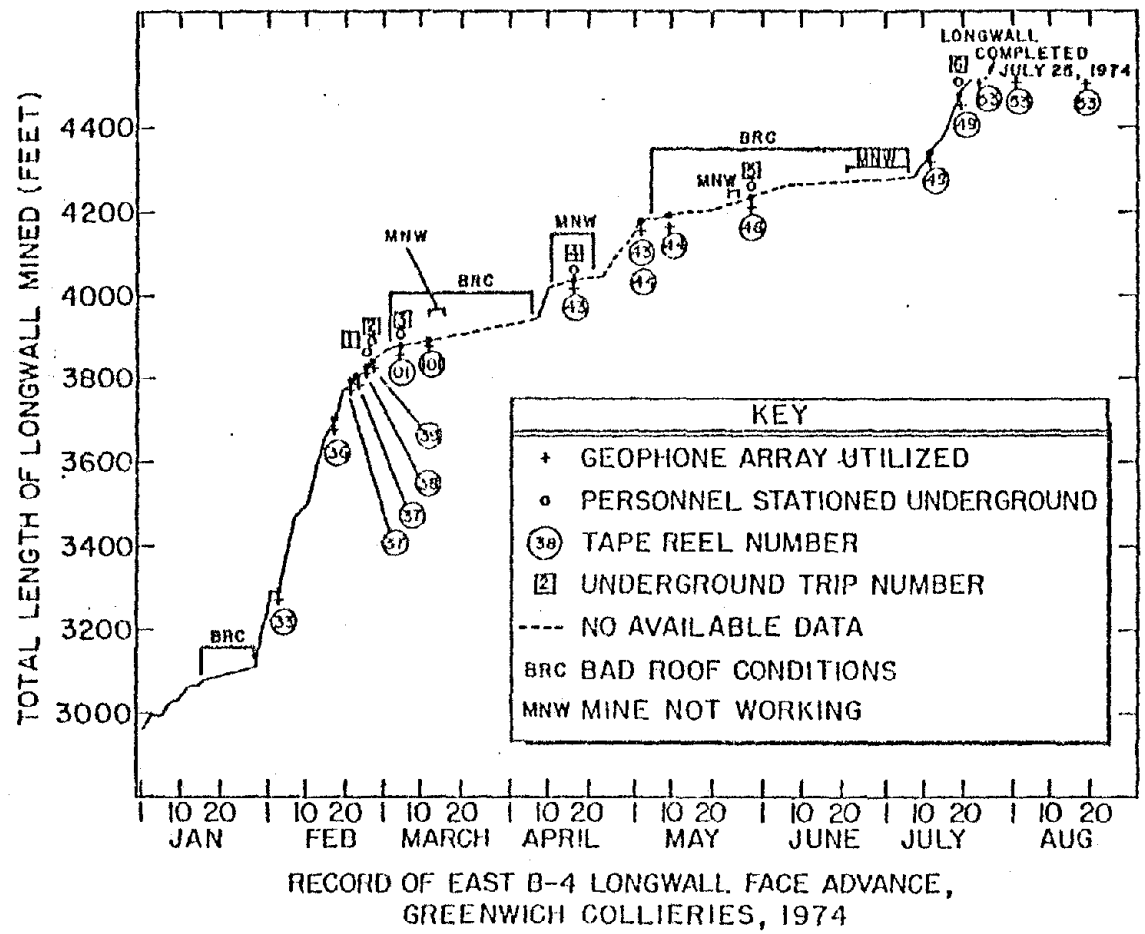

RECORD OF EAST B-4 LONGWALL FACE ADVANCE, GREENWICH COLLIERIES, 1974

Figure 24. Face Advance of the East B-4 Longwall.

(1) to establish the feasibility of using near-surface microseismic arrays to monitor underground mining activity,

(2) to provide field data for critical evaluation of microseismic source location techniques, and

(3) to provide microseismic field data typical of a longwall coal-mining operation under a variety of mining conditions.

This report is concerned mainly with the first and second objectives of these field measurements, although correlation of microseismic data with mining conditions are considered briefly in Chapter IX.

2. Feasibility of Surface Detection of Underground Events

2.1 General

Beginning November, 1973, and continuing through August, 1974, microseismic activity was monitored from surface in the proximity of the East B-4 longwall. The following sections of this chapter summarize the findings for a variety of longwall positions and operations. Table 1 gives the dates, the recording intervals, tape reel numbers, tape footages, and the sets of geophones utilized while recording microseismic data. In addition, this table lists the longwall position horizontally with respect to geophone station N-1, the total vector distance between the longwall face and N-1, and the maximum vector distance between the longwall face and the geophone station furtherest removed from the face.

TABLE 1

Brief Summary of Typical Microseismic Monitoring Sessions

Date	Recording Interval	Tape Reel	Footages	Geophones (N-)	Longwall Position	Total Distance From N-1	Distance From Furtherest Geophone
Feb. 18	13:27 - 16:21	36	101-3200	1 2 3 4 5 6 7	50' West[a]	433'[b]	N-6: 690'[b]
Feb. 18	17:06 - 17:36	36	3200-3750	8 9 10 11 12 14 15	50' West	433'	N-15: 1025'
Feb. 18	17:41 - 18:11	36	3750-4300	8 9 10 11 12 13 15	50' West	433'	N-15: 1025'
Feb. 26	14:07 - 15:58	38	10-2150	1 2 3 4 5 6 7	65' East	435'	N-6: 605'
Feb. 26	16:01 - 19:01	38	2160-5500	1 2 3 4 5 6 7	65' East	435'	N-6: 605'
Feb. 27	13:11 - 15:46	39	10-2900	1 2 3 4 5 6 7	75' East	436'	N-6: 605'
Feb. 27	16:06 - 18:56	39	2910-6060	1 2 3 4 15 6 7	75' East	436'	N-15: 917'
Apr. 17	12:18 - 13:49	43	10-1700	1 2 3 4 9 6 7	275' East	510'	N-9: 519'
Apr. 17	15:38 - 15:48	43	1710-1900	8 10 11 12 13 5 15	275' East	510'	N-15: 746'
Apr. 17	16:05 - 17:32	43	1910-3530	14 10 11 12 13 5 15	275' East	510'	N-15: 746'
Aug. 2	11:28 - 14:35	53	3311-6615	1 7 9 10 11 13 14	840' East	944'	N-1: 944'
Aug. 21	11:59 - 15:02	32	1430-4830	1 7 9 10 11 13 14	840' East	944'	N-1: 944'

(a) Longwall position measured horizontally from geophone station N-1 perpendicularly to longwall face.

(b) Longwall was assumed to be 430 ft below ground surface for computational purposes (vector distance).

2.2 Longwall face more than 1,000 ft west of geophone array

Initial monitoring of microseismic activity was conducted during the months of November and December, 1973, and all 15 geophones being utilized for a minimum of 30 minutes. At this time, geophone station N-1, which was the transducer nearest to the longwall face, was more than 1,000 ft east of the face. No positively identifiable microseismic activity was detected on any of the geophones during a total of 3-1/2 hours of recording. The equivalent ambient background particle velocities observed were 150 to 200 μips, and these were mainly associated with 60 Hz signals probably due to electrical power sources.

2.3 Longwall face 50 ft west of geophone array: mine operating--good longwall conditions

On February 18, 1974, nearly three hours of microseismic data were recorded from 13:27 to 16:21 utilizing geophones N-1 through N-7. During this time all mining operations were proceeding normally. The face was located approximately 50 ft west and 430 ft below geophone N-1 as shown in Figure 25.

This was the first monitoring session in which microseismic events were detected by the East B-4 array. The events themselves were of various amplitudes, frequencies, and durations. Each generally resembled a decaying sinusoidal waveform comprised of various frequency components. Typical microseismic activity is illustrated on Figure 26. A time-expanded version of the first two events are presented on Figure 27. Note that all geophones detected the events, which were most probably generated by either rock falls behind the chocks, bed separations, or other fracturing occurring in the vicinity of the face.

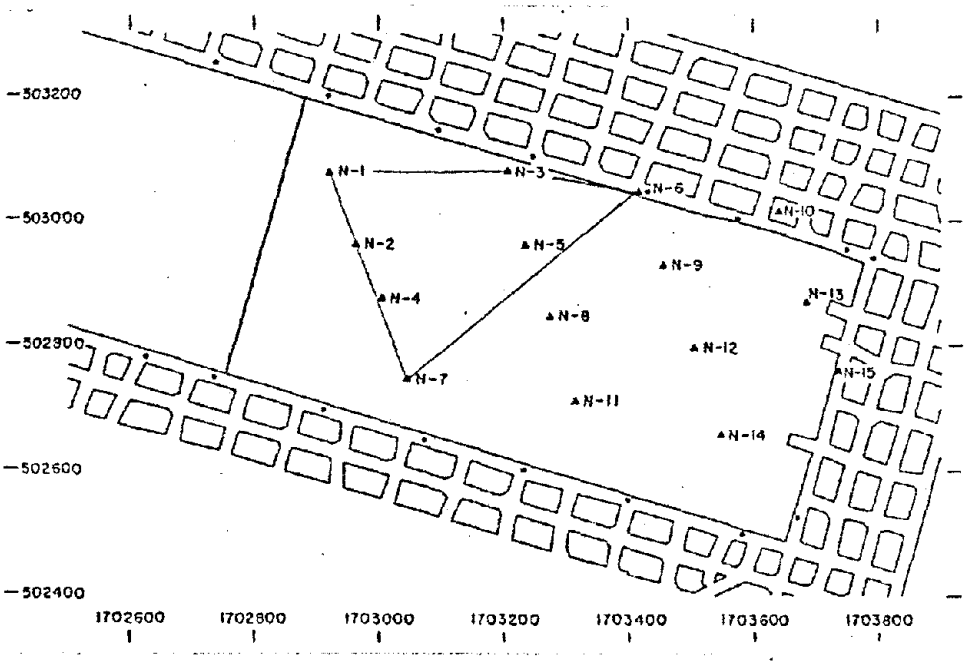

Figure 25. Location of Longwall Face and First Geophone Array Utilized: February 18, 1974.

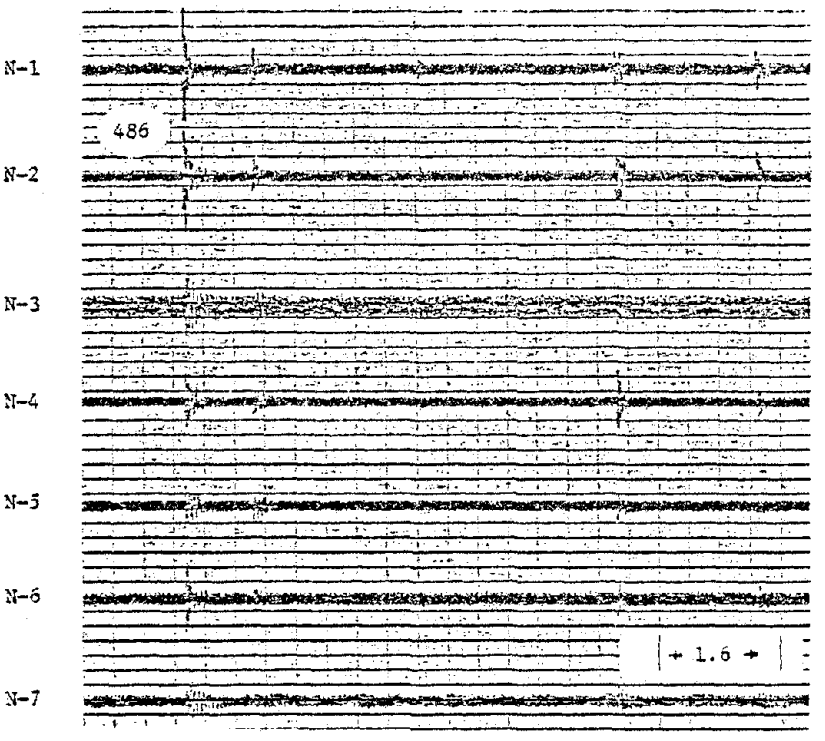

Figure 26. Typical Microseismic Events (36-1432), February 18, 1974. [Horizontal Scale: Time (s); Vertical Scale: Particle Velocity (μips/10 divisions).]

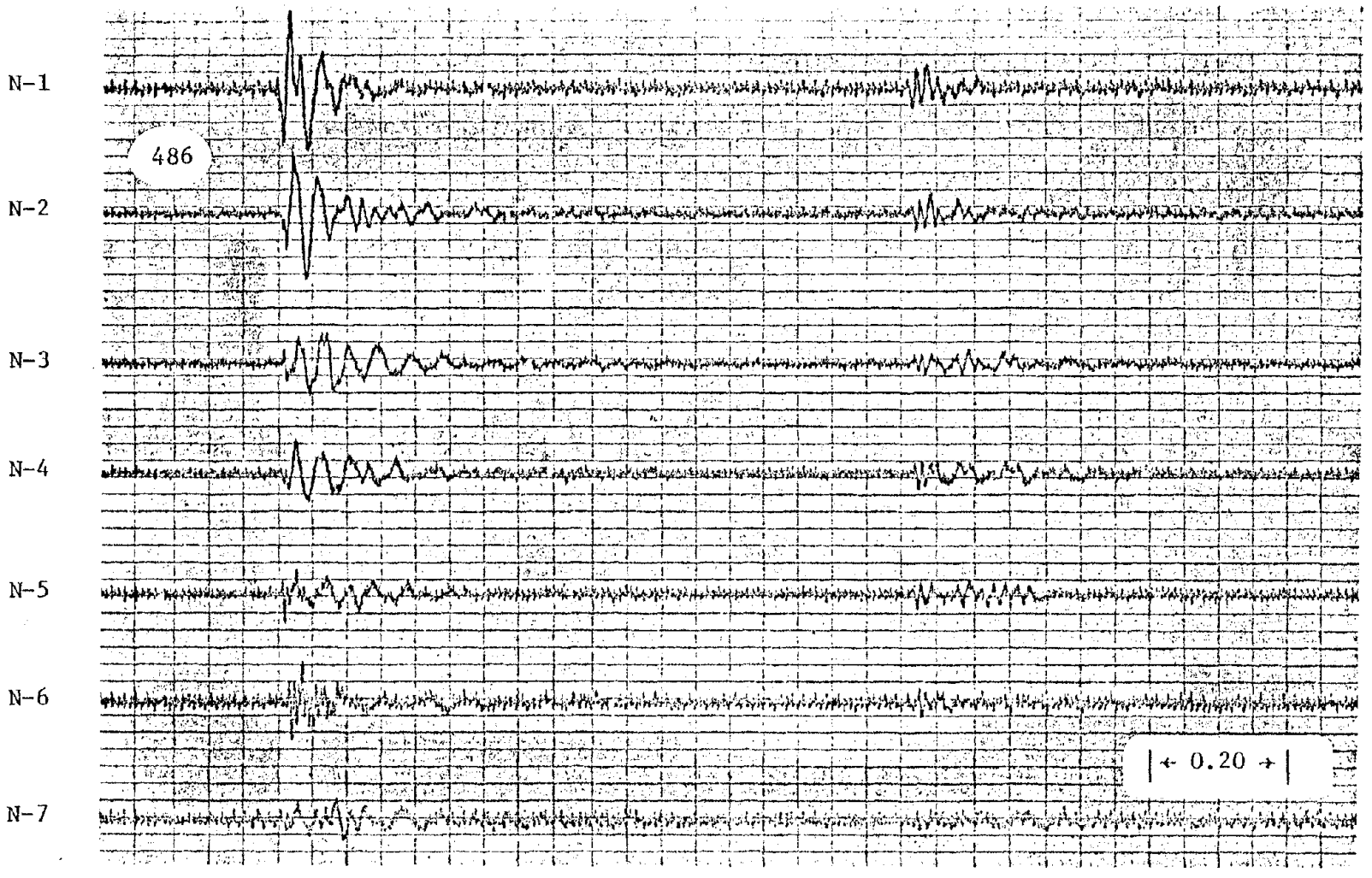

Figure 27. Event (36-1432), February 18, 1974--Time-Expanded. [Horizontal Scale: Time (s); Vertical Scale: Particle Velocity (μips/10 divisions).]

In Figure 27, the particle velocities ranged from 100 to 400 µips for the event on the left and 50 to 125 µips for the event on the right. Frequencies ranged from 20 to 80 Hz, with the highest frequencies usually arriving first. [As mentioned earlier, a simple method for obtaining frequencies is to measure the time interval between two peaks and calculate the reciprocal of this interval.] Station N-6 signals nearly always had a frequency content of 160 to 180 Hz initially.

Figure 28 shows the rate of microseismic activity for the day. As the longwall operation was progressing normally, the averate rate was 1.5 events per minute (epm) from 13:30 to 15:00 hours. A peak rate of more than 6 epm occurred at 14:45. An abrupt drop in the rate was observed from 15:00 to 16:00 hours. This period encompassed the shift change when operations were temporarily halted. Event activity increased rapidly again after 16:00 when the next crew of miners started to work.

Much of the time, the events were sufficiently separated to be considered individual events but, in a few instances, they appeared to overlap or be superimposed on one another as shown in Figure 29. "Rumblings" (higher than average background noise for a duration of more than 2 s) were occasionally observed as is illustrated in Figure 30. Possible origins of the rumblings included the coal shearer cutting hard rock, a machine drilling holes in the mine roof, aircraft, vehicular traffic, or numerous small microseismic events combining to form a rumbling effect. The normal frequency was a relatively constant 100 Hz and particle velocities were 50 to 100 µips.

Figure 31 shows an infrequently detected low-amplitude (50 to 100 µips) low-frequency (12 to 20 Hz) event of unknown cause or origin.

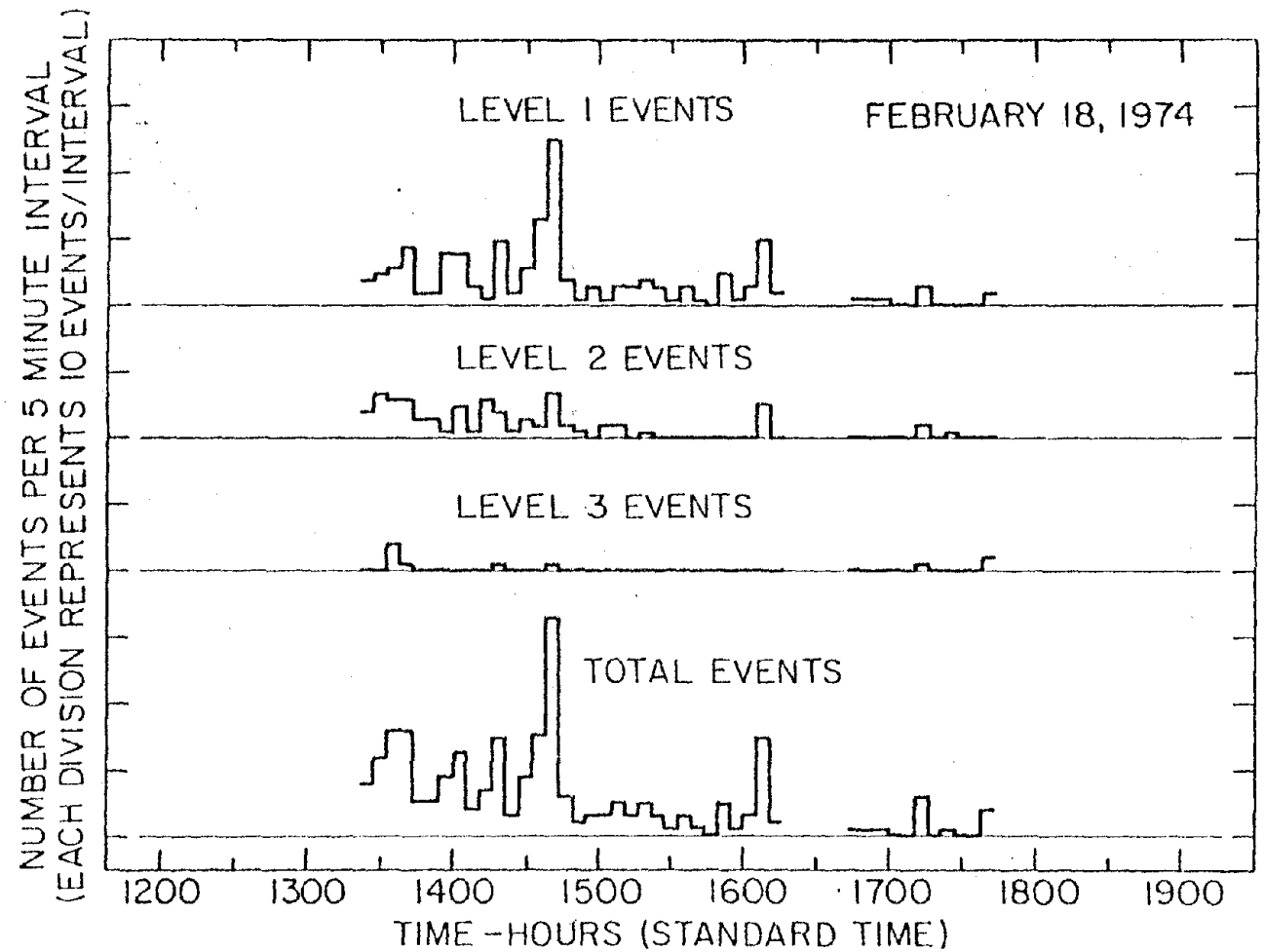

Figure 28. Event Activity Rate Histogram: February 18, 1974.

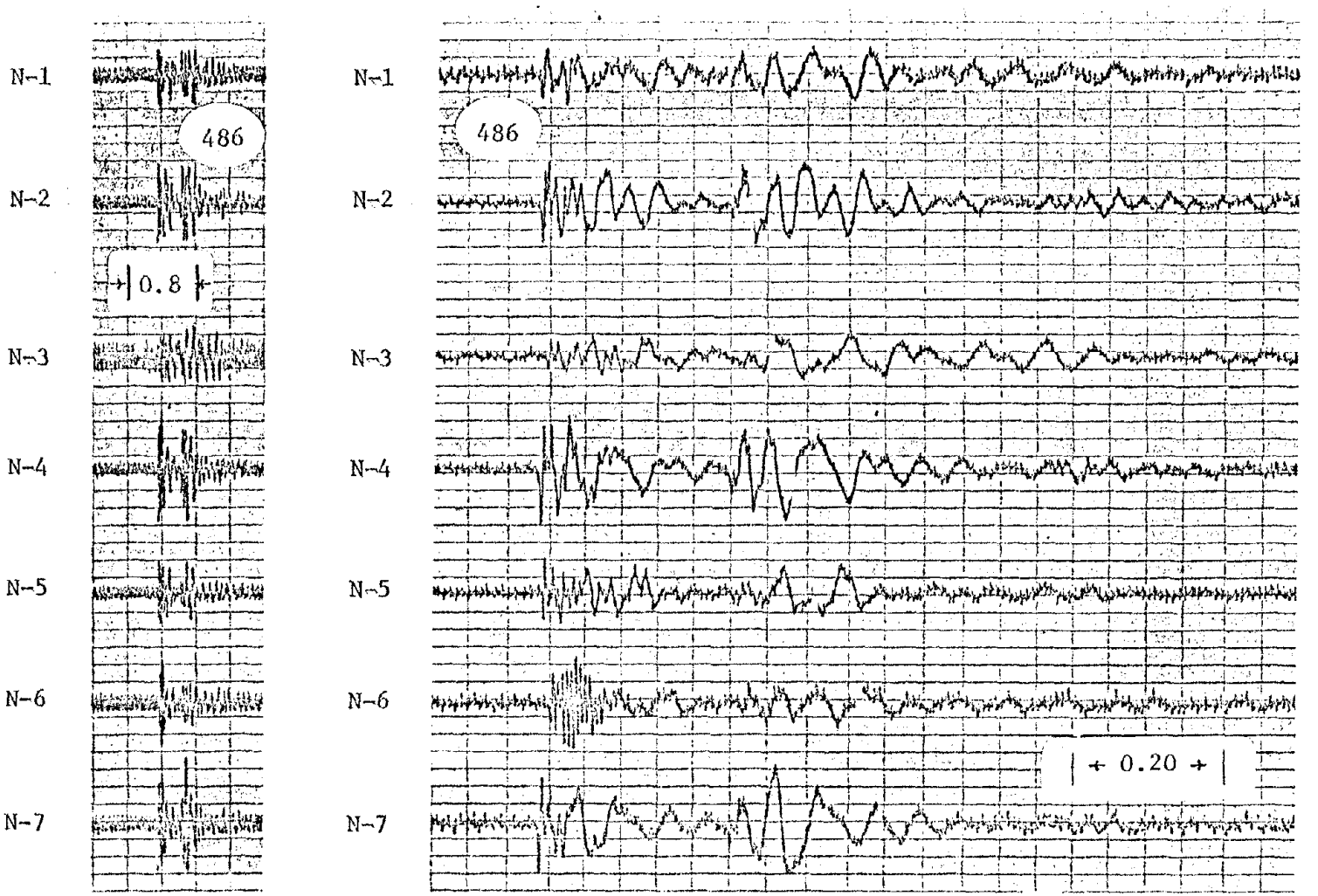

Figure 29. Event (36-1000), February 18, 1974. [Horizontal Scale: Time (s); Vertical Scale: Particle Velocity (μips/10 divisions).]

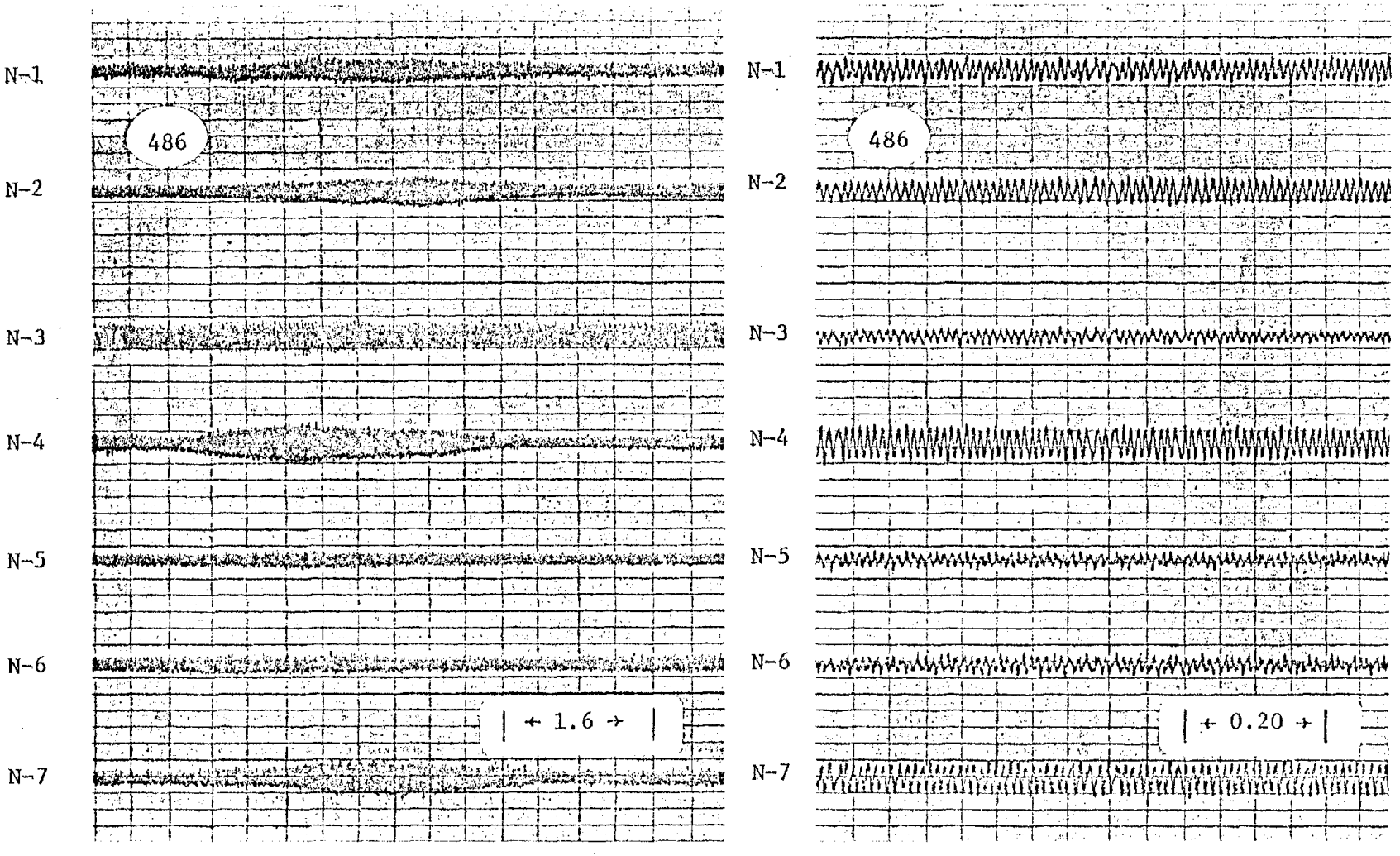

Figure 30. Event (36-1842), February 18, 1974. [Horizontal Scale: Time (s); Vertical Scale: Particle Velocity (μips/10 divisions).]

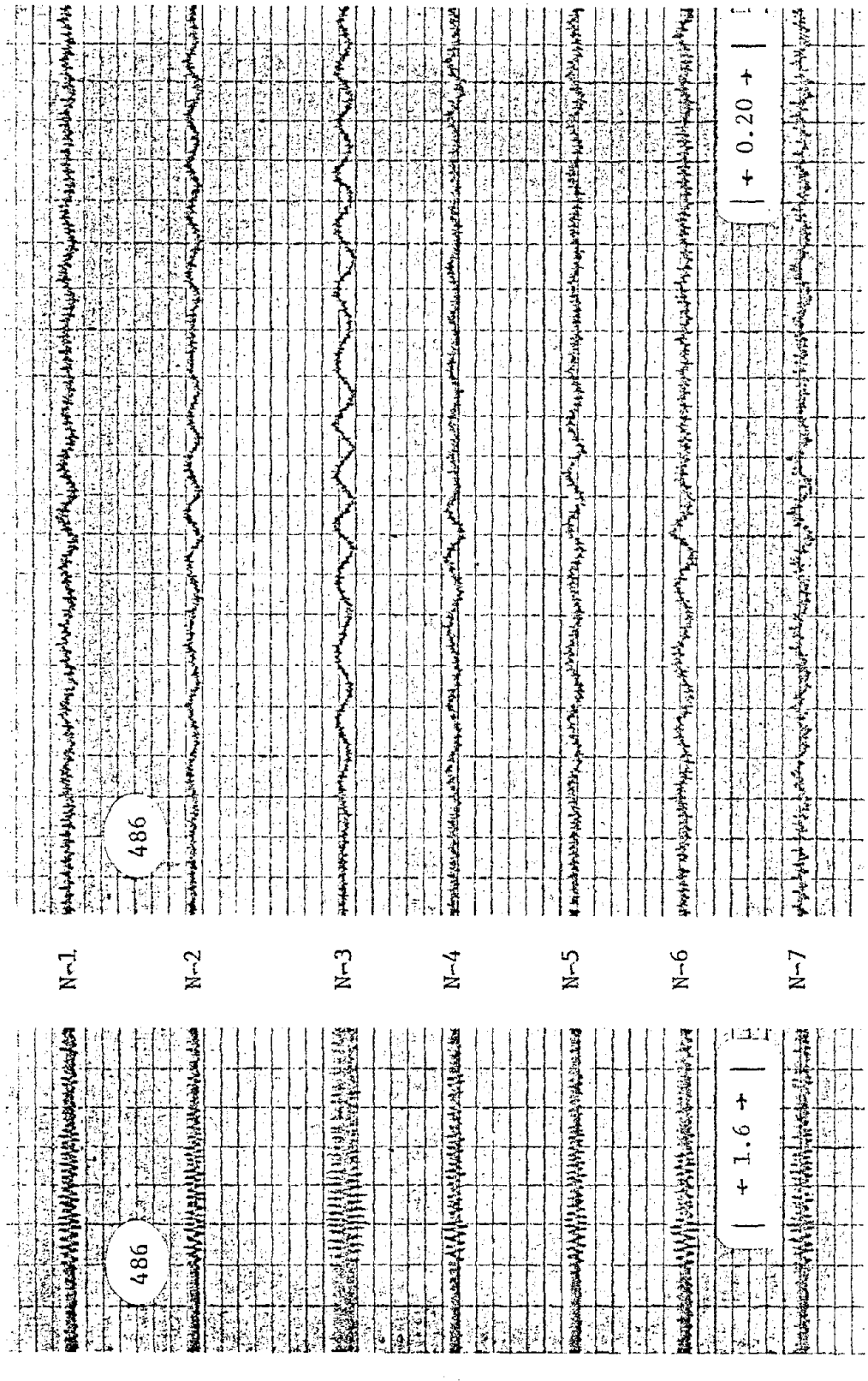

Figure 31. Event (36-2844), February 18, 1974. [Horizontal Scale: Time (s); Vertical Scale: Particle Velocity (μips/10 divisions).]

Stations N-3 and N-6 appeared to have the largest particle velocities as well as having the first arrival times. This suggested that the event originated outside the array, north of the longwall panel.

Using a second array on February 18, which is shown in Figure 32, a total of three level-3 events were detected. One such event is given in Figure 33. Its time-expanded version is given in Figure 34. This particular event, 36-4207, was believed to be either a major roof fall in the gob area, due to the high particle velocities (200 to 300 μips) at distances between 600 and 1,000 ft, or a fracture induced ahead of the face. Frequencies ranged from 50 to 200 Hz initially and then dropped to approximately 20 Hz. Another event, 36-3797, as shown in Figure 35, being of high-amplitude (more than 300 μips) and low-frequency (5 to 200 Hz) occurred 15 minutes before event 36-4207. The first arrivals were initially detected by N-15, N-14, and N-10, which indicated that this event originated east or southeast beyond the perimeter of the array.

2.4 Longwall face under geophone array: mine operating--good longwall conditions

Background data were recorded using geophones N-1 through N-7, as shown in Figure 36, for five hours (14:07 to 19:01) on February 26. For this day's monitoring, a ground rod was driven 7 ft into the ground and was connected to the grounding terminal on the side of the microseismic monitoring facility. This grounding scheme reduced the peak-to-peak electrical background noise at the system output from 1.5 V to 0.6 V and was used on all subsequent field trips.

Several typical microseismic events are presented in Figure 37, with the time-expanded version of the largest event (38-4894) given in

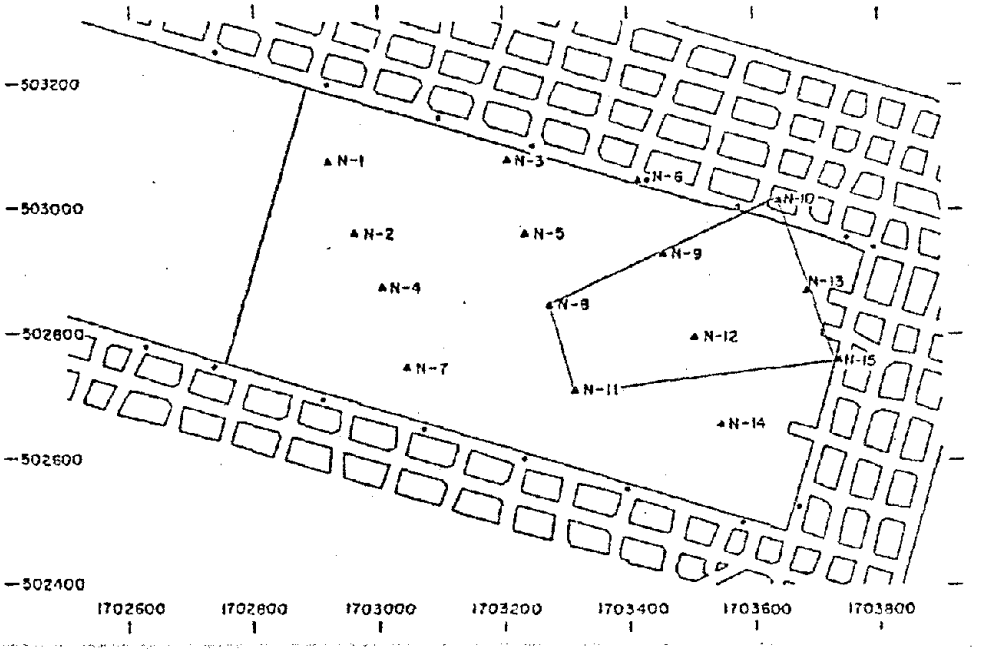

Figure 32. Location of Longwall Face and Second Geophone Array Utilized: February 18, 1974.

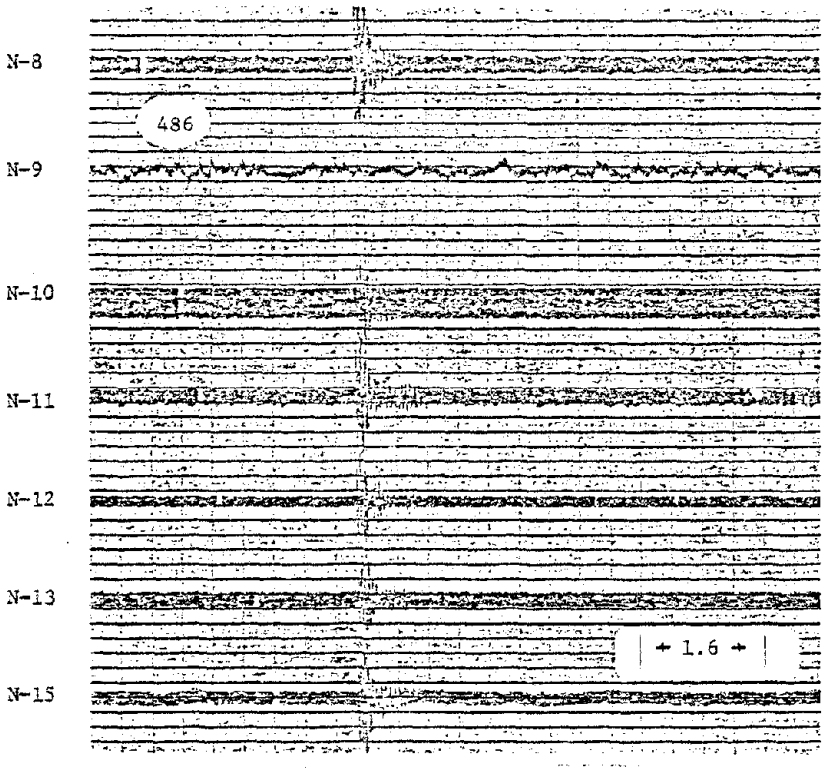

Figure 33. Typical Microseismic Event (36-4207), February 18, 1974. [Horizontal Scale: Time (s); Vertical Scale: Particle Velocity (μips/10 divisions).]

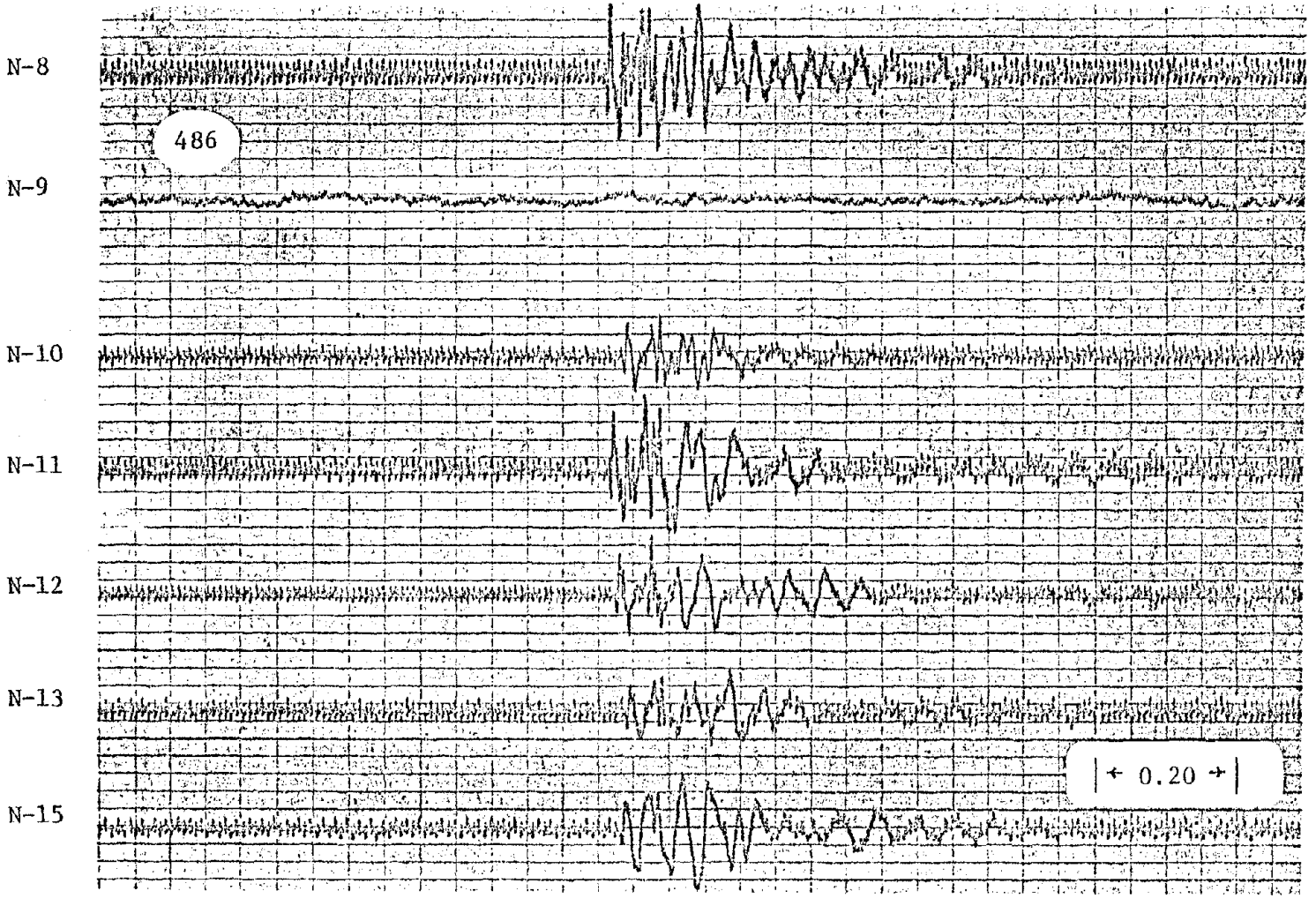

Figure 34. Event (36-4207), February 18, 1974--Time-Expanded. [Horizontal Scale: Time (s); Vertical Scale: Particle Velocity (μips/10 divisions).]

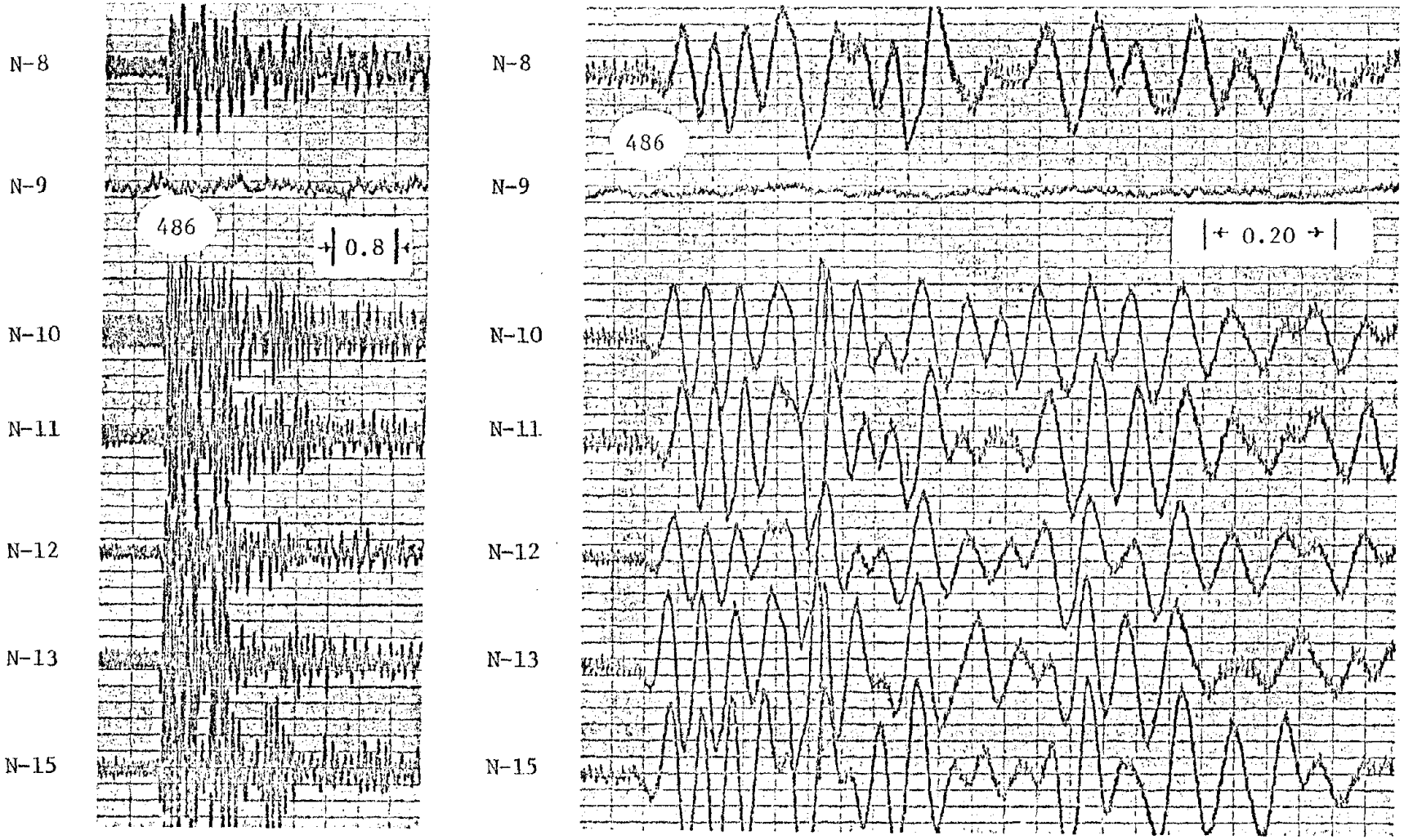

Figure 35. Event (36-3797), February 18, 1974. [Horizontal Scale: Time (s); Vertical Scale: Particle Velocity (μips/10 divisions).]

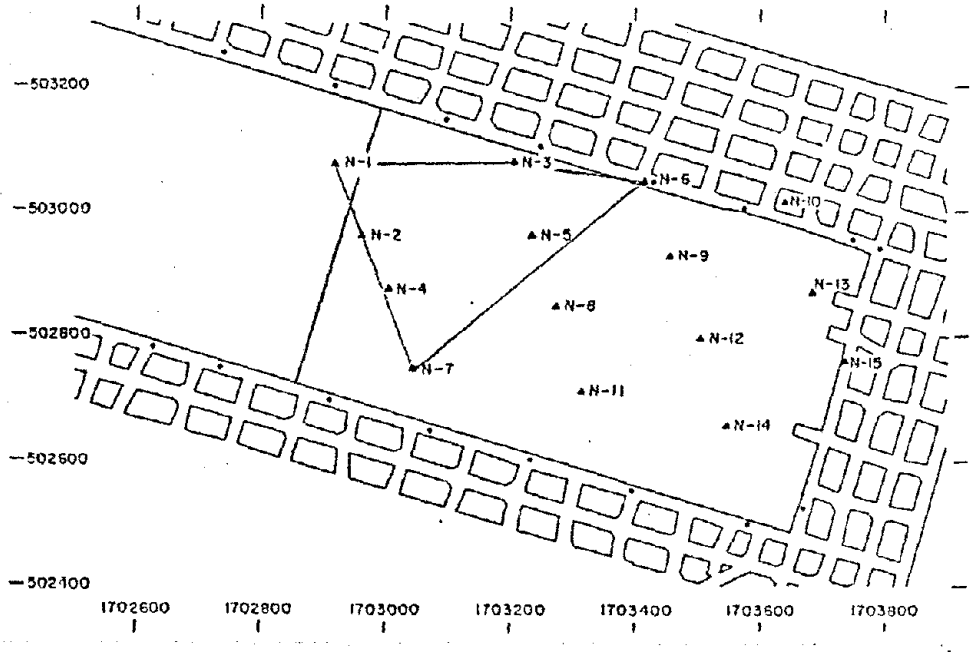

Figure 36. Location of Longwall Face and Geophone Array Utilized: February 26, 1974.

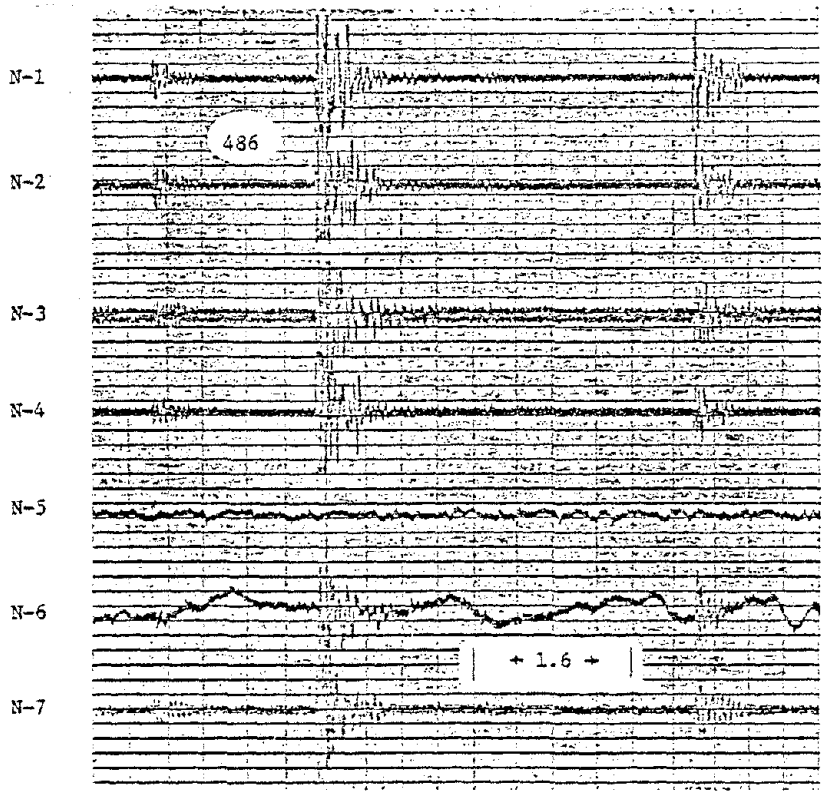

Figure 37. Typical Microseismic Events (38-4894), February 26, 1974. [Horizontal Scale: Time (s); Vertical Scale: Particle Velocity (μips/10 divisions).]

Figure 38. Particle velocities were approximately 300 to 500 µips and frequencies ranged from 15 to 100 Hz. Typical background was 10 to 15 µips and was basically composed of fundamental frequencies of 60 Hz and its harmonics. It should be noted that very satisfactory cutting of the coal seam by the shearer was typical for this day.

In Figure 39 many events are noted, particularly from 14:00 to 15:30 hours (2 epm) and from 17:00 to 19:00 hours (3.6 epm), while the normal longwall operations were proceeding smoothly. Also during this second period an increase in the event rates for both level-2 and level-3 is apparent. The period between 15:30 and 17:00 hours, which encompassed the crew change, had some activity (0.2 epm) but the rate was very minimal in comparison with those of the other two periods.

Mining operations were monitored following the crew change by R. Kim, a member of the project personnel, who stationed himself at the headgate to observe the operation of the shearer, hydraulic pump, belt conveyor, chain conveyor, and any other activities of possible value. Figure 40 graphically shows the operations and comments. Equipment "ON" conditions are the black regions and equipment "OFF" conditions are left white. Note that the longwall operation was progressing very well between 16:40 and 18:30, although no real microseismic activity was detected until 20 minutes later (Figure 39). Shortly before and after 17:30 the shearer was not in operation. This condition may have been observed by the level-1 event rate, as this rate sharply dropped at these times.

Figures 41 to 44 illustrate some typical microseismic events detected before underground observations began. Figure 41 shows two events occurring within a period of 1.5 s. The first event was then

Figure 38. Event (38-4894), February 26, 1974--Time-Expanded. [Horizontal Scale: Time (s); Vertical Scale: Particle Velocity (μips/10 divisions).]

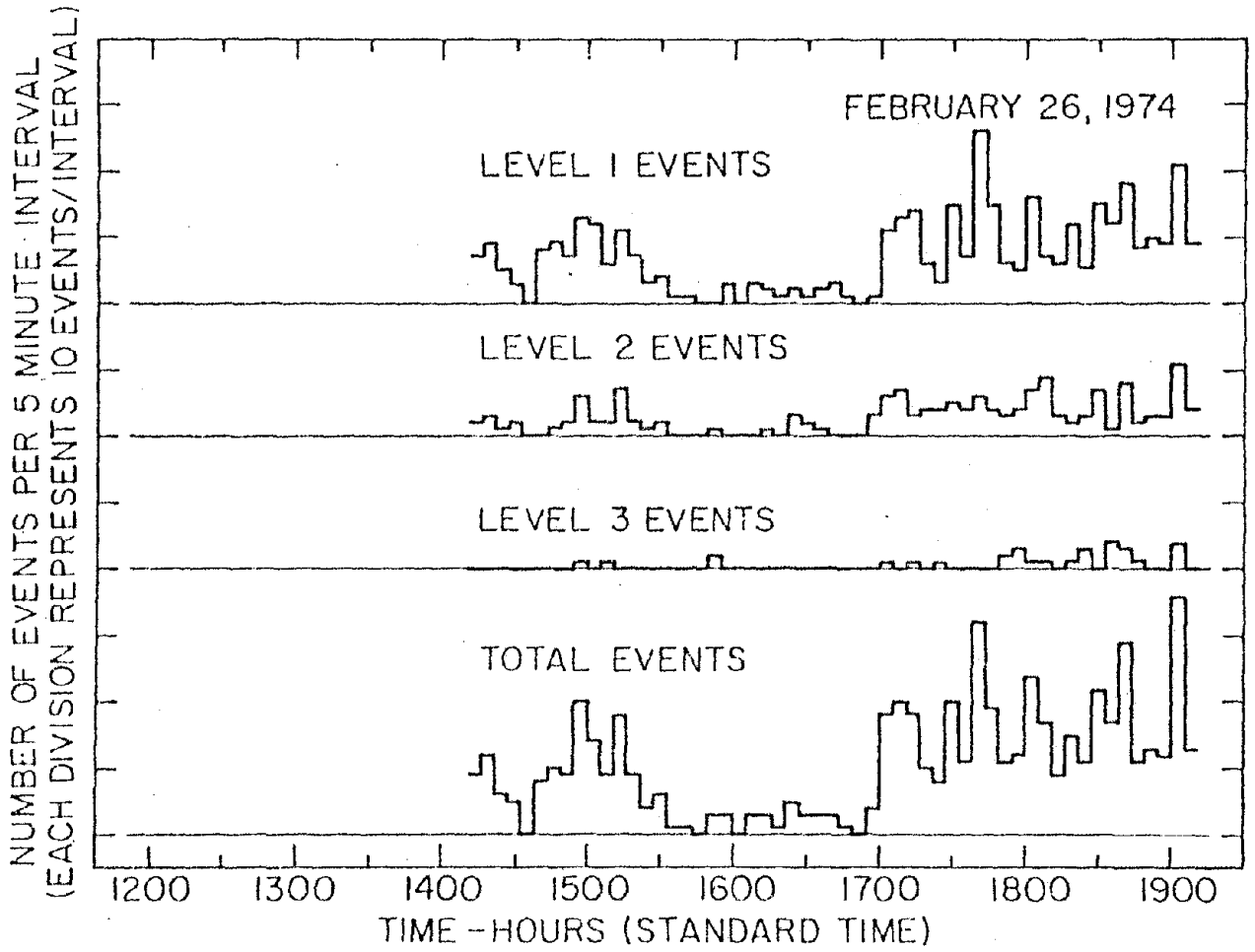

Figure 39. Event Activity Rate Histogram: February 26, 1974.

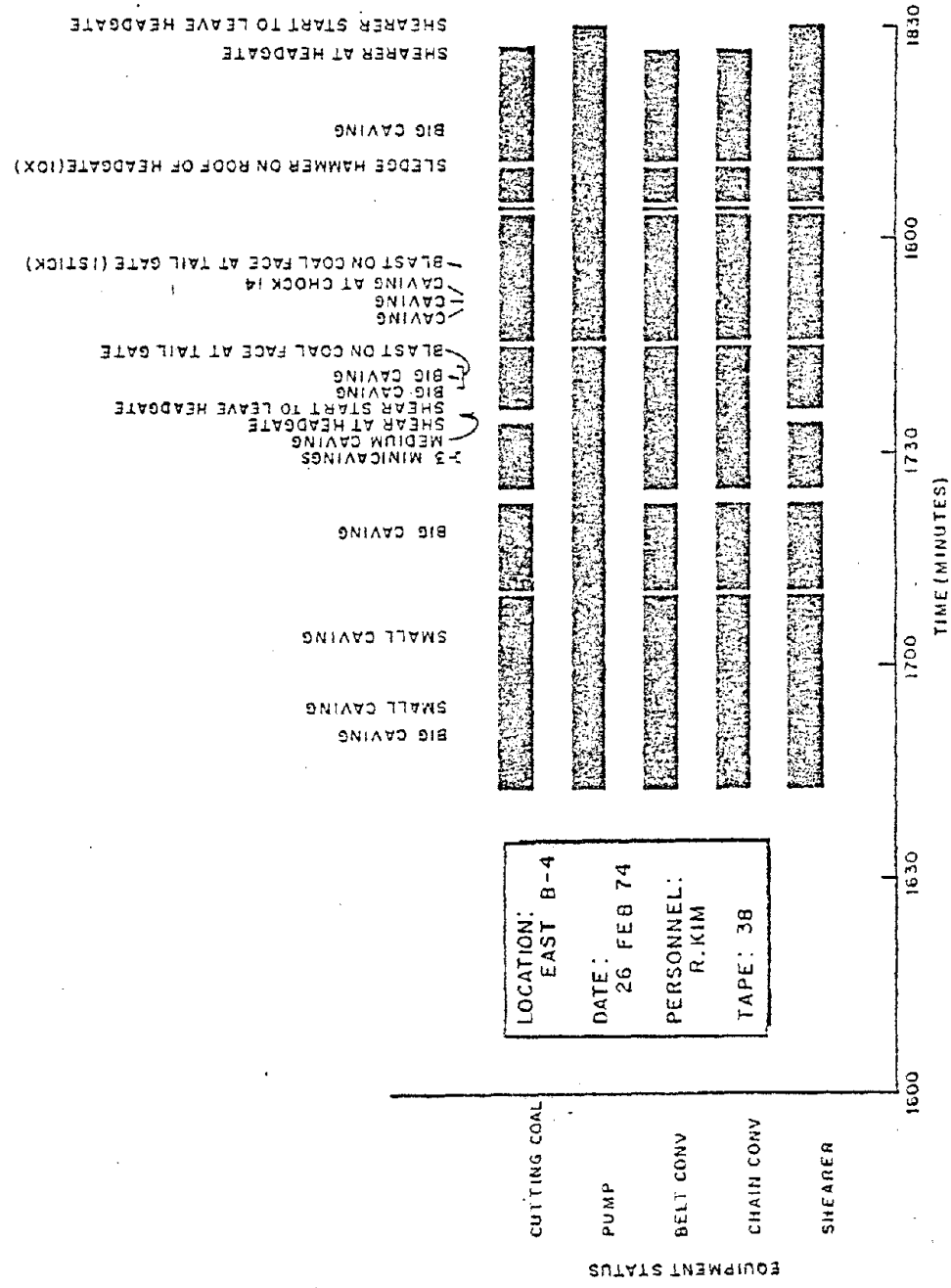

Figure 40. Underground Operations, February 26, 1974.

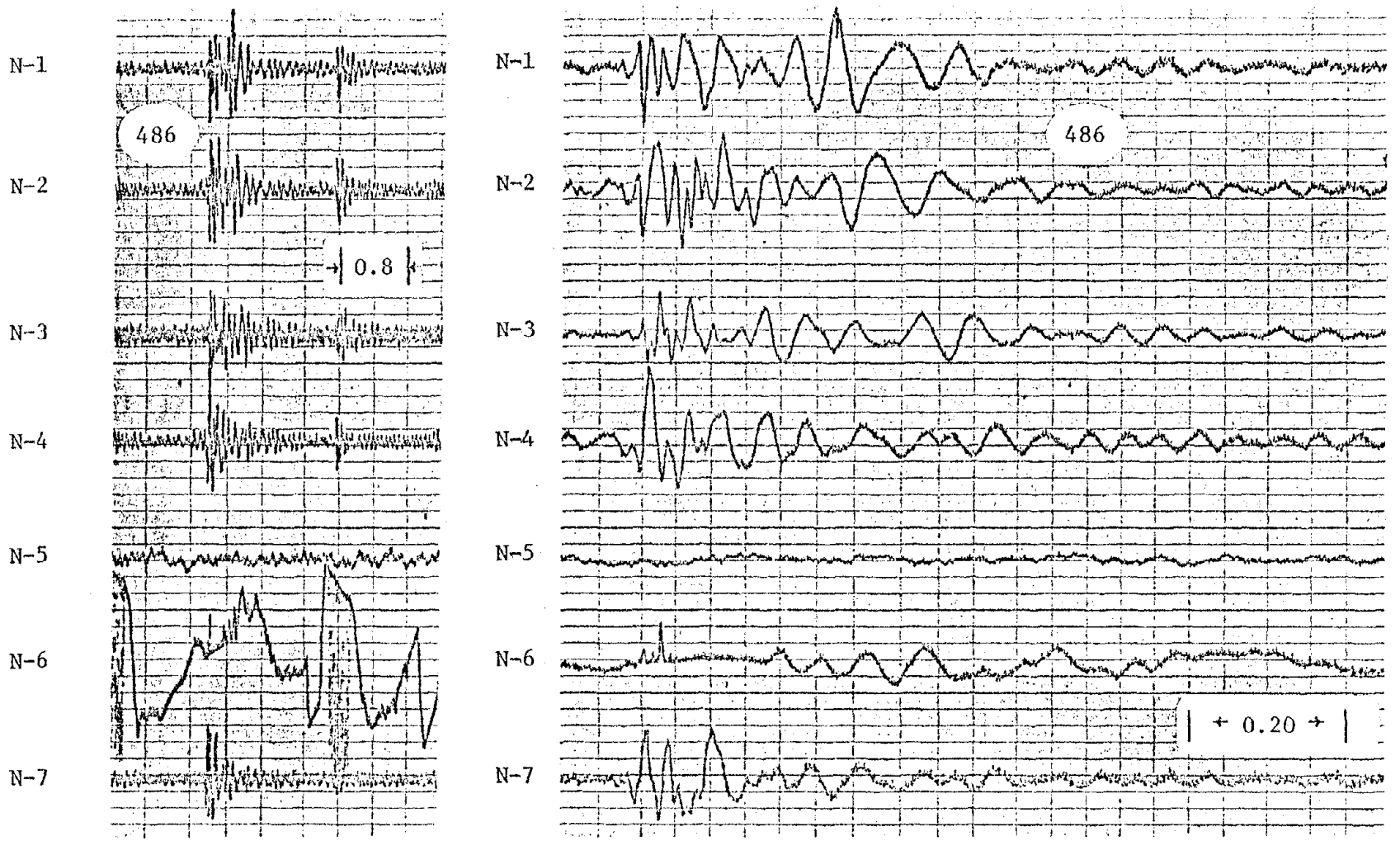

Figure 41. Event (38-1195), February 26, 1974. [Horizontal Scale: Time (s); Vertical Scale: Particle Velocity (μips/10 divisions).]

Figure 42. Event (38-1988), February 26, 1974. [Horizontal Scale: Time (s); Vertical Scale: Particle Velocity (µips/10 divisions).]

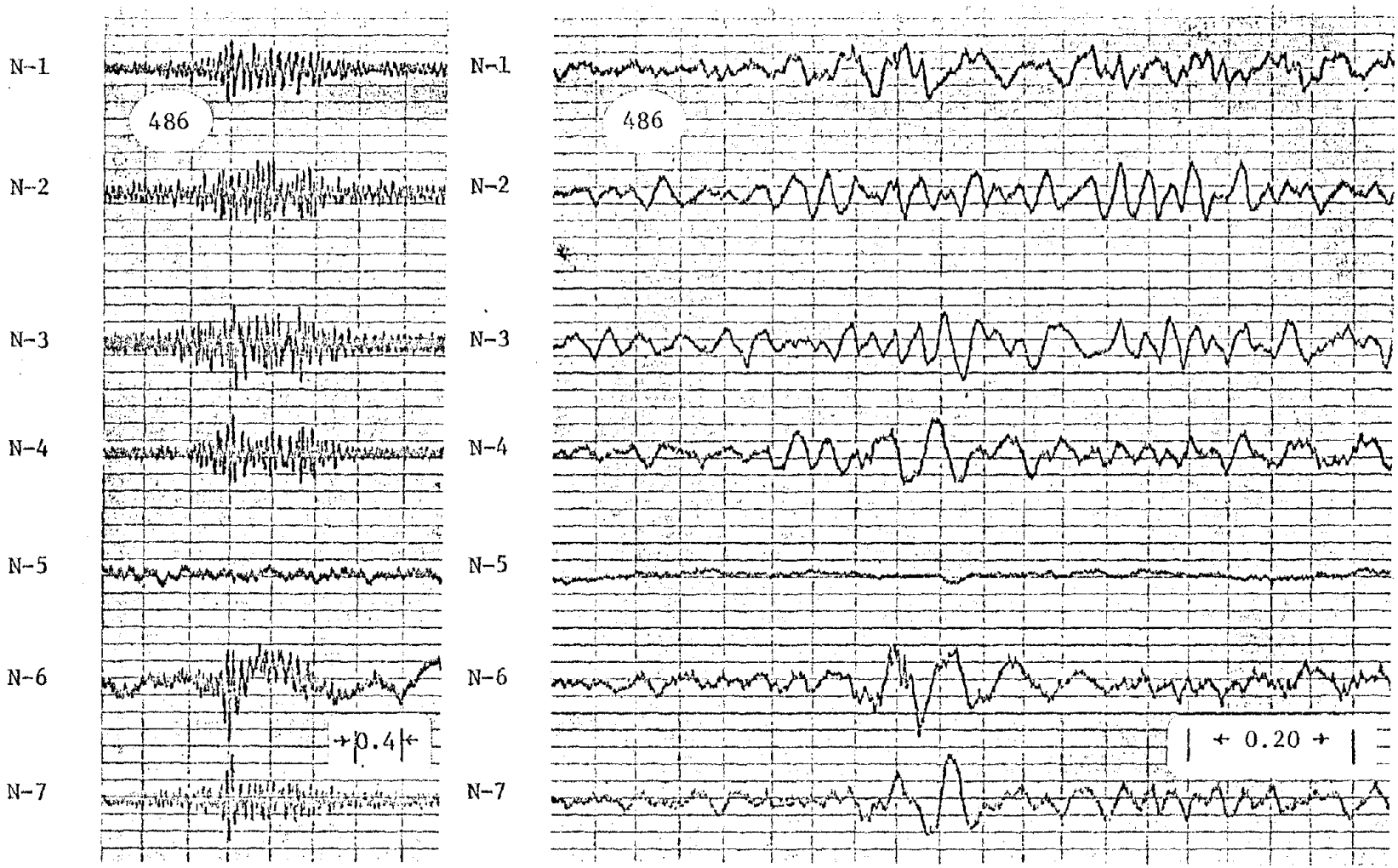

Figure 43. Event (38-3047), February 26, 1974. [Horizontal Scale: Time (s); Vertical Scale: Particle Velocity (μips/10 divisions).]

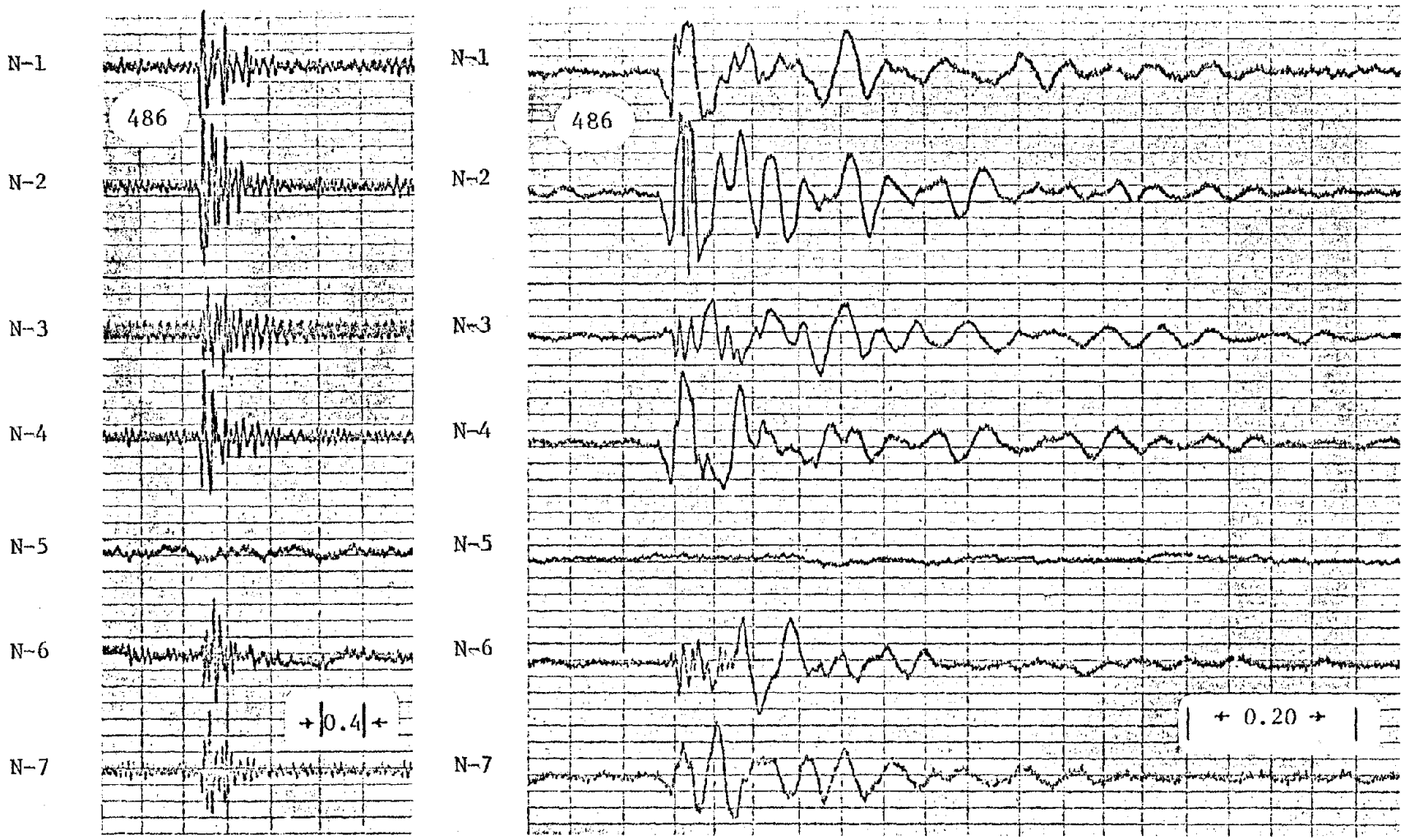

Figure 44. Event (38-3812), February 26, 1974. [Horizontal Scale: Time (s); Vertical Scale: Particle Velocity (μips/10 divisions).]

time-expanded to obtain particle velocities (125 to 350 µips) and basic frequencies (12 to 70 Hz). Figure 42 shows two closely spaced events of higher amplitude (250 to 550 µips) and generally lower frequencies (10 to 20 Hz). An uncommon event having a somewhat longer than normal duration of approximately 1.5 s is presented in Figure 43. This event had particle velocities of 150 to 250 µips and frequencies of 10 to 40 Hz. Figure 44 illustrates the most frequently observed type of event, whose duration was approximately 0.6 s. For this event the particle velocities were 200 to 450 µips, and frequencies were 12 to 80 Hz (except for geophone N-6 which had initial frequencies of 100 to 150 Hz). Particle velocities were greatest at geophones N-2 and N-4 and were smallest at geophones N-3 and N-6, which indicated that the event originated in the vicinity of the face.

Figures 45 to 47 give examples of known cavings as reported by R. Kim. His comments as to the amount of caving are based on subjective aural observations at the headgate and are included in the figure captions. Figure 45 illustrates "medium caving." Particle velocities were more than 500 µips for all geophones and frequencies were 20 to 40 Hz, although some low-amplitude higher frequencies (100 Hz) were observed superimposed on them.

Figure 46 shows two closely spaced events at the time "caving" was reported. Their particle velocities were 100 to 250 µips for the first event and 350 to 500 µips for the second. Frequencies for both events were 10 to 100 Hz. "Large caving" is shown on Figure 47, where particle velocities were 350 to 500 µips and frequencies were 12 to 80 Hz. Both events shown were attributed to the "large caving" reported as they were only 1.7 s apart.

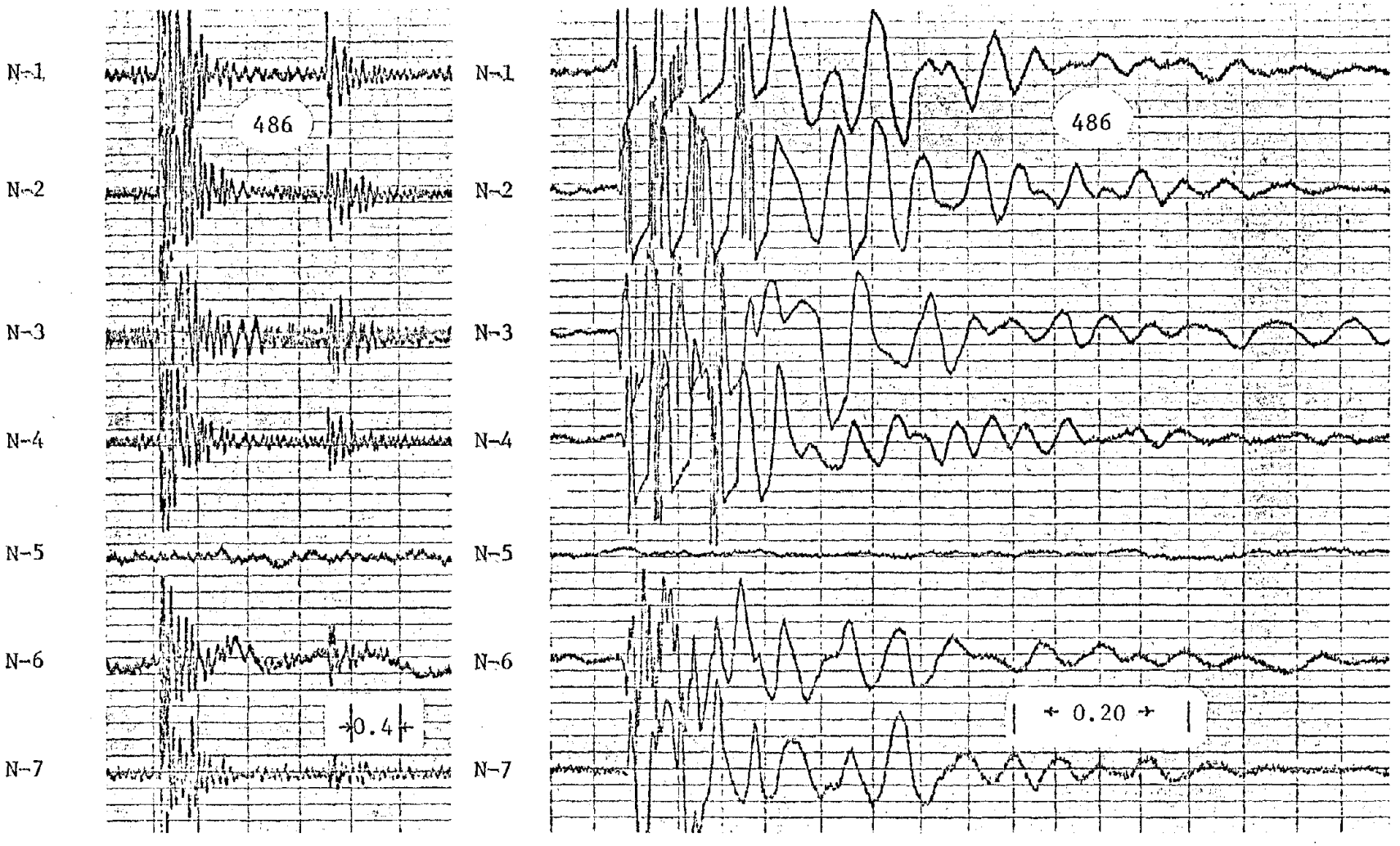

Figure 45. Event (38-3854), February 26, 1974, "Medium Caving." [Horizontal Scale: Time (s); Vertical Scale: Particle Velocity (µips/10 divisions).]

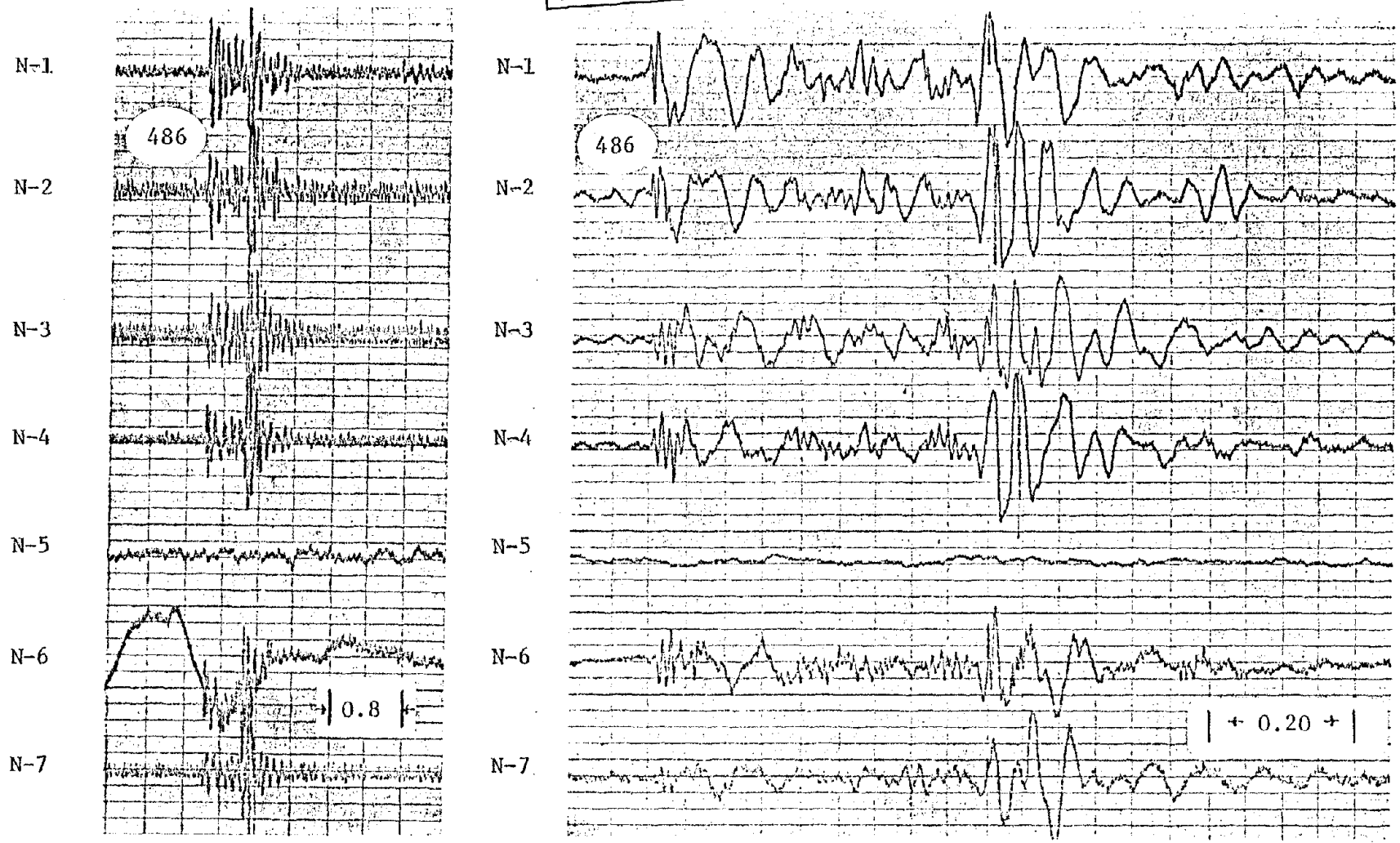

Figure 46. Event (38-4156), February 26, 1974, "Caving." [Horizontal Scale: Time (s); Vertical Scale: Particle Velocity (μips/10 divisions).]

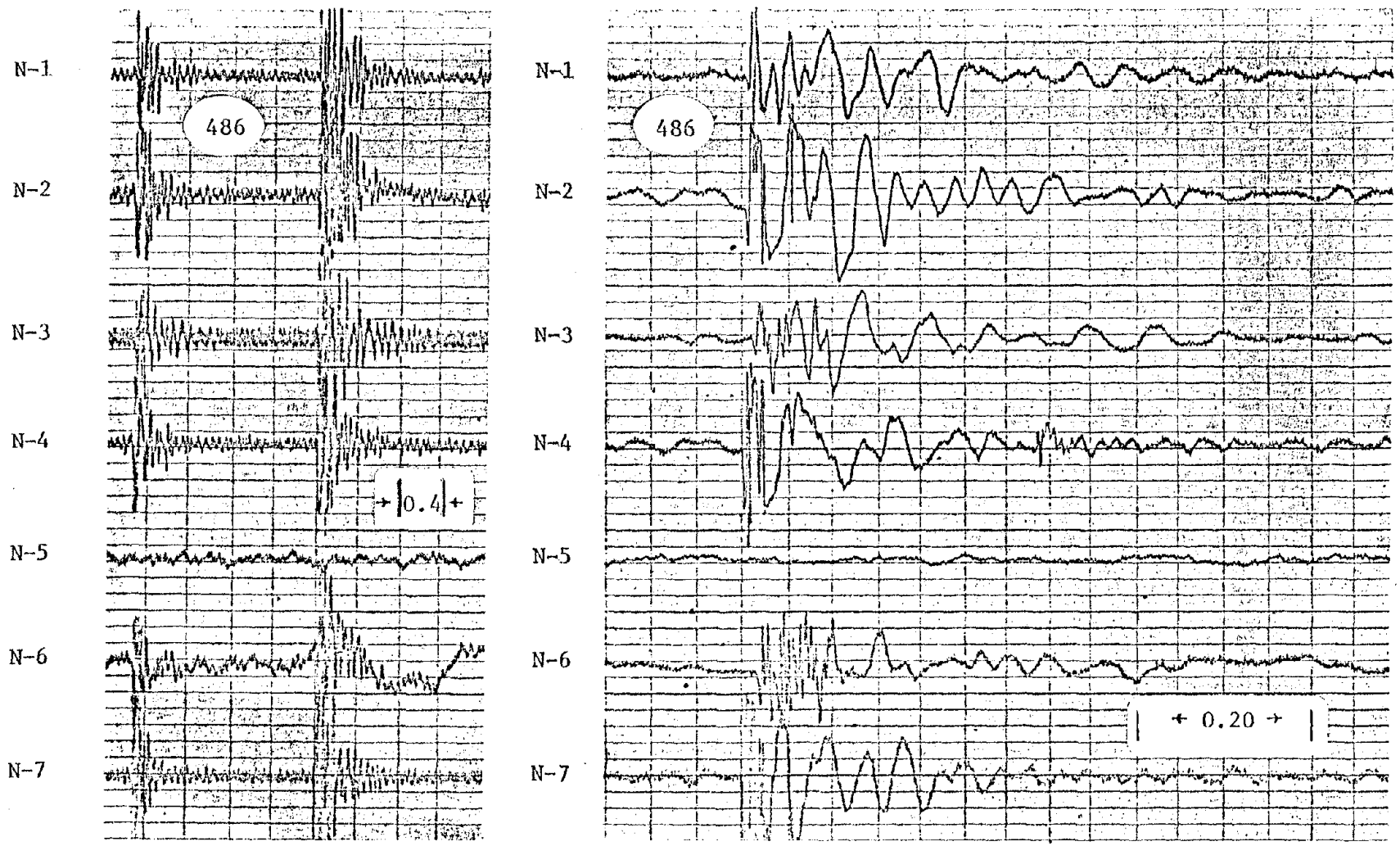

Figure 47. Event (38-4650), February 26, 1974, "Large Caving." [Horizontal Scale: Time (s); Vertical Scale: Particle Velocity (μips/10 divisions).]

2.5 Longwall face under geophone array: mine operating--poor longwall conditions

On February 27, the longwall roof was reported to be in poor condition with blocks falling from the roof in the middle of the longwall face. Approximately 2-1/2 hours of microseismic data were recorded beginning at 13:11 using geophones N-1 through N-7, as shown in Figure 48. One typical event observed during this time is presented in Figure 49, with its time-expanded version given in Figure 50. Particle velocities were 250 to 400 µips and frequencies were 10 to 100 Hz.

The event activity rate was very erratic (0.2 to 3 epm) as shown in Figure 51 during the first recording period. The general level of background noise increased several times between 13:00 and 15:00 hours, possibly due to mining activity and its associated cavings. Figure 52 shows a low-amplitude (125 to 175 µips), low-frequency (10 to 20 Hz) event, and Figure 53 illustrates a high-amplitude (more than 500 µips), low-frequency (12 to 40 Hz) event with some low-amplitude, high-frequency components (100 to 200 Hz) superimposed on the low-frequencies. Event 39-840 appeared to originate nearest N-3 because of its amplitude, while event 39-1024 was believed to have occurred nearest N-4 and N-7.

At 15:46 the first recording session was terminated. Geophone N-15 replaced N-5 and three additional hours of data were recorded beginning at 16:06. Figure 54 illustrates such data. W. Zuberek, one of the project personnel, was at this time stationed underground to monitor the longwall operation. As can be seen in Figure 56, the shearer was not in operation at any time from 16:30 to 19:00 hours and, therefore, no coal was being extracted.

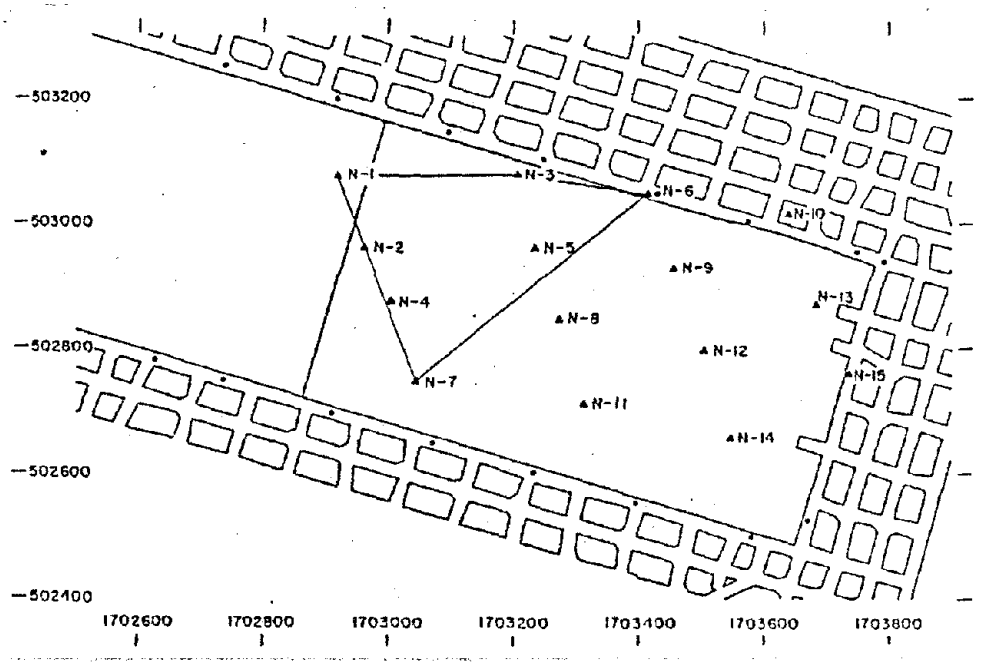

Figure 48. Location of Longwall Face and First Geophone Array Utilized: February 27, 1974.

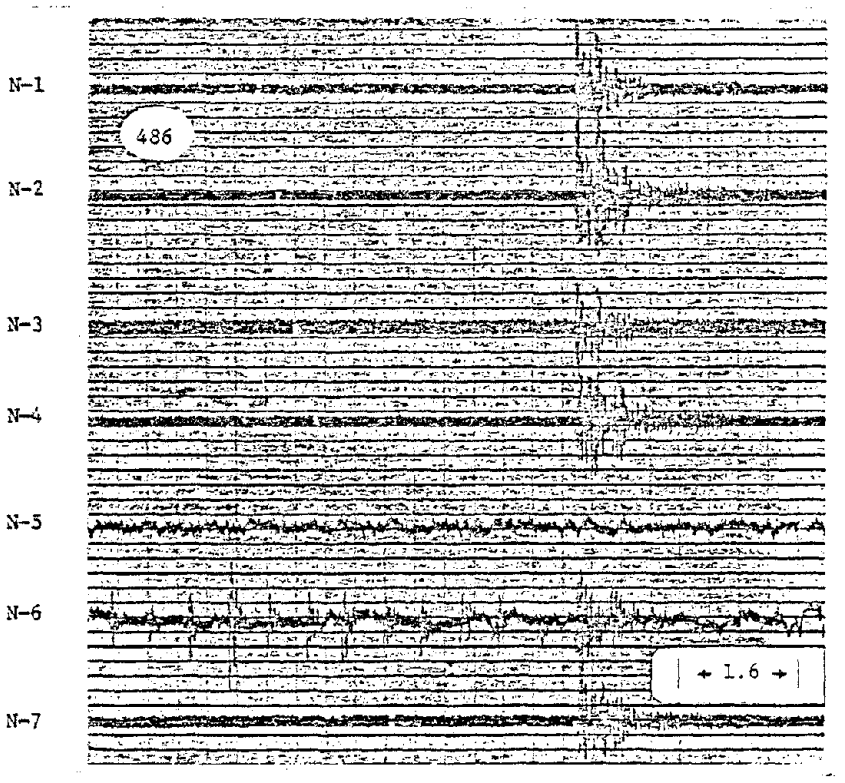

Figure 49. Typical Microseismic Event (39-867), February 27, 1974. [Horizontal Scale: Time (s); Vertical Scale: Particle Velocity (μips/10 divisions).]

Figure 50. Event (39-867), February 27, 1974--Time-Expanded. [Horizontal Scale: Time (s); Vertical Scale: Particle Velocity (μips/10 divisions).]

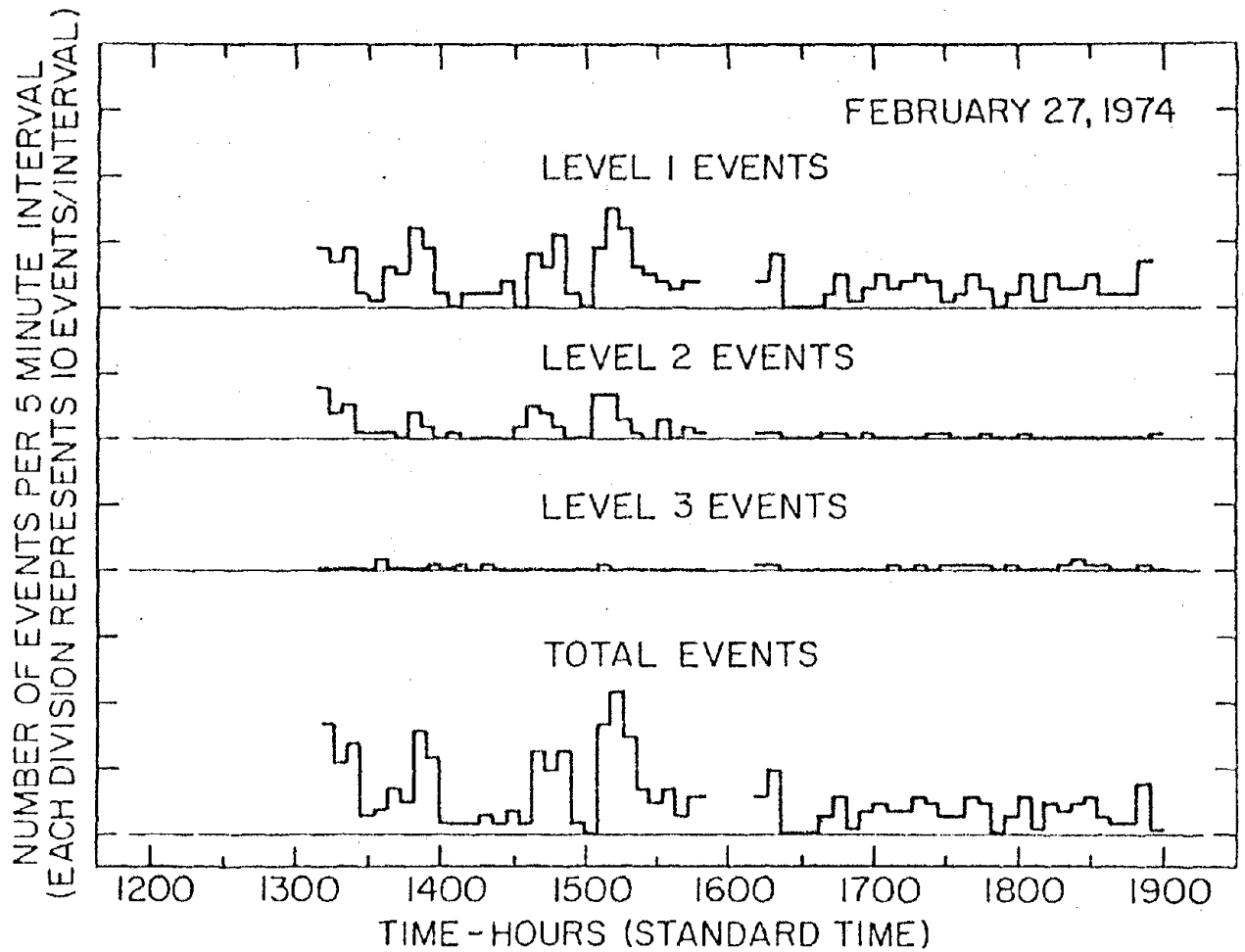

Figure 51. Event Activity Rate Histogram: February 27, 1974.

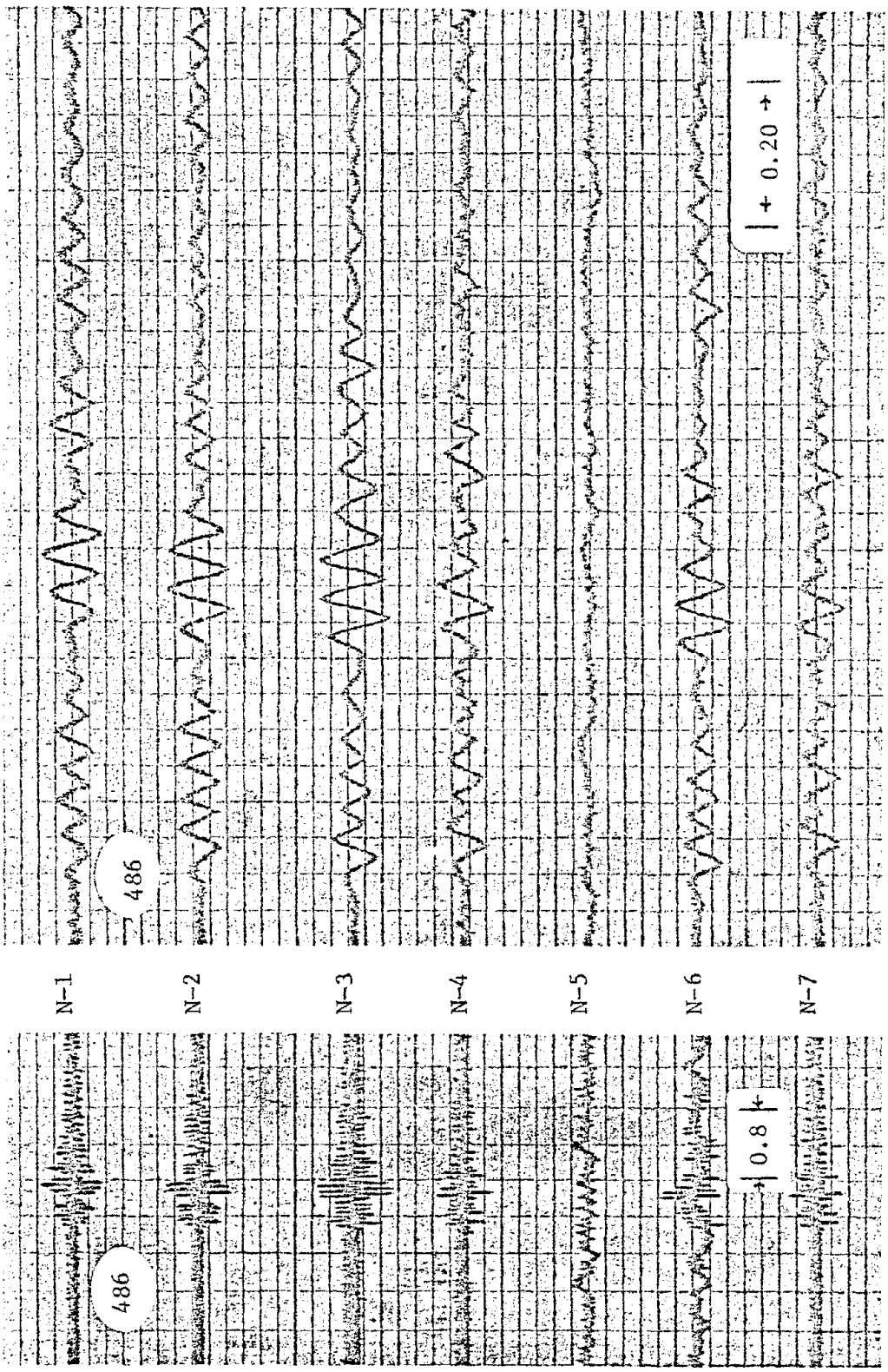

Figure 52. Event (39-840), February 27, 1974. [Horizontal Scale: Time (s); Vertical Scale: Particle Velocity (μips/10 divisions).]

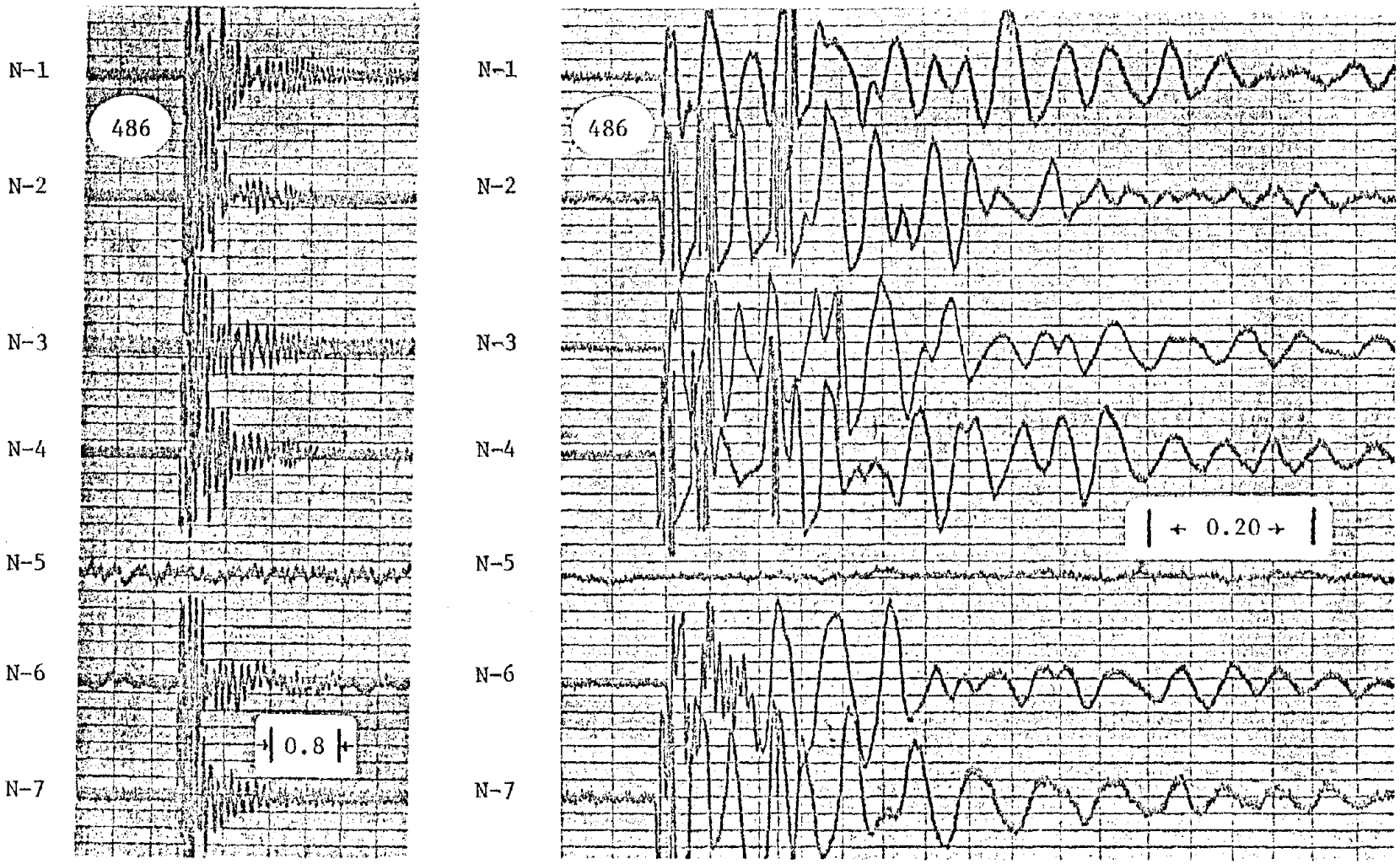

Figure 53. Event (39-1024), February 27, 1974. [Horizontal Scale: Time (s); Vertical Scale: Particle Velocity (μips/10 divisions).]

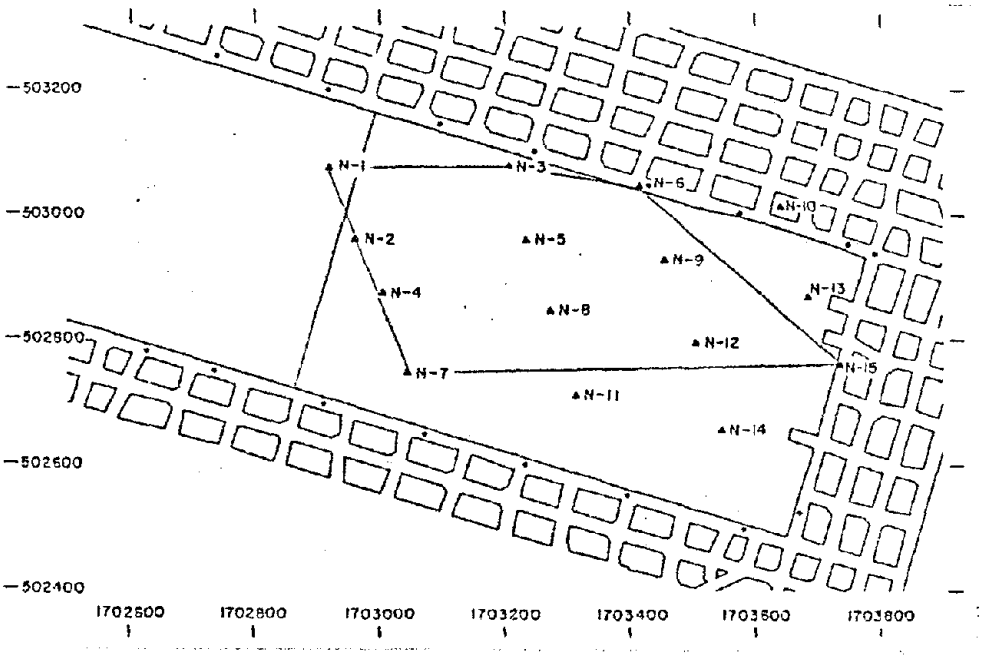

Figure 54. Location of Longwall Face and Second Geophone Array Utilized: February 27, 1974.

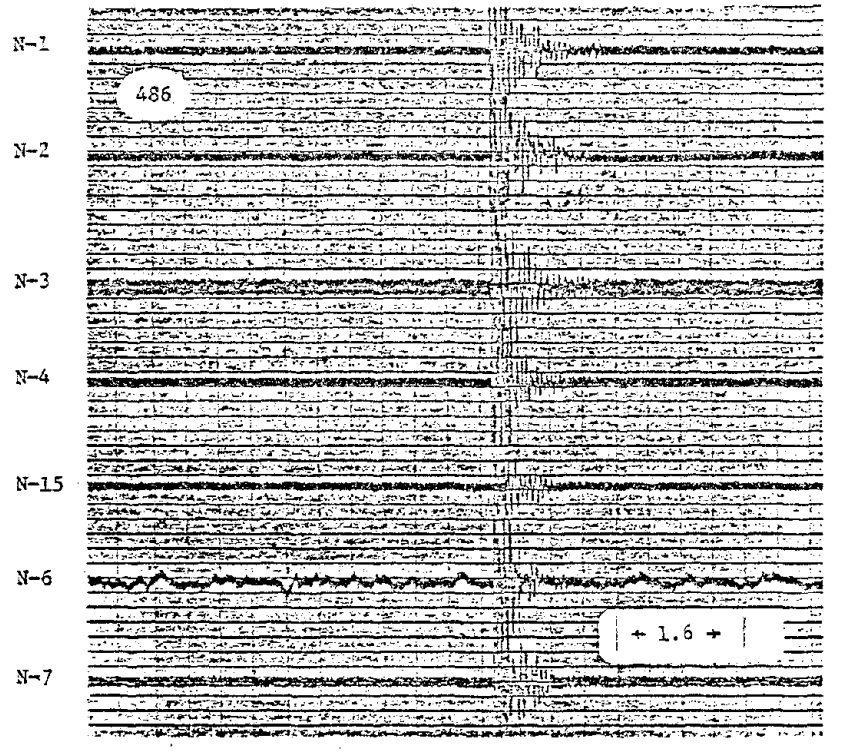

Figure 55. Blast (39-5009), February 27, 1974. [Horizontal Scale: Time (s); Vertical Scale: Particle Velocity (μips/10 divisions).]

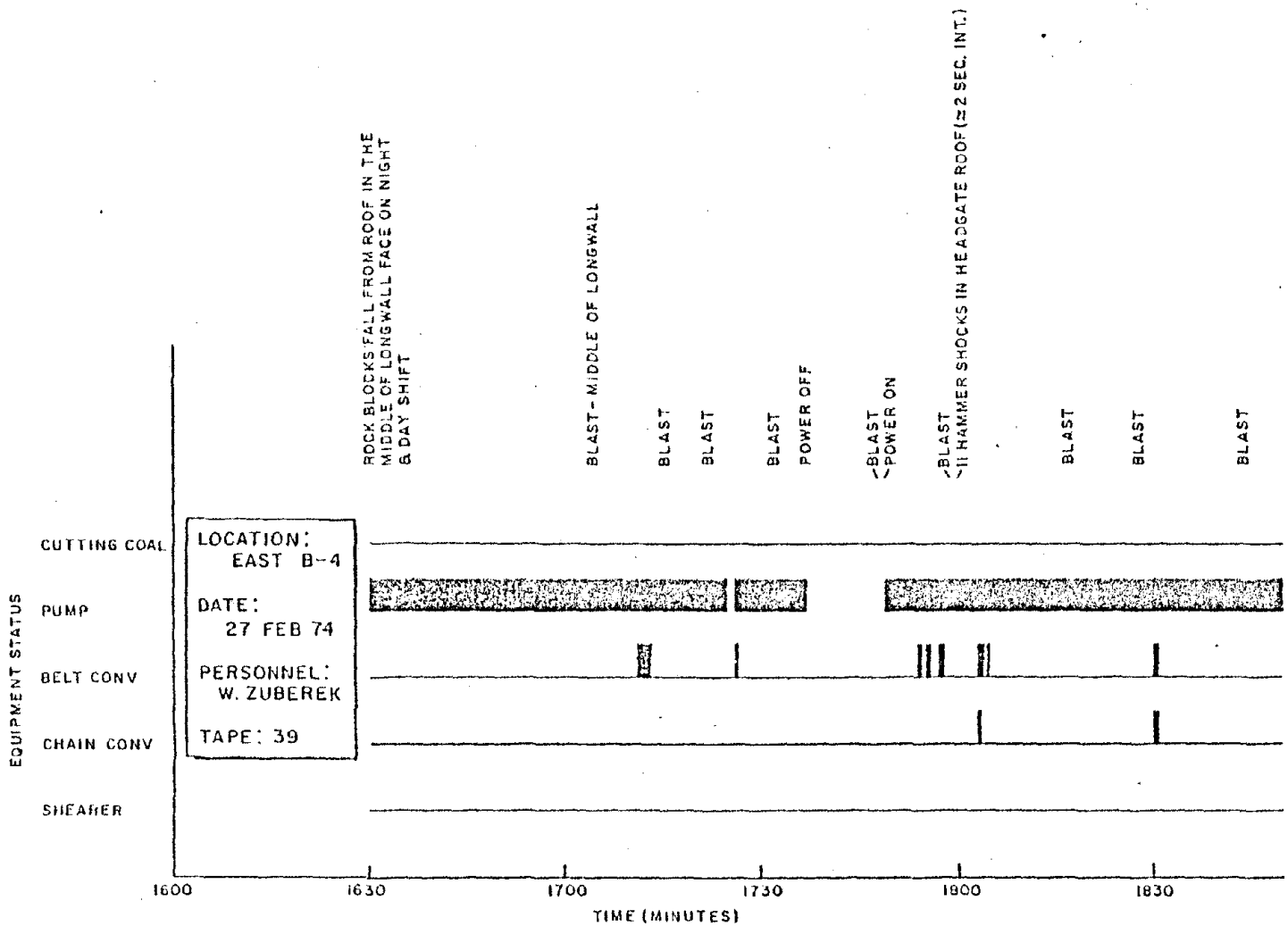

Figure 56. Underground Operations, February 27, 1974.

Unfortunately, insufficient data were recorded during the crew change and, thus, no effect of this change could be established (Figure 51). Most of the level-2 events dropped to 0.2 epm or less between 16:06 and 18:56. Level-1 events tended to stabilize at about 0.8 to 1.0 epm. The majority of the level-3 events were blasts, one of which is shown in Figure 55. Blast 39-5009, time-expanded, is presented in Figure 57. Particle velocities for this blast were 150 to 450 μips, and frequencies were basically 10 to 40 Hz.

Numerous other blasts were detected easily with the monitoring system. Blasting was performed to free the chocks and to break rock in the panline. The miners generally wedged from one to four sticks of permissible explosive between a stuck chock and the roof (or in some cases the floor). The dynamite upon detonation would fracture the rock sufficiently to free the chock. One other typical blast is given in Figure 58 which had particle velocities and frequencies basically identical as blast 39-5009.

Efforts were made to see if the system had sufficient sensitivity to detect hammer blows on the roof at the headgate. Despite attempts to filter the data at different frequency settings, no such hammer blows were observed in the data.

2.6 Longwall face under geophone array: mine not operating--poor longwall conditions

For nearly five days, the longwall had not been worked except to "smash rock in the panline" two days before microseismic data was recorded. Before the mine had temporarily halted operations, it was reported that the midface was in very poor condition and that rock was falling from the roof.

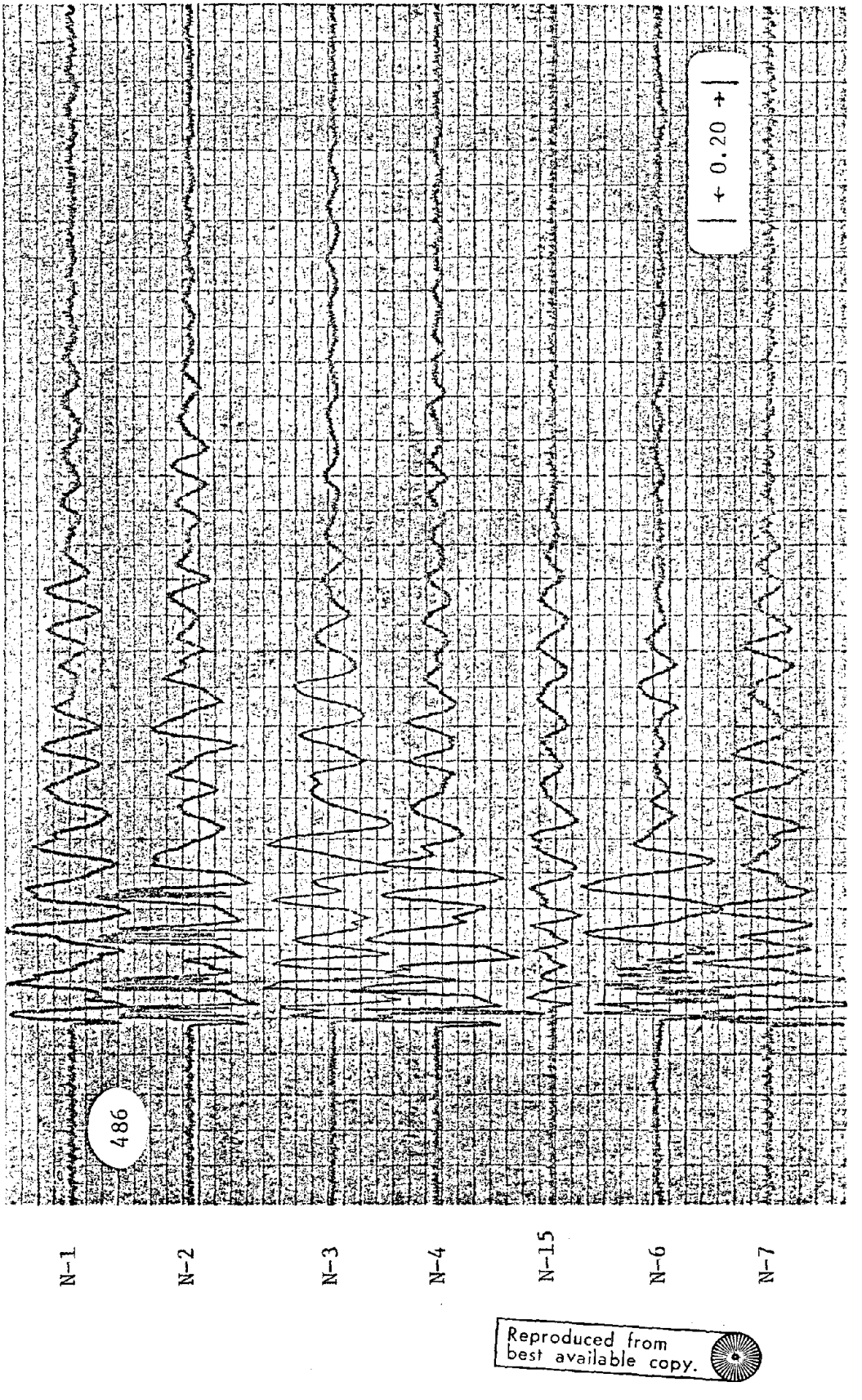

Figure 57. Blast (39-5009), February 27, 1974--Time-Expanded. [Horizontal Scale: Time (s); Vertical Scale: Particle Velocity (μips/10 divisions).]

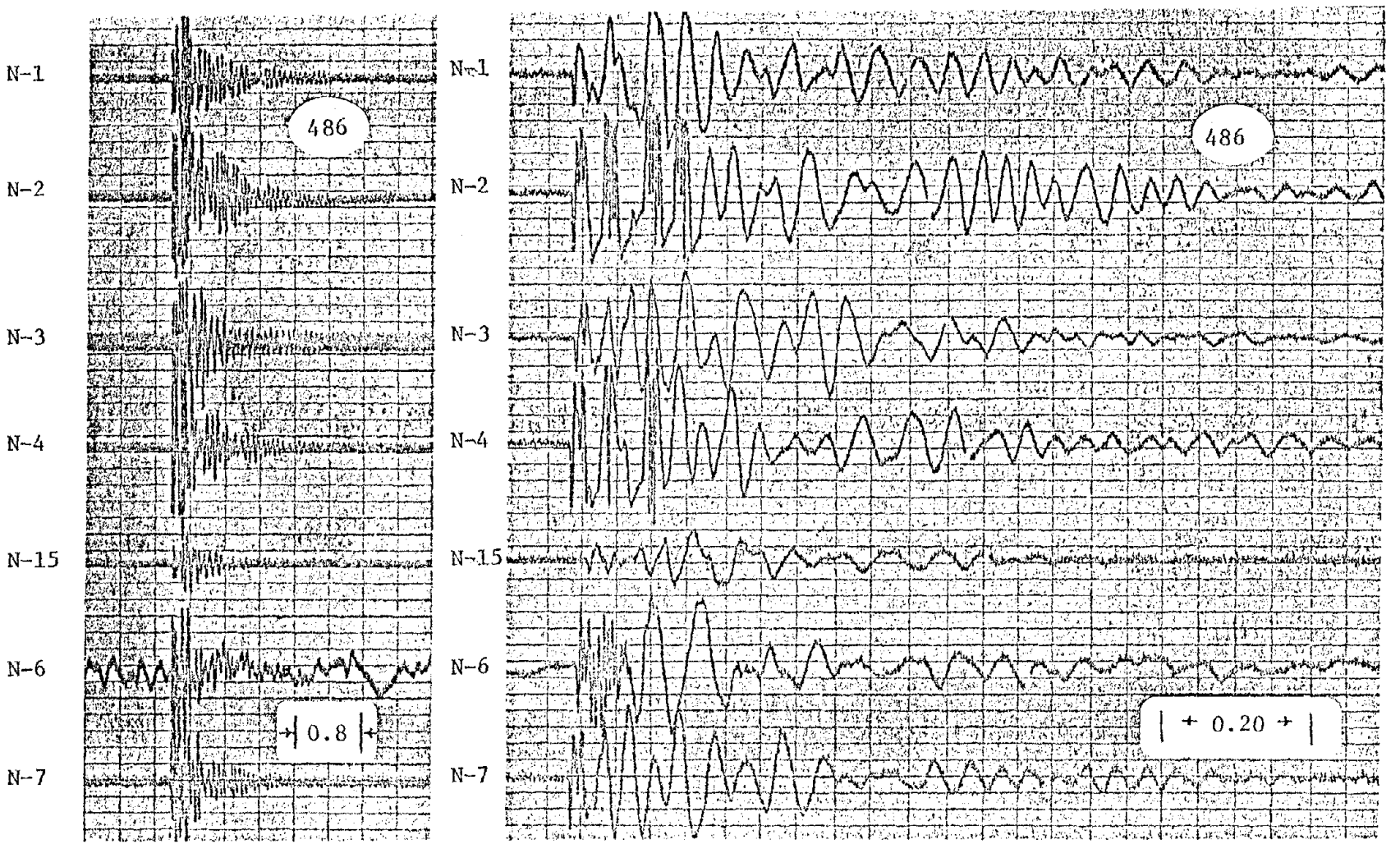

Figure 58. Blast (39-5855), February 27, 1974. [Horizontal Scale: Time (s); Vertical Scale: Particle Velocity (μips/10 divisions).]

Approximately 1-1/2 hours of microseismic data were initially recorded utilizing geophones N-1, N-2, N-3, N-4, N-6, N-7, and N-9 from 12:18 to 13:49 hours on April 17 as given in Figure 59. A level-2 event detected using this first array is given in Figure 60, with its time-expanded version presented in Figure 61. Note that only geophones N-1, N-2, N-3, and N-4 responded well to the event, and that N-2 and N-1 had the largest amplitudes, which implied that the event likely originated in the gob between the two geophones. Particle velocities were 20 to 50 µips, and the frequencies were 20 to 100 Hz. Ambient background was basically the same as the earlier field trips, being 10 to 20 µips.

Figure 62 shows the event rate associated with the first array. Only several level-1 events were detected in addition to the level-2 event presented.

A second array consisting of geophones N-5, N-10, N-11, N-12, N-13, N-14, and N-15 was next employed from 16:00 to 17:30 hours as presented in Figure 63. Several level-1 and level-2 events were detected (Figure 62), indicating that microseismic activity was occurring despite the fact that the mine had not been operating. This suggests that the strata surrounding the longwall panel were not yet completely stabilized. No level-3 events were observed. The average activity rate for April 17 was approximately 0.1 epm.

A microseismic event detected by the second geophone array is shown on Figure 64, and the event's time-expanded version is presented in Figure 65. Particle velocities were 60 to 80 µips, and frequencies were 12 to 40 Hz. Figure 66 shows another event whose particle velocities were 30 to 50 µips and had a relatively constant frequency of

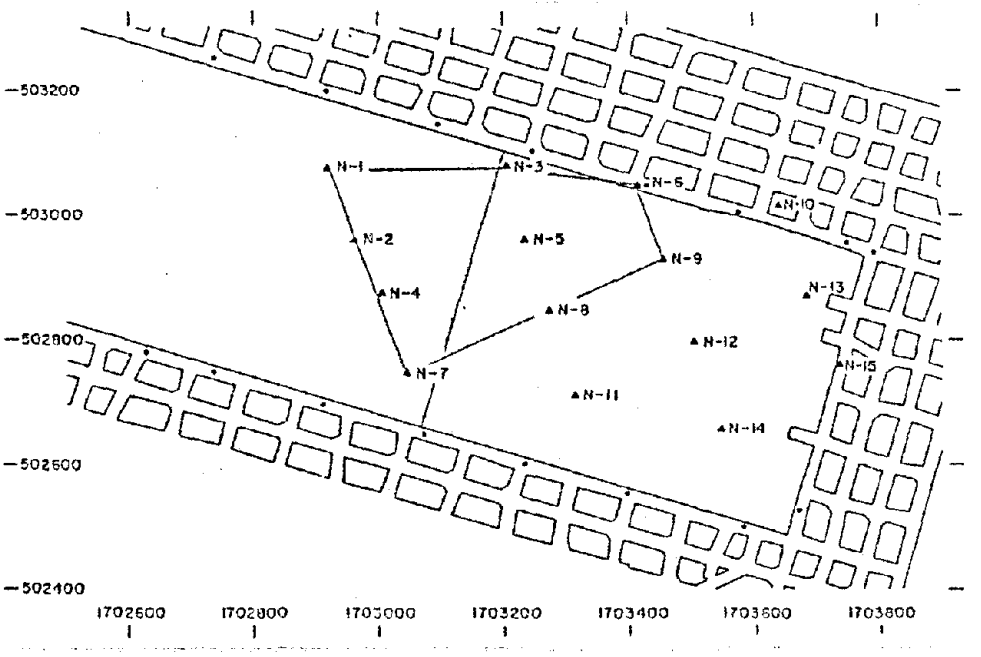

Figure 59. Location of Longwall Face and First Geophone Array Utilized: April 17, 1974.

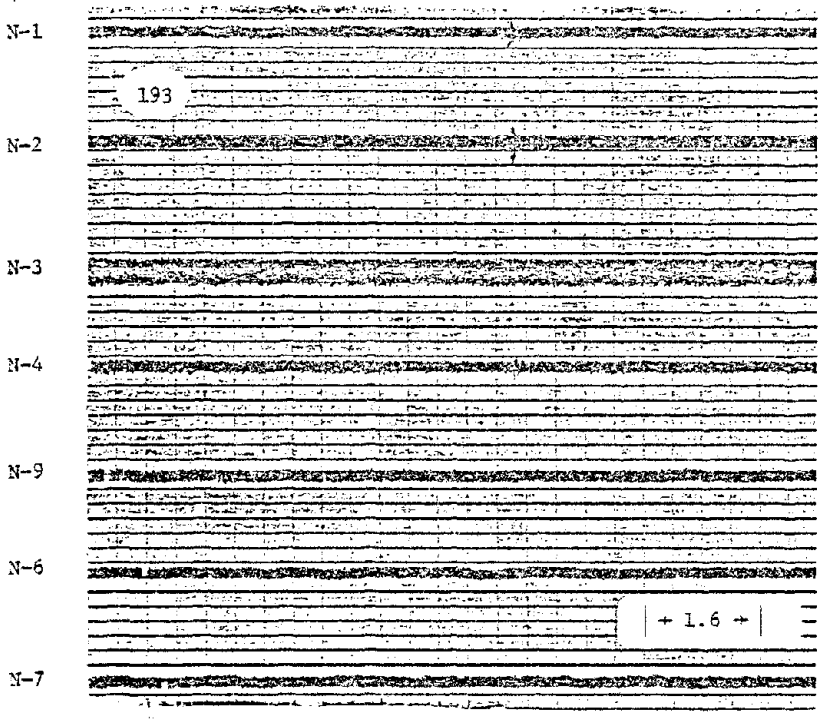

Figure 60. Typical Microseismic Event (43-491), April 17, 1974. [Horizontal Scale: Time (s); Vertical Scale: Particle Velocity (μips/10 divisions).]

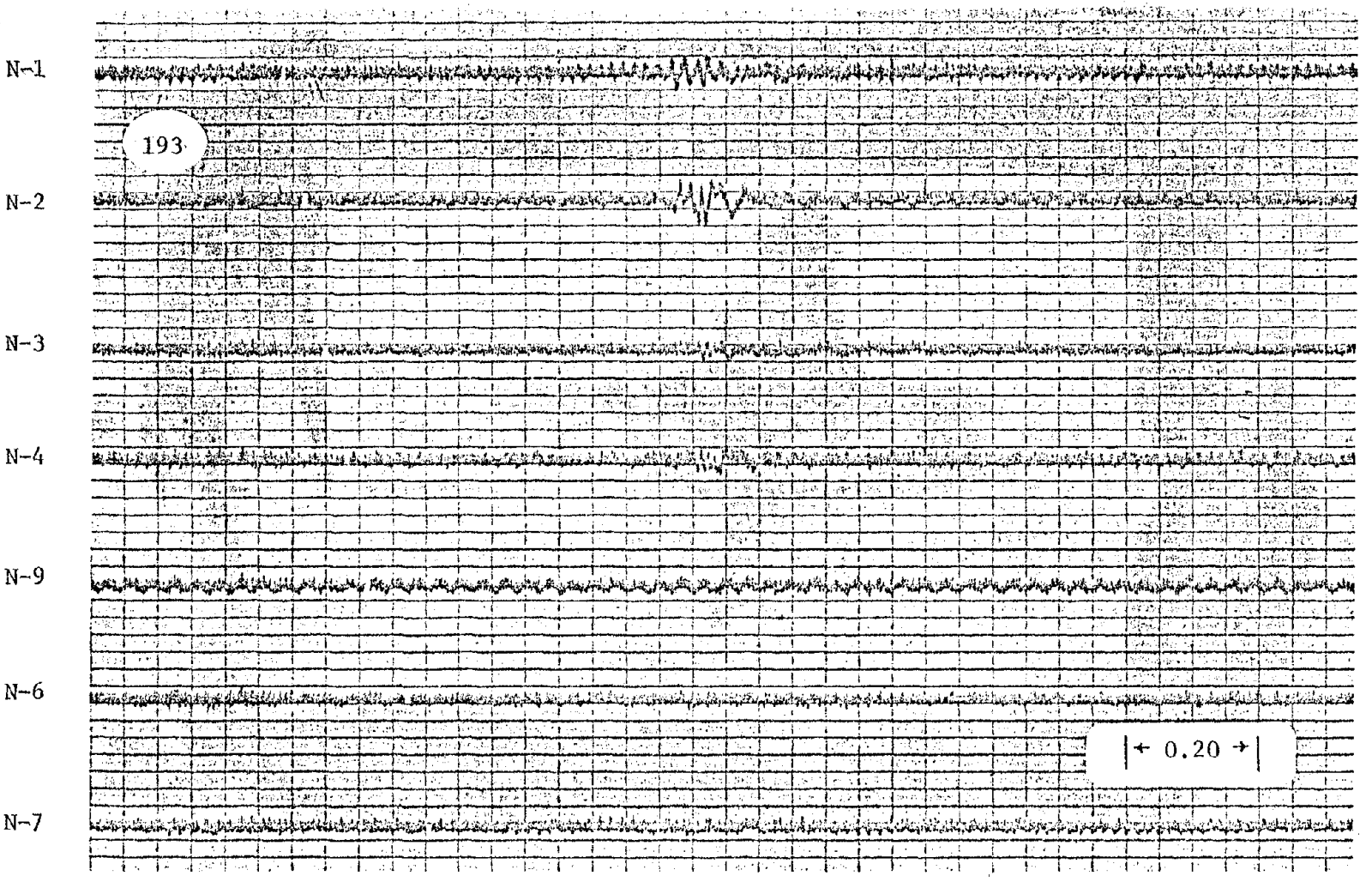

Figure 61. Event (43-491), April 17, 1974--Time-Expanded. [Horizontal Scale: Time (s); Vertical Scale: Particle Velocity (μips/10 divisions.)]

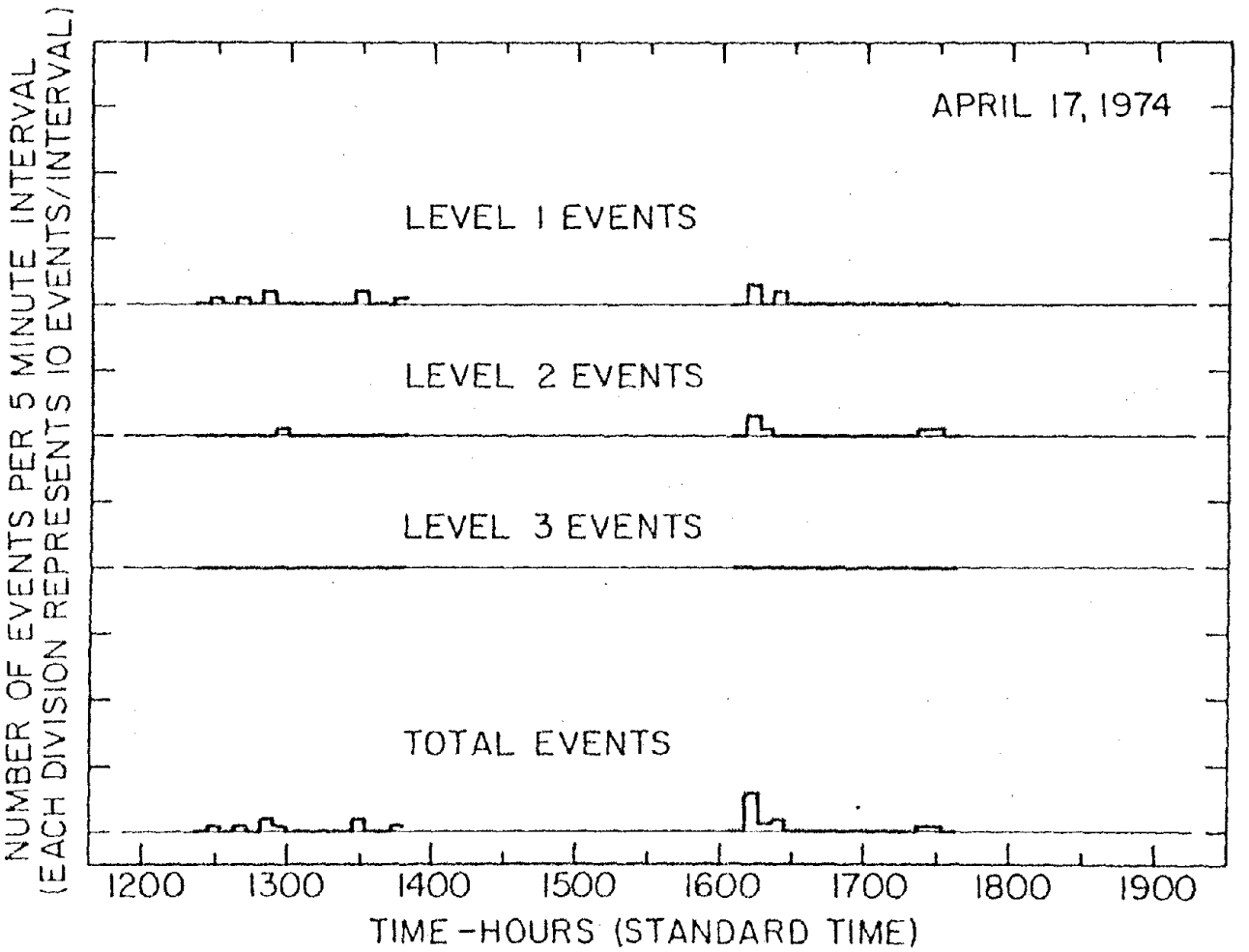

Figure 62. Event Activity Rate Histogram: April 17, 1974.

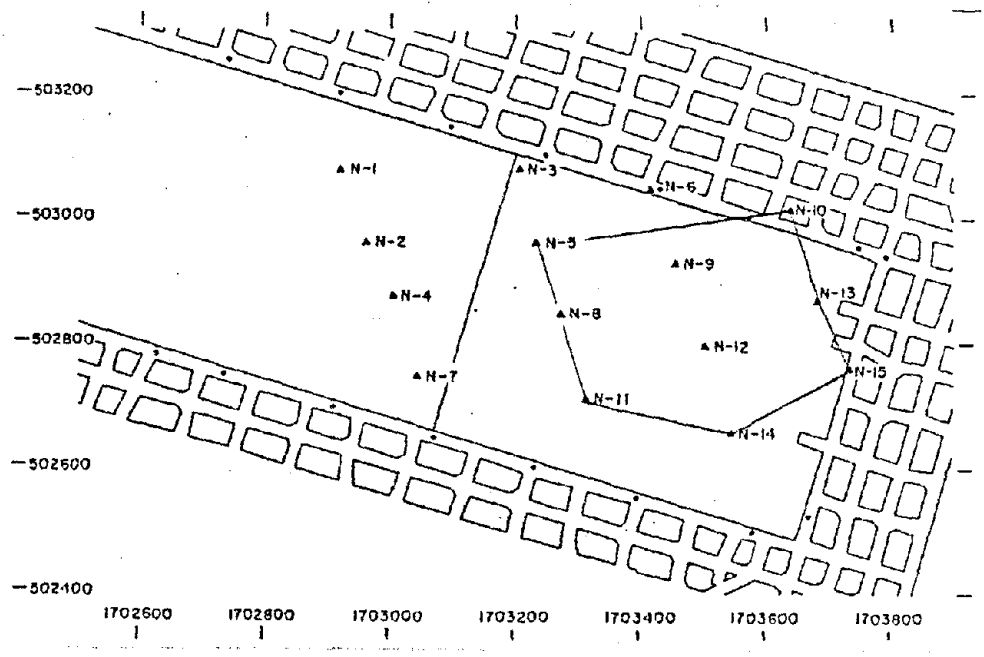

Figure 63. Location of Longwall Face and Second Geophone Array Utilized: April 17, 1974.

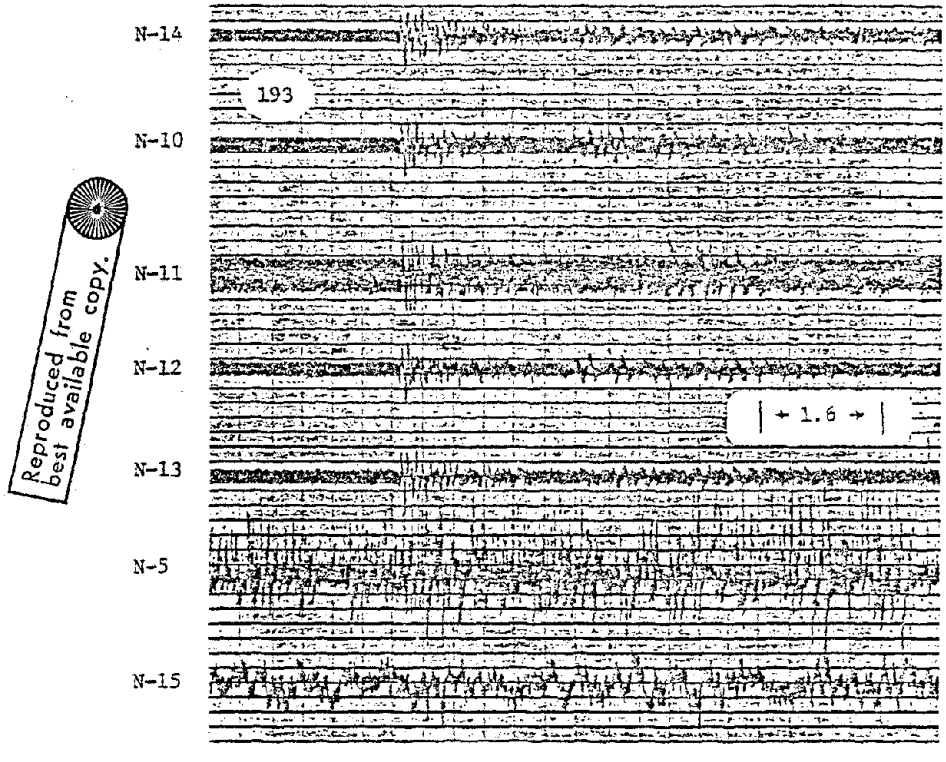

Figure 64. Typical Microseismic Event (43-3267), April 17, 1974. [Horizontal Scale: Time (s); Vertical Scale: Particle Velocity (μips/10 divisions).]

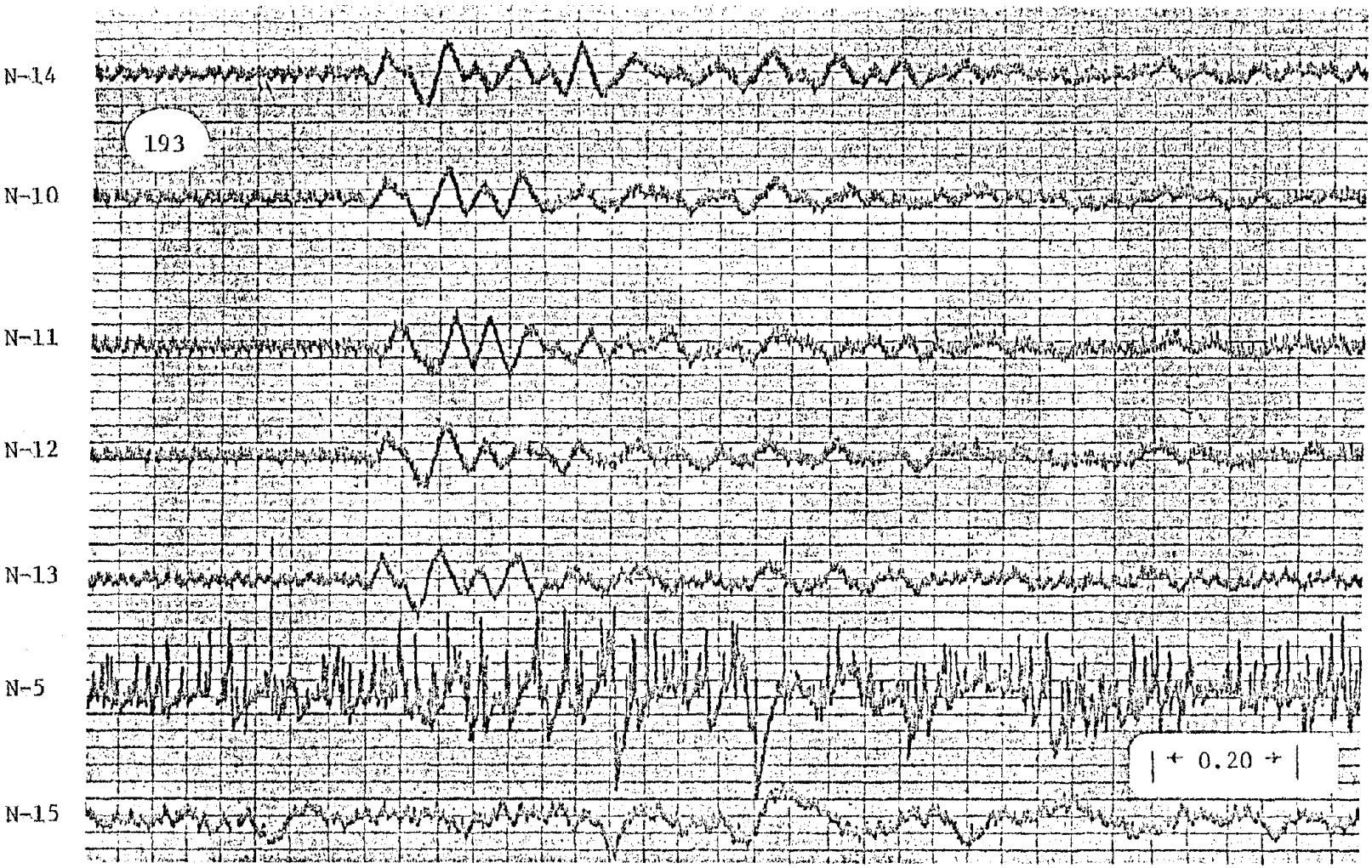

Figure 65. Event (43-3267), April 17, 1974--Time-Expanded. [Horizontal Scale: Time (s); Vertical Scale: Particle Velocity (μips/10 divisions).]

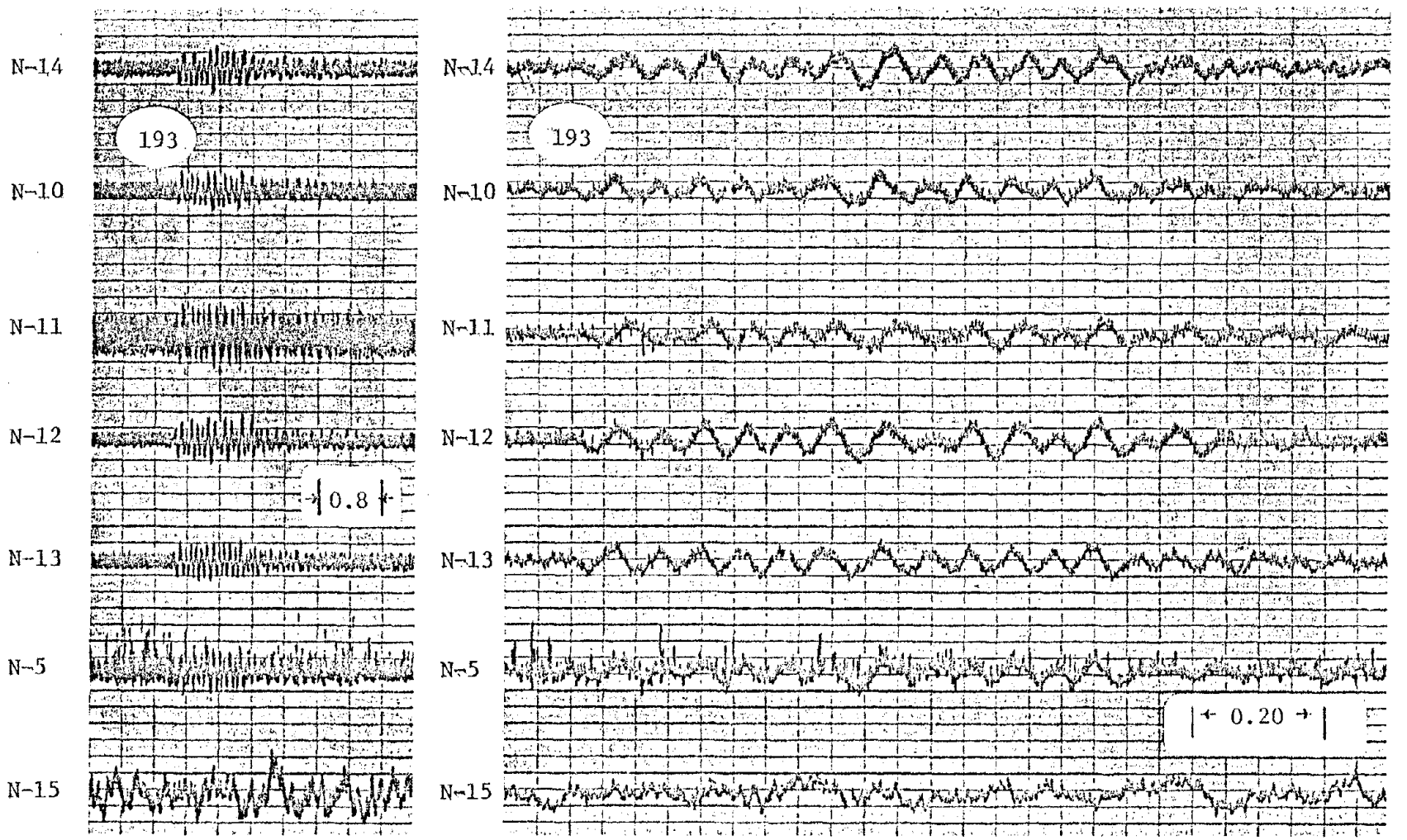

Figure 66. Event (43-1982), April 17, 1974. [Horizontal Scale: Time (s); Vertical Scale: Particle Velocity (μips/10 divisions).]

15 to 20 Hz. One additional event for this second array is given in Figure 67. Particle velocities associated with this event were 70 to 140 µips and, like event 43-1982, it had a fairly constant frequency of 12 to 15 Hz.

2.7 One week after longwall panel completed

The B-4 longwall panel was completed on July 25, 1974. Eight days later, 2-3/4 hours of microseismic data were recorded using the geophone array N-1, N-7, N-9, N-10, N-11, N-13, and N-14 as shown in Figure 68. Only a few level-1 and level-2 events were detected during recording, one of which is given in Figure 69. A time-expanded version of this event is presented in Figure 70. Particle velocities were 30 to 60 µips and frequencies were 10 to 30 Hz. Geophones N-9, N-10, and N-13 had the greatest response to the event, which indicated that it originated in that particular region which was then part of the gob area of the longwall.

Event activity was low (0.2 epm), as shown in Figure 71, due to the termination of mining operations. Nevertheless, such activity was indicative that there still existed certain instabilities somewhere in the vicinity of the longwall. The events occurring after 14:00 may have been due in part to the acoustical vibrations produced from a local thunderstorm. For example, one such event (which could be actually two events) is given in Figure 72. The duration of this event was somewhat longer than most other events detected during any of the past microseismic monitoring sessions. Particle velocities were 90 to 160 µips, and frequencies were 6 to 15 Hz, which were somewhat lower than the typical frequencies encountered.

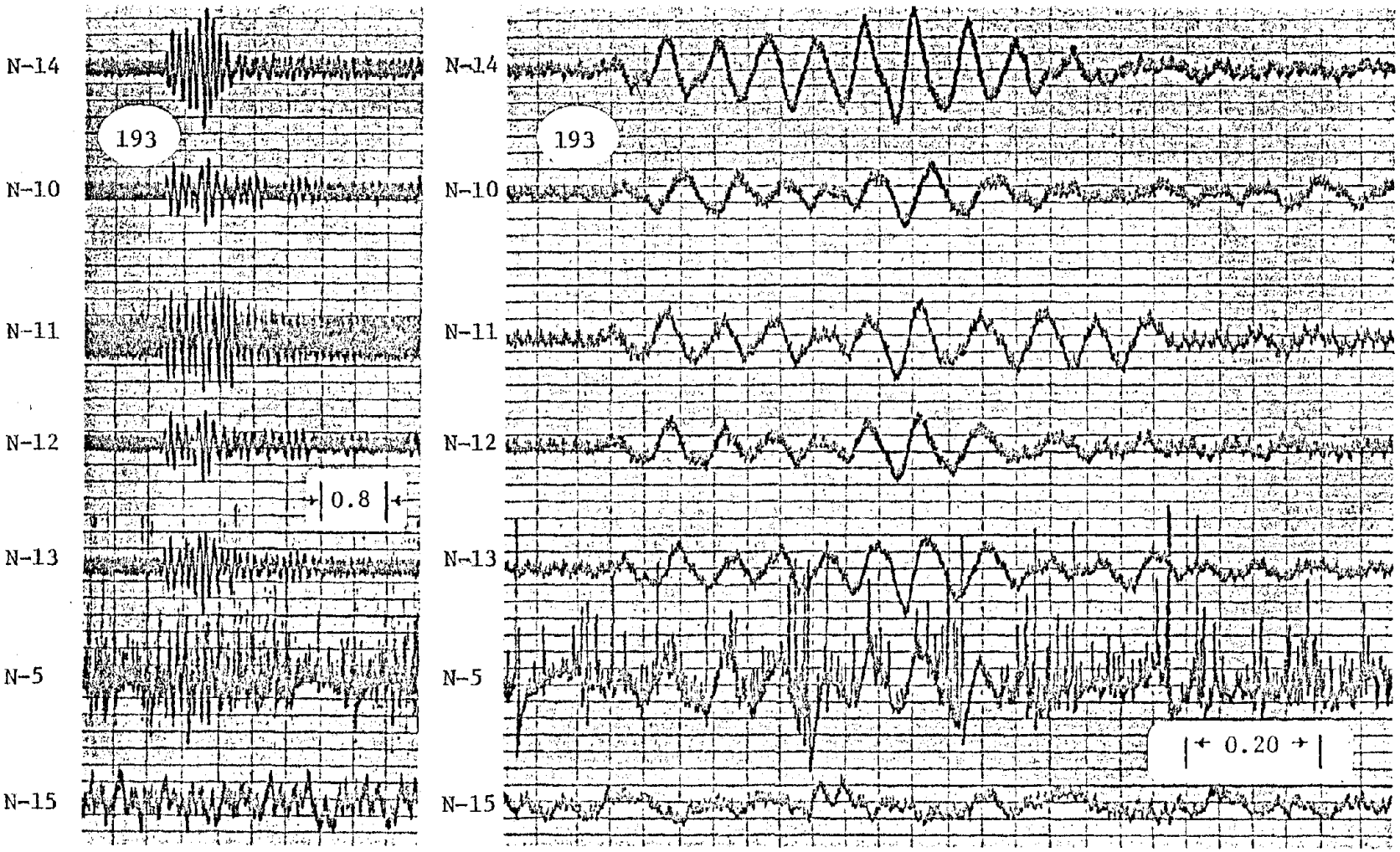

Figure 67. Event (43-3352), April 17, 1974. [Horizontal Scale: Time (s); Vertical Scale: Particle Velocity (μips/10 divisions).]

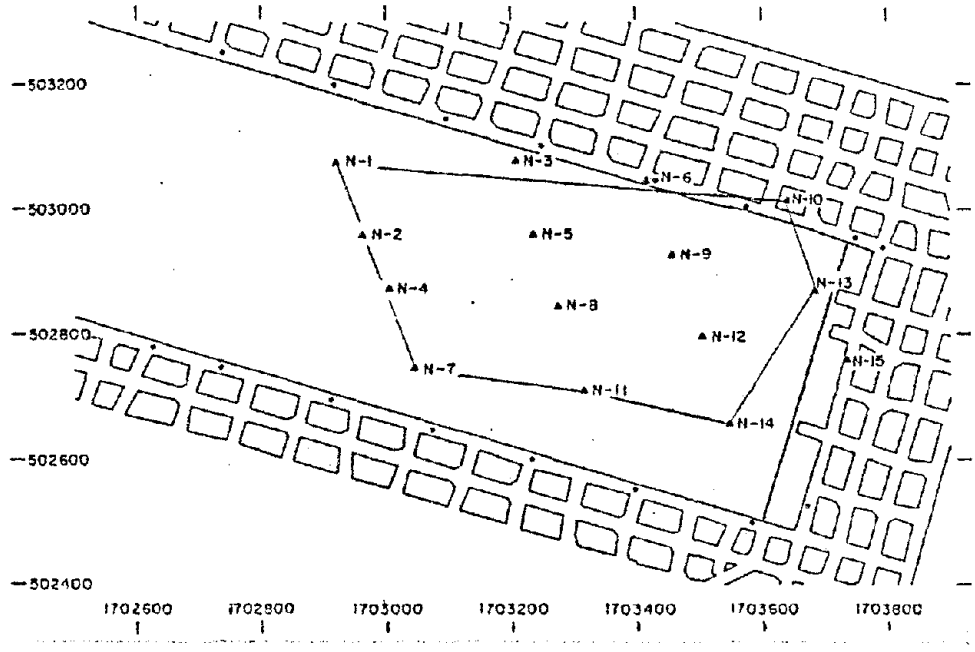

Figure 68. Location of Longwall Face and Geophone Array Utilized: August 2, 1974.

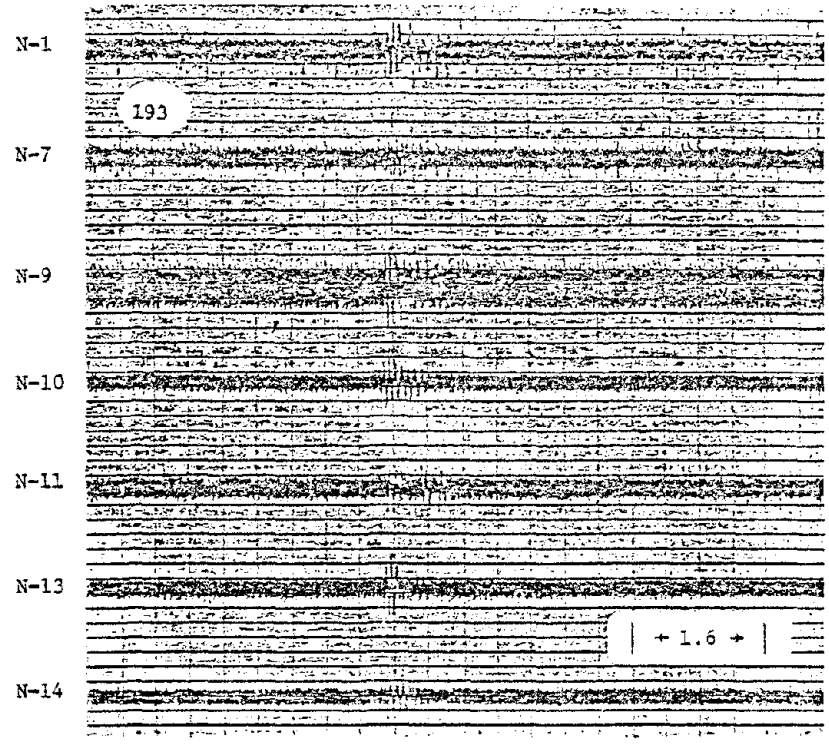

Figure 69. Typical Microseismic Event (53-3742), August 2, 1974. [Horizontal Scale: Time (s); Vertical Scale: Particle Velocity (μips/10 divisions).]

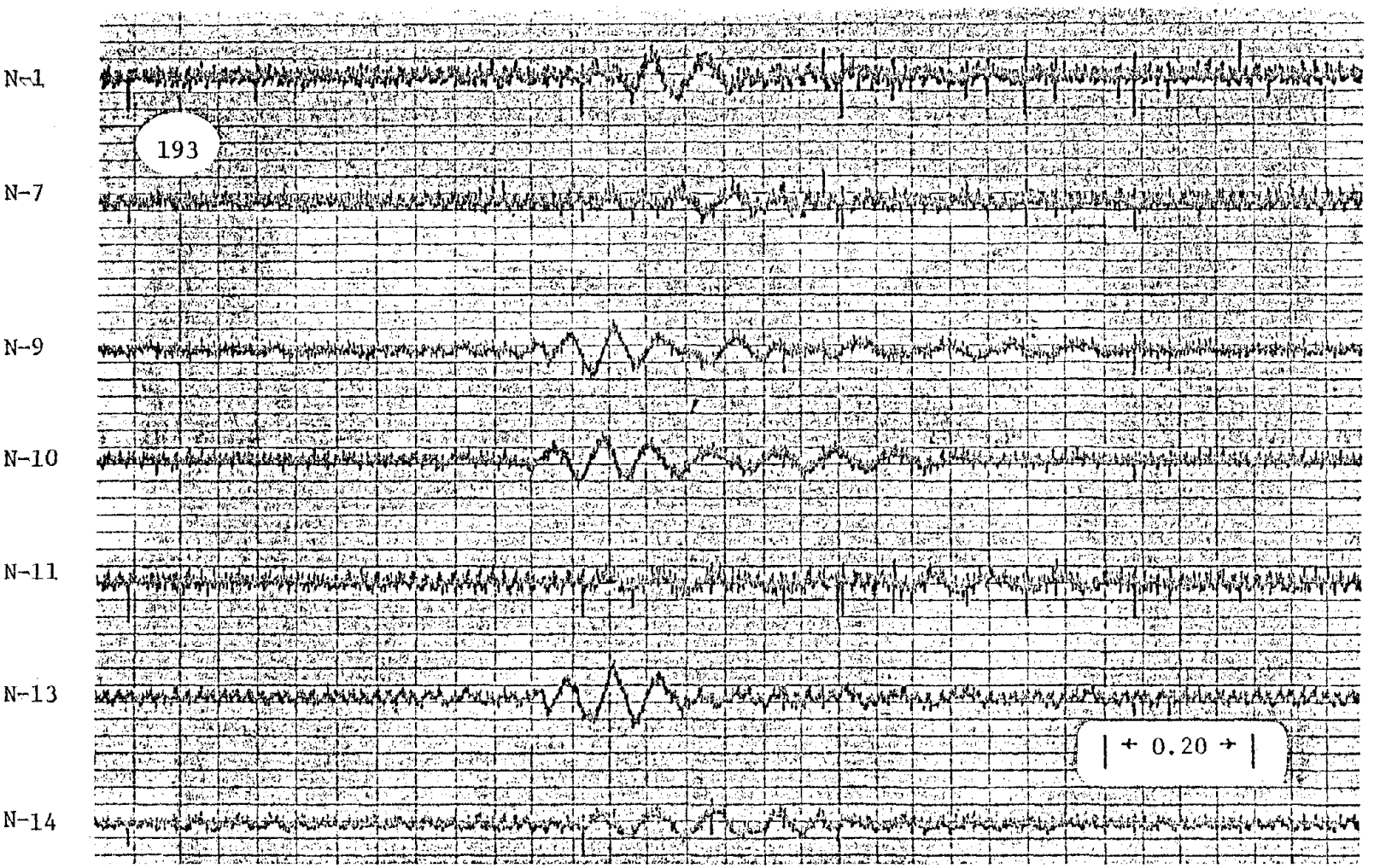

Figure 70. Event (53-3742), August 2, 1974--Time-Expanded. [Horizontal Scale: Time (s); Vertical Scale: Particle Velocity (μips/10 divisions).]

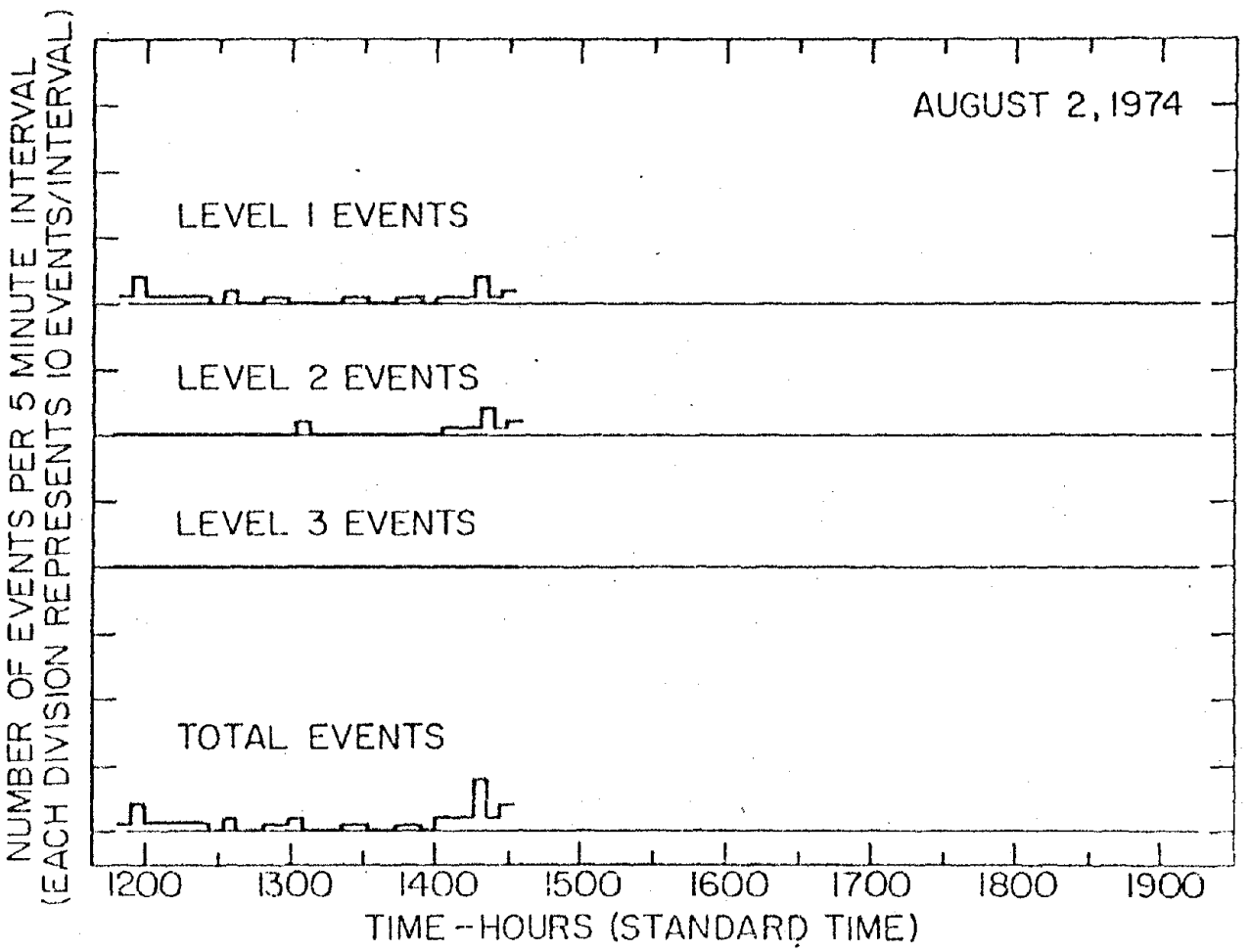

Figure 71. Event Activity Rate Histogram: August 2, 1974.

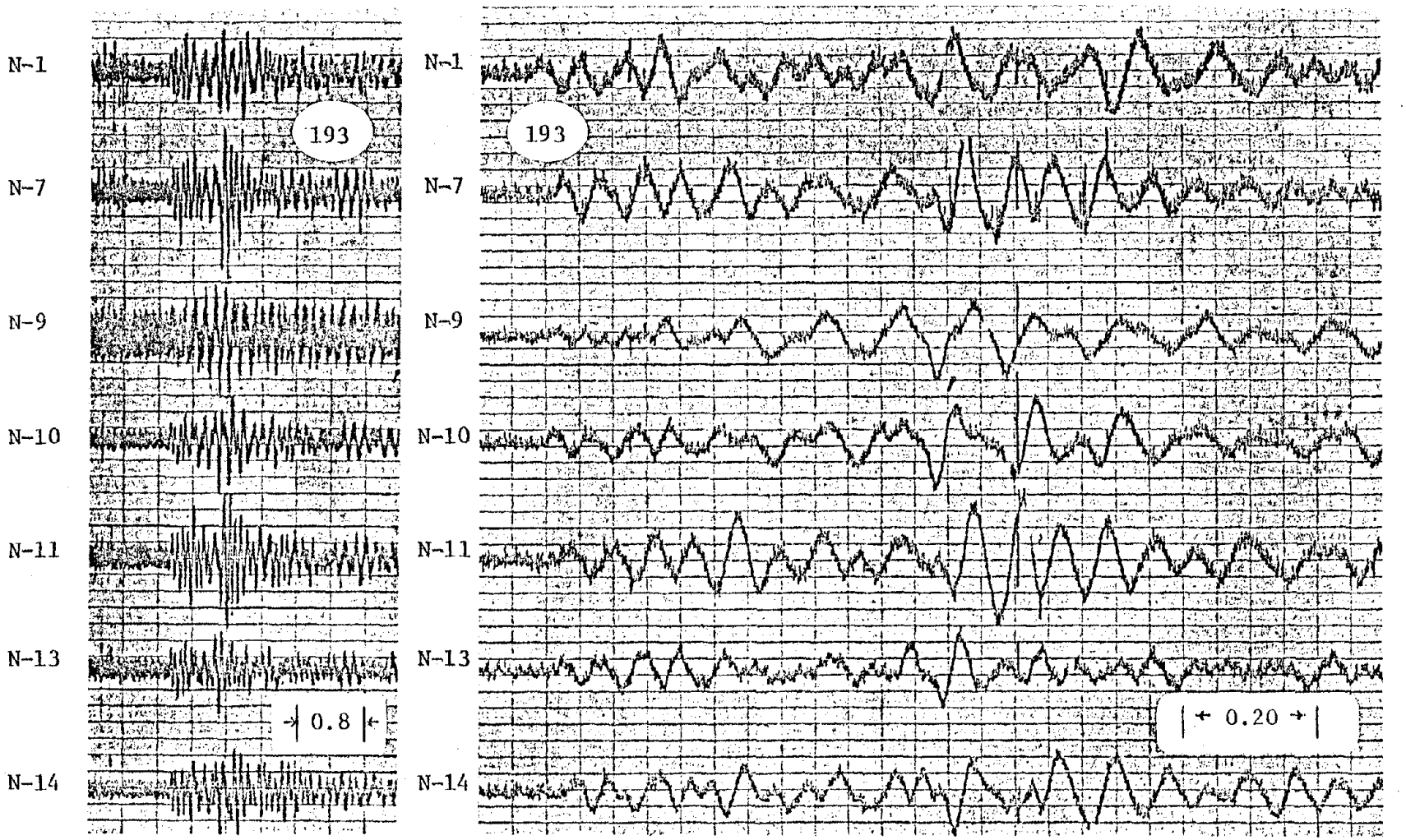

Figure 72. Event (53-4943), August 2, 1974--Time-Expanded. [Horizontal Scale: Time (s); Vertical Scale: Particle Velocity (μips/10 divisions).]

2.8 Four weeks after longwall panel completed

Approximately four weeks after the longwall was completed, a final microseismic data recording session of three hours was conducted utilizing the geophone array N-1, N-7, N-9, N-10, N-11, N-13, and N-14 on August 21. The geophone array is presented in Figure 73.

Only about five level-1 events were detected during the monitoring session. One of these events was of a type not observed in previous recording periods and is given in Figure 74, with a time-expanded version being presented in Figure 75. Note the extremely long arrival time difference between geophone stations N-10 and N-7. This could be indicative of an event occurring at a great distance from the array. This event might have generated a wave which traveled along the surface of the earth at a velocity of 1,000 to 3,000 fps, typical of wave propagation velocities in soils. One other similar event was detected about 1-1/2 hours earlier. A somewhat more typical microseismic event was detected mainly by N-10 and N-13 and is presented in Figure 76. Particle velocities were 10 to 80 µips, and frequencies were 15 to 30 Hz for this event, whose origin was assumed to lie near the headgate at the end of the longwall panel.

As can be seen in Figure 77, the rate of activity was essentially zero (0.02 epm) which suggested that the strata surrounding the completed longwall panel were finally stable.

2.9 Results

Field studies conducted in the proximity of the East B-4 longwall have definitely proven that many microseismic events were detected at

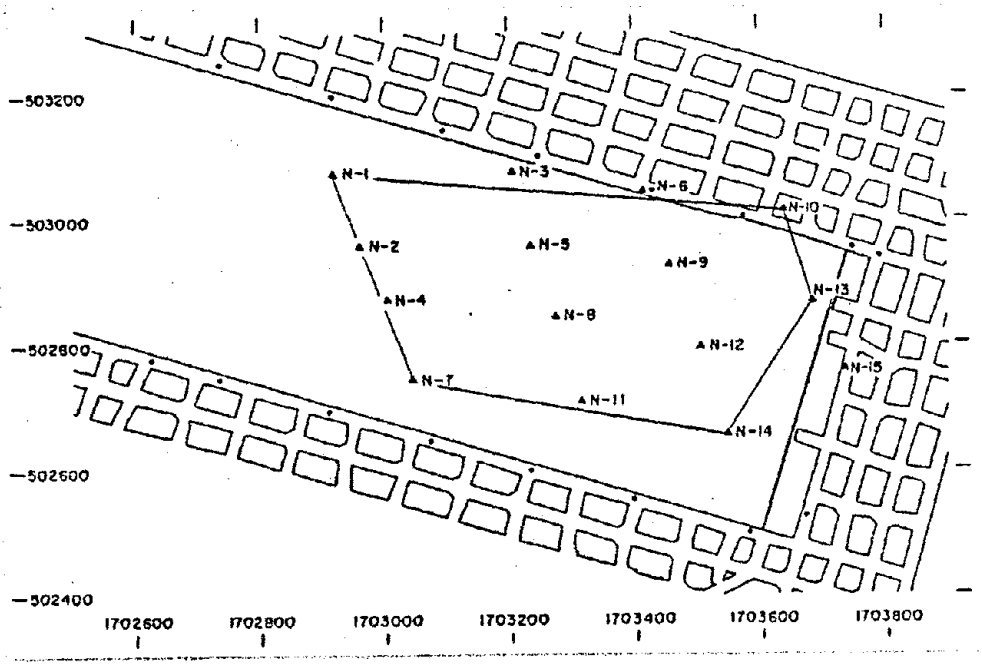

Figure 73. Location of Longwall Face and Geophone Array Utilized: August 21, 1974.

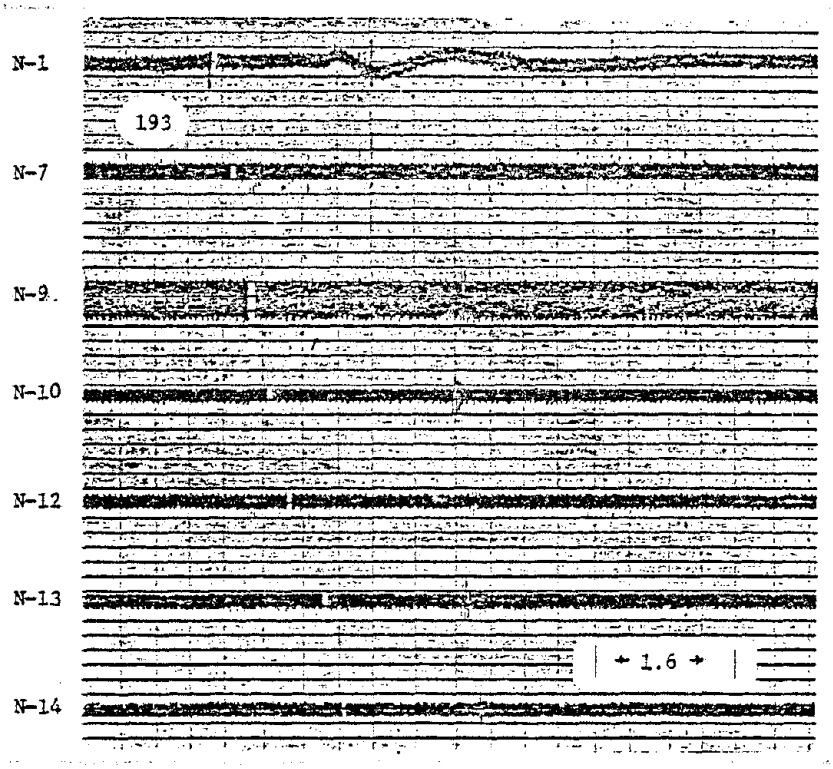

Figure 74. Typical Microseismic Event (32-4767), August 21, 1974. [Horizontal Scale: Time (s); Vertical Scale: Particle Velocity (μips/10 divisions).]

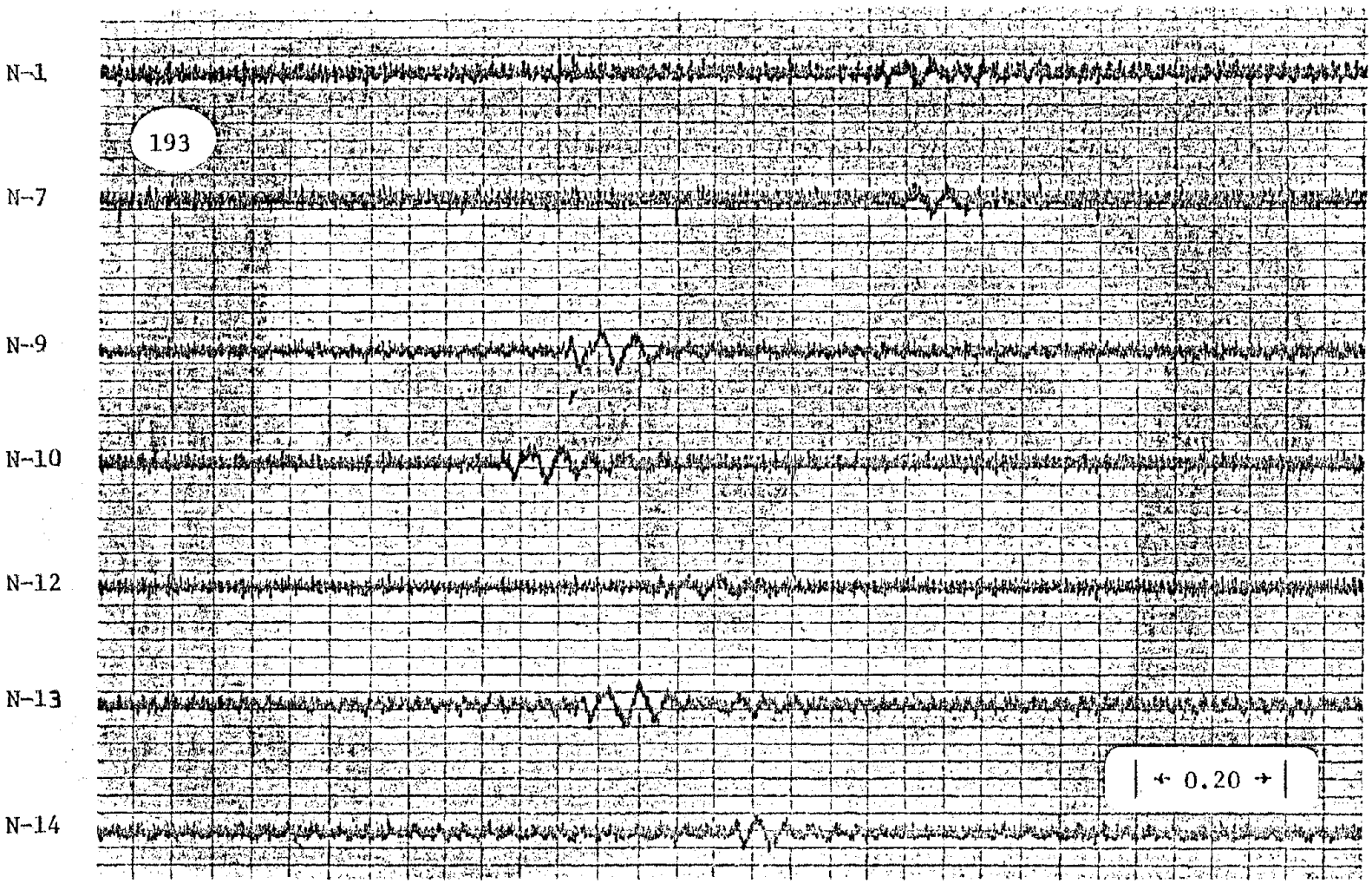

Figure 75. Event (32-4767), August 21, 1974--Time-Expanded. [Horizontal Scale: Time (s); Vertical Scale: Particle Velocity (μips/10 divisions).]

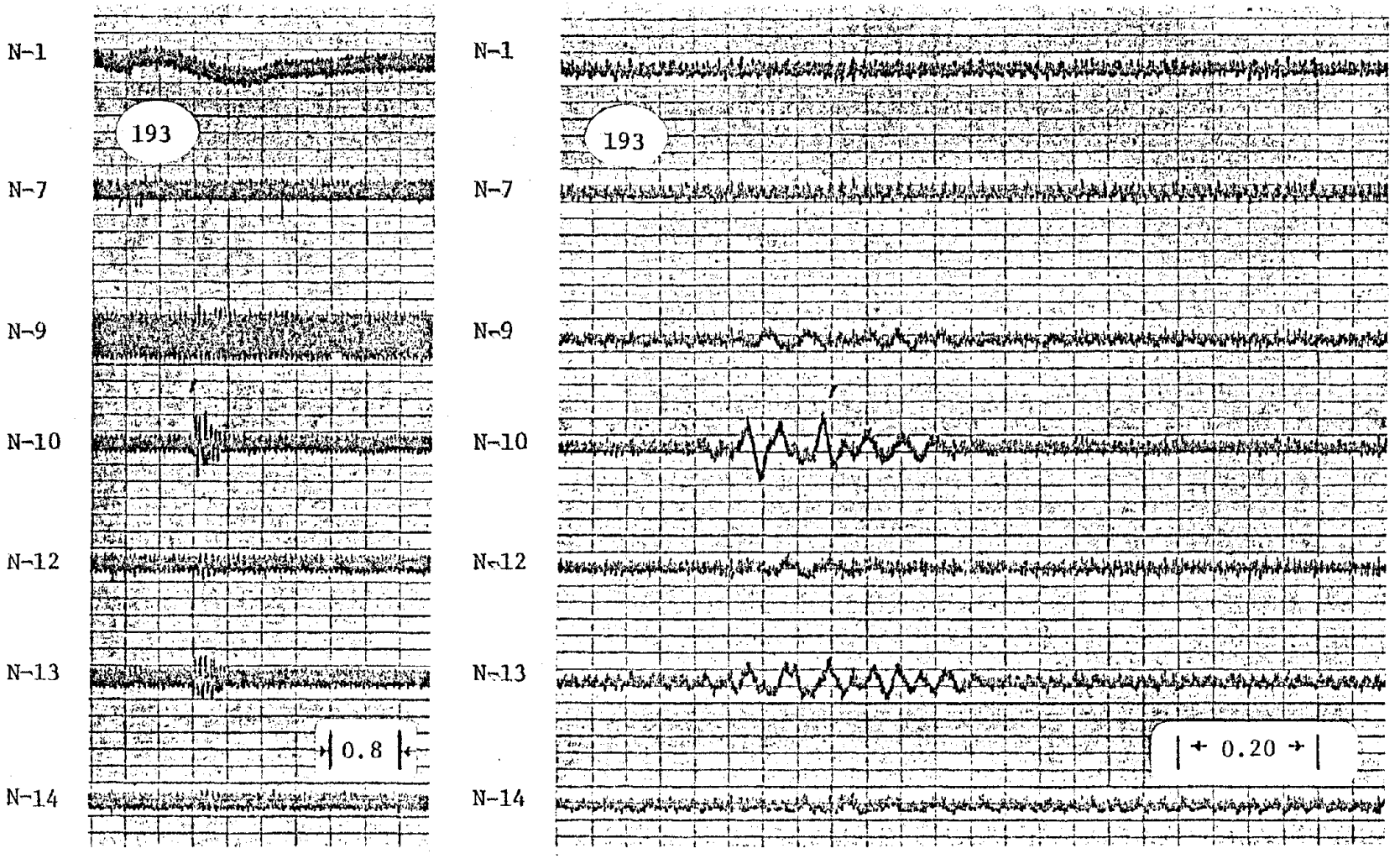

Figure 76. Event (32-2244), August 21, 1974. [Horizontal Scale: Time (s); Vertical Scale: Particle Velocity (μips/10 divisions).]

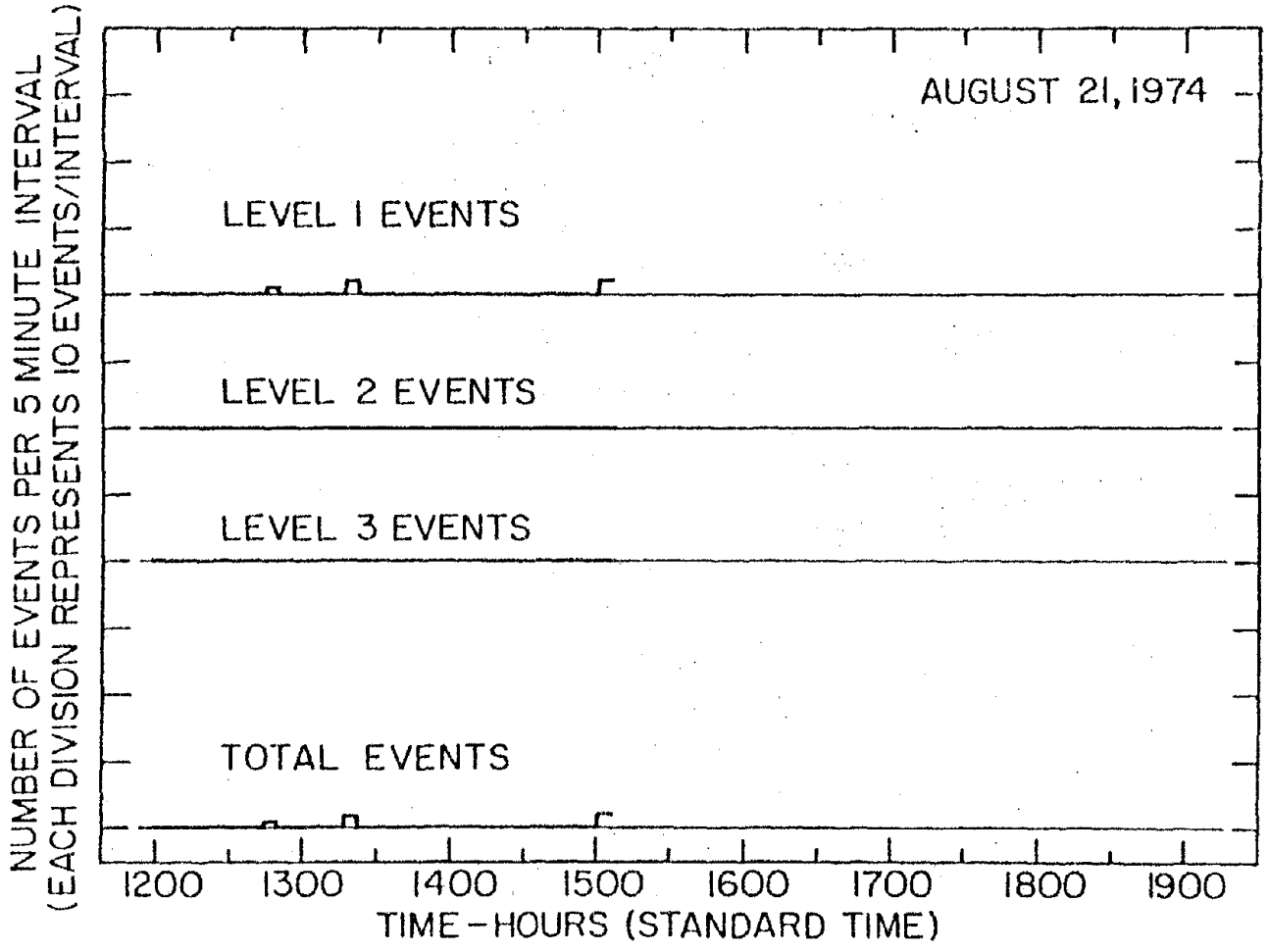

Figure 77. Event Activity Rate Histogram: August 21, 1974.

depths of at least 430 ft and horizontal distances of as much as 1,000 ft using various geophone arrays.

Typical particle velocities for the periods discussed ranged from 20 to more than 500 µips with most values being approximately 50 to 400 µips. Frequency components varied between 6 and 200 Hz, with most events having frequencies of 10 to 100 Hz. The ambient background had a particle velocity level of 10 to 20 µips, and a frequency content primarily composed of 60 Hz and its harmonics.

When the longwall was more than 1,100 ft away from the nearest geophone, no microseismic events were detected; hence, approximately 1,000 to 1,100 ft appeared to be the detection range limitation for the monitoring system.

Generally speaking, the rate of microseismic activity correlated well with both the condition of the longwall (roof, face, and/or gob) and the mining operations. Good cutting of coal (high rate of face advance) usually induced a moderate to high rate of microseismic activity (more than 1 epm), most probably due to good caving behind the chocks (e.g., February 26).

During short periods of longwall downtime such as shift changes, equipment repair, or stopping the shearer to change its direction of travel, the rate of event activity appeared to remain constant for a short time (0 to 15 minutes) after the downtime began and then to decrease rapidly thereafter to a low rate of less than 0.5 epm. Whenever coal was again being cut, the rate of activity rapidly increased to a moderate to high rate within 15 minutes (e.g., February 18 and 26).

For bad roof or face conditions, the rate of activity ranged erratically from 0.2 to 1.0 epm with an average rate of 0.6 epm (e.g.,

February 27). A variety of factors could have contributed to this fluctuating rate, including

(1) shooting rock in the panline, the face, and around the chocks,

(2) events occurring in the roof or on the face due to artificially induced fractures associated with the blasts, and

(3) events occurring due to the natural stress redistribution around the longwall workings.

If the mining operations stopped completely for more than a day, the microseismic activity rate was found to decrease to almost 0 epm (e.g., April 17).

Events observed on only one or two geophones were considered to be originating near the surface close to the responding geophones. Such events were assumed to be generated by fracturing strata below the soil and the subsidence of the immediate area.

3. Source Location of Microseismic Events

3.1 Empirical evaluation of source location techniques

After having proved that detecting microseismic events was feasible, the next step was to locate the origin of the major events as accurately as possible. This was not a simple task, particularly under field conditions. The only data available was a set of geophone traces whose arrival time differences could be determined to within ±1 ms, and the coordinates of each geophone with respect to the longwall. Consequently, the travel-time-difference source location method developed originally by Flinn (1960) and modified by the authors was employed as

it incorporated both quantities along with a wave propagation velocity associated with each geophone. Unfortunately, no velocity surveys had been conducted in the immediate vicinity of the longwall panel.

An empirical evaluation of the accuracy of the travel-time difference method was initially conducted. Four factors affecting the resulting source location solutions were investigated, namely,

(1) array geometry,

(2) arrival time error,

(3) initial source location estimates, and

(4) velocities.

Only a brief summary is included in this section as Appendix C describes this evaluation in detail.

First a set of 12 test points were selected which encompassed the general area of the East B-4 longwall. All points were positioned at the approximate depth of the coal seam. Arrival times were next calculated by dividing the vector distance between each test point and each geophone location by an isotropic velocity of 10,000 fps.

The influence of array geometry on source location accuracy was then evaluated, with a total of nine different array geometries being considered. Provided that the velocity was 10,000 fps in the source location program, array geometry was found to be unimportant as all test points were located to within 5 ft of their true positions for all nine arrays. However, when the velocity was varied from 8,000 fps to 12,000 fps, large errors (greater than 200 ft) in the locations were observed on some events for each array. Array-A, which consisted of geophones N-1 through N-7, and array-B, which was similar to array-A except the geophone N-5 was excluded, appeared to be the two arrays

least influenced by velocity changes. Both of these two arrays were utilized for studies carried out during the month of February.

The effect of arrival time errors on the accuracy of the source location solution was next investigated, as a possible reading error of as much as ±1 ms could exist. One test point was analyzed by introducing a deliberate error of 1 ms on one geophone at a time for array-A. Source locations were then computed with the velocities being incremented between 8,000 fps and 12,000 fps. Maximum errors of ±30 ft in the x-direction, ±20 ft in the y-direction, and ±60 ft in the z-direction resulted for this particular point. Other points were found to generate similar errors. Some source locations were influenced greatly by erroneous arrival times of certain geophones, while other geophones only slightly affected the location solutions.

In order to establish a starting point for the location program, an initial estimate of the approximate source location was needed. The effect of this initial estimate on the resulting source locations was investigated. Results indicated that the initial estimates of the x- and y-coordinates could be as much as 300 ft outside a given array and still provide the correct source location. For the z-coordinate, however, the initial estimate had to be lower than the deepest geophone in the array; otherwise, the source location results would yield z-coordinates located above, rather than below, the geophone array.

By means of such empirical investigations, the source location program was evaluated and found to be suitable, provided accurate input data was available. The only major source of error was that associated with establishing an appropriate velocity model for the longwall panel.

3.2 Application of source location techniques to field data

Source locations were calculated for all level-3 events detected during each microseismic monitoring session. Two velocity models for the longwall were assumed. A totally isotropic velocity model (wave propagation velocities being the same in all three directions) and a unique velocity model (an apparent wave propagation velocity being assigned to each geophone) were utilized to obtain source locations. The results of both models are presented below with Figure 78 giving the source location symbols and their associated descriptions.

Two other velocity models were considered but appeared to be no better than the isotropic velocity model. One such model was that obtained by Beck (1974) in which he used a geophone installed on a plate attached to the mine roof and a borehole probe to detect direct waves generated by shallow buried explosive charges having precisely known detonation times. Velocity values of 9,840 fps in the S30W direction, 9,551 fps in the N60W direction, and 10,739 fps in the vertical direction were determined from his field measurements. These values were incorporated into the source location program and the results were compared with those obtained using the isotropic and the unique velocity models. Overall the results were much less realistic than those of the unique velocity model and were therefore not considered further. The fundamental problems associated with this method were that

(1) the velocity surveys were conducted more than 4,000 ft away from the nearest geophone and could not be safely applied to the East B-4 site, and

KEY

SYMBOL	DESCRIPTION
▲	GEOPHONE LOCATION
○	GEOPHONE NOT UTILIZED
●	INITIAL ESTIMATE OF SOURCE
	SOURCE LOCATION { UPPER VELOCITY LIMIT: 12,000 FPS; AVERAGE VELOCITY LIMIT: 10,000 FPS; LOWER VELOCITY LIMIT: 8,000 FPS
	LOWEST VELOCITY LIMIT NOT SHOWN
	HIGHEST VELOCITY LIMIT NOT SHOWN
•	TEST POINT LOCATIONS
	SOURCE LOCATIONS LIE WITHIN THIS REGION
	SOURCE LOCATIONS LIE ABOVE THE ARRAY
------	LONGWALL FACE POSITION DURING SURVEY
	TOTAL LONGWALL ADVANCE (FEET)
⊙	SOURCE LOCATION - UNIQUE VELOCITY

Figure 78. Source Location Symbols.

(2) strata of varying thicknesses with joints, fractures, and other geologic anomalies, all of which could drastically alter wave paths (and consequently wave velocities), existed between each geophone and the source of any given microseismic event.

A generalized anisotropic velocity model was considered but it was found to be unsatisfactory due to the oversimplification of the true velocity structure. To develop this model, every possible incremental combination of x, y, and z velocity values were considered, between a minimum and a maximum for each velocity direction. Such a generalized approach took a considerable amount of computer time, making each source location very costly. In addition, as the true source locations of the events were not known, it was impossible to select the appropriate combination of x, y, and z velocity values.

Horizontal source locations: isotropic velocity model -- On February 18, two geophone arrays were utilized. Six events were detected using the first array and these were computed to be from 50 to 250 ft ahead of the longwall face as shown in Figure 79. These locations appeared to be unrealistic as current longwall studies have indicated that most fractures occur less than 30 ft ahead of the face. Three of the events were located outside the array about two-thirds down from the headgate. Many of the bad face and roof conditions were reported by the mine crew to frequently occur in this region, but they existed at the face rather than ahead of it. Figure 80 shows the three events detected by the second array. All three events were computed

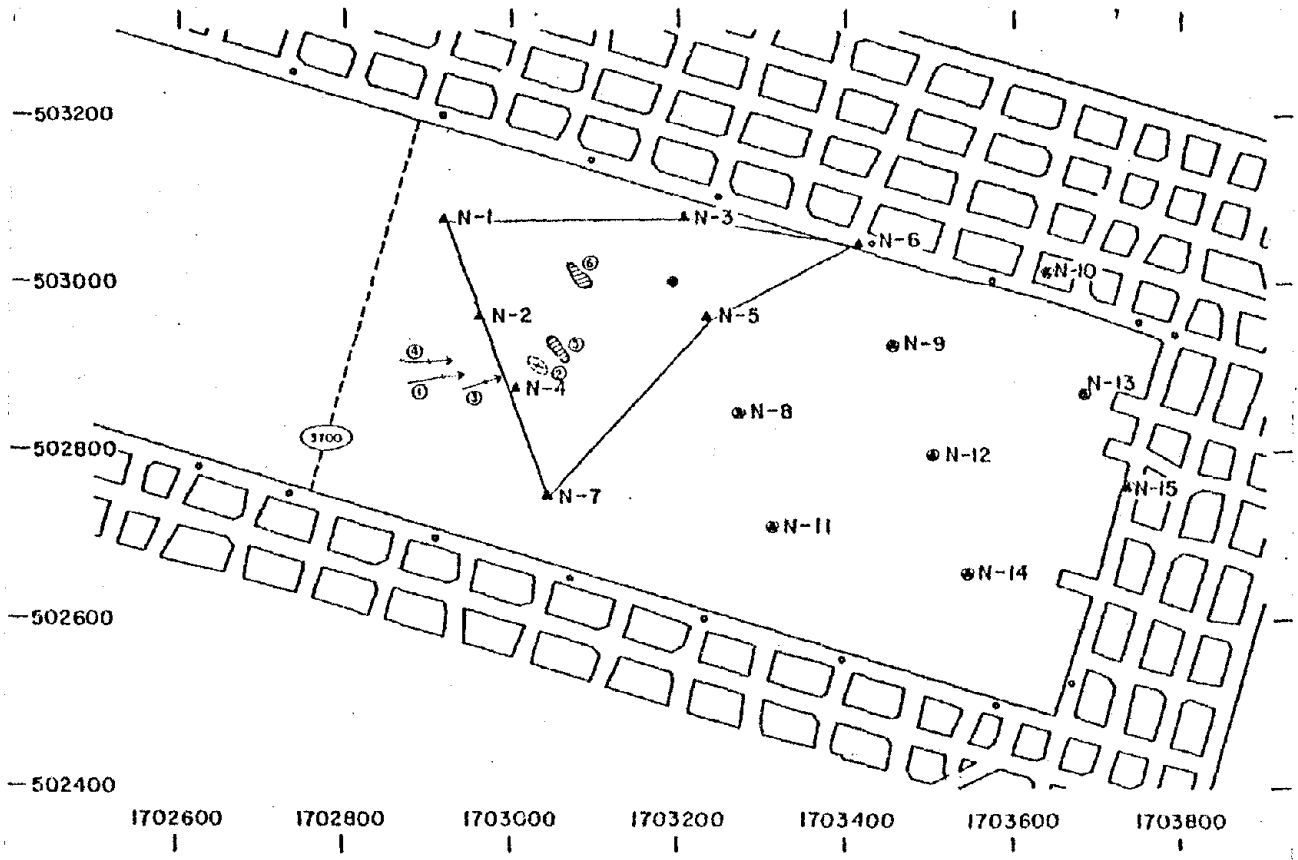

Figure 79. Source Location Plot, First Geophone Array, February 18, 1974: Isotropic Velocity Model.

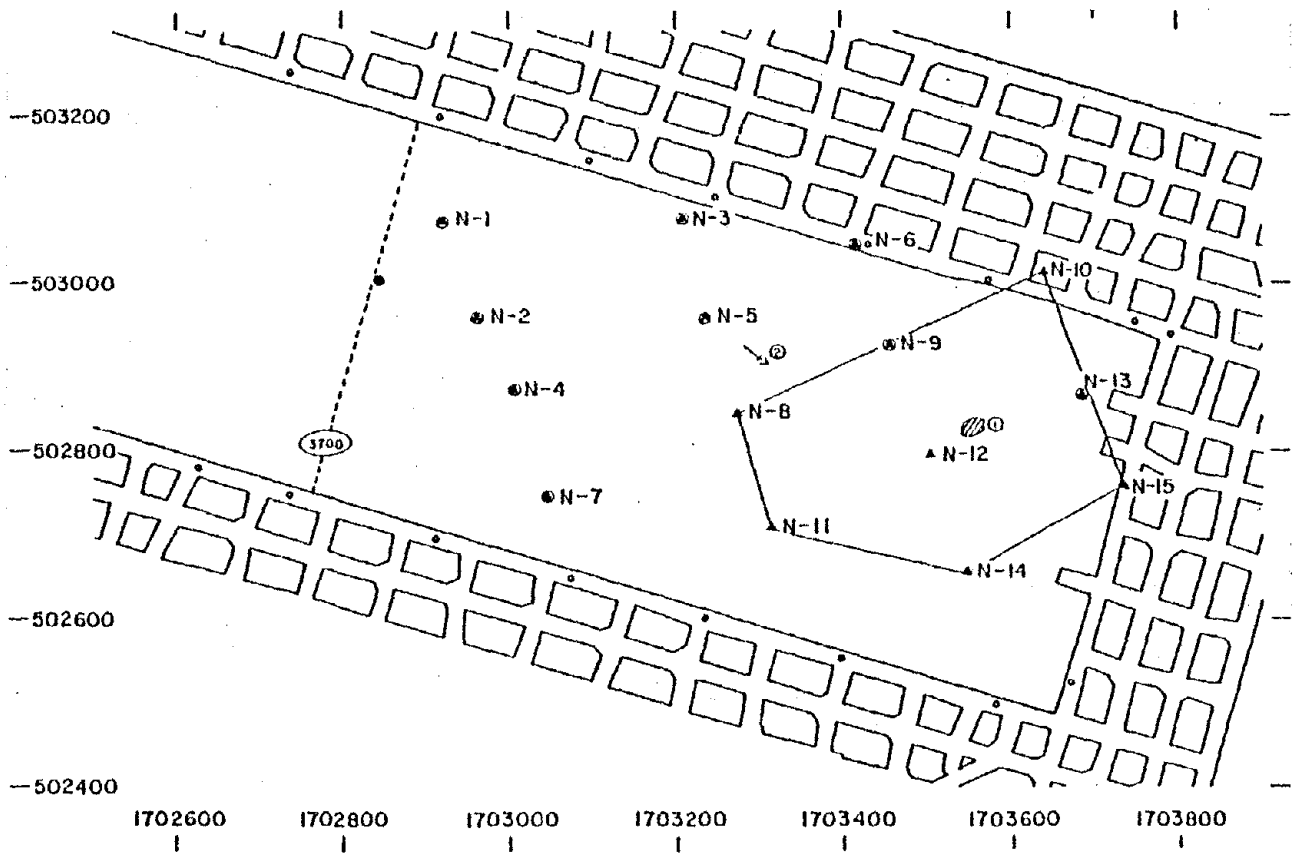

Figure 80. Source Location Plot, Second Geophone Array, February 18, 1974: Isotropic Velocity Model.

to be more than 400 ft ahead of the face. Instabilities in the strata at these distances from the face were again highly unlikely.

On February 26, a total of 39 events were located as shown in Figure 81. Four of the events, namely 3, 7, 16, and 18, were computed to lie 50 to 200 ft behind the face. The majority of the events clustered inside the boundaries of the array and from 30 to 250 ft ahead of the longwall face. Three events (9, 11, and 36) were located above ground level. Events 14 and 27 were just in front of the headgate pillar. Event 20, the blast, was located underneath the center of a pillar 150 ft ahead of the tailgate. This particular event was accurately located by mine personnel, and its coordinates were documented (x = 2,880 ft; y = 2,716 ft; and z = 1,325 ft) by R. Kim, one of the project personnel stationed underground during this time to record mining activities. Consequently, the isotropic velocity model appeared to shift event 20 approximately 150 ft southeast from the blast site. This suggested that the other events might have had similar location shifts.

Two array configurations were employed on the following day, February 27. Seven events were located using the first array as shown in Figure 82. Events 1 and 6 were 50 to 100 ft ahead of the face, event 3 was two pillars northeast of the headgate, and events 4 and 7 were more than 100 ft ahead of the face. When the second array was used, in which geophone N-15 replaced N-5, most events clustered about two-thirds of the distance south of the headgate and were located up to 150 ft ahead of the face as shown in Figure 83. Events 9, 12, and 15 were localized between two pillars approximately 200 ft southeast of

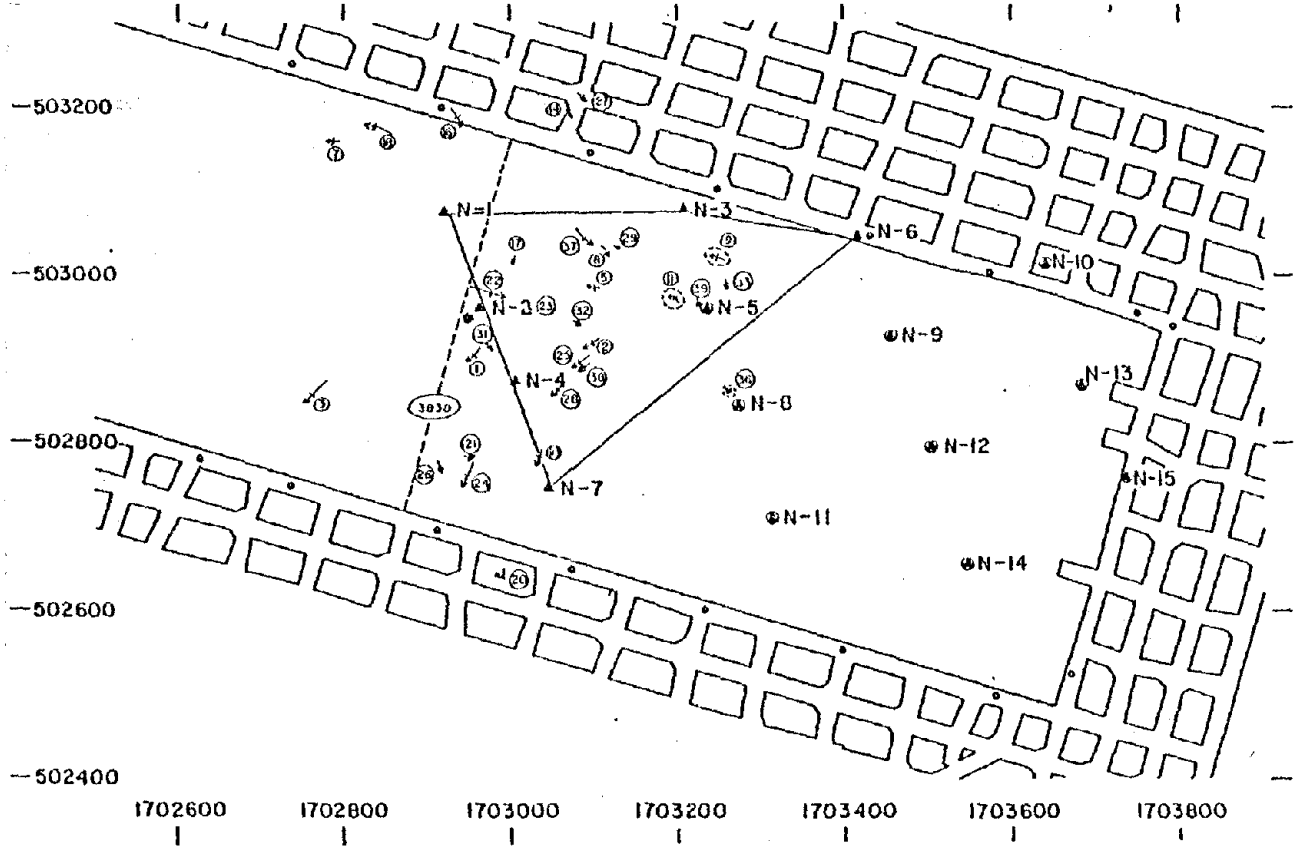

Figure 81. Source Location Plot, February 26, 1974: Isotropic Velocity Model.

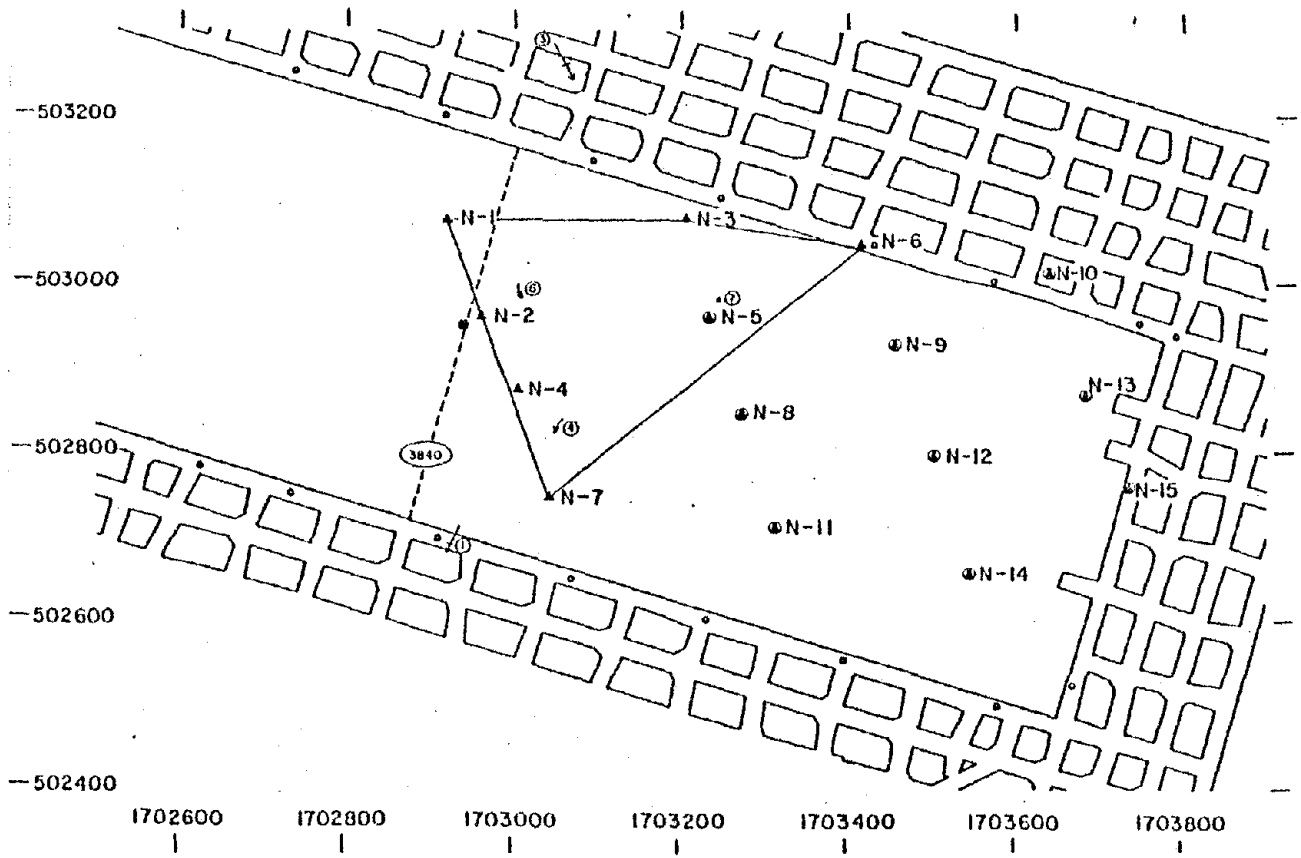

Figure 82. Source Location Plot, First Geophone Array, February 27, 1974: Isotropic Velocity Model.

the tailgate. Events 1 and 17 were between 50 and 100 ft behind the face, both being in the gob area.

Microseismic data from other field trips discussed in this report did not exhibit level-3 events; consequently, source location calculations were not carried out in these cases.

Horizontal source locations: unique velocity model -- Microseismic data from a blast which occurred on February 26, having a location of x = 2,880 ft; y = 2,716 ft; and z = 1,325 ft, was used in conjunction with a source location subroutine program (Leighton, 1970) to obtain unique velocities for each geophone employed in the array. The waveform generated by the blast and its time-expanded version are presented in Figure 84. The unique velocities calculated for each geophone were as follows: N-1 = 8,985 fps; N-2 = 8,556 fps; N-3 = 9,542 fps; N-4 = 8,740 fps; N-6 = 10,790 fps; and N-7 = 8,891 fps.

Applying the resulting unique velocities to the analysis of data obtained for February 18, it was found, as shown in Figure 85, that source locations were shifted considerably towards the longwall face as compared with those obtained with the isotropic velocity model (Figure 79). For example, events 5 and 6 were not located within 50 ft behind the face in the gob and events 1, 2, and 3 were less than 70 ft in front of the face. Only event 4 appeared to be erroneous, being approximately 150 ft ahead of the longwall.

As shown in Figure 86, analysis of the data obtained on February 26, exhibited an extremely good event distribution. It should be noted that the distribution of events congregated fairly evenly within 100 ft on either side of the longwall face. Event 20, the blast,

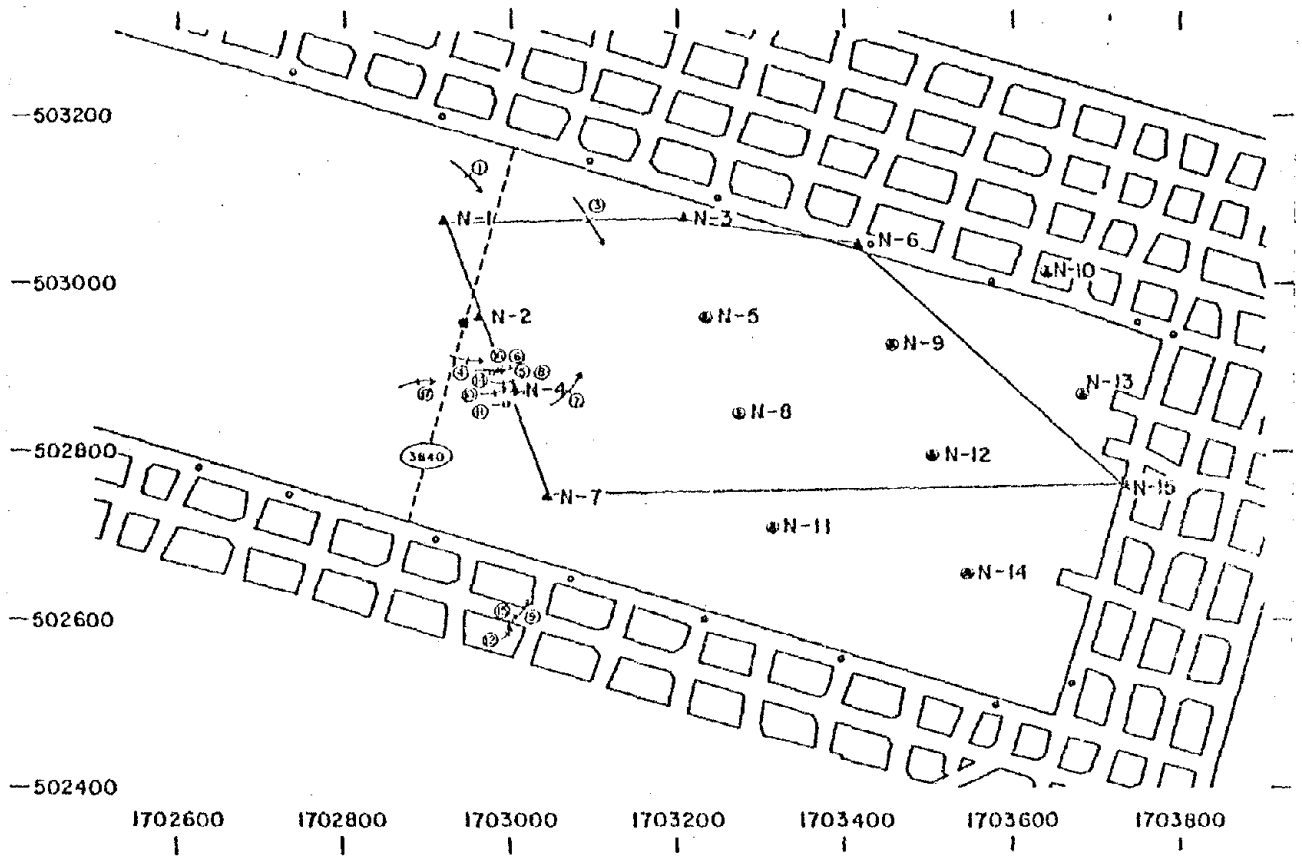

Figure 83. Source Location Plot, Second Geophone Array, February 27, 1974: Isotropic Velocity Model.

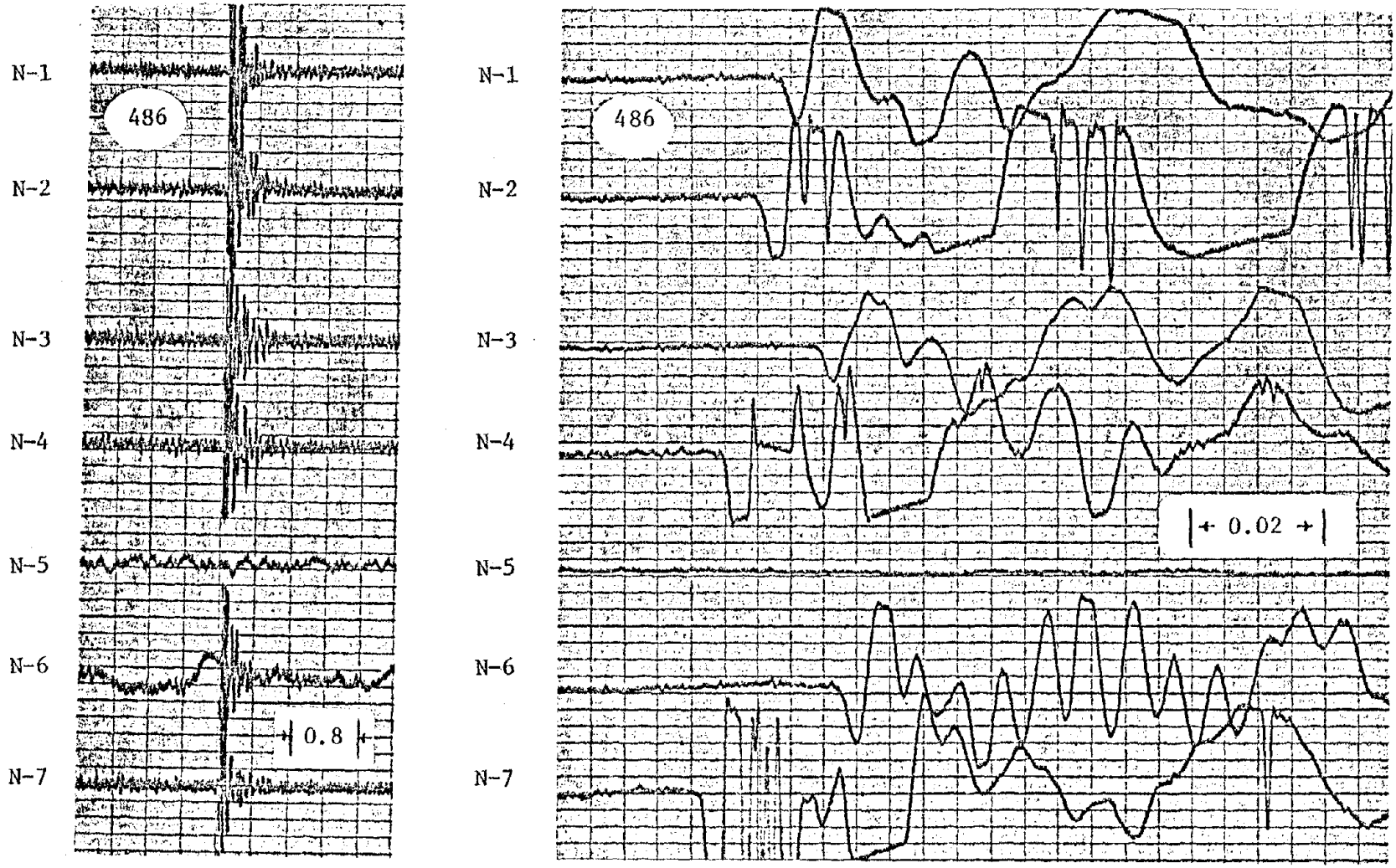

Figure 84. Blast (38-4280) Used to Determine Unique Velocity Model.

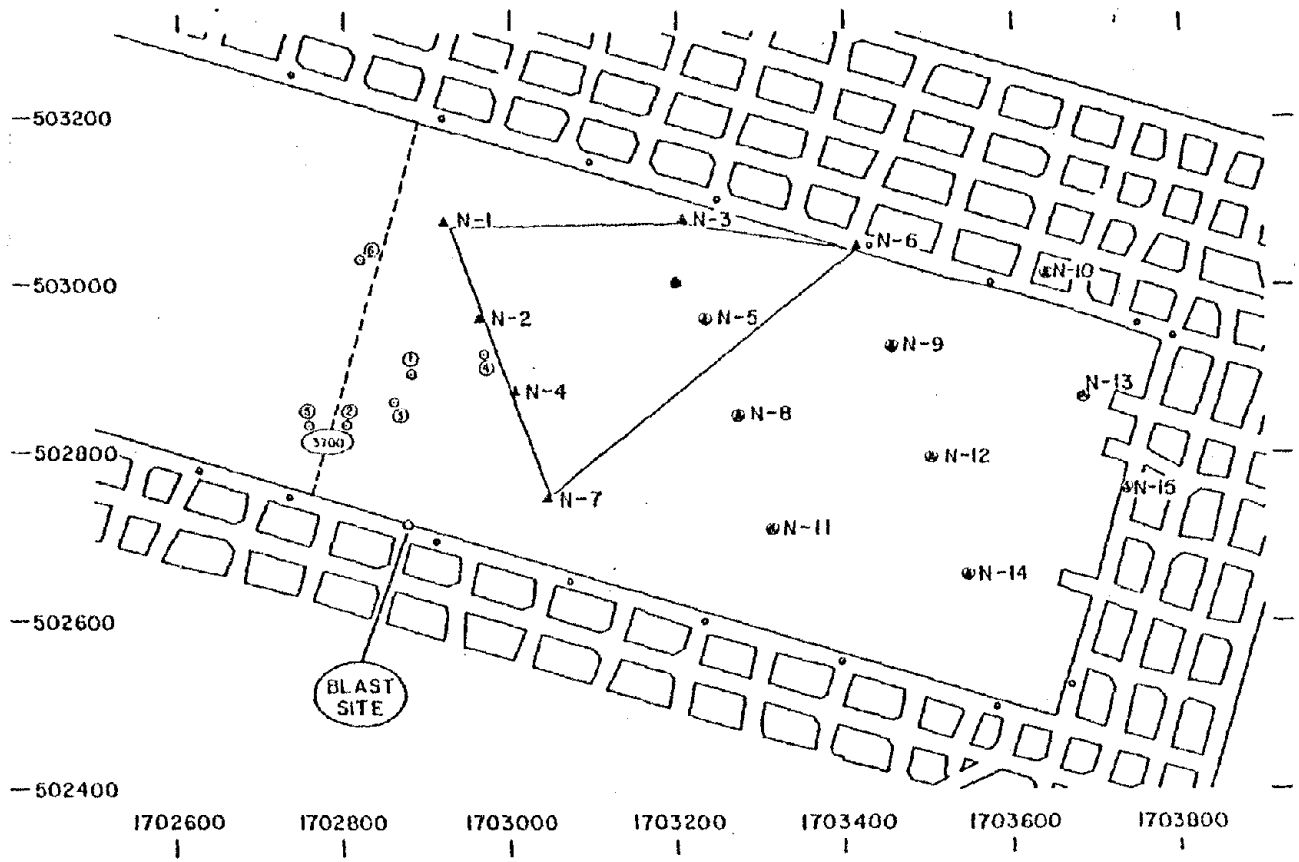

Figure 85. Source Location Plot, First Geophone Array, February 18, 1974: Unique Velocity Model.

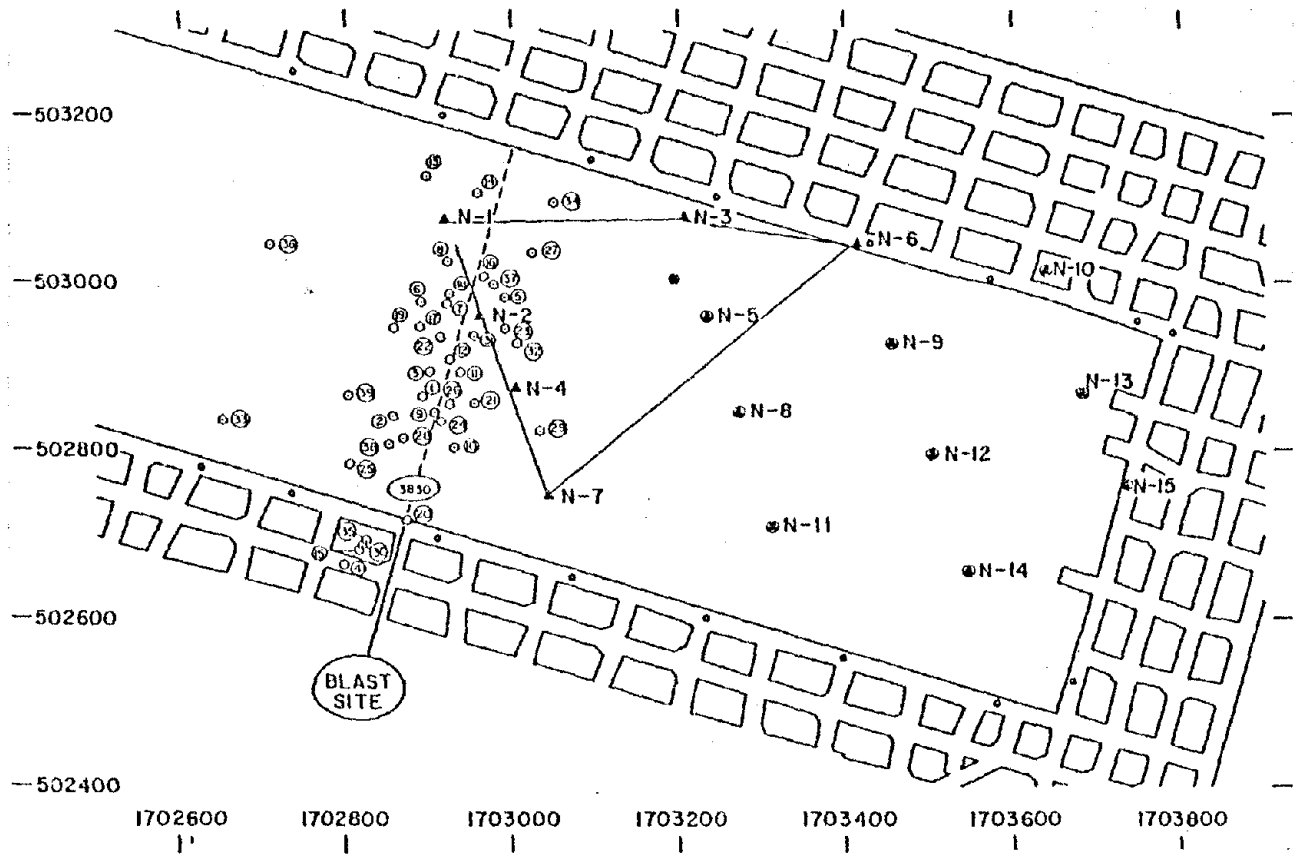

Figure 86. Source Location Plot, February 26, 1974: Unique Velocity Model.

occurred at its correct location. Events 33 and 36 were more than 200 ft back from the face. Events 4, 15, 30, and 35 were clustered around the center of a pillar just behind the tailgate. This strongly suggested that the pillar was undergoing a change in stress and may have become unstable.

As shown in Figure 87, on February 27, using the first array and unique velocities, all events were located at or slightly ahead of the face except for event 7, which was located in the gob about 150 ft back from the face. Using the second array which included geophone N-15, however, introduced some problems since the unique velocity associated with N-15 was unknown. In order to carry out source location calculations, a velocity value of 10,000 fps was assumed for N-15. Figure 88 illustrates the results, which were extremely scattered. Many of the events were more than 200 ft ahead of the longwall face, with only events 3, 5, 6, 7, 10, and 11 falling within 100 ft of the face. Since these results were considered erroneous, source locations of these events were recomputed, this time excluding data from geophone N-15. The results, shown in Figure 89, indicated that most of the events now clustered within 50 ft of the face and at a position about two-thirds of the distance from the headgate, where bad face and roof conditions were not uncommon. Events 4 and 11 were located just ahead of the tailgate, a region also subjected to higher than normal stresses.

Vertical source locations: unique velocity model -- Only the vertical source location data calculated by means of the unique velocity model were considered sufficiently accurate to be discussed here. Source locations calculated for the isotropic model had too much scatter

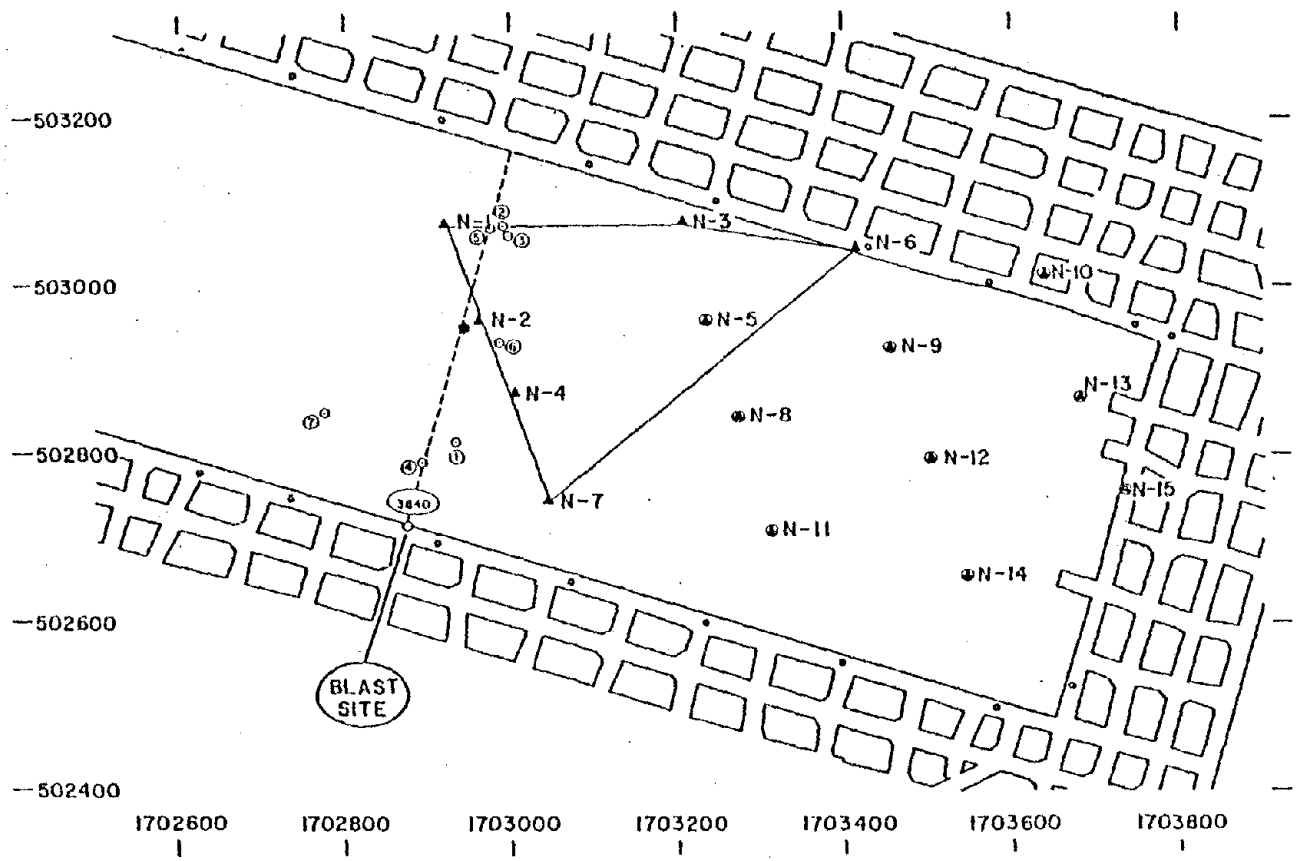

Figure 87. Source Location Plot, First Geophone Array, February 27, 1974: Unique Velocity Model.

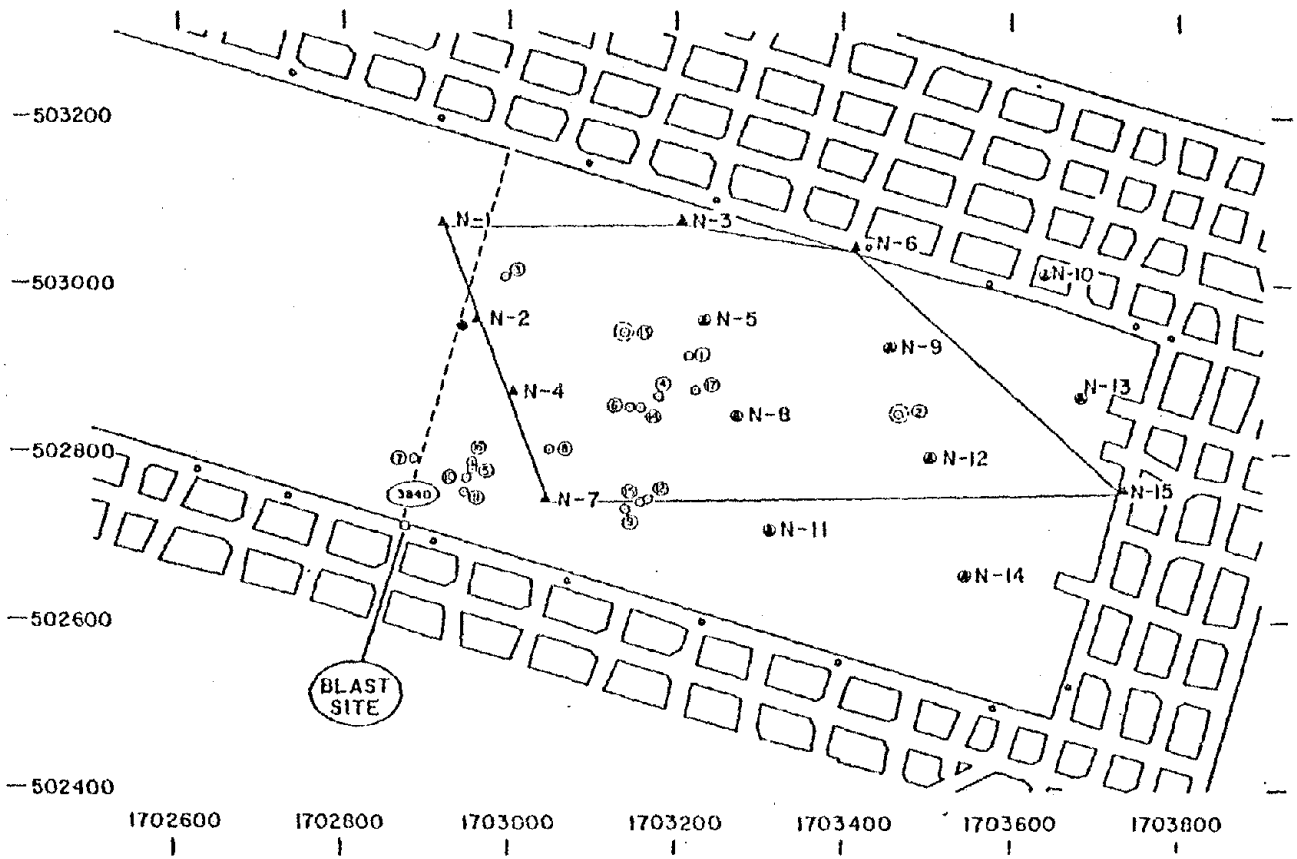

Figure 88. Source Location Plot, Second Geophone Array, February 27, 1974: Unique Velocity Model.

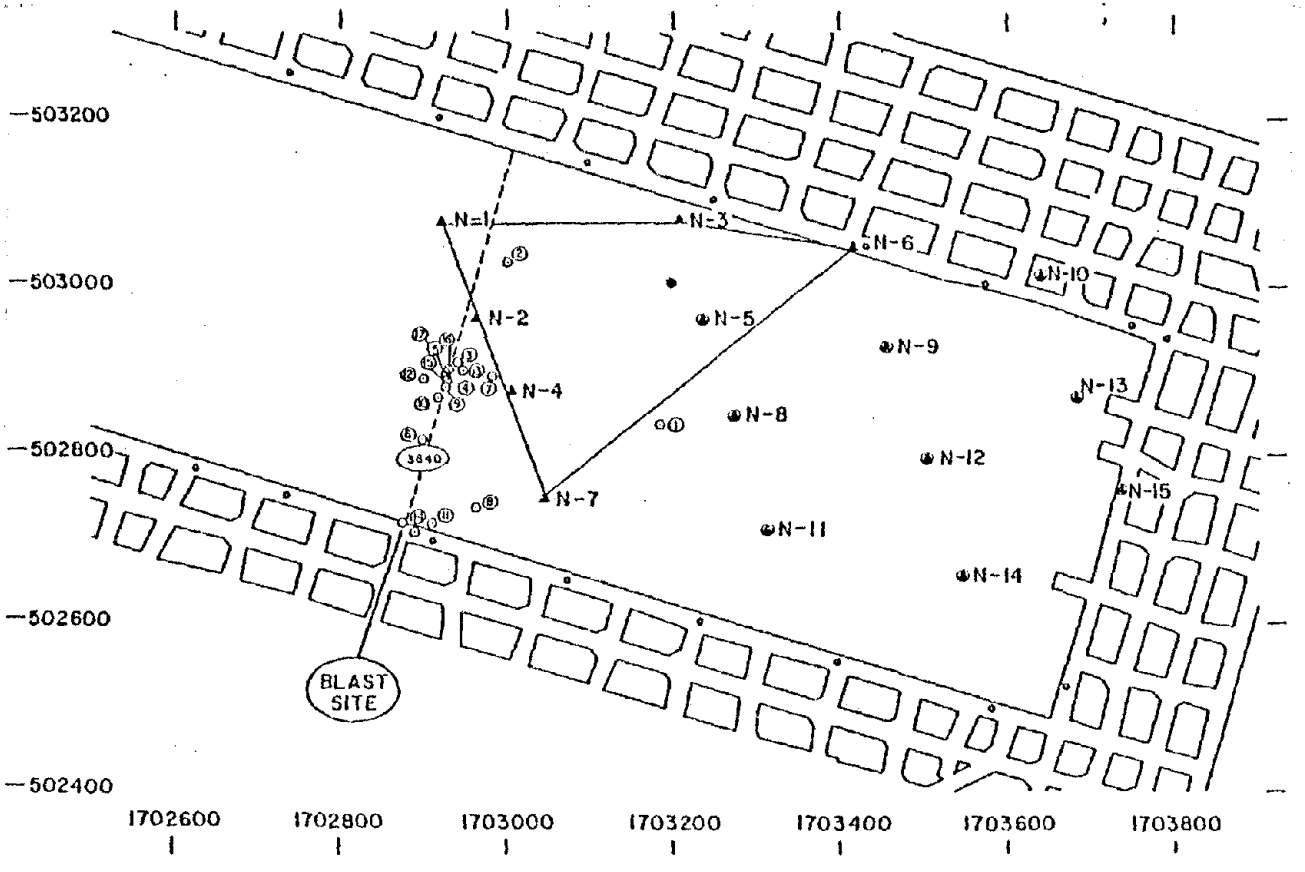

Figure 89. Source Location Plot, Modified Second Geophone Array, February 27, 1974: Unique Velocity Model.

in the vertical direction (z-coordinate) to present meaningful plots. For display of this data, it was plotted on a vertical cross-section of the longwall. In the associated graphs the headgate is located on the left-hand side of the graph, and the tailgate (460 ft from the headgate) is located on the right.

Figures 90 to 93 illustrate the projections of the source location data on vertical cross-sections of the longwall. Figure 90 (February 18) shows a considerable scatter in the points plotted, with four events lying above and two events lying below the coal seam. Fracturing in the intermediate and main roof is normal in longwall mining operations. However, fracturing beneath a solid floor is rather unlikely unless the strata below the seam had pre-existing fractures. Also all events tended to lie between midface and the tailgate, where roof problems frequently occurred. As illustrated in Figure 91, on February 26 events were found to lie as much as 200 ft above or below the seam. Generally, the majority of events were vertically located within 50 ft of the seam. Event 20, the calibration blast, was found to be located precisely where it was known to have originated. Events 15, 30, and 35 were clustered 40 ft to the right of and about 50 ft below the tailgate. Major fracturing appeared to be occurring along the entire longwall face, while the coal was being successfully extracted. Figure 92, illustrating data obtained using the first geophone array on February 27, shows all but one event lying beneath the coal seam; nevertheless, every event, except for event 7, was within 60 ft of the seam. Figure 93 illustrates the source locations obtained on February 27, using the modified second geophone array in which data from N-15 was excluded in the calculations. It should be noted that

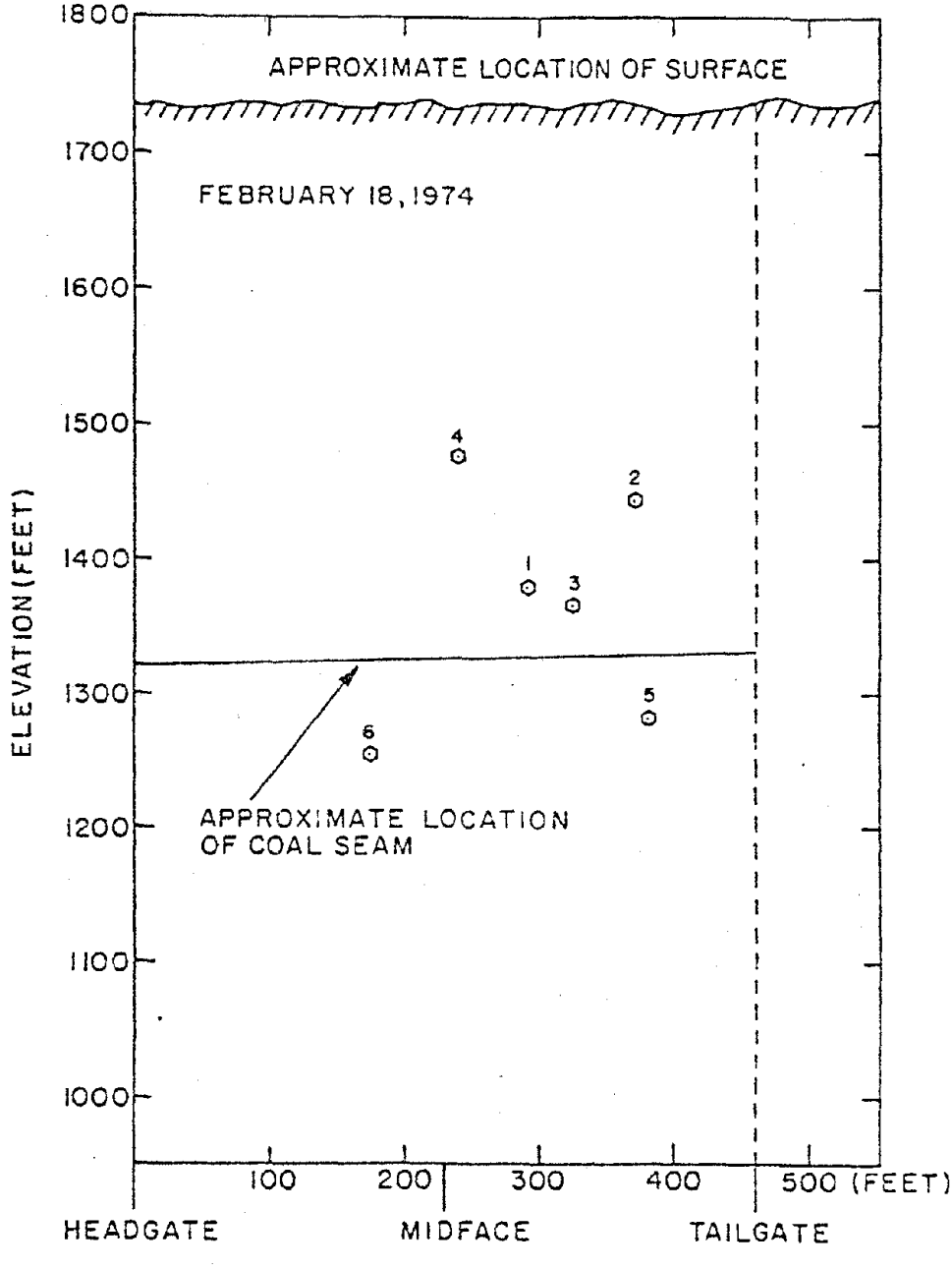

Figure 90. Projections of Source Locations Plotted on Vertical Cross-Sections of Longwall, February 18, 1974: Unique Velocity Model.

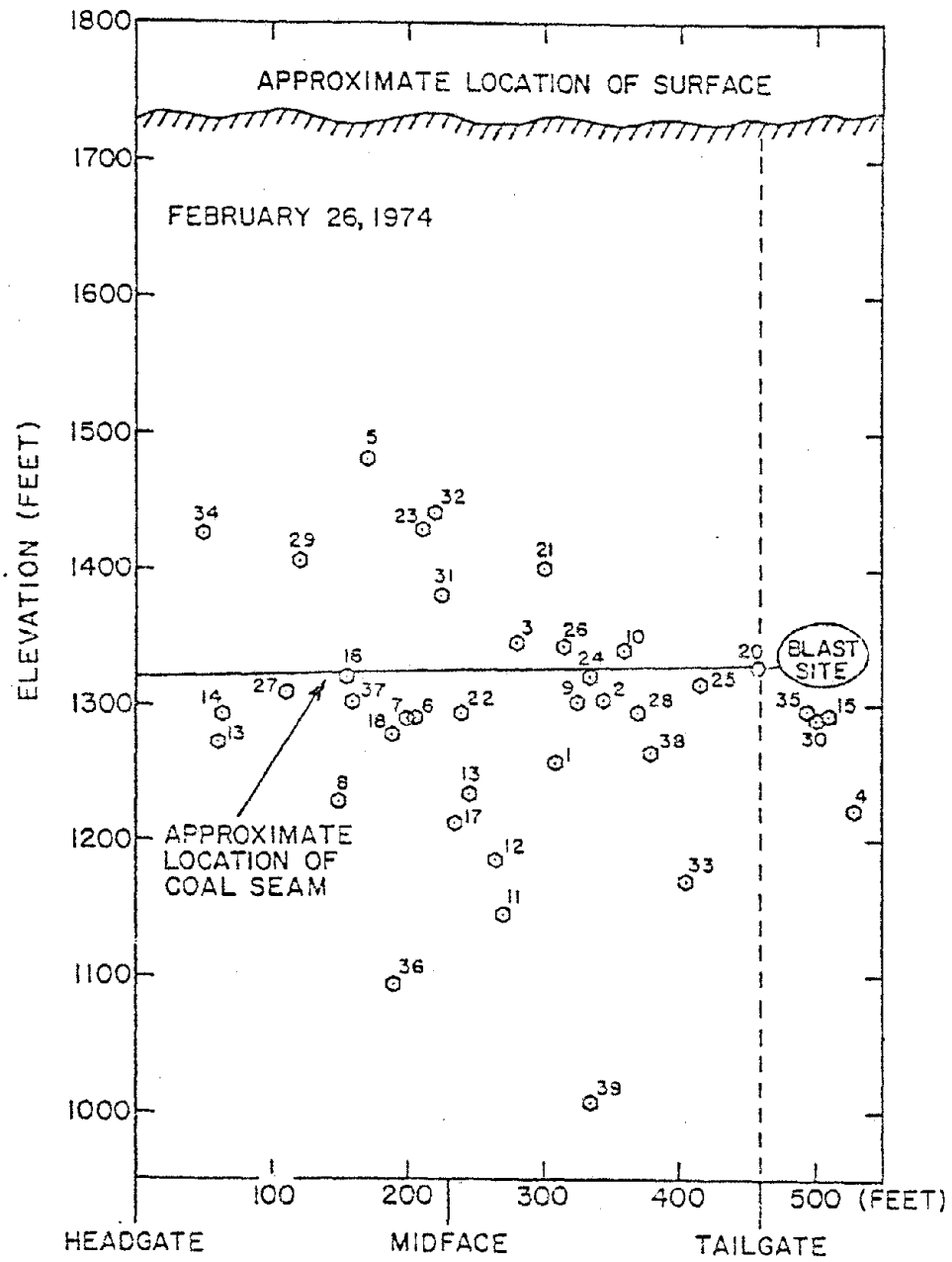

Figure 91. Projections of Source Locations Plotted on Vertical Cross-Sections of Longwall, February 26, 1974: Unique Velocity Model.

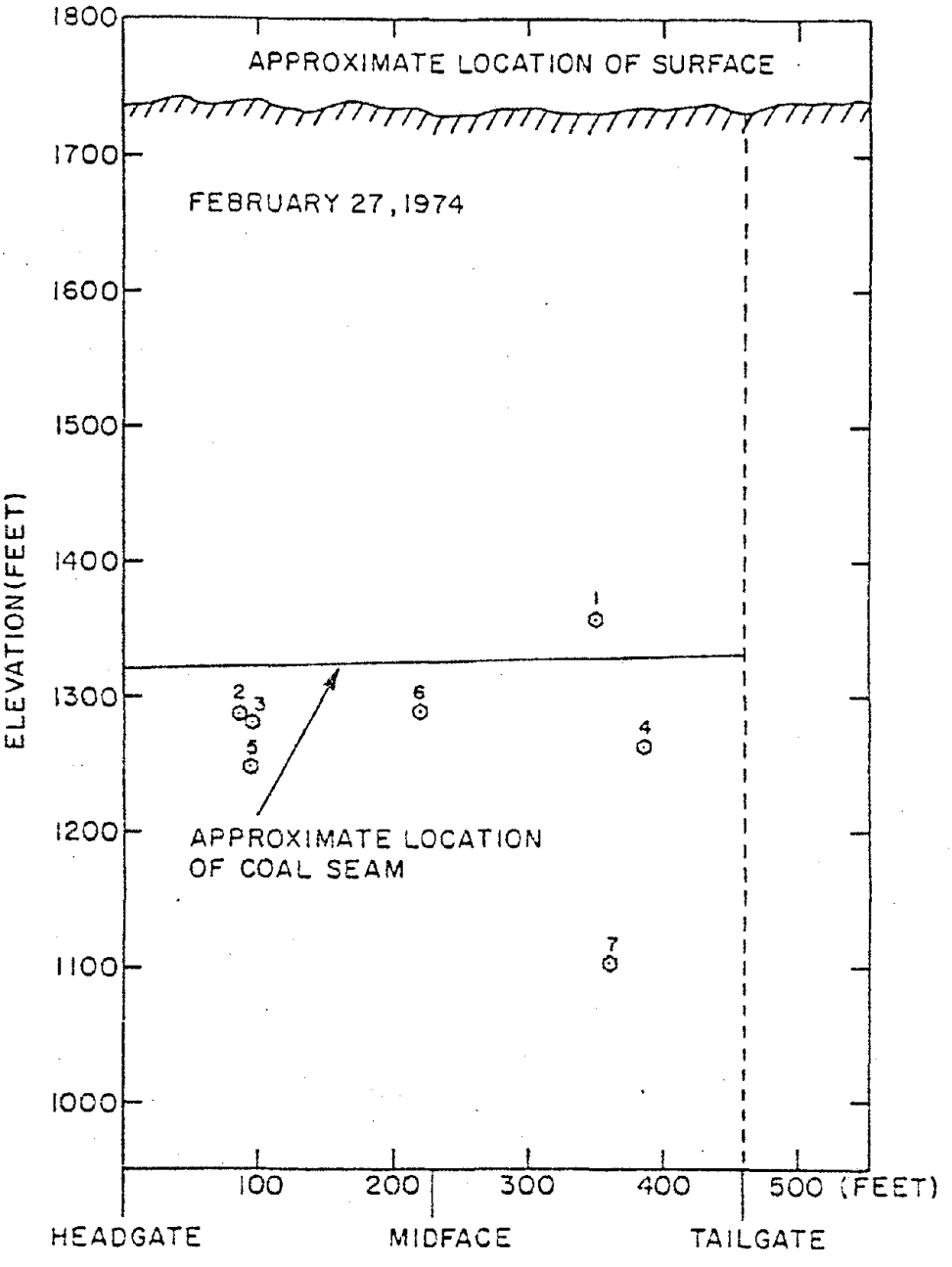

Figure 92. Projections of Source Locations Plotted on Vertical Cross-Sections of Longwall, February 27, 1974: Unique Velocity Model, First Geophone Array.

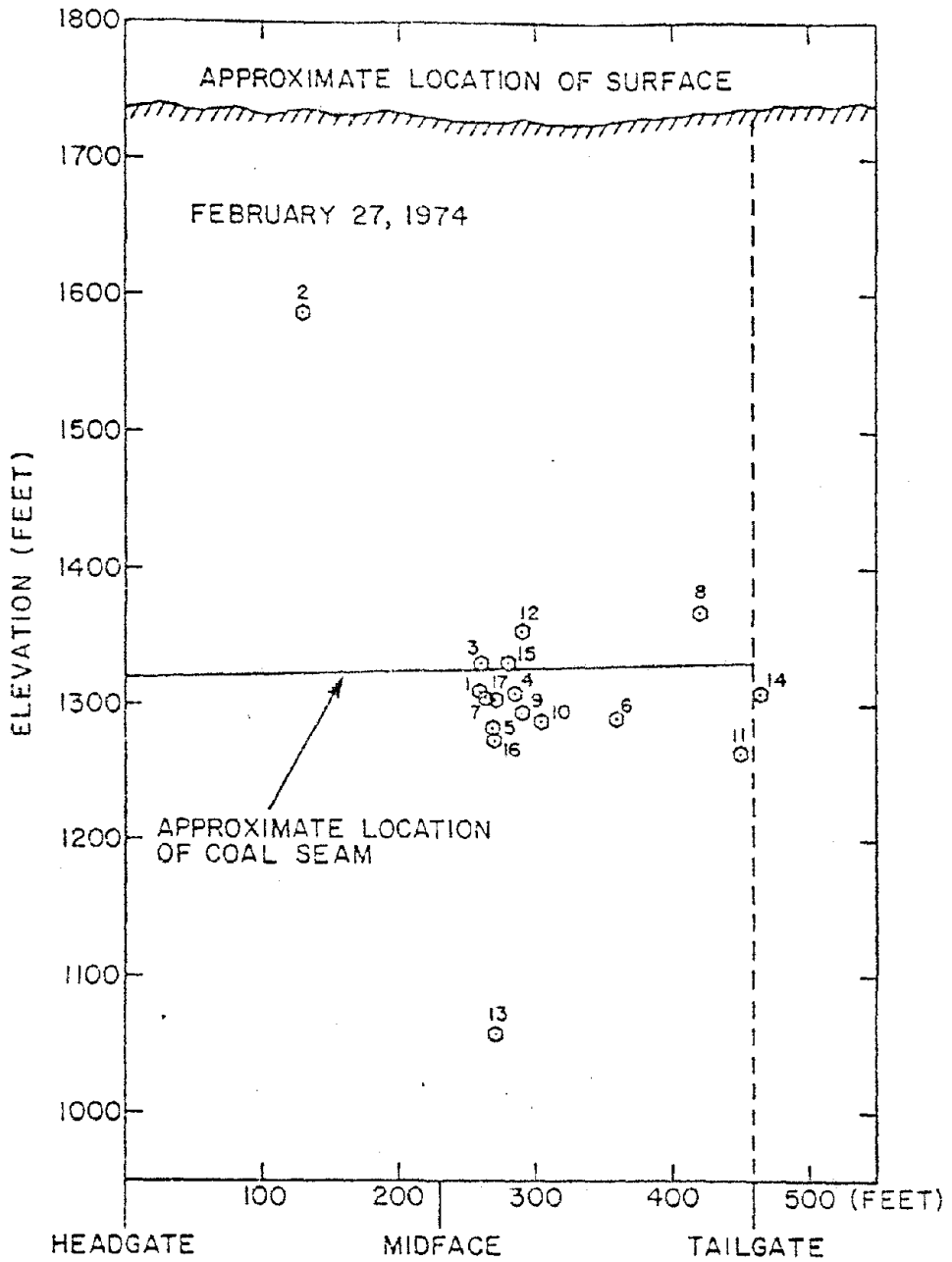

Figure 93. Projections of Source Locations Plotted on Vertical Cross-Sections of Longwall, February 27, 1974: Unique Velocity Model, Modified Second Geophone Array.

good clustering of events, about 50 ft to the right of midface, was observed. The majority of these events were blasts, associated with the necessity of freeing support chocks stuck as a result of the rapid deterioration of the midface area which occurred over a period of less than 24 hours.

Overall, the vertical source locations obtained using the unique velocity model appeared to be from 10 to 100 ft too deep. It is felt that in reality only a few events really occurred beneath the coal, with the remaining events occurring in the immediate vicinity at or above the seam. Only a true three-dimensional array will make it possible to obtain more accurate z-coordinate data.

Source location distributions -- Graphs were constructed to illustrate horizontal and vertical distributions of source locations (unique velocity model only) for the level-3 events detected. Figure 94 shows the daily event distribution, horizontally, with Figure 95 showing a composite plot for the complete longwall study. Note that when the coal was being extracted easily (good longwall conditions), events were occurring primarily at and behind the longwall face as shown in Figure 94B but when roof problems rapidly developed at midface one day later, the majority of the events occurred at or ahead of the face as shown in Figure 94C, suggesting that uncontrolled fracturing and poor caving were taking place. Figure 95 gives a somewhat similar plot to that of Figure 94C, again indicating that longwall problems existed during other monitoring sessions as well.

Vertical distributions are presented in Figures 96 and 97. Note that the majority of the events appeared to be occurring about 50 ft

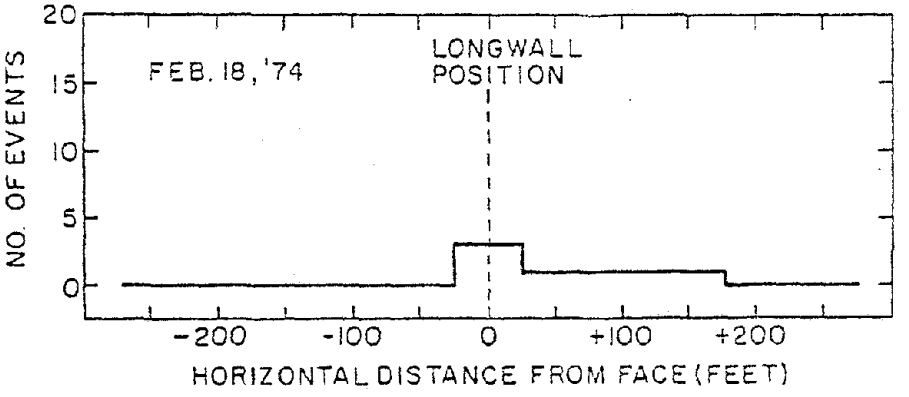

(A) Event Distribution on February 18, 1974

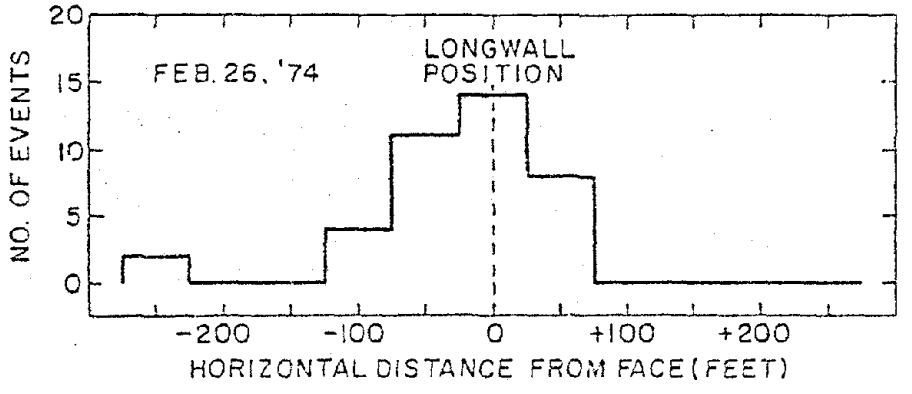

(B) Event Distribution on February 26, 1974

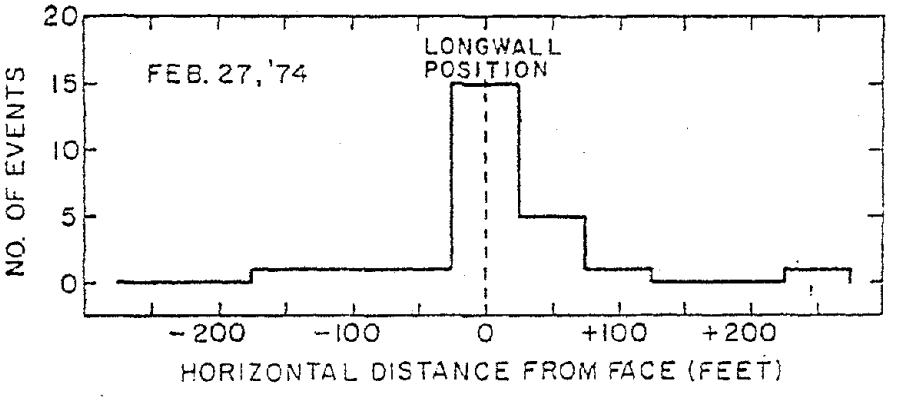

(C) Event Distribution on February 27, 1974

Figure 94. Horizontal Distribution of Events: Unique Velocity Model.

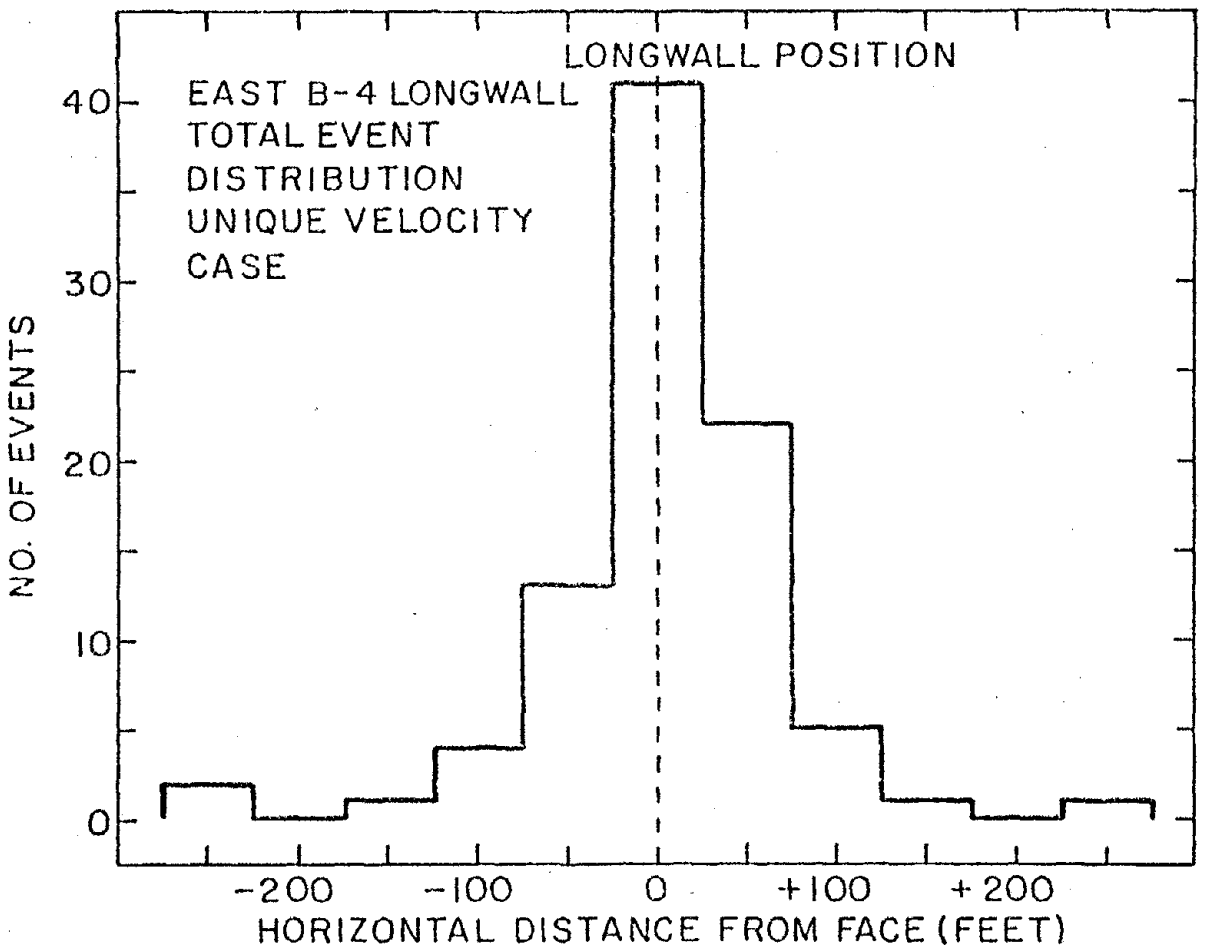

Figure 95. Total Horizontal Distribution of Events: Unique Velocity Model.

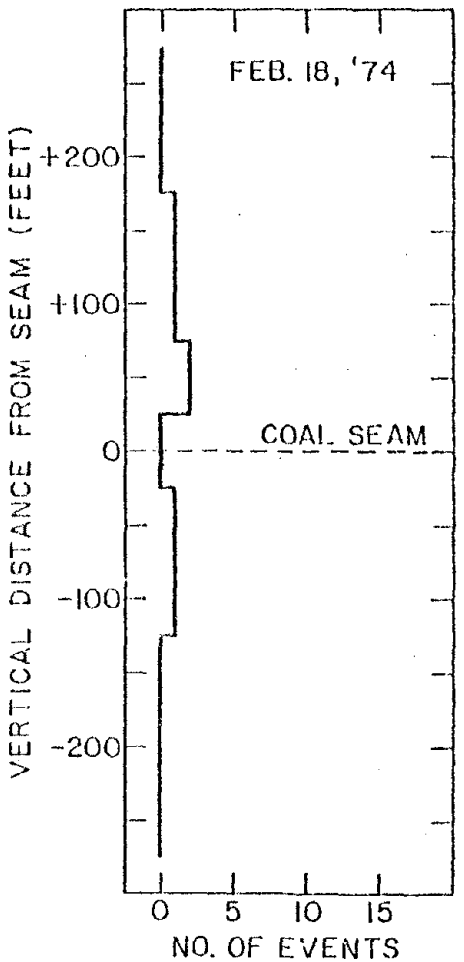

(A) February 18, 1974

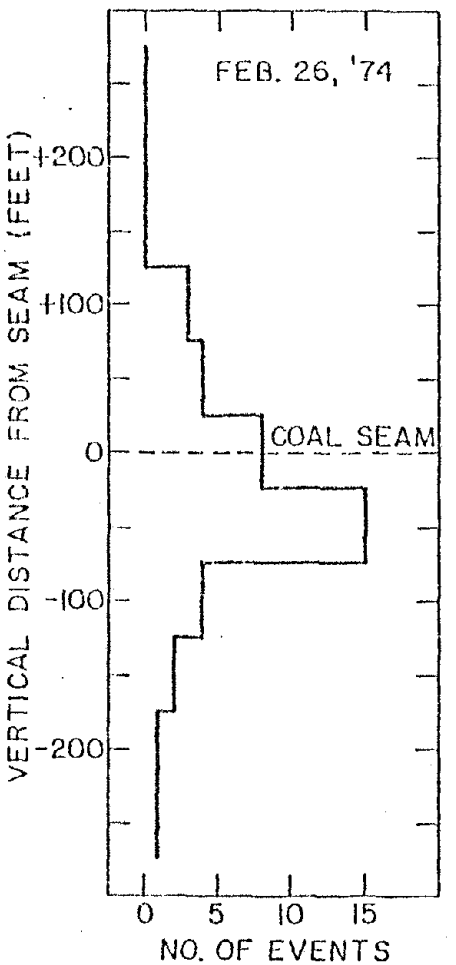

(B) February 26, 1974

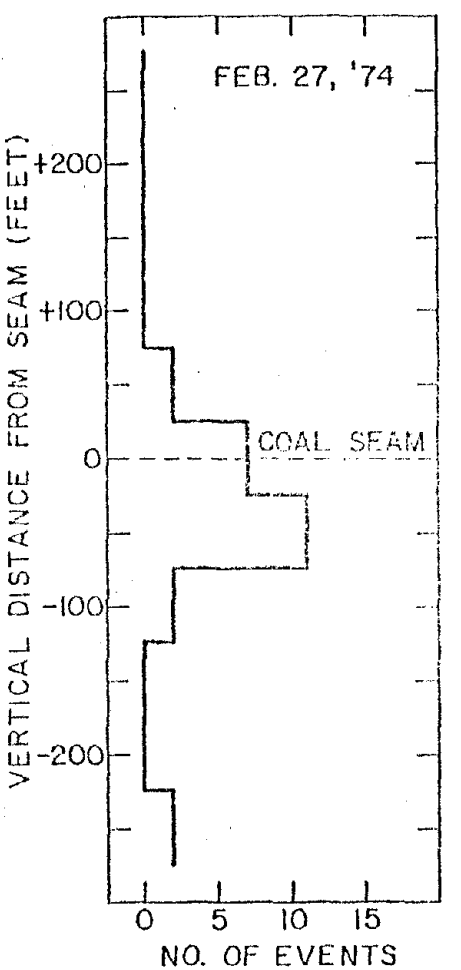

(C) February 27, 1974

Figure 96. Vertical Distribution of Events for Three Monitoring Periods: Unique Velocity Model.

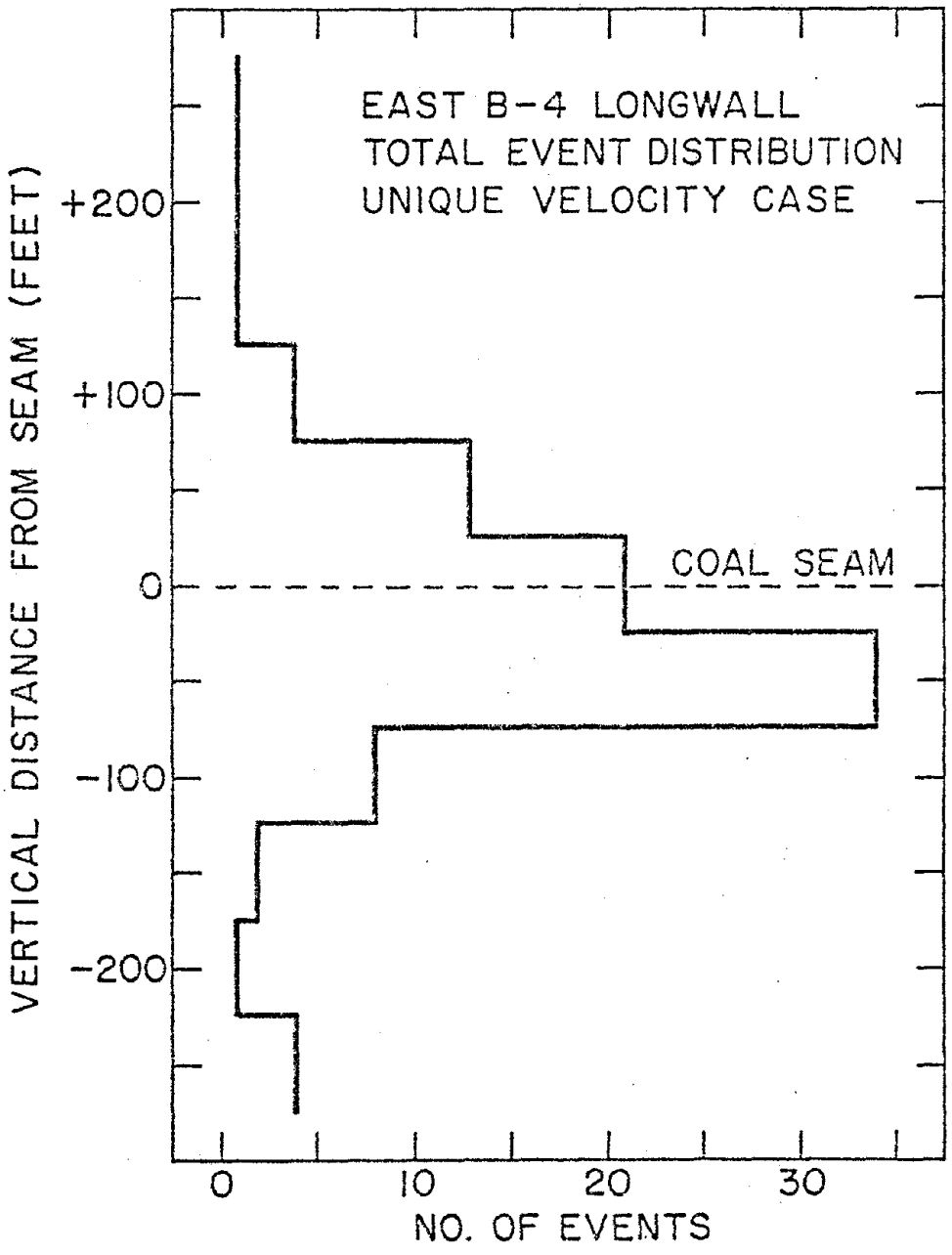

Figure 97. Total Vertical Distribution of Events: Unique Velocity Model.

beneath the coal seam. Such results were considered to be unrealistic and were, therefore, assumed to be in error by as much as 125 ft in depth. Data obtained from blasting of chocks on February 27 helped to substantiate this conclusion. Such blasts, identified by locations 4, 5, 6, 8, 10, 11, 13, 14, 16, and 17 as presented in Figure 93, were generally located beneath rather than at the coal seam depth.

3.3 Results

Source locations (isotropic velocity model) gave only very crude estimates of where each event occurred. Generally the event locations computed by this method were found to be 50 to 200 ft horizontally ahead of the longwall face. Such locations were considered to be unreasonable both in a theoretical and practical sense. However, if no wave propagation velocities are known, the isotropic velocity method is suggested to establish an approximate source location horizontally. Appendix D lists all level-3 events with their arrival times. Appendix E contains the complete listing of source locations using the isotropic velocity model. Vertical locations varied greatly and ranged from 0 to more than 1,800 ft.

The unique velocity model applied to the source location of events generated much more reasonable solutions. These appeared to be within accuracies of ±50 ft horizontally and ±100 ft vertically. Unfortunately, a blast at a known location is required in order to obtain unique velocity values for each geophone. Using the unique velocity model, the majority of the events were found to originate in the proximity of the face line, which agrees with both theory and field observations.

This method is recommended if such velocities are available. Appendix F contains the complete listing of source locations using the unique velocity model.

VIII. DISCUSSION--MICROSEISMIC FIELD STUDY

1. General

The basic hypothesis assumed when applying the microseismic monitoring method to mining operations is that redistribution of stress, especially in the extraction of coal, causes abrupt micro- to macro-fractures in the mechanically weakest bonds of the rock in the proximity of the longwall face. The nature and intensity of the stress distribution is mainly dependent upon the type of mining employed, the amount of load imposed by the surrounding rock strata, and the mining rate of advance. The rate of fracturing is likewise dependent upon such factors, as well as the degree of homogeneity of the strata. Such fracturing generates acoustic signals, termed microseismic activity, which propagate through the geologic strata, and may be detected and recorded for later analysis.

In this investigation such microseismic activity was successfully detected at depths of more than 400 ft and at horizontal distances exceeding 800 ft from the source. The majority of the analyzed events were locatable to within ±100 ft vertically of the coal seam and to within ±50 ft horizontally of the longwall face, provided accurate unique velocity values were available. For this study, the feasibility of microseismically monitoring a longwall mining operation using a surface geophone array has proven to be highly successful and should provide a fundamental initial step towards a long range goal of improving mine safety.

The microseismic monitoring sessions carried out above a longwall coal mining operation have provided the following conclusions:

(1) A geophone array installed on or near surface can be effectively utilized in detecting events occurring during longwall mining operations.

(2) These events can be approximately located if accurate arrival time differences, geophone locations, and wave propagation velocities are determined.

(3) Typical frequencies of observable events ranged from 10 to 100 Hz for those events originating in the vicinity of the roof, seam, or floor of the longwall panel. The majority of events observed had frequency components of 200 Hz or less. Events, whose frequencies exceed 200 Hz and which were detected by only one or two geophones, were considered to be very localized events due to subsidence, or tree root motion due to the wind load on the tree branches.

(4) Particle velocities of observable events ranged from 20 to more than 500 μips. Typical events had particle velocities of 50 to 300 μips.

(5) Various types of noises observed during monitoring included periodic electrical noises such as 60 Hz, 120 Hz, and 180 Hz signals originating from internal and external a-c power sources; electrical transient noises due to electrical switching of heavy machinery; periodic mechanical noises due to such sources as aircraft and ground vibrations from the motor generator; and transient mechanical noises due to such sources as people walking near the transducers.

(6) Amplitude and frequency data both produced clues as to the source of the various events. Geophones which show signals with the greatest amplitudes (particle velocities) and highest frequencies usually were the nearest to the event. As the distance between an event and a given geophone increased, the amplitude and frequency content of the event became lower. Events observed on only one geophone probably originated very near that geophone and most likely released a limited amount of energy. Distant events were believed to have released considerable quantities of energy because they were detected by all geophones. No energy determinations as such, however, were carried out in the current study.

(7) Some events appeared to be triggered by other events as several events would sometimes occur within a few seconds of one another.

(8) Numerous small events could have been occurring continuously in the vicinity of the longwall face. Such small events would have small individual amplitudes, but when they are superimposed on each other a dominant energy or noise field (background noise level) could be generated. Some of the so-called "rumblings" discussed earlier could have been caused in such a manner.

2. Source Location

The source location studies both theoretical (Appendix C) as well as those involving actual field data have suggested the following conclusions:

(1) For an isotropic velocity model of the region encompassing the longwall, it is generally true that the fewer the number of iterations, the closer the solution approaches the correct one. It was noted that if the required number of iterations was greater than eight, the source location was generally inaccurate.

(2) The true source should lie inside the array in order to obtain the most accurate source location.

(3) Within a given boundary outside of the array, the source location program is fairly accurate, provided that accurate input data is available (e.g., arrival times, velocities, geophone coordinates, and initial location estimates).

(4) Using a seven-geophone array rather than a six-geophone array does not significantly improve the source location solution and, in fact, may be detrimental if one of the geophones has an abnormal arrival time or if a geological discontinuity exists between the source and that geophone.

(5) The initial estimate rarely affects the source location solution except for extreme points outside the array boundaries. The x- and y-coordinates of the initial estimate may be in error as much as ±300 ft from the true source location coordinates for a suitable location computation but the z-coordinate should not be in error more than the estimated depth of the structure under study.

(6) Each array geometry has its own error boundaries. Numerous test points, encompassing the area of interest, should be employed to determine the amount of possible error at a given location for a given velocity model.

(7) The best source location solutions were obtained when the unique velocity model was employed, as the majority of solutions were found to be in the immediate region surrounding the longwall face. This strongly suggested that in such studies field velocity surveys should be made, using blasts at numerous known underground locations, to determine a unique velocity for each geophone location.

3. Limitations

For effectively evaluating underground structural stability, there exist several limitations in utilizing microseismic techniques, namely:

(1) Microseismic events having particle velocities of less than 30 µips are difficult to differentiate from the ambient background noise.

(2) Location of events is highly dependent upon accurate velocity measurements, arrival times, and optimum array geometry.

(3) The depths (z-coordinates) of the source locations are subject to a high degree of error when a planar geophone array configuration is employed. A three-dimensional array with transducers effectively surrounding the area of interest would provide data for obtaining much more accurate depth locations.

IX. GENERAL DISCUSSION OF OVERALL PROJECT

1. Review of Current Project

During the period October 1, 1973 to September 31, 1978, a USBM funded research project (Grant G0144013) has been carried by the Department of Mineral Engineering at The Pennsylvania State University. The primary phase of this project involved a series of microseismic field studies which were conducted over a longwall mining operation in Central Pennsylvania to study the feasibility of using these techniques to detect and locate potential zones of instability around the longwall. Transducers located in an array of shallow boreholes positioned above the active area of the longwall were employed to detect any microseismic activity, and a mobile microseismic monitoring facility was used to condition and record the activity sensed by the transducers. Results indicate that the primary studies were highly successful and that the feasibility of using near-surface transducers has been verified. Secondary studies associated with the evaluation of seismic velocities (necessary for accurate microseismic source location) and surface subsidence due to the longwall mining process were also carried out. A three volume final report (of which the present report is Volume I) has been prepared describing both the primary and secondary studies in detail, however, a brief review of each of the three studies will be included here for completeness.

1.1 Microseismic field studies

From both a safety and economic standpoint, microseismic monitoring of underground rock structures have in recent years proven to be a valuable nondestructive testing technique which can in many situations rapidly detect and locate areas of possible instability (Hardy and Leighton, 1977). The current study is unique in that the transducers were located near-surface rather than within the mine itself. Consequently, two immediate advantages are realized, namely, that mining operations can continue normally because there is no monitoring equipment in the mine, and that there is no electrical limitation on the microseismic monitoring system. On the negative side, the distances between the microseismic source and the transducers are generally much greater, and the stratified geologic media through which the signals must pass subjects them to additional attenuation, dispersion, and other waveform alternating processes. As a result the microseismic signals tend to be weaker and more distorted than those encountered using a monitoring system located in the mine itself. It is the authors' opinion, however, that in many field situations the advantages far outweigh the disadvantages. Furthermore, it is felt that with additional research the disadvantages due to surface transducer location may be greatly minimized.

In this context it is recommended that additional research should be undertaken in the following areas: use of three-dimensional transducers, development of improved signal acquisition and processing techniques, correlation of observed activity with specific sources, and development of more meaningful velocity models. Further details on these proposed research areas will be presented later in this chapter.

1.2 Determination of seismic velocity

In general the secondary study carried out to determine seismic velocity data was successful. A number of practical field techniques were developed, and the results obtained were found to be reasonably reproducible and, within the study itself, consistent. However, when attempts were made to use this velocity data for microseismic source location, extremely poor results were obtained. This may be due to the highly complex stress and fracture pattern existing in the neighborhood of an active longwall face. Further research in this area is obviously necessary.

1.3 Field study of mine subsidence

The secondary study carried out to monitor surface subsidence over the longwall panel being evaluated by microseismic techniques was highly successful. Excellent subsidence data was obtained at a very minimal cost. The study indicated extensive regions of very non-uniform surface subsidence which it is felt may well be a reflection of the difficult roof conditions experienced during various phases of the longwall operation. The original purpose for carrying out this study was to provide subsidence data which could possibly be correlated, along with underground observations, with the observed microseismic activity. This aspect of the study will be considered further in the next section.

2. Correlation of Microseismic Activity with Underground Mine Observations and Surface Subsidence

If the microseismic technique is to reach its full potential as a tool in the geomechanics field, it will be necessary that definite correlations between observed activity and actual physical behavior of

the associated rock mass be firmly established. This can only be accomplished by detailed examination of microseismic activity observed during specific and well defined rock mass behavior. This aspect was investigated to a very limited degree in the current study. For example, the results quoted in section 2 of Chapter VII indicate that during the current study at the Greenwich mine different types of microseismic behavior were noted during periods of satisfactory and unsatisfactory longwall operation. Similarly during an earlier study at the Greenwich mine (see item (5), section 2, Chapter I of this report), the character of the observed microseismic data also appeared to be influenced by the longwall operating conditions.

During the current study considerable detail on behavior of the longwall area (face condition, roof support, caving quality, etc.) and the resulting surface subsidence has been collected. This data is presented in Appendices H, I, and J of this volume, and in Volume III. Unfortunately, time and funds were not available to attempt other than a casual correlation of this data with observed microseismic behavior, however, the following scheme for such a study is recommended.

(1) Short-Term Analysis

In this analysis it is suggested that attempts be made to correlate observed microseismic activity with underground data obtained from selected detailed longwall reports (Appendix H) and detailed underground observations (Appendix I). First such a study would provide information with respect to possible correlations with short-term (hours) longwall behavior (caving quality, rate of advance, face quality, etc.). Secondly such a study would be useful to delineate the characteristic microseismic signals generated by such face activity as pump, conveyor and shearer operation, support motion, and blasting. A better classification of these signals is certainly a prerequisite to future application of the microseismic technique in high noise environments.

(2) Long-Term Analysis
It is suggested here that attempts be made to correlate observed microseismic activity with underground data obtained from brief daily longwall reports (Appendix G) and from surface subsidence data (Final Report Volume III). Such a study would be useful to determine the potential of the microseismic technique as a means of evaluating general face quality, the development of local caving over the face and adjacent support area, and the development of large scale caving over the gob area and eventual surface subsidence.

It is important to note that in both the preceding analyses, it is important that signal processing techniques be developed to better separate low level microseismic signals (level-1 and -2 type events) from ambient noise; and that attempts be made to obtain more accurate source depth (z-direction) coordinates.

3. Suggested Future Microseismic Research

Based on the recent study the following additional research is recommended:

(1) Three-Dimensional Transducers
The use of three-dimensional geophones rather than the uniaxial vertical motion geophones used to date would be very useful in separating P-wave and the S-wave components and in providing data on the direction from which a microseismic event originated. A better knowledge of the types of waves present should also provide further insight into the mechanisms causing the event, and further information on the geologic materials and discontinuities which exist between the event source and the various geophones in the monitoring array.

(2) Three-Dimensional Transducer Arrays
Where possible future studies should employ a realistic three-dimensional transducer array. In the recent study the apparent errors in the depths (z-coordinates) of the computed sources are at least partially due to the fact that a nearly planar transducer array was employed. The use of such an array is particularly important when investigating three-dimensional problems such as underground caving and development of surface subsidence.

(3) Data Acquisition Techniques
Microseismic data acquisition techniques should be investigated, including the effect of data cable length and

associated phase shifts on source location accuracy, the use of local radio telemetry at field sites, and the use of long-distance telephone lines for acquisition of microseismic data from remote field sites.

(4) Signal Processing and Storage

Due to the very large volumes of data acquired during microseismic studies, a system, which selectively screens the data based on certain criteria (amplitude threshold, frequency components, and coincidence), is definitely needed if the volume of field data is to be reduced to a manageable level. A suitably programmed minicomputer coupled to an analog-to-digital converter, multiplexer, and digital storage device would be suitable for such a data reduction and storage task. In particular, the problems of signal processing associated with low-level microseismic signals occurring in a high ambient background should be investigated. Such an investigation is considered extremely important since the majority of microseismic signals associated with problems in the geomechanics area, other than rock bursts, are in this category.

(5) Monitoring System Optimization

In order to optimize the overall monitoring system, an active controlled seismic source should be used in the field to effectively calibrate the study area. Small explosive charges, ground impactors, and spark- or air-guns could be used for this purpose. Graphs could then be plotted of frequency versus distance, amplitude versus distance, and energy versus distance. If t_o (source origin time) is known, traveltimes and wave propagation velocities could also be calculated. This technique should be employed first in soil and in soft medium, and hard rock areas to provide practical field data. The results could also provide data to enable narrower bandpass filter setting to be utilized, thereby resulting in a more sensitive and low noise monitoring system.

(6) Source Recognition and Site Characteristics

Microseismic measurements should be made at various types of field sites such as a quiesient one which has no sources of electricity nearby and no abnormal subsurface stresses for a background-noise-level check; a mine where the mechanical activity is accurately known (mining machine operations, blasting, roof falls, and/or rock bursts), and a gas storage reservoir undergoing hydrofracturing. Such a variety of field conditions is necessary in order to learn to more efficiently distinguish between microseismic events, man-made events, noises inherent in the monitoring system itself, background surface noises, and subsurface noises. Increased knowledge of the frequency spectra observed at each geophone for a known event should provide clues as to the frequency attenuation and dispersive properties of the area under study

and possible geologic discontinuities. A determination of the amplitude or energy loss of waves travelling through geologic media would prove to be of significant value for computing the energy released at the source of each event.

(7) Velocity Models

One of the most critical factors involved in using microseismic techniques in the field is the necessity of developing a meaningful velocity model for the field site under study. At sites similar to the one investigated in the current study due to the complexity of the associated structural geology (e.g., joints and faults), the differences in wave propagation characteristics of the layered geologic media involved, and the dynamic structural changes associated with a longwall mining operation, it is suggested that seismic velocity data be determined from in-situ velocity surveys conducted as often as possible. Furthermore, it is suggested that the locations of various known sources, such as blasts, be determined before employing such velocity data to determine locations of unknown sources. There is no doubt that a more accurate velocity model, either for each geophone (unique velocity) or for the entire longwall region under study, will greatly improve source location accuracy.

ACKNOWLEDGEMENTS

Funds for this project were provided by the U.S. Bureau of Mines under Grant No. G0144013. Financial assistance to the graduate program in the Mining and Geomechanics Sections of the Department of Mineral Engineering at The Pennsylvania State University is gratefully acknowledged. Staff of the Denver Mining Research Center have been extremely helpful during all phases of the project. Particular thanks must go to Wilbur I. Duvall who, in 1970, assisted in launching initial microseismic field studies at Penn State (Grant No. G0101743), and to Dr. Wilson Blake who acted as Technical Project Officer during these earlier studies. Mr. F. W. Leighton served as Technical Project Officer during the current study; his technical assistance and encouragement throughout the project has contributed greatly to its successful completion.

This project could not have been possible without the continuous assistance provided by the administrative and technical staff of the Greenwich Collieries. Mr. Robert H. Foley (former president) was enthusiastic even in the early stages of the project and this continuing interest and enthusiasm was reflected through the encouragement and assistance provided by Joseph Kreutzberger (former mine manager), Jack Emerick (former chief engineer), and Garry Reeder (former assistant chief engineer). Technical assistance provided by Nick Letizia (superintendent North Mine), Frank Burzanski (foreman North Mine), Ed Leish (superintendent of longwalls), Ken Woodring (assistant superintendent of No. 2 Mine), John Wagner (survey party chief), Joe Phillips (who assisted in providing longwall records), and the general office staff

is gratefully acknowledged. Project progress was only possible due to their day-to-day assistance.

Since most experiments during this project were carried out from surface, the authors would like to thank the owners of the property overlying the B-4 east longwall, Mrs. Lola Cowan and Mr. Edger Buterbaugh, for their permission to install transducers and locate monitoring facilities on their property during the study. Entrance to the study area was through the adjacent property owned by Mr. H. C. Wilson. His permission for access was greatly appreciated.

The authors would like to express their appreciation to members of the administrative and technical staff of the Penn State College of Earth and Mineral Sciences for their assistance on this project. A particular vote of thanks is extended to G. Reisinger (assistant supervisor) and other members of the Mineral Industries shop staff, all of who assisted greatly in construction and modification of microseismic monitoring facilities.

The authors were assisted in the microseismic field studies by Dr. A. W. Khair, Dr. R. Y. Kim, and Dr. W. Zuberek, departmental Research Associates. Dr. Zuberek, a visiting scientist from the Polish Central Mining Institute in Katowice, Poland (December 1973 to November 1974), also provided considerable assistance in the analysis of field data. A number of Penn State graduate assistants contributed a great deal to the study and in particular the assistance of B. A. Anani, L. A. Beck, J. W. Comeau, M. Gopwani, S. T. Harding, and S. Luesatja is gratefully acknowledged. The field studies associated with this project involved long hours often under extremely difficult working conditions. The authors were fortunate to have the assistance of such a hard working and unselfish field research group.

REFERENCES

Antsyferov, M. S., Ed., (1966), Seismo-Acoustic Methods in Mining, Consultants Bureau, New York.

Beard, F. D., (1962), "Microseismic Forecasting of Excavation Failures," Civil Engineering, Vol. 32, No. 5, pp. 50-51.

Beck, L. A., (1974), "Determination of Seismic Velocity with Application to Microseismic Field Studies," M.S. Thesis, Department of Mineral Engineering, The Pennsylvania State University.

Beck, L. A. and A. W. Khair, (1974), "Report on Greenwich Mine," Internal Report RML-IR/74-11, The Pennsylvania State University.

Blake, W., (1971), "Rock Burst Research at the Galena Mine, Wallace, Idaho," U.S. Bureau of Mines, TPR 39, 22 pp.

Blake, W. and W. I. Duvall, (1969), "Some Fundamental Properties of Rock Noises," Transactions, SME, Vol. 244, pp. 388-290.

Blake, W., F. Leighton, and W. I. Duvall, (1974), "Microseismic Techniques for Monitoring the Behavior of Rock Structures," U.S. Bureau of Mines, Bulletin 665.

Broadbent, C. D. and C. W. Armstrong, (1968), "Design and Application of Microseismic Devices," Proceedings Fifth Canadian Rock Mechanics Symposium, Toronto, pp. 91-103.

Cete, A., (1975), Geophysics Institute, Ruhr University, Bocham, Germany, personal communication.

Cook, N. G. W., (1963), "The Seismic Location of Rockbursts," Proceedings Fifth Symposium on Rock Mechanics," Minneapolis (1962), pp. 493-516, Pergamon Press, New York.

Crandell, F. J., (1955), "Determination of Incipient Roof Failures in Rock Tunnels by Microseismic Detection," Jour. Boston Soc. Civil Engineers, January, pp. 39-59.

Flinn, E. A., (1960), "Earthquake Location with an Electronic Computer," Bulletin of the Seismological Society of America, Vol. 50, pp. 467-470.

Goodman, R. E. and W. Blake, (1964), "Microseismic Detection of Potential Earth Slumps and Rock Slides," Report No. MT-64-6, Inst. of Engineering Research, University of California, Berkeley.

Goodman, R. E. and W. Blake, (1966), "Rock Noise in Landslides and Slope Failures," Highway Research Board, 44th Annual Meeting, Washington, D.C.

Harding, S. T., (1970), "A Least Squares Seismic Location Technique and Error Analysis," Internal Report RML-IR/71-8, Department of Mineral Engineering, The Pennsylvania State University.

Harding, S. and R. Rothman, (1974), Departments of Mineral Engineering and Geophysics, The Pennsylvania State University, personal communication.

Hardy, H. R., Jr., (1972), "Application of Acoustic Emission Techniques to Rock Mechanics Research," ASTM, STP 505, pp. 41-83.

Hardy, H. R., Jr., (1975), "Evaluating the Stability of Geologic Structures Using Acoustic Emission," ASTM, STP 571, pp. 80-106.

Hardy, H. R., Jr., (1974), "Microseismic Techniques Applied to Coal Mine Safety," USBM Grant No. G0101743 (Min-45), The Pennsylvania State University, USBM Open File #23-75, NTIS, PB 241-208/AS.

Hardy, H. R., Jr., (1976), "Microseismic Monitoring of Storage Reservoirs," (Progress Report on PR-12-75 prepared for 1976 AGA Transmission Conference - Las Vegas), Internal Report RML-IR/76-14, Geomechanics Section, Department of Mineral Engineering, The Pennsylvania State University.

Hardy, H. R., Jr. and A. W. Khair, (1973), "Applications of Acoustic Emission in the Evaluation of Underground Gas Storage Reservoir Stability," Proceedings Ninth Canadian Symposium on Rock Mechanics, Montreal.

Hardy, H. R., Jr. and E. J. Kimble, Jr., (1972), "Design and Development of a Mobile Microseismic Monitoring Facility," Internal Report RML-IR/72-20, Department of Mineral Engineering, The Pennsylvania State University.

Hardy, H. R., Jr. and F. Leighton, (1977), First Conference on Acoustic Emission/Microseismic Activity in Geologic Structures and Materials, Proceedings of Conference held at Penn State University, June 9-11, 1975, Trans Tech Publications, Clausthal, Germany, 490 pp.

Jones, M. F., III, (1972), "Development of Stratigraphic Cross-Sections from Selected Drill Holes at the Greenwich Colliery, Barnesboro, Pennsylvania," Internal Report RML-IR/72-13, Department of Mineral Engineering, The Pennsylvania State University.

Leighton, F. and W. Blake, (1970), "Rock Noise Source Location Techniques," U.S. Bureau of Mines, RI 7432.

Leighton, F. and B. J. Steblay, (1977), "Applications of Microseismics in Coal Mines," Proceedings First Conference on Acoustic Emission/ Microseismic Activity in Geologic Structures and Materials, The Pennsylvania State University, June 1975, Trans Tech Publications, Clausthal, Germany.

Kellmel, D., S. Fortune, and J. Vosenilek, (1974), Department of Electrical Engineering, The Pennsylvania State University, personal communication.

Mowrey, G. L., (1977), "Computer Processing and Analysis of Microseismic Data," Proceedings First Conference on Acoustic Emission/ Microseismic Activity in Geologic Structures and Materials, The Pennsylvania State University, June 1975, Trans Tech Publications, Clausthal, Germany.

Mowrey, G. L., (1975), "Computer Programs for the Processing and the Analysis of Microseismic Data," Internal Report RML-IR/75-3, Department of Mineral Engineering, The Pennsylvania State University.

Neyman, B., Z. Szecowka, and W. Zuberek, (1972), "Effective Methods for Fighting Rock Bursts in Polish Collieries," Proceedings Fifth International Strata Control Conference, London.

Obert, L., (1941), "Use of Subaudible Noise for Prediction of Rock Bursts," U.S. Bureau of Mines, RI 3555.

Obert, L. and W. I. Duvall, (1945), "Microseismic Method of Predicting Rock Failure in Underground Mining. Part I. General Method," U.S. Bureau of Mines, RI 3797.

Obert, L. and W. I. Duvall, (1942), "Use of Subaudible Noise for Prediction of Rock Bursts. Part II," U.S. Bureau of Mines, RI 3654.

Oudenhoven, M. S. and R. E. Tipton, (1973), "Microseismic Source Locations Around Block Caving at the Climax Molybdenum Mine," U.S. Bureau of Mines, RI 7798.

Paulsen, J. C., R. B. Kistler, and L. L. Thomas, (1967), "Slope Stability Monitoring at Boron," Mining Congress Journal, Vol. 53, p. 28.

Scott, J. J., (1971), "Key Note Address," Proceedings of Conference on Underground Mining Environment, University of Missouri, Rolla, October, pp. 1-15.

Stas, B. et al., (1971), "Development Trends and Application of Geophysical Research in Mines of the Ostrava-Karvina Coal Field," Proceedings Twelfth Symposium on Rock Mechanics, Rolla, (1970), AIME, New York, pp. 109-119.

Trevorrow, George C., Jr., (1975), "Taking Bottom Rock at Greenwich Collieries," Mining Congress Journal, July, pp. 28-34.

Weller, J. M., (1930), "Cyclical Sedimentations in the Pennsylvania and Its Significance," Jour. Geol., Vol. 38, No. 2, pp. 97-135.

Whittaker, B. N., (1974), "General Comments on Caving Characteristics of Roof Strata, B-Seam, Greenwich North Mine," RML-IR/74-25.

Wisecarver, David W., R. H. Merrill, and R. M. Stateham, (1969), "The Microseismic Technique Applied to Slope Stability," Transactions SME, Vol. 244, December, pp. 278-385.

Yonkoske, J. W., (1972), "Incompetent Roof Conditions at Greenwich Collieries North Portal," Internal Report RML-IR/72-26, Department of Mineral Engineering, The Pennsylvania State University.

APPENDIX A

TRANSDUCER LOCATIONS AT THE EAST B-4 LONGWALL SITE, GREENWICH NORTH MINE

This appendix contains the three-dimensional coordinates of transducer locations for the East B-4 longwall sites at the Greenwich North mine. The associated surveys were carried out by project personnel using instrument station coordinates provided by the Greenwich mine survey group.

The geophone identifying label such as "N-1" denotes the transducer location as shown, for example, in Figure 23. Localized coordinates are given in Table 2. To obtain the absolute coordinates, it is necessary to add 1,700,000 ft to the Easting coordinate and 500,000 ft to the Northing coordinate. The elevation listed is with reference to sea level in both the local and absolute coordinate systems.

TABLE 2

Three-Dimensional Coordinates of Transducer Locations
at Greenwich East B-4 Longwall Site

Geophone Identifying Label	Location (Ft)		
	Easting (x)	Northing (y)	Elevation (z)
N-1	2919.93	3075.16	1724.62
N-2	2961.58	2968.24	1725.76
N-3	3206.28	3075.47	1716.58
N-4	3003.64	2872.67	1719.26
N-5	3232.39	2958.39	1700.04
N-6	3412.18	3044.03	1712.40
N-7	3043.42	2747.25	1710.89
N-8	3270.61	2844.99	1696.12
N-9D	3454.46	2924.15	1710.02
N-9SH	3454.46	2924.15	1721.52
N-9SF	3454.46	2924.15	1724.52
N-10	3639.16	3012.05	1716.17
N-11	3312.49	2709.13	1696.29
N-12	3501.34	2793.85	1698.41
N-13	3682.73	2869.38	1699.29
N-14	3543.20	2655.64	1700.57
N-15	3732.99	2759.53	1698.72

APPENDIX B

IBMSL--A SOURCE LOCATION COMPUTER PROGRAM

1. General

The source location program, IBMSL, is Mowrey's modification of the program of Harding and Rothman (1974). This program utilizes a least-mean-squares reduction technique to give a "best average" source location if five or more seismic stations are used. IBMSL was designed to be used with The Pennsylvania State University's IBM 370/168 computer system.

Basically, the program uses a least-squares iteration technique which contains the x_i, y_i, and z_i ($i = 1, 2, \ldots, n$) coordinates of "n" geophone stations and corresponding arrival times and velocities t_i and v_i respectively:

$$(x_i - x)^2 + (y_i - y)^2 + (z_i - z)^2 = v_i^2(t_i - t)^2 \qquad \text{(Eq. 26)}$$

where x, y, and z are the true coordinates of the source and t is the true origin time.

As there are four unknowns (x, y, z, and t), data from at least four geophone stations are necessary to solve equation (26) exactly. However, due to inherent experimental errors related to this equation (e.g., geophone location errors, determination of travel-time differences, accuracy of velocity measurements), data from five geophone

stations should be employed such that this equation is overdetermined to allow the computer to minimize such error terms and arrive at a best fit solution. Data from additional geophone stations will yield an even better value for the average solution because of further redundancy in equation (26).

This program requires the following input data information, namely:

(1) the maximum number of iterations,

(2) a isotropic or anisotropic velocity for the field site,

(3) the desired velocity increment(s),

(4) an initial estimate as to the x, y, z, and t values of the source,

(5) the initial minimum velocity value,

(6) the maximum velocity value,

(7) the x, y, and z coordinates of the geophone stations, and

(8) the estimated arrival time at each station.

The IBM 370/168 computer then calculates and prints out the x, y, z, and t values of the source at each incremental value of velocity. If the actual velocity is unknown, this program is particularly useful because the computer will increment the velocity within the minimum/maximum boundaries selected by the user. The resulting x, y, and z values for each velocity can then be plotted (as shown on Figure 79) and the velocity effect on source location evaluated.

2. Special Features

Essentially, IBMSL was written to read the x, y, and z coordinates and arrival times of from five to eight geophones situated in an array

and then to print the best location of the source for one or more selected velocities.

The user currently has the following options with IBMSL.

(1) Velocities can be chosen to be either isotropic (one-dimensional case), anisotropic (three-dimensional case), or unique.

(2) Velocities can be incremented between a minimum and a maximum value for both the isotropic and the anisotropic cases.

(3) Boundary conditions can be incorporated to prevent print-out of those source locations which are found to lie outside of the selected boundaries.

(4) For the anisotropic velocity option, a print-out of the calculated resultant velocities associated with each geophone can be obtained for each event.

(5) Data for one or two geophones can be skipped, provided that there are still data for at least five geophones. Such a technique is particularly useful whenever one geophone has an anomalous arrival time (possibly due to fractures, joints, or faults in the wave path) which is not readily apparent. In automatic skipping, the program disregards data from one of the geophones and evaluates the source location; it then reinserts the data from the skipped geophone and skips the data from the next geophone and re-evaluates the source location. This procedure is repeated until data from all geophones have been skipped. If one geophone is skipped at a time, the specific geophone which most influences the source location solution can be easily determined.

(6) One coordinate (x, y, or z) may be held constant during the computation of the source location.

(7) Seismic data from a blast, whose location is accurately known, may be used in this program to establish a more realistic velocity model.

3. Basic Names of Variables Used

Numerous variable names are present in the source location program. To assist the reader in deciphering these terms, a list with a brief description of each term is presented here. The sequence of these terms follows the same order as they occur in the program.

Term	Description
DESC	Literal description of the data to be processed this run
KICK	Maximum number of iterations
XINC	Increment of x-component of velocity
YINC	Increment of y-component of velocity
ZINC	Increment of z-component of velocity
XMX	Maximum x-velocity component allowed
YMX	Maximum y-velocity component allowed
ZMX	Maximum z-velocity component allowed
X1	Minimum acceptable x-coordinate for print-out of source location
X2	Maximum acceptable x-coordinate for print-out of source location
X3	Minimum acceptable y-coordinate for print-out of source location
X4	Maximum acceptable y-coordinate for print-out of source location

Term	Description
X5	Minimum acceptable z-coordinate for print-out of source location
X6	Maximum acceptable z-coordinate for print-out of source location
X7	Minimum acceptable z-coordinate employed during mathematical computations
X8	Maximum acceptable z-coordinate employed during mathematical computations
N	Number of geophone stations to be used
XO(1-4)	Initial estimate of source location: (x, y, z, time = 0.000001)
XVEL	Initial x-component velocity
YVEL	Initial y-component velocity
ZVEL	Initial z-component velocity
ICASE =0:	Anisotropic velocity case, print-out of resultant velocities
=1:	Isotropic velocity or unique velocity case
=2:	Anisotropic velocity case, no print-out of resultant velocities
ISKIP1=0:	No effect on program
=n:	n^{th} geophone to be neglected or skipped
ISKIP2=0:	No effect on program
=m:	m^{th} geophone to be neglected or skipped
ISEL =0:	No effect on program
=1:	Keep x-coordinate in solution constant
=2:	Keep y-coordinate in solution constant
=3:	Keep z-coordinate in solution constant
IA1 =0:	No effect on program
=1:	Skips one geophone at a time, re-evaluates the solution for each disregarded geophone, until all geophones have been skipped

Term	Description
XX(1-3)	x-, y-, or z-coordinate values to be held constant if ISEL is used; only one of the three coordinate values may be held constant per run
IBST =0:	No effect on program
=1:	Determines unique velocities for each geophone provided a blast occurs at a known location
=2:	Allows a unique velocity to be assigned to each geophone
ICHG =0:	No effect on program
=1:	Will alter geophone travel times and/or coordinates if/when implemented
X(n,1-4)	x-, y-, z-coordinate values of n^{th} geophone station [The value for X(n,4) is employed on a separate card and is therefore unnecessary here.]
STA(n)	Station identification of geophone "n"
X(1-N,4)	Travel times of each geophone from 1 to n
V(n)	Unique velocity value associated with geophone "n"
REF	Reference code which consists of a tape reel number followed by a tape footage number

4. Data Card Formats

The basic card format for running the program on the IBM 370/168 computer is given by the list below. FORTRAN formats are given in brackets [ ] as a reader's aid.

Card	Description
A	Job card
B	Compile, execute card
C	Source code card
D	Source program
E	Data code card

Card	Description
F	Description card [10A8]
G	KICK, XINC, YINC, ZINC, XMX, YMX, ZMX [I10, 10X, 6F10.2]
H	X1, X2, X3, X4, X5, X6, X7, X8 [8F10.2]
I	N, XO(1), XO(2), XO(3), XO(4), XVEL, YVEL, ZVEL [I2, 3F10.2, F10.6, 3F10.2]
J	ICASE, ISKIP1, ISKIP2, ISEL, IA1, XX(1), XX(2), XX(3) [5I2, 3F10.2]
K	IBST, ICHG [2I2]
L	X(n,1), X(n,2), X(n,3), X(n,4), STA(n) [3F10.2, F10.6, A8]
M	If IBST = 0, omit this card from the program; if IBST = 1, X(1-n,4) [8F10.6] [Arrival times of the blast); if IBST = 2, V(1-n) [8F10.2] (Unique velocity for each geophone)
N	X(1-n,4) [8F10.6]
O	REF [A8]
P	End of data/job card

Tables 3, 4, and 5 illustrate the three basic data input card configurations with the variable IBST = 0, 1, and 2 respectively. The first case (IBST = 0) assumes that the wave propagation velocities are incremented at 200 fps steps between a range of 8,000 to 12,000 fps. All three velocities (v_x, v_y, and v_z) are identical for each velocity step as this run is the isotropic velocity case.

The second case (IBST = 1) assumes that a blast has occurred at a known location. Unique velocities for each geophone are calculated by the subroutine VLDT by knowing the arrival times of the blast. These velocities are subsequently utilized for all other events given on that particular run.

TABLE 3

Computer Card Sequence for IBST = 0

```
Code        Card Listing

      //AQ1XXXXX JOB
A...../                'P3783,T=50,R=2500', 'MOWREY GARY L'
B...../EXEC FWGG, PARM=NOSOURCE
C...../SYSIN DD *
D...../*INCLUDE GLMO2.$IBMSL6
D...../*INCLUDE GLMO2,$IBMSL7
E...../DATA. INPUT DD *
F.....         THIS IS PROGRAM $IBMSL6, $IBMSL7
F.....
G.....          20              200.       200.       200.       12000.     12000.     12000.
H.....  0.           6000.       0.          6000.      0.          3000.      0.          3000.
I..... 6   2880.     2716.       1325.       0.00001    8000.      8000.      8000.
J..... 1
K.....
L..... 2919.93    3075.16    1724.62      .       N-1
L..... 2961.58    2968.24    1725.76      .       N-2
L..... 3206.28    3075.47    1716.58      .       N-3
L..... 3003.64    2872.67    1719.26      .       N-4
L..... 3412.18    3044.03    1712.40      .       N-6
L..... 3043.42    2747.25    1710.89      .       N-7
N..... 0.0458     0.0473     0.0530     0.0435     0.0600     0.0550
O.....38-1993
N..... 0.0450     0.0476     0.0514     0.0490     0.0578     0.0514
O.....38-3170
N..... 0.0417     0.0428     0.0462     0.0443     0.0518     0.0470
O.....38-3171
P...../*          THIS IS A SLASH ASTERISK CARD
```

TABLE 4

Computer Card Sequence for IBST = 1

```
Code            Card Listing

      //AQ1XXXXX JOB
A...../                'P3783,T=50,R=2500', 'MOWREY GARY L'
B...../ EXEC FWCG,PARM=NOSOURCE
C...../SYSIN DD *
D...../*INCLUDE GLMO2.$IBMSL6
D...../*INCLUDE GLMO2.$IBMSL7
E...../DATA.INPUT DD *
F.....        THIS IS PROGRAM $IBMSL6,$IBMSL7
F.....
G.....          20              200.        200.        200.        12000.     12000.     12000.
H.....  0.          6000.       0.          6000.       0.          3000.      0.         3000.
I..... 6   2880.     2716.       1325.       0.00001   8000.       8000.      8000.
J..... 1
K..... 1
L..... 2919.93    3075.16    1724.62      .        N-1
L..... 2961.58    2968.24    1725.76      .        N-2
L..... 3206.28    3075.47    1716.58      .        N-3
L..... 3003.64    2872.67    1719.26      .        N-4
L..... 3412.18    3044.03    1712.40      .        N-6
L..... 3043.42    2747.25    1710.89      .        N-7
M..... 0.0562     0.0524     0.0616     0.0468     0.0644     0.0435
N..... 0.0458     0.0473     0.0530     0.0435     0.0600     0.0550
O.....38-1993
N..... 0.0450     0.0476     0.0514     0.0490     0.0578     0.0514
O.....38-3170
N..... 0.0417     0.0428     0.0462     0.0433     0.0518     0.0470
O.....38-3171
P...../*          THIS IS A SLASH ASTERISK CARD
```

TABLE 5

Computer Card Sequence for IBST = 2

```
Code            Card Listing

      //AQ1XXXXX JOB
A...../'                'P3783,T=50,R=2500','MOWREY GARY L'
B...../' EXEC FWCG,PARM=NOSOURCE
C...../'SYSIN DD *
D...../*INCLUDE GLMO2,$IBMSL6
D...../*INCLUDE GLMO2.$IBMSL7
E...../'DATA.INPUT DD *
F.....        THIS IS PROGRAM $IBMSL6,$IBMSL7
F.....
G.....          20              200.        200.        200.        12000.      12000.      12000.
H.....  0.            6000.       0.          6000.       0.          3000.       0.          3000.
I..... 6    2880.      2716.       1325.       0.00001     8000.       8000.       8000.
J..... 1
K..... 2
L..... 2919.93    3075.16     1724.62       .         N-1
L..... 2961.58    2968.24     1725.76       .         N-2
L..... 3206.28    3075.47     1716.58       .         N-3
L..... 3003.64    2872.67     1719.26       .         N-4
L..... 3412.18    3044.03     1712.40       .         N-6
L..... 3043.42    2747.25     1710.89       .         N-7
M..... 8985.37    8555.74     9542.35     8739.69     10789.82    8891.48
N..... 0.0458     0.0473      0.0530      0.0435      0.0600      0.0550
O.....38-1993
N..... 4.0450     0.0476      0.0514      0.0490      0.0578      0.0514
O.....38-3170
N..... 0.0417     0.0428      0.0462      0.0443      0.0518      0.0470
O.....38-3171
P...../*          THIS IS A SLASH ASTERISK CARD
```

The third case (IBST = 2) permits one to assign unique velocities to each geophone. As in the second case, these velocities are employed for all other events given on that particular run.

5. Source Listing

This section contains the complete source listing of the IBMSL source location program utilized in this thesis. The program is written in FORTRAN IV and is currently run on The Pennsylvania State University's IBM 370/168 computer. The program is generally stored on disk files identified by GLMØ2.$IBMSL6 and GLMØ2.$IBMSL7. A listing of this program is presented in Table 6.

TABLE 6

Listing of IBMSL Source Location Program

```
C      SEISMIC SOURCE LOCATION PROGRAM
C      LAST UPDATE  02 APRIL 1975
C
C      GARY L. MOWREY
C         119 MINERAL INDUSTRIES BUILDING
C            THE PENNSYLVANIA STATE UNIVERSITY
C               UNIVERSITY PARK, PENNSYLVANIA  16802
C         PHONE:  (814) 865-3437
C
C      THIS PROGRAM IS A LEAST SQUARES REDUCTION OF SEISMIC ARRIVAL TIMES
C      WHICH SHOULD GIVE A BEST AVERAGE LOCATION IF 5 OR MORE SEISMIC
C      STATIONS ARE USED.
C
C     ASSUMPTIONS NEEDED:
C       1. GEOPHONE X, Y, AND Z COORDINATES MUST BE ACCURATELY KNOWN
C       2. RELATIVE TIME DIFFERENCES BETWEEN GEOPHONES ARE KNOWN
C       3.  THERE MUST BE AT LEAST 5 AND NO MORE THAN 8 GEOPHONES UTILIZED
C       4. THE FIRST GEOPHONE TO DETECT THE EVENT IS THE REFERENCE GEOPHONE
C             AND IS ASSIGNED A VALUE BETWEEN 37 AND 45 MILLISECONDS
C            ALL OTHER GEOPHONES HAVE THEIR TIME DIFFERENCES IN REFERENCE
C            TO THE REFERENCE GEOPHONE
C       5. THE EVENT SHOULD BE LOCATED WITHIN THE BOUNDARIES OF THE GEOPHONE
C             ARRAY FOR BEST RESULTS
C       6. THE VELOCITY MODEL MAY BE EITHER ISOTROPIC OR ANISOTROPIC
C       7. THE P-WAVE METHOD IS EMPLOYED AS FIRST ARRIVALS ARE ASSUMED TO
C             BE P-WAVES
C
```

```
      IMPLICIT REAL * 8 (A-H, O-Z)
      DIMENSION XO2(4)
      DIMENSION XO1(4),SUM(4),STOR(100,4),SUM1(4)
      DIMENSION XX(3),XCK(8,4),DESC(20),STACK(8)
      DIMENSION XO(4), X(8,4), V(8), STA(8), D(8,4), R(8), B(4,8),
     1C(4,4), DA(8), E(8), F(4,9), GA(4), SAM(4,4), VEC(4,4)
      DIMENSION XMAX(4),YMAX(4),ZMAX(4),XMIN(4),YMIN(4),ZMIN(4)
C
C     READ IN A DESCRIPTION OF THE DATA IF DESIRED
C
      READ(5,132)(DESC(I),I=1,10)
      READ(5,132)(DESC(I),I=11,20)
  132 FORMAT(10A8)
      WRITE(6,133) DESC
  133 FORMAT(' ',10A8/' ',10A8)
C
C     READ IN THE FOLLOWING
C
C    KICK = THE NUMBER OF ITERATIONS, MAXIMUM
C    XINC = THE INCREMENT OF THE X COMPONENT OF VELOCITY
C    YINC = THE INCREMENT OF THE Y COMPONENT OF VELOCITY
C    ZINC = THE INCREMENT OF THE Z COMPONENT OF VELOCITY
C    XMX  = THE MAXIMUM X VELOCITY COMPONENT ALLOWED
C    YMX  = THE MAXIMUM Y VELOCITY COMPONENT ALLOWED
C    ZMX  = THE MAXIMUM Z VELOCITY COMPONENT ALLOWED
C
      READ(5,102) KICK,XINC,YINC,ZINC,XMX,YMX,ZMX
  102 FORMAT(I10,10X,6F10.2)
C
C     READ IN THE BOUNDARY CONDITIONS OF THE ARRAY
C     THIS THEREBY PLACES THE SOURCE WITHIN THE ARRAY UNDER CONSIDERATION
C     ALL VALUES OUTSIDE THESE LIMITS WILL NOT BE PRINTED
```

```
C
C     X1 = MINIMUM ACCEPTIBLE X COORDINATE
C     X2 = MAXIMUM ACCEPTIBLE X COORDINATE
C     X3 = MINIMUM ACCEPTIBLE Y COORDINATE
C     X4 = MAXIMUM ACCEPTIBLE Y COORDINATE
C     X5 = MINIMUM ACCEPTIBLE Z COORDINATE
C     X6 = MAXIMUM ACCEPTIBLE Z COORDINATE
C     X7 = MINIMUM ACCEPTIBLE Z COORDINATE FOR THE MATHEMATICAL COMPUTATIONS
C     X8 = MAXIMUM ACCEPTIBLE Z COORDINATE FOR THE MATHEMATICAL COMPUTATIONS
C
      READ(5,121)X1,X2,X3,X4,X5,X6,X7,X8
  121 FORMAT(8F10.2)
C
C     READ NUMBER OF OF STATIONS AND THE FIRST GUESS AS TO THE HYPOCENTER AND
C     ORIGIN TIME, AND THE PRINCIPAL VELOCITIES, AND THE REFERENCE NUMBER (REF)
C
C
C     NUM2 = COUNTER FOR TELLING COMPUTER TO ENTER CO-ORDINATES ONLY ONCE
C     NUM10 = FLAG TO EMPLOY SKIP ROUTINE ONLY ONCE
C
      NUM2=0
      NUM10=0
   53 IF (NUM2.GT.0) GO TO 139
C
C     N = NUMBER OF STATIONS WHICH ARE TO BE READ
C     XO = INITIAL GUESS FOR THE SOURCE LOCATION
C     THE GUESS LOCATION IS READ IN X,Y,Z,TIME
C     THE THREE PRINCIPAL VELOCITIES ARE READ IN AS XVEL YVEL & ZVEL.
C
      READ (5,100,END=1000) N,(XO(J),J=1,4),XVEL,YVEL,ZVEL
  100 FORMAT(I2,3F10.2,F10.6,3F10.2)
      DO 599 I=1,4
  599 XO2(I)=XO(I)
      IF (N.GT.8) N=8
```

```
C
C     ICASE = THE ISOTROPIC, HOMOGENEOUS CASE (1) OR ANISOTROPIC,
C             HOMOGENEOUS CASE (ANY OTHER INTEGER EXCEPT  1)
C             <ANISOTROPIC, HOMOGENEOUS CASE REFERS TO ORTHORHOMBIC CASE>
C             IF THE RESULTANT VELOCITY FOR THE ORTHORHOMBIC CASE IS NOT
C             DESIRED TO BE PRINTED OUT, THE USER SHOULD MAKE ICASE = 3,
C             THUS MAKING THE OUTPUT FORMAT APPROXIMATELY THE SAME AS THE
C             ISOTROPIC, HOMOGENEOUS CASE  (THIS ALSO SAVES PAPER AND
C             LOWERS LINE PRINTING COSTS)
C      ISKIP1 = GEOPHONE TO BE NEGLECTED OR SKIPPED
C      ISKIP2 = A SECOND GEOPHONE TO BE SKIPPED
C      ISEL = CO-ORDINATE TO BE HELD CONSTANT 1=X, 2=Y, 3=Z
C      IA1 = OPTION TO SKIP ONE GEOPHONE AT A TIME, RE-EVALUATING THE
C         SOLUTION FOR EACH DISGARDED GEOPHONE
C      XX = CO-ORDINATE VALUES, ANY ONE OF WHICH MAY BE HELD CONSTANT BY ISEL
C
      READ (5,150) ICASE,ISKIP1,ISKIP2,ISEL,IA1,(XX(I),I=1,3)
  150 FORMAT(5I2,3F10.2)
C
C      IBST = USE BLAST AT KNOWN LOCATION TO DETERMINE VELOCITY FOR EACH GEOPHONE
C      ICHG = ALTER GEOPHONE TIMES AND COORDINATES
C      IBST HAS PRIORITY OVER ICASE
C
      READ(5,151) IBST,ICHG
  151 FORMAT(2I2)
      WRITE(6,162)KICK,ISKIP1,ISKIP2,ICASE,XINC,YINC,ZINC,XMX,YMX,ZMX
  162 FORMAT(' ',' KICK = ',I4,'   ISKIP1 = ',I3,'   ISKIP2 = ',I3,
     1'   ICASE = ',I3,//,' XINC = ',F10.2,'   YINC = ',F10.2,'   ZINC =
     1',F10.2,//,' XMX = ',F10.2,'   YMX = ',F10.2,'   ZMX = ',F10.2///)
      WRITE(6,161)X1,X2,X3,X4,X5,X6,X7,X8
  161 FORMAT(' ',' X1 = ',F10.2,'   X2 = ',F10.2,'   X3 = ',F10.2,//
     1' X4 = ',F10.2,'   X5 = ',F10.2,'   X6 = ',F10.2,//
     1,' X7 = ',F10.2,'   X8 = ',F10.2///)
```

```
      WRITE(6,160) ISEL, XX, IA1, IBST, ICHG
  160 FORMAT(' ',' ISEL = ',I3,'   XX(1) = ',F10.2,'   XX(2) = ',F10.2,
     1'   XX(3) = ',F10.2/'   IA1 = ',I3,'   IBST = ',I3,'   ICHG = ',
     1I3,///)
      WRITE(6,164) XO
  164 FORMAT(' ',' SOURCE ORIGIN HAS BEEN INITIALLY SET AT: '
     1,' -----> X  = ',F10.2,'     Y  = ',F10.2,'     Z  = ',F10.2,
     1'   <-----',/' WITH T ZERO  = ',F10.6///)
  138 CONTINUE
      IF (NUM2.GT.0) GO TO 136
      NUM2=1
C
C     READ CO-ORDINATES OF STATION, ARRIVAL TIME AND STATION NAME
C     X = STATION CO-ORDINATES AND ARRIVAL TIME OF THE EVENT
C     THESE ARE READ IN X,Y,Z,ARRIVAL TIME
      DO 70 J=1,N
   70 READ(5,101)(X(J,I),I=1,4),STA(J)
  101 FORMAT(3F10.2,F10.6,A8)
C
C     READ IN ARRIVAL TIMES OF EACH STATION RESPECTIVELY
C
      IF(IBST.EQ.1) CALL VLDT(N,V,X,XO)
      IF(IBST.EQ.2) GO TO 700
  702 CONTINUE
C
C     NUM4 = COUNTER:  LIST GEOPHONE COORDINATES ONLY ONCE (IBST)
C     NUM5 = COUNTER:  SEQUENTIALLY NUMBERS EVENTS (IBST)
C
      NUM4=0
      NUM5=0
  136 READ (5,134,END=1000) (X(I,4),I=1,N)
  134 FORMAT(8F10.6)
C
```

```
C       READ IN REFERENCE NUMBER
C
        READ (5,135) REF
C
C       NUM3 = COUNTS NUMBER OF TIMES SOLUTION FALLS WITHIN LIMITS
C
        NA1=0
        NAA2=0
  562   CONTINUE
        NUM = 0
        NUM1=0
        NUM3=0
        IF(IBST.EQ.2) GO TO 1801
        IF(IBST.EQ.1) GO TO 1801
  135   FORMAT(A8)
        WRITE(6,222)REF
  222   FORMAT('1','***** TAPE NO.-FOOTAGE-REF. NO.: ',A8,' *****')
        XPVEL=XVEL
        YPVEL=YVEL
        ZPVEL=ZVEL
C
C       ZERO AND INITIALIZE ARRAYS
C
        DO 1780 I=1,4
        XMAX(I)=-999999.
        YMAX(I)=-999999.
        ZMAX(I)=-999999.
        XMIN(I)=0.
        YMIN(I)=0.
        ZMIN(I)=0.
 1780   CONTINUE
        XMIN(1)=999999.
        YMIN(2)=999999.
```

```
      ZMIN(3)=999999.
C
C     AT THIS POINT THE COMPUTER CONSIDERS A NEW VELOCITY EACH INCREMENT
C
      DO 1700  I=1,8
 1700 V(I)=0.
      DO 1781 I=1,4
      DO 1787 J=1,100
 1787 STOR(J,I)=0.
      SUM(I)=0.
      SUM1(I)=0.
 1781 CONTINUE
 1801 CONTINUE
      IF(IA1.EQ.1) GO TO 560
      IF((ISKIP1.GT.0).AND.(NUM10.NE.0)) GO TO 568
 1805 IF((ISKIP2.GT.0).AND.(NUM10.NE.0)) GO TO 567
 1806 CONTINUE
      IF((ISKIP1.GT.0).AND.(NUM10.EQ.0)) CALL SKIP(N,ISKIP1,X,STA)
      IF((ISKIP2.GT.0).AND.(NUM10.EQ.0)) CALL SKIP(N,ISKIP2,X,STA)
      NUM10=1
C*************************************************************************
C     THIS IS THE ENTRY INTO THE LEAST SQUARES METHOD
C*************************************************************************
   54 NUM=0
      DO 598 I=1,4
  598 XO(I)=XO2(I)
      DEL = 1000000.0
   51 DO 10 J=1,N
C
C     CALCULATE DISTANCE COMPONENTS FROM EACH STATION TO ASSUMED HYPOCENTER
C    AND TRAVEL TIME. MULTIPLY TRAVEL TIME BY THE VELOCITY SQUARED.
C
      DO  6 I=1,4
```

```
    6 D(J,I)=X(J,I)-XO(I)
      IF(IBST.EQ.1) GO TO 1800
      IF(IBST.EQ.2) GO TO 1800
      IF(ICASE.EQ.1) GO TO 1790
      CALL VELOC (J, XVEL, YVEL, ZVEL,D, V )
      GO TO 1800
 1790 V(J)=XVEL
 1800 CONTINUE
      D(J,4)=-(V(J)*V(J)*D(J,4) )
C
C     CALCULATE THE RESIDUALS.
C
      R(J) = ( D(J,1)**2 + D(J,2)**2 + D(J,3)**2 -((D(J,4)**2) / (V(J)
     1**2))) / 2.0
C
C     FIND TRANSPOSE OF DISTANCE MATRIX.
C
      DO 21 I=1,4
      B(I,J)=D(J,I)
   21 CONTINUE
   10 CONTINUE
C
C     PREMULTIPLY DISTANCE MATRIX BY ITS TRANSPOSE.
C
      DO 32 I=1,4
      DO 32 J=1,4
      C(I,J)=0.0
      DO 32 K=1,N
   32 C(I,J)=C(I,J)+B(I,K)*D(K,J)
C
C     CALCULATE THE VARIANCE.
C
      SIGMA=0.0
```

```
      DO 15 I=1,N
   15 SIGMA = SIGMA + R(I) * R(I)
      OUT = DEL
      IF(N.LT.5) GO TO 1779
      DEL=DSQRT(SIGMA/DFLOAT(N-4))
C
C     CHECK CONTINUED CONVERGENCE
C
      IF(DABS(DEL-OUT).LT.0.00000002) GO TO 50
C
C     CHECK THE NUMBER OF ITERATIONS.
C
      NUM=NUM+1
      IF(NUM .EQ. KICK) GO TO 50
      DO 33 I=1,4
      DA (I) = 0.0
C
C     PREMULTIPY RESIDUAL VECTOR BY THE TRANSPOSE OF DISTANCE MATRIX.
C
      DO 33 K = 1,N
   33 DA (I   )=DA (I   )+B(I,K)*R (K   )
C
C     SOLVE FOUR SIMULTANEOUS EQUATIONS FOR THE UNKNOWN DELTAS, C IS PRODUCT OF
C     DISTANCE MATRIX AND ITS TRANSPOSE, DA IS THE TRANSPOSE OF DISTANCE
C     MAXTRIX TIMES THE RESIDUAL MATRIX. E IS THE ERROR MATRIX, F IS A WORKING
C     MATRIX IN THE SUBROUTINE.  THE LAST 4 COL OF F ARE THE INVERSE OC.
C     THE 5TH COL OF F IS E THE DELTAS WE ARE SOLVING FOR. GA IS THE DIAGONAL
C     OF THE INVERSE OF C.
C
      CALL EQUN(C,DA,E,F,GA)
      DO 20 L=1,4
   20 XO(L)=XO(L)+E(L)
      IF(XO(3).LT.X7) XO(3)=X7
```

```
      IF(XO(3).GT.X8) XO(3)=X8
      IF(ISEL.GT.0) XO(ISEL)=XX(ISEL)
C
C     MAKE NEW GUESS AS TO EPICENTER AND ORIGIN TIME
C
      GO TO 51
   50 IF (NUM1.GT.0) GO TO 302
      NUM1=1
      GO TO 330
C*******************************************************************************
C     THIS IS THE END OF THE LEAST SQUARES METHOD
C*******************************************************************************
  700 READ(5,701) V
  701 FORMAT(8F10.2)
      GO TO 702
  330 CONTINUE
      IF(NUM4.EQ.0) WRITE(6,109)
  105 FORMAT(' ',3F15.3,F15.6,F15.3,5X,I3,11X,3(F10.2,2X))
  109 FORMAT('3',3X,'X COORD',4X,'Y COORD',4X,'Z COORD','  TRAVEL TIME'
     1,2X,'LOCATION')
      IF(NUM4.NE.0) GO TO 1803
      DO 56 J=1,N
   56 WRITE(6,106)(X(J,I),I=1,4),STA(J)
  106 FORMAT(' ',3(F10.2,1X),F10.6,5X,A5)
 1803 CONTINUE
      IF (ISEL.GT.0) WRITE (6,156) ISEL
  156 FORMAT(' ',' ISEL = ',I2,'.',' THIS COORDINATE WAS HELD CONSTANT'
     1)
      IF(IBST.EQ.1) GO TO 1802
      IF(IBST.EQ.2) GO TO 1802
      WRITE(6,222) REF
      WRITE(6,103)
  103 FORMAT ('0',10X,'X',14X,'Y',14X,'Z',14X,'T',12X,'SIGMA',4X,
```

```
     1'ITERATIONS',11X,'XVEL',8X,'YVEL',8X,'ZVEL')
       GO TO 302
  303  NUM3=NUM3+1
       DO 1783 I=1,4
       SUM(I)=SUM(I)+XO(I)
 1783  STOR(NUM3,I)=XO(I)
  306  XVEL=XVEL+XINC
       IF(ICASE.EQ.1) YVEL=XVEL
       IF(ICASE.EQ.1) ZVEL=XVEL
       IF(XVEL.GT.XMX) GO TO 300
       GO TO 54
  300  IF(ICASE.EQ.1) GO TO 460
       XVEL=XPVEL
       YVEL=YVEL+YINC
       IF(YVEL.GT.YMX) GO TO 301
       GO TO 54
  301  XVEL=XPVEL
       YVEL=YPVEL
       ZVEL=ZVEL+ZINC
       IF(ZVEL.GT.ZMX) GO TO 460

       GO TO 54
C
C      CHECK THE BOUNDARY CONDITIONS IMPOSED ON X, Y, AND Z COORDINATES
C
  302  IF(XO(1).LE.X1.OR.XO(1).GE.X2) GO TO 306
       IF (XO(2).LE.X3.OR.XO(2).GE.X4) GO TO 306
       IF(XO(3).LE.X5.OR.XO(3).GE.X6) GO TO 306
       IF (ICASE.EQ.1) GO TO 476
       IF (ICASE.EQ.3) GO TO 476
       WRITE(6,120)V,XVEL,YVEL,ZVEL
  120  FORMAT(11(F10.2,2X))
  476  WRITE(6,105) XO,DEL,NUM,XVEL,YVEL,ZVEL
C
```

```
C       SEARCH FOR THE MAXIMUM AND MINIMUM VALUES OF X, Y, AND Z COORDINATES
C       THESE VALUES ARE WRITTEN OUT AT THE END OF THE RUN
C
        IF(XO(1).GT.XMAX(1)) GO TO 400
  473   IF(XO(1).LT.XMIN(1)) GO TO 410
  470   IF(XO(2).GT.YMAX(2)) GO TO 420
  474   IF(XO(2).LT.YMIN(2)) GO TO 430
  471   IF(XO(3).GT.ZMAX(3)) GO TO 440
  475   IF(XO(3).LT.ZMIN(3)) GO TO 450
  472   IF(ZVEL.GT.ZMX) GO TO 460
        GO TO 303
  400   DO 1720 I=1,4
 1720   XMAX(I)=XO(I)
        XA1=XVEL
        XA2=YVEL
        XA3=ZVEL
        GO TO 473
  410   DO 1730 I=1,4
 1730   XMIN(I)=XO(I)
        XB1=XVEL
        XB2=YVEL
        XB3=ZVEL
        GO TO 470
  420   DO 1740 I=1,4
 1740   YMAX(I)=XO(I)
        XC1=XVEL
        XC2=YVEL
        XC3=ZVEL
        GO TO 474
  430   DO 1750 I=1,4
 1750   YMIN(I)=XO(I)
        XD1=XVEL
        XD2=YVEL
```

```
      XD3=ZVEL
      GO TO 471
  440 DO 1760 I=1,4
 1760 ZMAX(I)=XO(I)
      XE1=XVEL
      XE2=YVEL
      XE3=ZVEL
      GO TO 475
  450 DO 1770 I=1,4
 1770 ZMIN(I)=XO(I)
      XF1=XVEL
      XF2=YVEL
      XF3=ZVEL
      GO TO 472
  460 CONTINUE
      IF(NUM3.EQ.0) GO TO 1795
      WRITE(6,231) SUM,NUM3
  231 FORMAT('0',3F15.3,F15.6,5X,I5)
      WRITE(6,232)
  232 FORMAT('+',100X,'GRAND TOTAL')
      DO 1784 I=1,4
 1784 SUM(I)=SUM(I)/NUM3
      WRITE(6,231) SUM, NUM3
      WRITE(6,233)
  233 FORMAT('+',100X,'AVERAGE VALUE')
      IF (ICASE.EQ.3) GO TO 520
      DO 1786 J=1,4
      DO 1785 I=1,NUM3
      STOR(I,J)=(STOR(I,J)-SUM(J))**2
 1785 SUM1(J)=SUM1(J)+STOR(I,J)
 1786 SUM1(J)=DSQRT(SUM1(J)/NUM3)
      WRITE(6,234) SUM1
  234 FORMAT('0',4F15.6,40X,'STANDARD DEVIATION')
```

```
520 CONTINUE
    WRITE(6,222) REF
    WRITE(6,131)
131 FORMAT('0',11X,'X',14X,'Y',14X,'Z',14X,'T',
   112X,'XVEL',12X,'YVEL',12X,'ZVEL')
    WRITE(6,130) XMAX,XA1,XA2,XA3
    WRITE(6,500)
500 FORMAT('+',113X,'X MAX VALUE')
    WRITE(6,130)YMAX,XC1,XC2,XC3
    WRITE(6,501)
501 FORMAT('+',113X,'Y MAX VALUE')
    WRITE(6,130)ZMAX,XE1,XE2,XE3
    WRITE(6,502)
502 FORMAT('+',113X,'Z MAX VALUE')
    WRITE(6,130)XMIN,XB1,XB2,XB3
    WRITE(6,503)
503 FORMAT('+',113X,'X MIN VALUE')
    WRITE(6,130)YMIN,XD1,XD2,XD3
    WRITE(6,504)
504 FORMAT('+',113X,'Y MIN VALUE')
    WRITE(6,130) ZMIN,XF1,XF2,XF3
    WRITE(6,505)
505 FORMAT('+',113X,'Z MIN VALUE')
130 FORMAT('0',5X,3(F10.2,5X),F10.6,5X,3(F10.2,5X))
    XMAX(1)=XMAX(1)-XMIN(1)
    YMAX(2)=YMAX(2)-YMIN(2)
    ZMAX(3)=ZMAX(3)-ZMIN(3)
    WRITE(6,506) XMAX(1),YMAX(2),ZMAX(3)
506 FORMAT('0',5X,3(F10.2,5X),63X,'MAX - MIN')
    XMAX(1)=XMAX(1)/2.
    YMAX(2)=YMAX(2)/2.
    ZMAX(3)=ZMAX(3)/2.
    WRITE(6,507)XMAX(1),YMAX(2),ZMAX(3)
```

```
 507 FORMAT('0',5X,3(F10.3,5X),63X,'(MAX - MIN)/2.')
     XMAX(1)=XMAX(1)+XMIN(1)
     YMAX(2)=YMAX(2)+YMIN(2)
     ZMAX(3)=ZMAX(3)+ZMIN(3)
     WRITE(6,508) XMAX(1),YMAX(2),ZMAX(3)
 508 FORMAT('0',5X,3(F10.3,5X),63X,'AVERAGE VALUE')
1795 IF(NUM3.EQ.0) WRITE(6,509)
 509 FORMAT('2*****  THERE EXISTS NO SOLUTIONS WHICH FALL WITHIN THE BO
    1UNDARIES SELECTED  *****')
     NUM2=1
     IF (IA1.EQ.1) GO TO 565
     IF(ISKIP1.GT.0) N=N+1
     IF(ISKIP2.GT.0) N=N+1
     GO TO 53
 568 DO 569 J=1,N
     JA=J
     IF(J.GE.ISKIP1) JA=J+1
     IF(JA.GT.N) JA=N
     X(J,4)=X(JA,4)
 569 CONTINUE
     N=N-1
     GO TO 1805
 567 DO 519 J=1,N
     JA=J
     IF (J.GE.ISKIP2) JA=J+1
     IF(JA.GT.N) JA=N
     X(J,4)=X(JA,4)
 519 CONTINUE
     N=N-1
     GO TO 1806
 139 CONTINUE
     XVEL=XPVEL
     YVEL=YPVEL
```

```
      ZVEL=ZPVEL
      GO TO 138
  560 IF(NAA2.EQ.1) N=N+1
      DO 561 I=1,4
      DO 561 J=1,N
      XCK(J,I)=X(J,I)
      STACK(J)=STA(J)
  561 CONTINUE
      NA1=NA1+1
      IF (NA1.GT.N) GO TO 53
      CALL SKIP(N,NA1,X,STA)
      GO TO 54
  565 DO 566 I=1,4
      NAA1 = N+1
      DO 566 J=1,NAA1
      X(J,I)=XCK(J,I)
      STA(J)=STACK(J)
  566 CONTINUE
      NAA2=1
      XVEL=XPVEL
      YVEL=YPVEL
      ZVEL=ZPVEL
      GO TO 562
 1802 CONTINUE
      IF((NUM4.EQ.0).AND.(IBST.EQ.2)) WRITE(6,194) (V(I),I=1,N)
  194 FORMAT('0',5X,'VELOCITY = ',8(F10.2,3X))
      IF(NUM4.EQ.0) WRITE(6,190)
  190 FORMAT('0',10X,'X',14X,'Y',14X,'Z',14X,'T',12X,'SIGMA',4X,
     1'ITERATIONS',11X,'REFERENCE NO.')
      NUM4=1
      NUM5=NUM5+1
      WRITE(6,191)XO,DEL,NUM,REF,NUM5
  191 FORMAT('0',3F15.3,F15.6,F15.3,5X,I3,16X,A8,2X,I2)
```

```
      DO 193 I=1,N
  193 X(I,4)=X(I,4)*1000.
      WRITE(6,192) (X(I,4),I=1,N)
  192 FORMAT(' ',60X,'TRAVEL TIMES = ',8F6.1)
      NUM2=1
      IF(IA1.EQ.1) GO TO 565
      IF(ISKIP1.GT.0) N=N+1
      IF(ISKIP2.GT.0) N=N+1
      GO TO 136
 1779 WRITE(6,1778)N
 1778 FORMAT('0','      ERROR *******  N=',I5)
 1000 STOP
      END
      SUBROUTINE EQUN(C,D,E,F,GA)
      IMPLICIT REAL * 8 (A-H,O-Z)
      DIMENSION C(4,4), D(6), E(6), F(4,9), G(4,6), GA(4)
      N=4
      NP=N+1
      NPM=NP+1
      NM=N-1
      NPP=NP+N
      DO 1 J=1,N
      F(J,NP)=D(J)
      DO 1 K=1,N
    1 F(J,K)=C(J,K)
      DO 7 J=NPM,NPP
      DO 7 K=1,N
    7 F(K,J)=0.0
      DO 8 J=1,N
      K=NP+J
    8 F(J,K)=1.
      DO 2 L=1,N
      LP=L+1
```

```
      Y=1./F(L,L)
      DO 3 J=L,NPP
    3 F(L,J)=F(L,J)*Y
      IF(LP-N) 13,13,6
   13 DO 4 J=LP,N
      Y=F(J,L)
      DO 4 K=L,NPP
    4 F(J,K)=F(J,K)-Y*F(L,K)
    2 CONTINUE
    6 DO 5 J=2,N
      IM=N-J+1
      IMP=IM+1
      DO 5 II = 5,9
      DO 5 K=IMP,N
    5 F(IM,II) = F(IM,II) - F(IM,K )* F(K,II)
      DO 15 J = 1,4
      NNN = J + 5
   15 GA(J) = F(J, NNN)
      DO 14 I = 1,4
   14 E(I) = F(I,5)
      RETURN
      END
      SUBROUTINE VELOC( J, XVEL, YVEL,ZVEL,  DIST, VEL )
C
C******** ORTHORHOMBIC CASE MAY 14, 1974  R.L.ROTHMAN**************************
C
      IMPLICIT REAL * 8 (A-H,O-Z )
      DIMENSION DISMA(8), EL(8),X(3), Y(3), Z(3),DIST(8,3), VEL(8),EM(8)
      DIMENSION EN(8),A(3)
      DISMSQ=0.
      DO 1 I=1,3
      A(I)=DIST(J,I)*DIST(J,I)
    1 DISMSQ=DISMSQ+A(I)
```

```
      VEL(J)=DSQRT((XVEL*XVEL*A(1)+YVEL*YVEL*A(2)+
     1ZVEL*ZVEL*A(3))/DISMSQ)
      RETURN
      END
      SUBROUTINE SKIP(N,ISKIP,X,STA)
      IMPLICIT REAL*8 (A-H,O-Z)
      DIMENSION X(8,4),STA(8)
      NCK=0
      DO 61 J=1,N
      JA=J
      IF(ISKIP.EQ.J) GO TO 64
      IF(NCK.GT.0) GO TO 64
      IF(JA.GT.N) GO TO 61
   62 CONTINUE
      DO 63 I=1,4
      X(J,I)=X(JA,I)
   63 CONTINUE
      STA(J)=STA(JA)
      GO TO 61
   64 JA=J+1
      NCK=1
      IF(JA.GT.N) GO TO 61
      GO TO 62
   61 CONTINUE
      N=N-1
      RETURN
      END
      SUBROUTINE VLDT(N,CV,X,XO)
C     05 DECEMBER 1974
C     THIS SUBROUTINE IS DESIGNED TO DETERMINE THE VELOCITY,
C     ASSUMING THAT A BLAST HAS BEEN ACCURATELY LOCATED.
C     GOOD DELTA T'S AND/OR ARRIVAL TIME ESTIMATES ARE NEEDED FOR A
C     GOOD SOLUTION
```

```
C      ***** TAKEN FROM F. LEIGHTON'S PROGRAM AND MODIFIED BY G. L. MOWREY ****
       IMPLICIT REAL*8(A-H,O-Z)
       DIMENSION CV(8),X(8,4),XO(4),DA(8),T(8),CD(8),TI(8),VI(8)
       READ(5,134)(X(I,4),I=1,N)
  134  FORMAT(8F10.6)
       DO 5 I=1,8
       DA(I)=0.
       CV(I)=0.
       CD(I)=0.
       VI(I)=0.
       TI(I)=0.
    5  T(I)=0.
       DO 1 I=1,N
       A=X(I,1)-XO(1)
       B=X(I,2)-XO(2)
       C=X(I,3)-XO(3)
    1  DA(I)=DSQRT(A*A+B*B+C*C)
       AA=1000.
       DO 27 I=1,N
       IF(X(I,4).GT.AA) GO TO 27
       AA=X(I,4)
       MM=I
   27  CONTINUE
       DO 28 I=1,N
   28  T(I)=X(I,4)-X(MM,4)
       M=0
       TII=0.
       DO 37 I=1,N
       CD(I)=DA(I)-DA(MM)
       IF (T(I)) 37,37,33
   33  VI(I)=CD(I)/T(I)
       M=M+1
       TI(I)=DA(I)/VI(I)-T(I)
```

```
      TII=TII+TI(I)
   37 CONTINUE
      SP=TII/DFLOAT(M)
      DO 42 I=1,N
      IF (T(I)) 42,41,41
   41 CV(I)=DA(I)/(T(I)+SP)
   42 CONTINUE
      WRITE(6,500) CV,VI,CD,DA,TI,T,TII,SP,M
  500 FORMAT('1COMPENSATED VELOCITY = ',   8(F10.2,3X)/
     1       'OUNCOMPENSATED VELOCITY ',8(F10.2,3X)/
     1       'ODELTA DISTANCE  =      ',8(F10.2,3X)/
     1       'OTOTAL DISTANCE =       ',8(F10.2,3X)/
     1       'OTIME TI =              ',8(F10.6,3X)/
     1       'ODIFFERENCE TRAVEL TIME ',8(F10.6,3X)///
     1'OTTI = ',F10.6/'OSP = ',F10.6/'OM = ',I3)
      RETURN
      END
```

APPENDIX C

EVALUATION OF SOURCE LOCATION TECHNIQUES

1. Effect of Array Geometry

In this appendix, various factors affecting the quality of microseismic source location are considered. These factors include array geometry, arrival time error, and initial source location estimates.

To obtain a rudimentary concept of how specific source locations and array geometries affect the source location solutions, a series of tests were conducted. First, 12 test points were arbitrarily chosen encompassing the East B-4 longwall under study. All 12 points were positioned at the approximate depth of the longwall (1,300 ft above sea level). An isotropic velocity model was selected for simplicity as no true velocities were known in this study. A velocity value of 10,000 fps was used. Table 7 delineates the test point coordinates and their computed arrival times to the various geophone locations. The arrival times were calculated by dividing the vector distance (assuming a direct path between the source [test point] and each geophone location) by the isotropic velocity, 10,000 fps. The FORTRAN IV computer program utilized to calculate these arrival times is presented in Table 8.

A total of nine different array geometries were considered, array-A through array-I, as shown in Table 9. The location of the various geophone stations are shown in Figure 98. The basic procedure was to use the arrival times corresponding to the appropriate geophones

TABLE 7

Test Point Locations and Associates Arrival Times

Ref. No.	Source Coordinates-Ft (x)	(y)	(z)	Geophone Stations N-1	N-2	N-3	N-4	N-5	N-6	N-7	N-8
				Arrival Times - Ms							
1	2900	3200	1300	44.30	48.86	53.18	54.19	57.35	67.58	62.80	64.83
2	2900	3000	1300	43.17	43.14	52.25	45.03	52.18	65.90	50.33	56.42
3	2700	2700	1300	60.78	56.71	75.55	54.57	71.43	89.20	53.76	70.96
4	3000	2600	1300	64.23	56.42	66.50	50.01	58.52	73.29	43.86	53.87
5	3000	2900	1300	46.63	43.29	49.69	42.02	46.63	60.06	44.05	48.29
6	3000	3200	1300	44.98	48.63	48.12	53.19	52.19	60.36	61.29	59.68
7	3200	2600	1300	69.61	61.13	63.22	53.73	53.81	64.21	46.37	47.11
8	3200	2900	1300	53.80	49.27	45.21	46.38	40.56	48.56	46.55	40.61
9	3200	3100	1300	50.93	50.54	41.73	51.58	42.56	46.71	56.37	47.64
10	3400	2800	1300	69.75	63.39	53.57	58.15	46.17	47.93	54.66	41.91
11	3700	2900	1300	90.53	85.51	66.94	81.33	61.81	52.31	78.95	58.68
12	3600	2600	1300	93.20	85.11	74.47	77.83	65.09	63.44	70.73	57.05

TABLE 7 (Continued)

Ref. No.	Source Coordinates-Ft (x)	(y)	(z)	Geophone Stations N-9D	N-9SH	N-9SF	N-10	N-11	N-12	N-13	N-14	N-15
				Arrival Times - Ms								
1	2900	3200	1300	74.27	74.76	74.91	86.88	75.38	82.78	93.88	93.30	102.32
2	2900	3000	1300	69.38	69.90	70.06	84.84	64.17	75.02	88.83	83.23	95.43
3	2700	2700	1300	88.75	89.15	89.28	107.36	72.96	89.98	107.42	93.46	110.89
4	3000	2600	1300	69.26	69.78	69.95	86.69	51.63	66.91	83.55	67.72	84.95
5	3000	2900	1300	61.26	61.85	62.03	77.09	53.96	64.91	79.15	71.78	84.62
6	3000	3200	1300	67.14	67.68	67.85	78.55	70.40	75.83	85.72	86.71	94.35
7	3200	2600	1300	58.13	58.75	58.95	73.20	42.62	53.58	68.19	53.04	68.45
8	3200	2900	1300	48.32	49.06	49.30	61.53	45.40	51.07	62.72	58.13	68.03
9	3200	3100	1300	51.36	52.06	52.28	61.14	56.79	58.59	66.76	68.97	74.76
10	3400	2800	1300	43.19	44.02	44.28	52.47	41.59	41.11	49.41	44.92	52.11
11	3700	2900	1300	47.85	48.60	48.84	43.53	58.62	45.77	40.08	49.47	42.40
12	3600	2600	1300	54.26	54.92	55.13	58.70	50.16	45.39	48.87	40.84	44.96

TABLE 8

Computer Program for Computing Theoretical Arrival Times for the Test Set of Points

```
      IMPLICIT REAL*8 (A-H, O-Z)
      DIMENSION AR(17,3),CO(3),E(17)
      DIMENSION JA(3)
      DO 1 1=1,17
      READ(5,100)(AR(I,J),J=1,3)
  100 FORMAT(3F10.2)
    1 CONTINUE
   10 READ(5,100,END=1000) CO
      DO 2 I=1,17
      A=AR(I,1)-CO(1)
      B=AR(I,2)-CO(2)
      C=AR(I,3)-CO(3)
      D=DSQRT(A*A+B*B+C*C)
      E(I)=D/10.
    2 CONTINUE
      DO 11 J=1,3
   11 JA(J)=CO(J)/100.
      WRTTE(6,101) JA,E
  101 FORMAT(' ',3I3,17(F6.2))
      GO TO 10
 1000 STOP
      END
```

TABLE 9

Array Configurations: East B-4 Longwall

Array ID	Geophones Used						
A	N-1	N-2	N-3	N-4	N-5	N-6	N-7
B	N-1	N-2	N-3	N-4	N-6	N-7	
C	N-1	N-2	N-3	N-4	N-6	N-7	N-15
D	N-1	N-7	N-9D	N-9SH	N-9SF	N-12	
E	N-1	N-7	N-9	N-10	N-11	N-13	N-14
F	N-1	N-9D	N-9SH	N-9SF	N-11	N-14	
G	N-3	N-7	N-9	N-10	N-11	N-14	
H	N-3	N-7	N-9	N-10	N-14		
I	N-8	N-10	N-11	N-12	N-14	N-15	

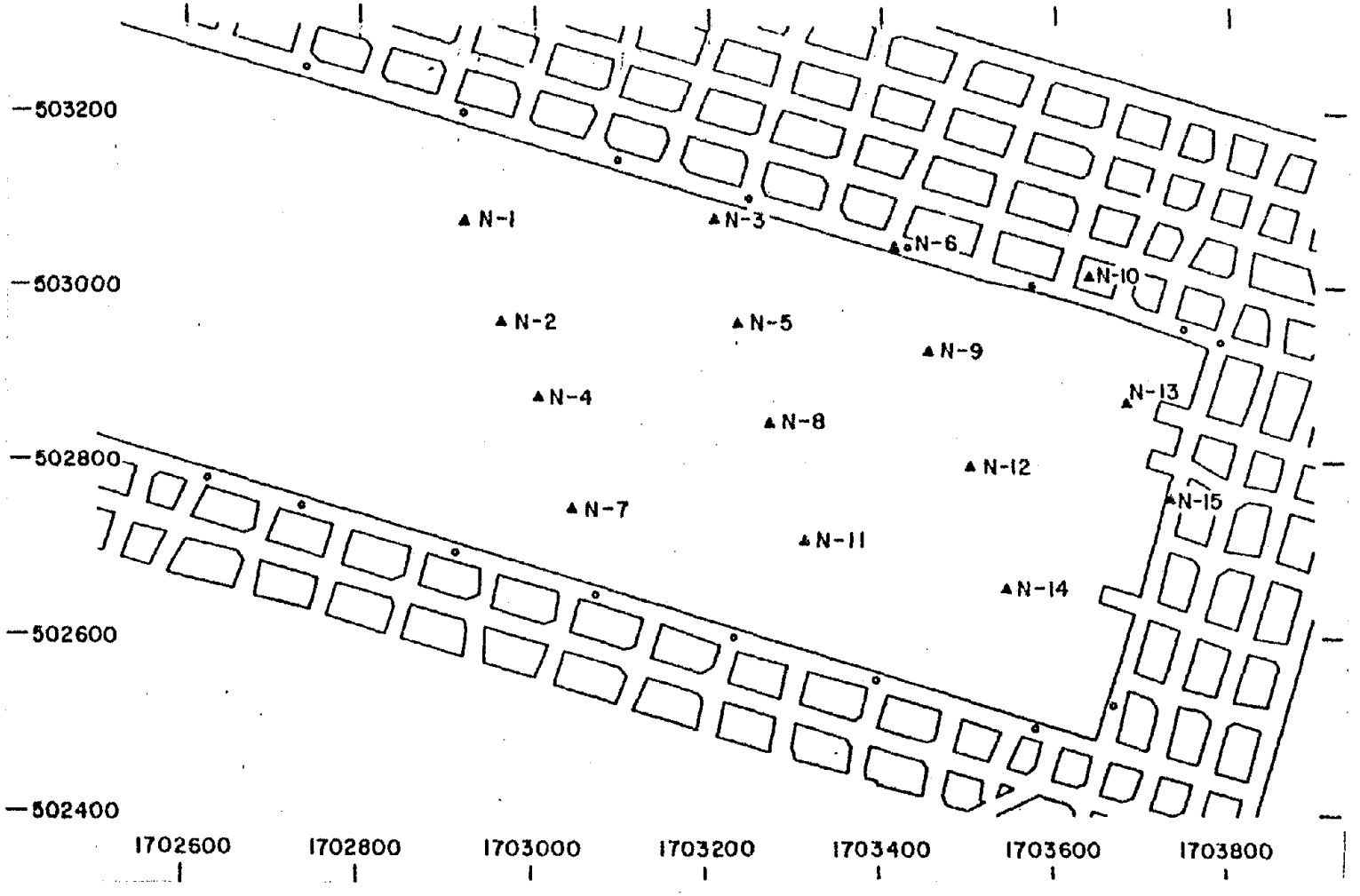

Figure 98. Map of the East B-4 Longwall and the Geophone Stations.

of a given array and utilize the source location program (IBMSL) to compute the location limits of each of the 12 points. A homogeneous, isotropic velocity model was employed, with the velocity values ranging from 8,000 fps to 12,000 fps in 200 fps increments. Thus, for each test point, a total of 21 isotropic velocity values were considered in IBMSL, giving 21 corresponding source location solutions. A continuous line was then constructed, which connected all 21 solutions. In this manner it was possible to note the general trend of the source location solutions as the isotropic velocities were increased.

Figures 99 through 107 illustrate graphically the results of this investigation. For array-A, the source location solutions (represented as arrows, with the tip of the arrow representing the maximum isotropic velocity model [12,000 fps] and the tail of the arrow representing the minimum isotropic velocity model [8,000 fps]) tended to migrate toward the center of the array. The greatest location deviations (longest arrows) were found to be those test points lying outside the array boundaries and the smallest location deviations were those test points nearest the center of the array. For array-B, the vector lengths of the arrows were shorter than for array-A, but the plots were otherwise essentially the same.

Greater location deviations were noted in the left-hand section of array-C, as compared with array-A. For array-D, the arrows in the bottom half were found to point away from the array rather than toward the center of the array, as was the case in array-A. Also the location deviations for array-D were generally larger than array-A. Array-E was similar to array-D in that the arrows in the bottom half pointed away from the array; however, in array-E the deviations in the southern half

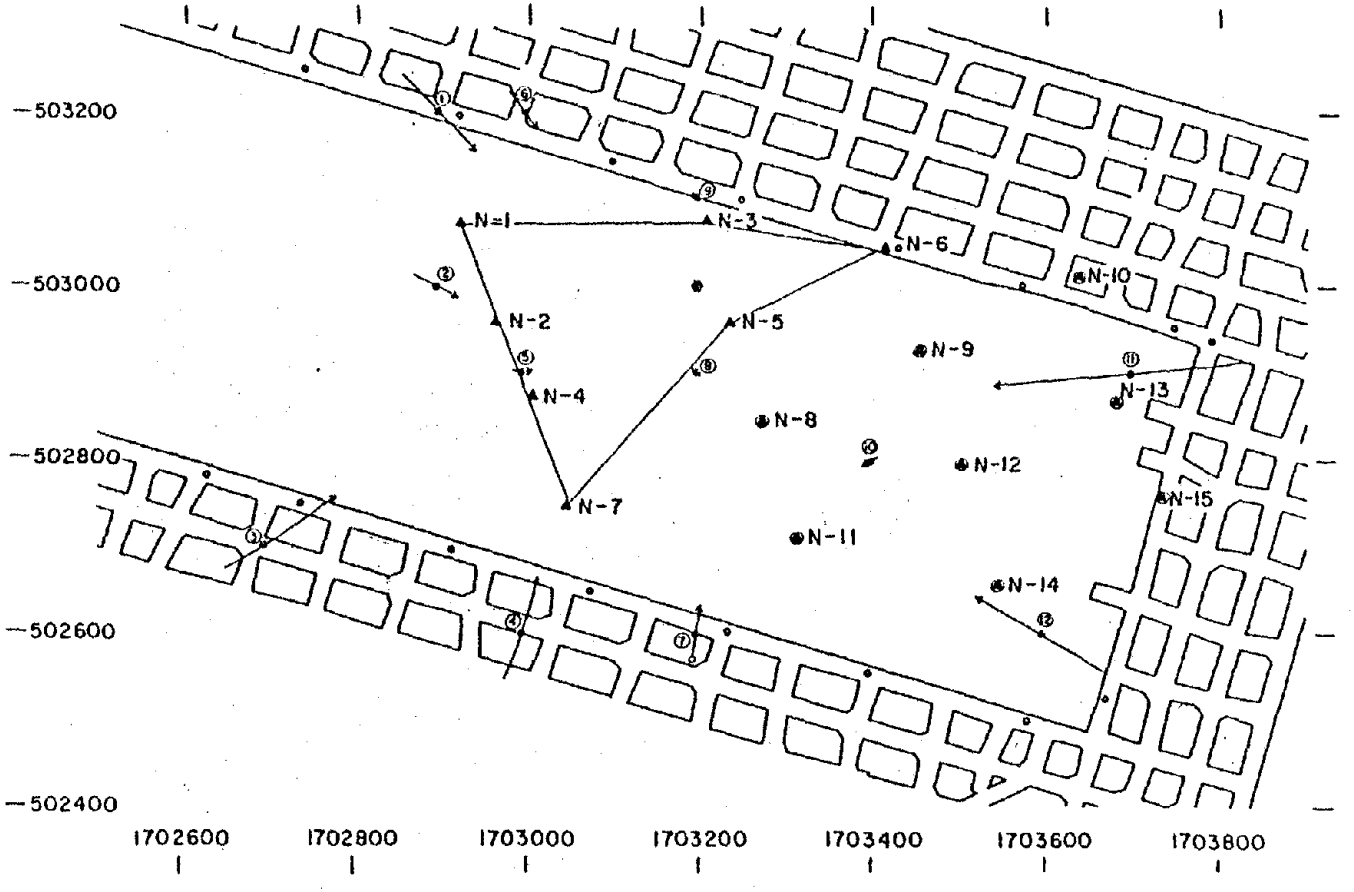

Figure 99. Source Location Plot: Array A, Isotropic Velocity Model.

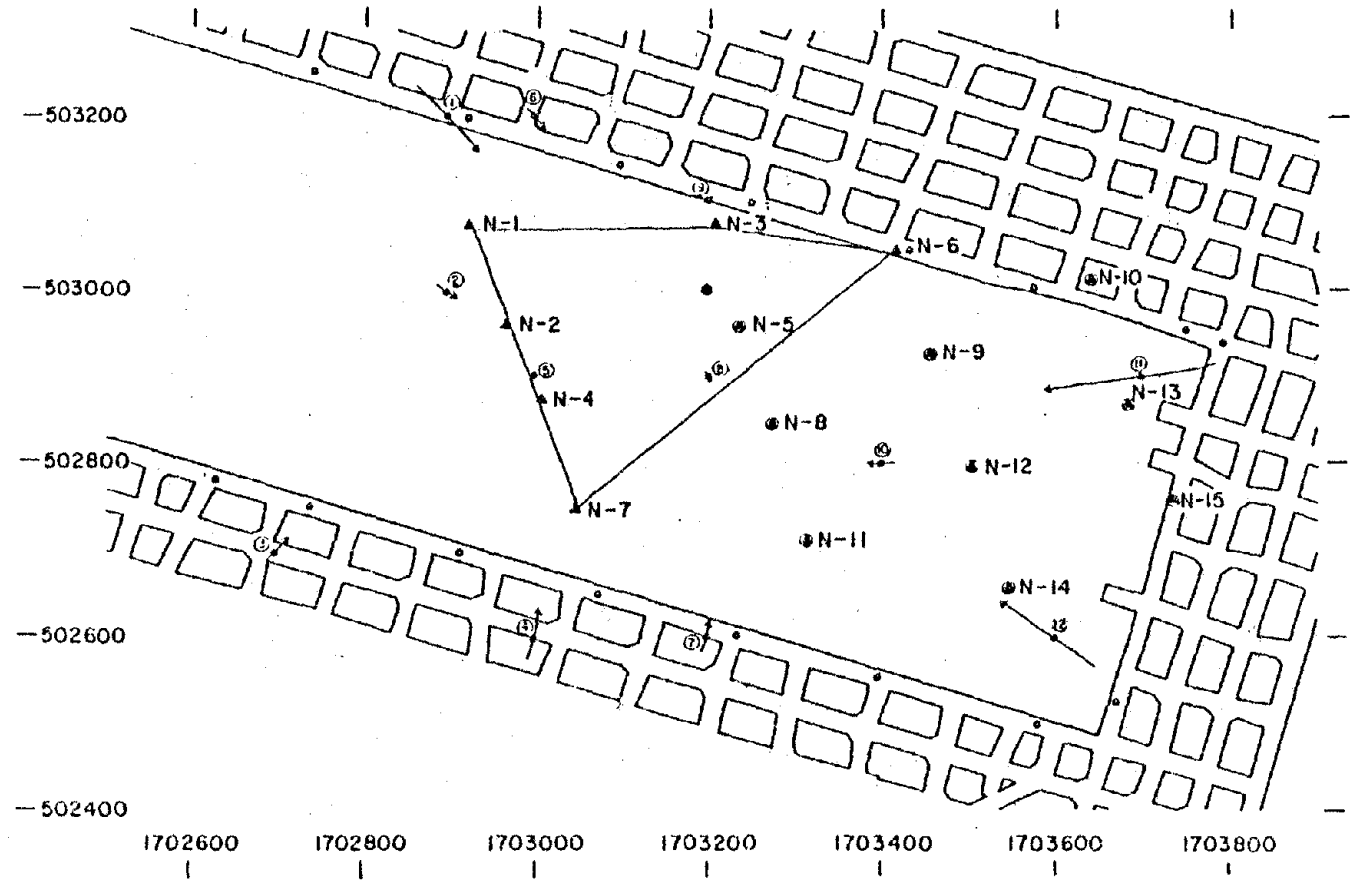

Figure 100. Source Location Plot: Array B, Isotropic Velocity Model.

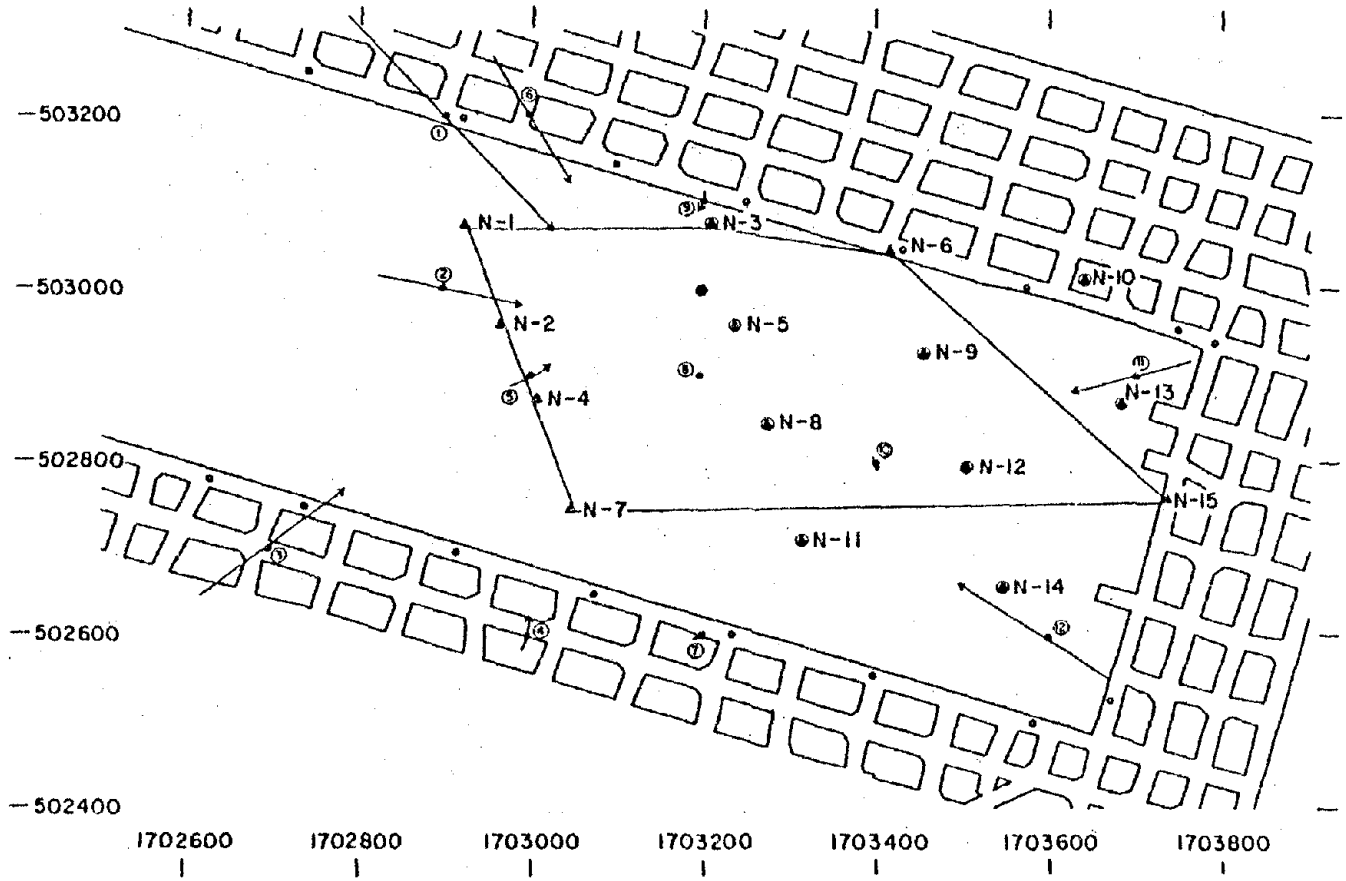

Figure 101. Source Location Plot: Array C, Isotropic Velocity Model.

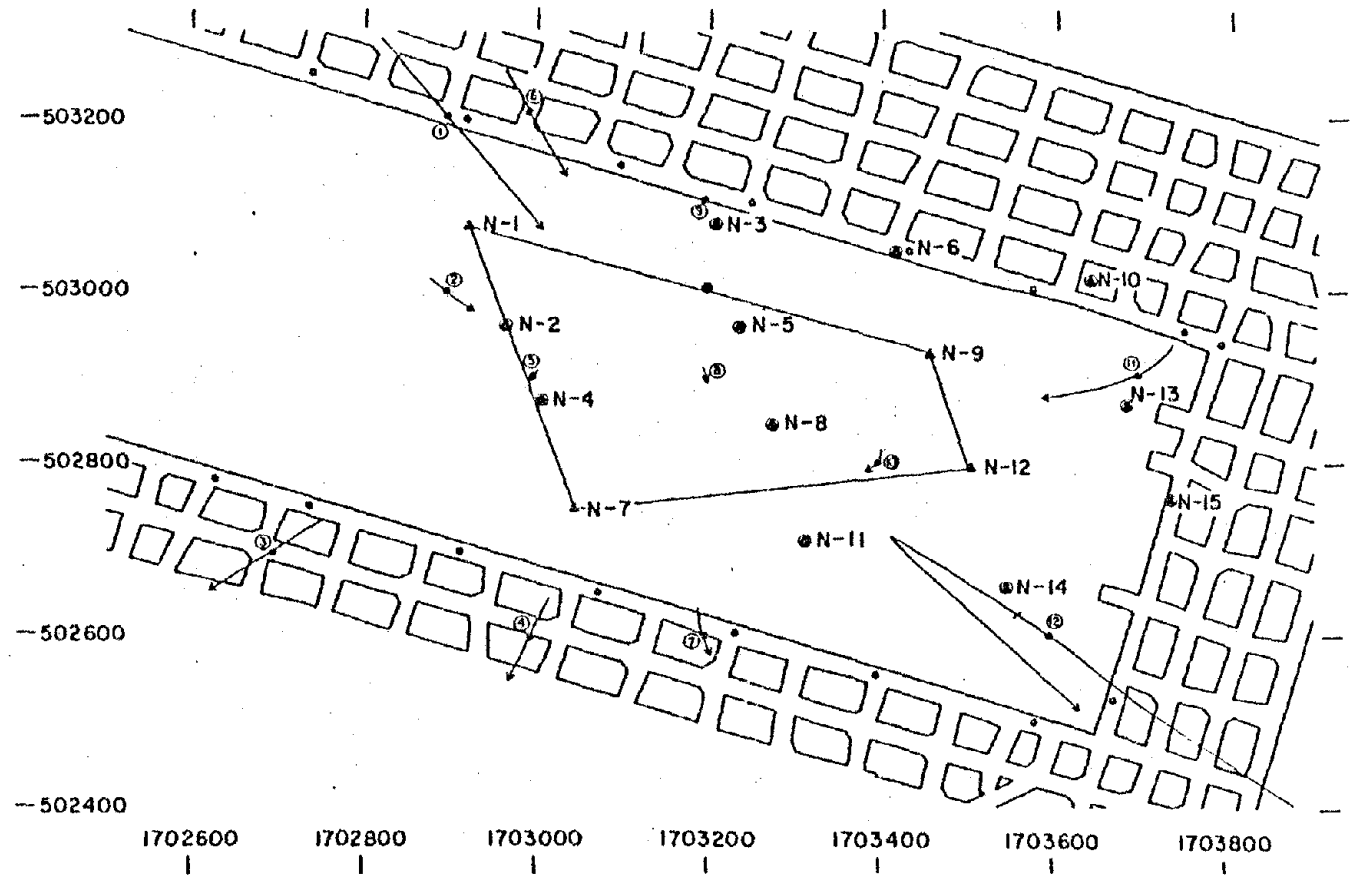

Figure 102. Source Location Plot: Array D, Isotropic Velocity Model.

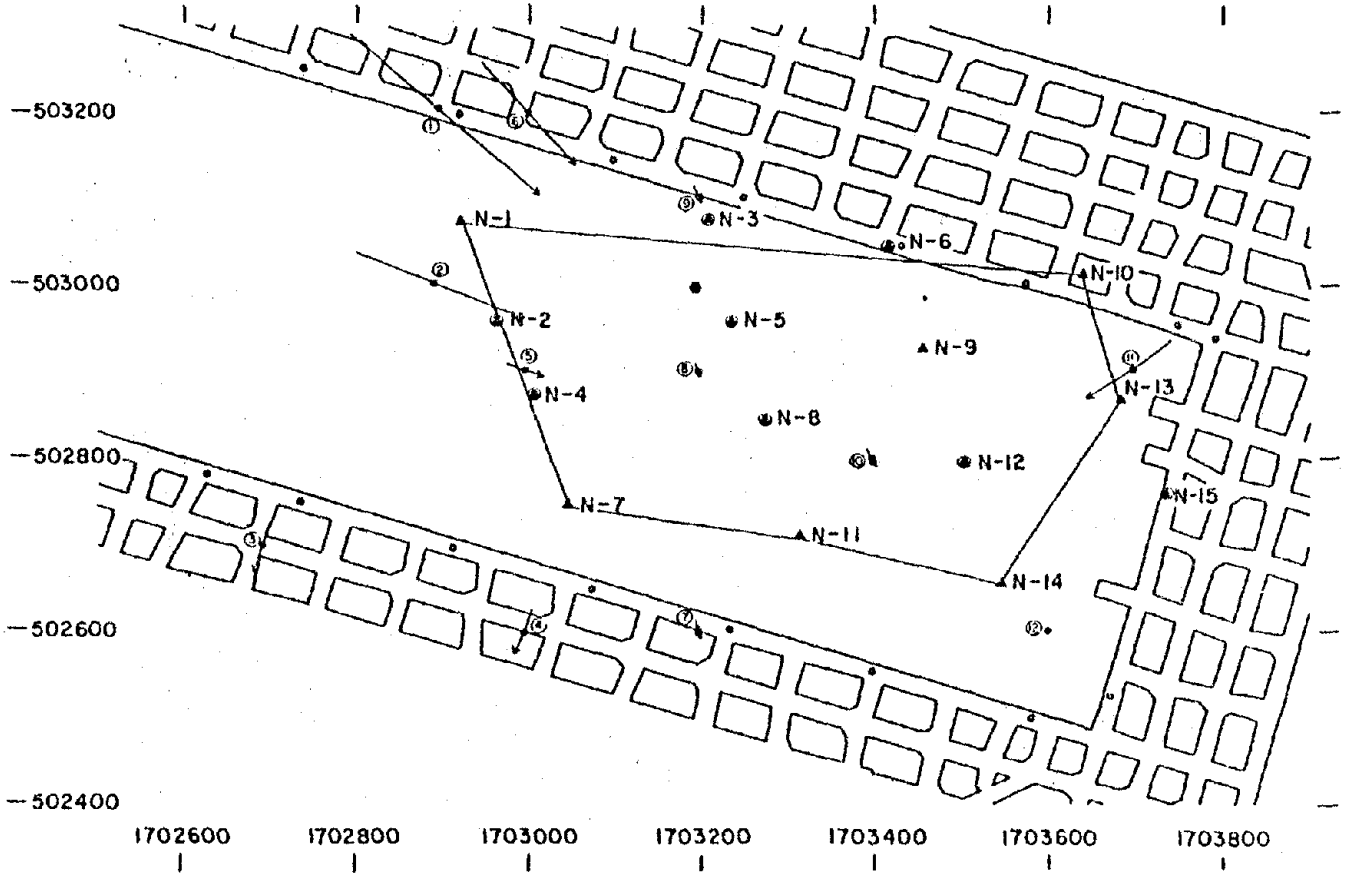

Figure 103. Source Location Plot: Array E, Isotropic Velocity Model.

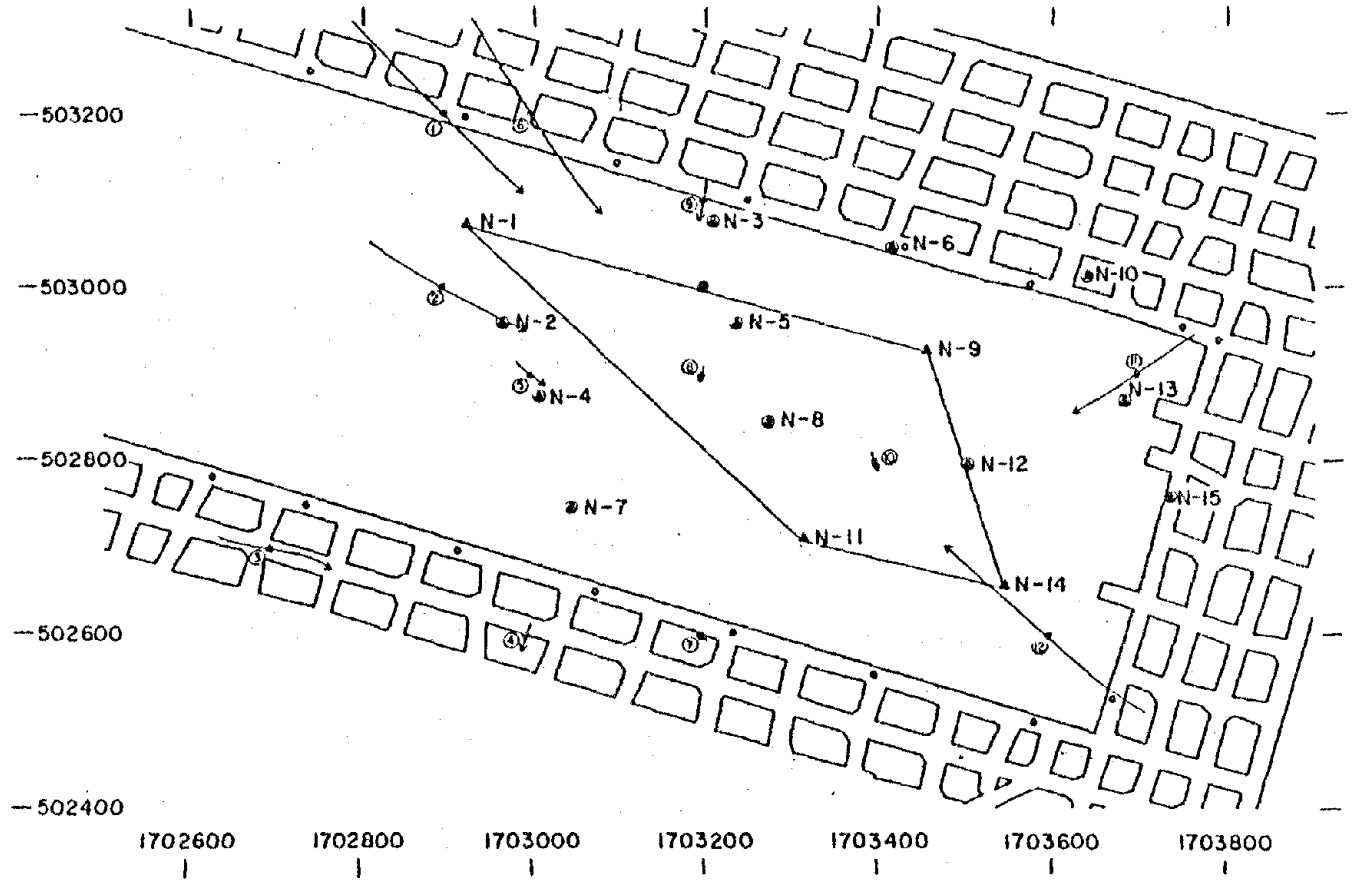

Figure 104. Source Location Plot: Array F, Isotropic Velocity Model.

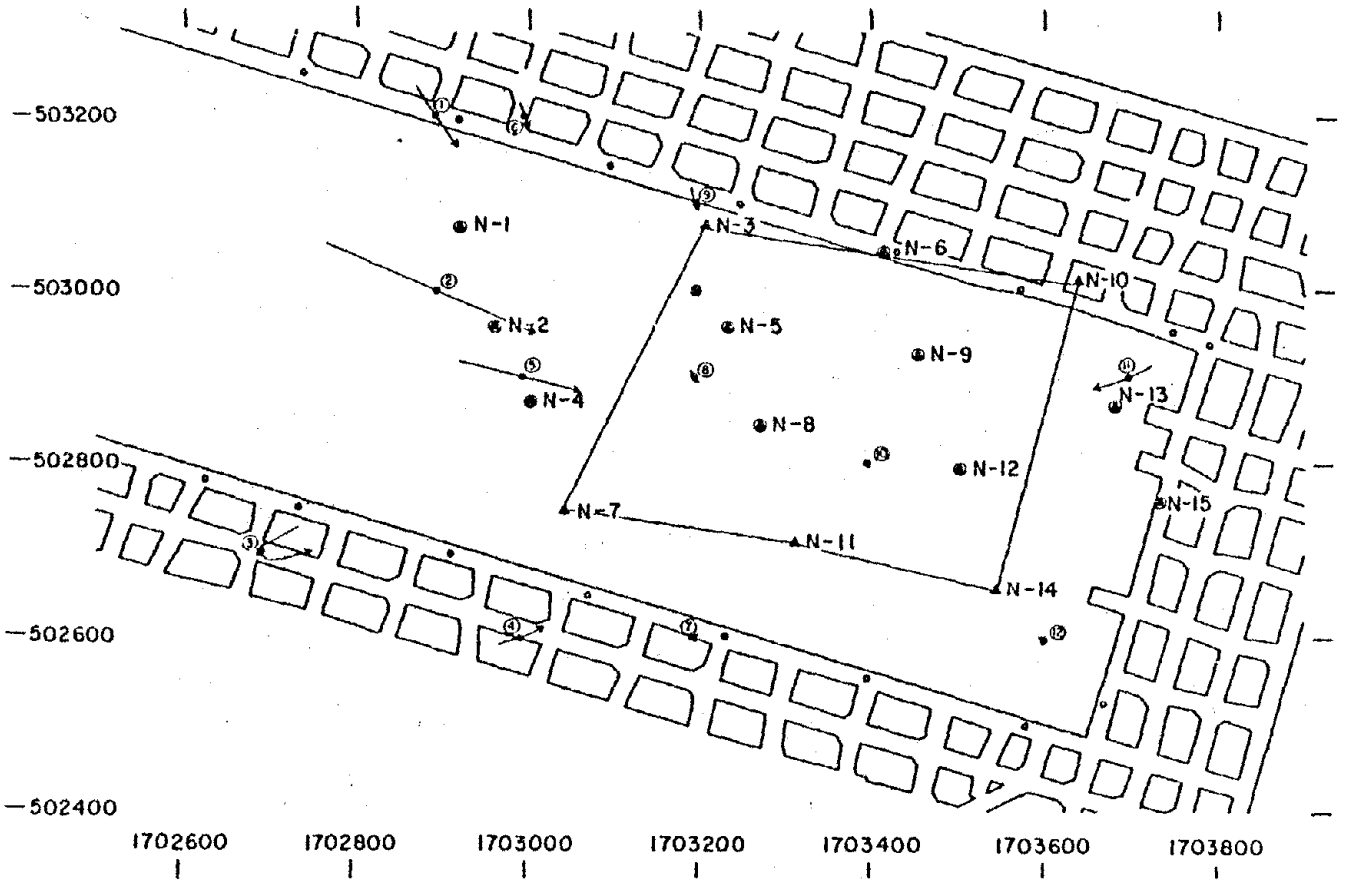

Figure 105. Source Location Plot: Array G, Isotropic Velocity Model.

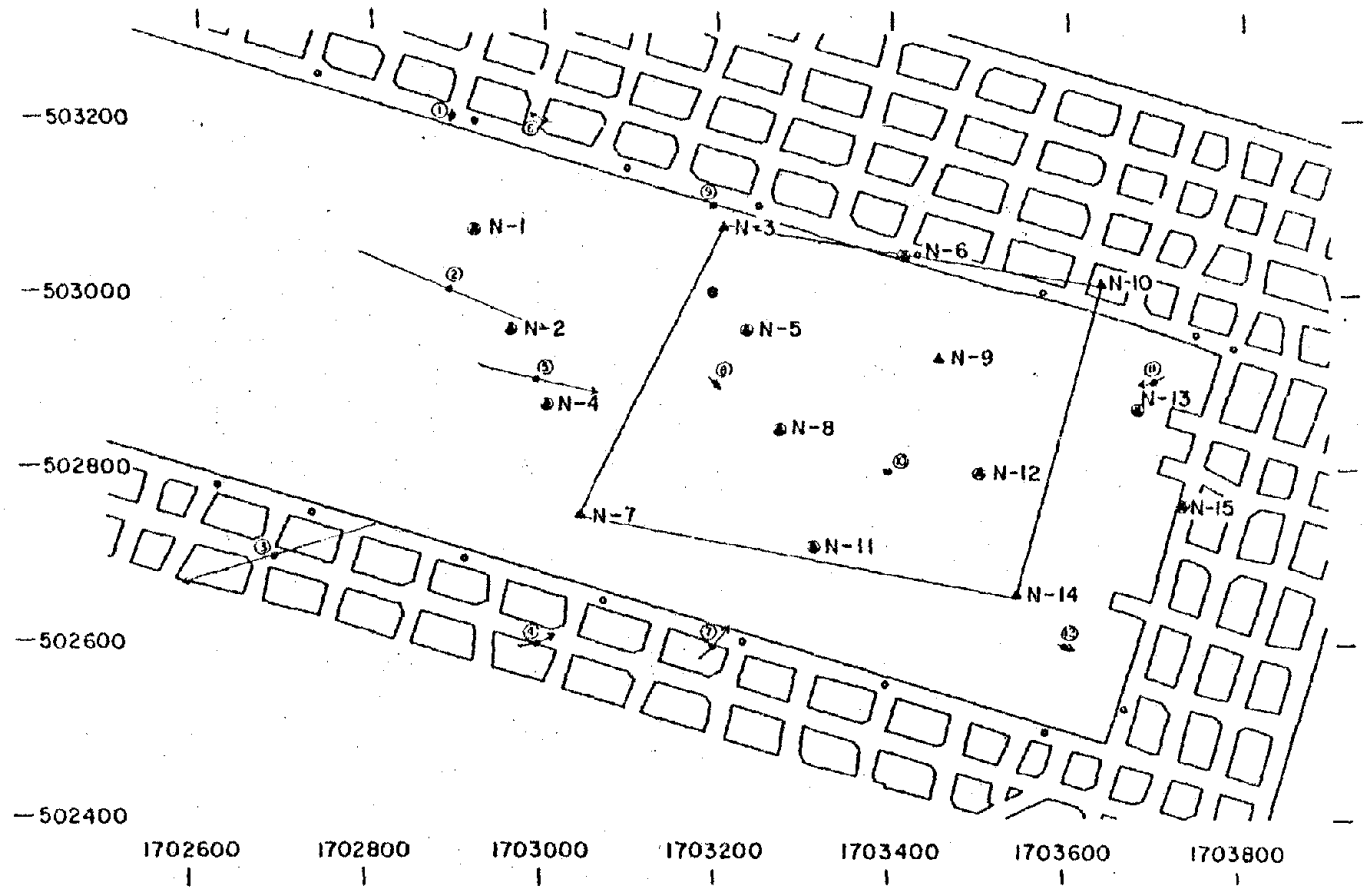

Figure 106. Source Location Plot: Array H, Isotropic Velocity Model.

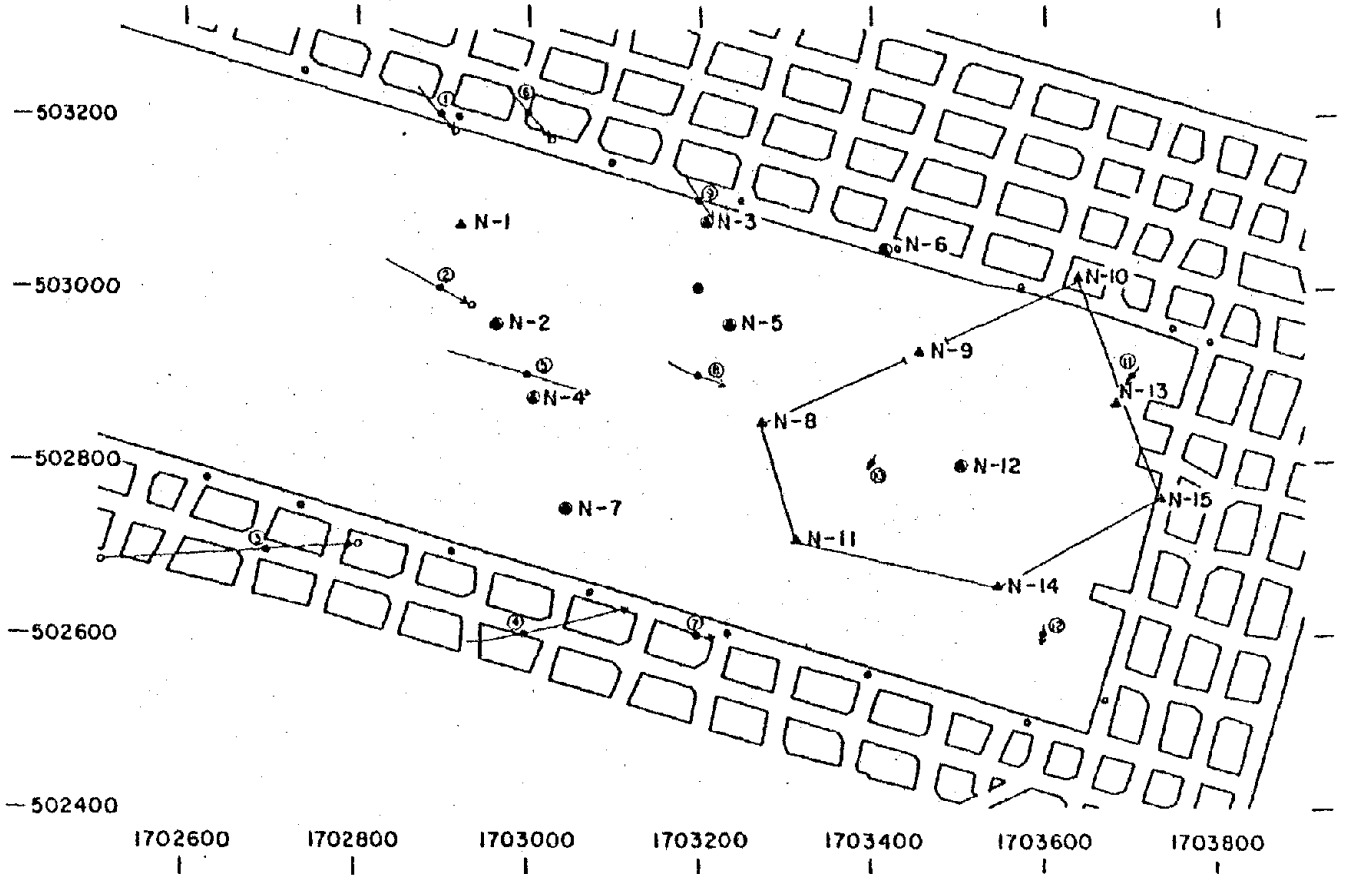

Figure 107. Source Location Plot: Array I, Isotropic Velocity Model.

of the array were usually smaller than those in array-A. Array-F was somewhat elongated as compared to other arrays; also the location deviations here tended to be larger than those in array-A. Array-G was approximately square in shape. The location deviations for array-G basically were smaller than those found for array-A, except for the left-hand region.

Array-H was quite similar to array-G in geometric shape and area, and the location deviations obtained were approximately the same as those for array-G. Finally, array-I appeared to give the poorest location solutions for any of the nine arrays considered. Numerous instabilities and large deviations in the location solution were prevalent, particularly at test points far removed from the array.

From the results obtained, the following set of general conclusions can be drawn.

(1) The geometry of the array influences the deviation and the direction of the source location.

(2) Source locations which lie within the boundaries of the array generally have smaller location deviations than those which lie outside the array boundaries.

(3) No real quantitative evaluation of the effect of array size or geometry can be made unless many test points are considered for the array under study.

(4) In a field study, the array to be utilized should be examined thoroughly to observe which regions are subject to large deviations in solution.

2. Effect of Arrival Time Error

To determine the amount of error introduced when the arrival time for a single geophone is incorrectly read, it is necessary to first ascertain the maximum possible error in reading the first break point for that geophone. During the current field study, the arrival times were generally assumed to be accurate to within ±1 ms. The time error was then incorporated into the IBMSL program by giving geophone station N-1 a time error of -1 ms and assuming that all other geophones had no timing errors. Using the arrival times associated with test point 2 (coordinates: x = 2,000 ft; y = 3,000 ft; and z = 1,300 ft) and array-A, the corresponding source location was determined. The standard isotropic velocity model (velocity maximum = 12,000 fps; velocity minimum = 8,000 fps; velocity increments = 200 fps) was employed for these tests, such that 21 velocity models (and consequently 21 source locations) were obtained. The calculated source location points for the various velocities were connected as shown in Figure 108. In like manner, all other geophones were, in turn, each given a -1 ms timing error and their corresponding source location variations with respect to velocity are also plotted in Figure 108. The reader can readily observe that certain geophone locations are highly sensitive to arrival time errors, e.g., N-3 and N-7.

An error of +1 ms was then introduced to each of the geophones in the same way as described above. Figure 109 shows the variation in source location as a function of velocity (assuming in each case that only one geophone has been read incorrectly). Again, one can easily see that certain geophone locations are susceptible to small arrival time errors. Considering the worst cases, an error of +1 ms results

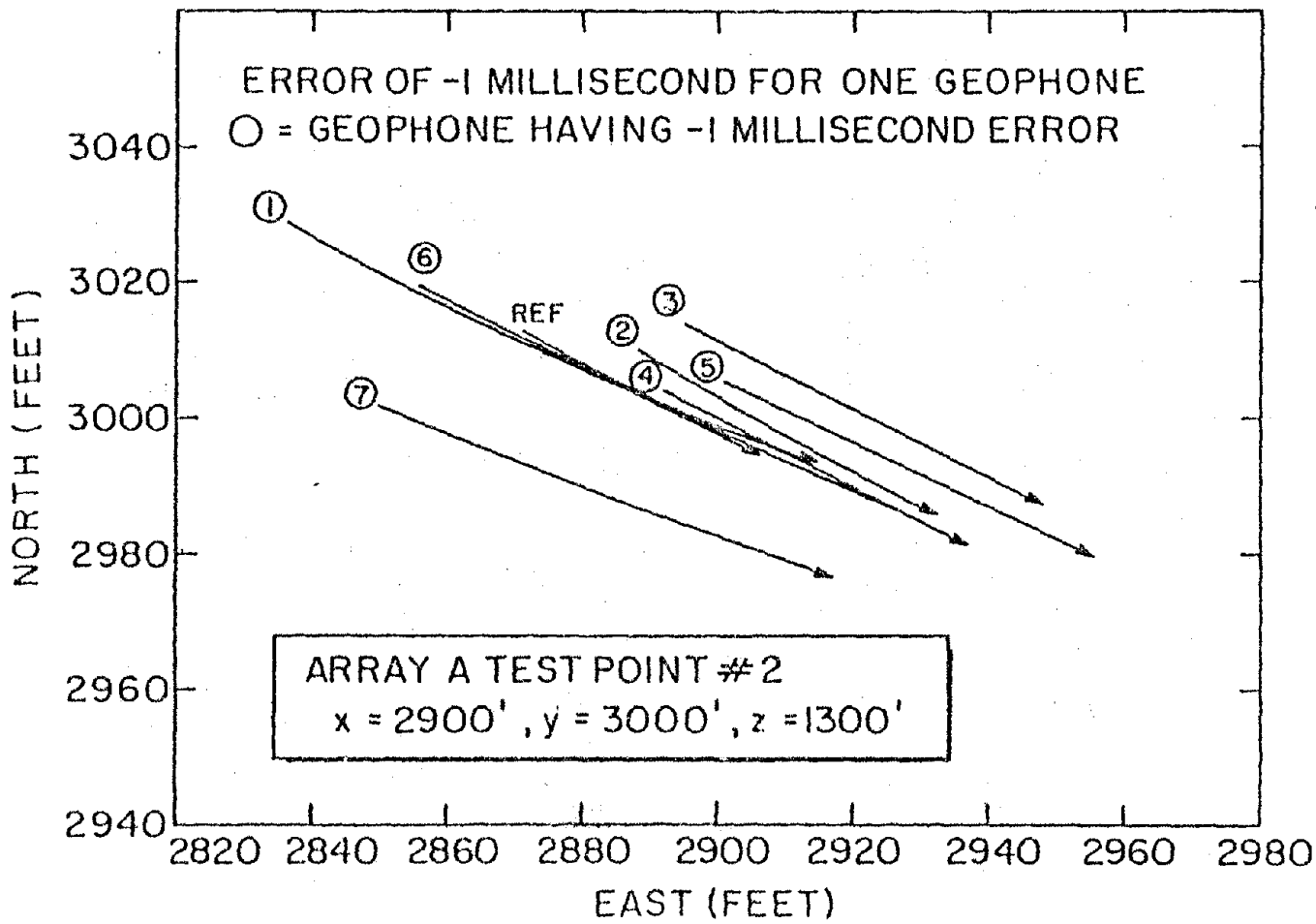

Figure 108. Location Error Resulting from a -1 Ms Time Error.

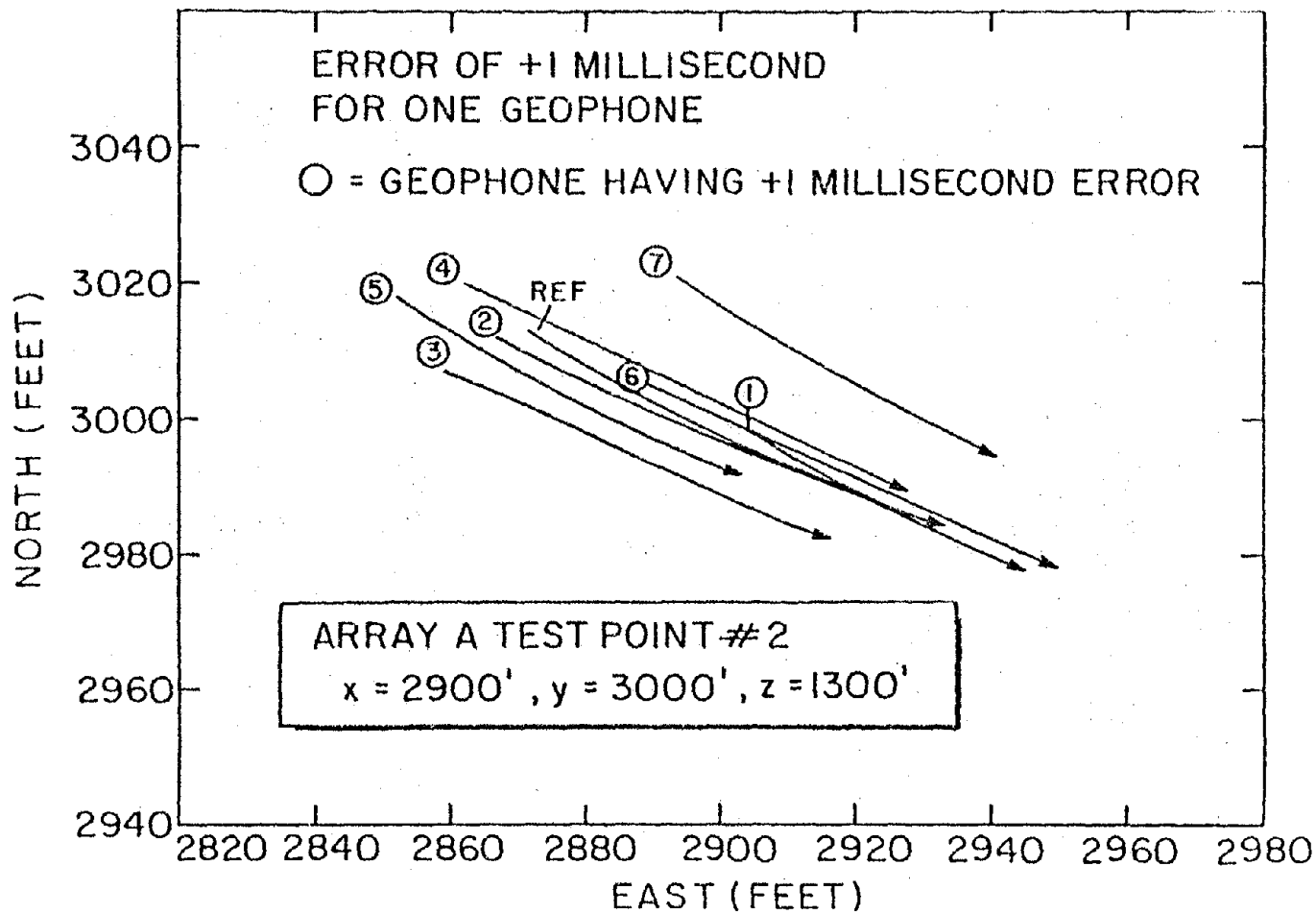

Figure 109. Location Error Resulting from a +1 Ms Time Error.

in a ±30 ft error in the x-direction, ±10 ft in the y-direction, and ±60 ft in the z-direction. Such error estimates are only valid for test point 2 in array-A. Error estimates for all other test points and/or arrays could be computed in the manner described above.

In general, therefore, the solution for one geophone whose arrival time is in error of +1 ms is located on one side of a plane whose edge runs roughly parallel to the exact solution (no arrival time errors). If the same geophone has an error of -1 ms, the solution lies on the other side of the plane nearly symmetrically opposite the +1 ms solution.

It is imperative, therefore, that arrival times be determined as accurately as possible for the best solution.

3. Effect of Initial Source Location Estimate

To establish a starting point for IBMSL, an approximate source location point is needed, i.e., an initial estimate. Generally, this initial estimate is not critical. Initial estimates as much as 300 ft outside a given array have been found to be adequate to obtain the desired source location.

Using array-A and the 12 test points defined earlier, a study was conducted to determine what effect, if any, the initial estimate had on the source location solution. The original initial estimate was used as a standard, i.e., x = 3,200 ft; y = 3,000 ft; and z = 1,300 ft. Next, the x-coordinate of the initial estimate was increased to 3,400 ft, the y-coordinate was decreased to 2,900 ft, and the z-coordinate was held constant at 1,300 ft. The solutions for all 12 test points were the same as determined for the standard initial estimate.

The x-coordinate was then decreased to 2,800 ft, the y-coordinate was increased to 3,000 ft, while the z-coordinate was held constant at 1,300 ft. Again, the solutions were the same as determined for the standard initial estimate.

Next, the z-coordinate was varied, keeping the x- and y-coordinates the same as the original initial estimate. The z-coordinate was first set at 0 ft and the resultant solutions were identical to the standard initial estimate. Finally, the z-coordinate was set at 1,800 ft (100 ft above the plane of the array). For this condition, all solutions were found to lie above rather than below the array. Also the x- and y-coordinates were observed, for the most part, to lie somewhat closer to the center of the array than for the standard initial estimate. None of these solutions intersected their appropriate test points, as shown in Figure 110.

Overall, as long as the initial z-coordinate estimate lies below the plane of the array, the solutions obtained are correct. However, if the initial estimate lies above the array, an incorrect solution is obtained. This is probably due to the squaring of terms, which can generate two solutions, one solution of which is unrealistic, i.e., a solution which exists above the plane of the array.

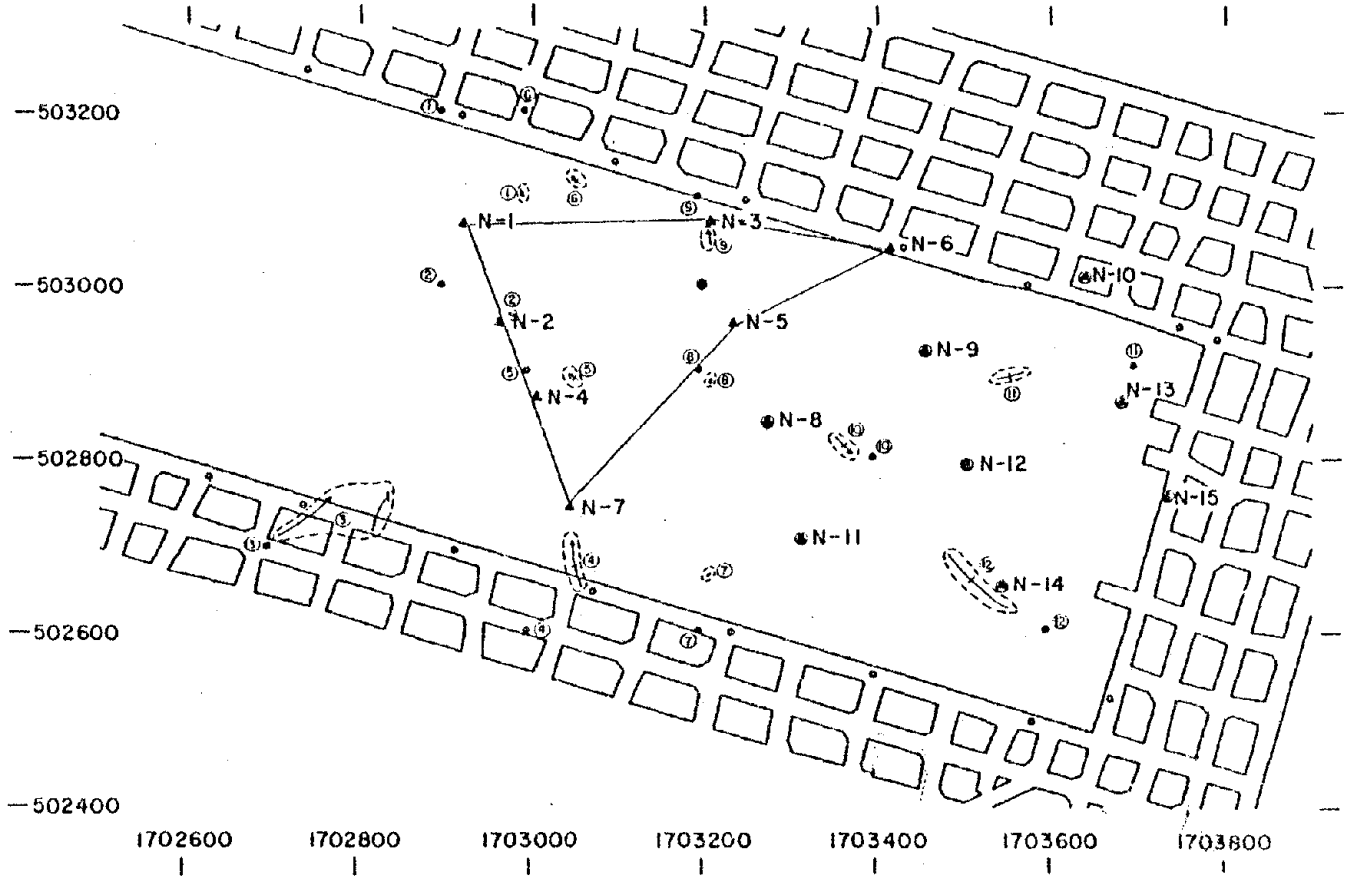

Figure 110. Source Locations Obtained with an Unsatisfactory Initial Estimate (x = 3,200; y = 3,000; z = 1,800 ft).

APPENDIX D

ARRIVAL TIMES OF EVENTS

Approximately 150 events were of sufficient amplitude (level-3) to accurately determine their relative arrival times. In Table 10, the events are numbered sequentially in time in the "Event No." column. The "Event No." represents the cumulative number of events selected from the initial to the final field trip. The "Tape-Footage" data gives the tape reel number and tape footage at which each event was recorded. If two or more events occurred nearly simultaneously (having less than 2 ft of tape between them), each event was given a letter attached to the footage, with the first event being given the suffix of A after the footage, the second event being given a B suffix, and so on. For each field trip a sequential identity number ("ID") was assigned for each qualifying event, with the first event being identified as "1." The remaining columns contain the relative arrival times for the various geophones. These times are given in milliseconds.

TABLE 10

Arrival Times of Events

Event No.	Date	Tape Footage	ID	Geophone Arrival Times (Ms) N-1	N-2	N-3	N-4	N-5	N-6	N-7
1	Feb. 18	36-0244	1	43.5	43.0	52.0	43.0	47.0	59.5	43.0
2	Feb. 18	36-0387	2	43.7	46.0	58.4	41.8	53.3	66.8	42.6
3	Feb. 18	36-1000A	3	46.0	45.5	55.0	44.0	48.5	62.0	44.5
4	Feb. 18	36-1000B	4	45.0	45.0	51.0	44.0	49.0	61.0	45.0
5	Feb. 18	36-1072	5	43.5	43.0	54.5	42.5	47.5	59.3	43.0
6	Feb. 18	36-1489	6	43.5	47.3	53.0	52.0	49.0	59.0	54.5

				N-8	N-10	N-11	N-12	N-14	N-15
7	Feb. 18	36-3797	1	61.8	41.0	50.0	41.8	41.7	42.3
8	Feb. 18	36-4207	2	45.5	66.0	50.8	57.8	66.5	72.5
9	Feb. 18	36-4241	3	42.5	66.0	47.7	56.0	61.8	68.6

				N-1	N-2	N-3	N-4	N-6	N-7
10	Feb. 23	37-6412	1	43.0	48.0	50.0	52.0	58.0	57.0
11	Feb. 26	38-0807	1	46.8	45.0	51.8	44.0	54.9	44.8
12	Feb. 26	38-1070	2	48.4	46.8	56.3	43.5	60.0	46.3
13	Feb. 26	38-1100	3	45.8	45.0	52.3	44.5	58.8	45.5
14	Feb. 26	38-1196	4	53.5	53.4	60.8	44.5	61.0	43.6
15	Feb. 26	38-1993	5	45.8	47.3	53.0	43.5	60.0	55.0
16	Feb. 26	38-3170	6	45.0	47.6	51.4	49.0	57.8	51.4
17	Feb. 26	38-3171	7	41.7	42.8	46.2	44.3	51.8	47.0
18	Feb. 26	38-3175B	8	40.8	46.0	44.5	46.1	49.5	49.3
19	Feb. 26	38-3310	9	45.3	44.0	54.5	47.8	55.5	41.2
20	Feb. 26	38-3560	10	53.2	49.6	57.1	45.0	60.7	44.8

TABLE 10 (Continued)

Event No.	Date	Tape Footage	ID	Geophone Arrival Times (Ms) N-1	N-2	N-3	N-4	N-6	N-7
21	Feb. 26	38-3812	11	43.3	44.5	45.0	45.5	45.8	41.4
22	Feb. 26	38-3817	12	42.7	42.7	46.7	42.7	46.6	47.0
23	Feb. 26	38-3854A	13	41.5	51.6	49.5	55.4	56.0	58.5
24	Feb. 26	38-3854B	14	45.2	48.6	48.4	51.8	53.2	59.6
25	Feb. 26	38-4001	15	52.5	49.0	59.3	43.5	61.1	40.7
26	Feb. 26	38-4063	16	44.3	46.3	47.0	47.6	53.4	51.5
27	Feb. 26	38-4101	17	43.7	45.3	48.2	45.0	51.9	47.5
28	Feb. 26	38-4131	18	43.6	44.6	47.8	47.0	53.0	49.2
29	Feb. 26	38-4134	19	43.0	44.8	49.5	45.9	54.3	47.3
30	Feb. 26	38-4280	20	56.1	52.5	61.5	47.0	64.5	43.5
31	Feb. 26	38-4387	21	48.3	46.3	52.3	42.7	58.9	42.5
32	Feb. 26	38-4448	22	42.4	44.8	47.5	43.5	53.4	45.0
33	Feb. 26	38-4501	23	44.9	43.0	47.2	42.4	55.0	46.5
34	Feb. 26	38-4650	24	50.5	48.0	55.0	45.2	59.3	45.0
35	Feb. 26	38-4652	25	47.0	45.2	56.1	41.7	60.5	41.5
36	Feb. 26	38-4655	26	46.5	45.0	51.1	42.0	56.5	42.0
37	Feb. 26	38-4824	27	47.0	48.3	45.5	50.5	50.3	54.0
38	Feb. 26	38-4862	28	50.0	48.5	56.2	44.3	60.0	44.9
39	Feb. 26	38-4894	29	44.6	47.5	45.3	44.5	50.7	54.0
40	Feb. 26	38-4897	30	53.8	50.8	60.3	45.0	62.4	41.6
41	Feb. 26	38-4939	31	43.1	43.8	47.4	42.0	54.8	45.3
42	Feb. 26	38-4957	32	44.5	47.2	47.4	43.5	55.7	44.4
43	Feb. 26	38-4979	33	41.2	42.0	54.4	40.7	55.0	44.2
44	Feb. 26	38-4999	34	43.3	52.0	43.5	54.5	52.0	58.0
45	Feb. 26	38-5313	35	55.0	51.6	61.6	46.0	63.7	43.3
46	Feb. 26	38-5325	36	44.5	47.5	55.7	52.3	55.5	56.2
47	Feb. 26	38-5327	37	45.0	49.0	47.0	49.3	53.0	50.8
48	Feb. 26	38-5329	38	47.7	45.7	54.0	42.7	57.0	42.8
49	Feb. 26	38-5377	39	41.8	42.2	46.2	42.1	44.0	42.0

TABLE 10 (Continued)

Event No.	Date	Tape Footage	ID	Geophone Arrival Times (Ms) N-1	N-2	N-3	N-4	N-6	N-7
50	Feb. 27	39-0456	1	50.0	46.0	54.1	43.5	58.7	42.0
51	Feb. 27	39-0470	2	41.0	45.0	41.7	47.5	47.3	51.5
52	Feb. 27	39-0867	3	43.5	47.3	44.0	50.5	49.3	53.3
53	Feb. 27	39-1024	4	50.8	48.6	55.4	44.6	58.0	44.0
54	Feb. 27	39-1243	5	40.0	45.0	41.6	48.3	46.4	50.0
55	Feb. 27	39-2176	6	43.5	42.8	44.2	42.6	48.2	44.0
56	Feb. 27	39-2177	7	44.6	44.4	52.0	44.1	51.8	45.2

				N-1	N-2	N-3	N-4	N-6	N-7	N-15
57	Feb. 27	39-2939	1	42.3	42.4	44.4	44.6	49.7	47.0	68.1
58	Feb. 27	39-3070	2	48.0	53.5	60.8	63.7	58.6	79.0	81.5
59	Feb. 27	39-3079	3	43.4	46.5	44.4	49.2	50.8	50.8	81.5
60	Feb. 27	39-3977	4	45.0	44.3	48.5	43.0	53.5	44.5	70.3
61	Feb. 27	39-4193	5	46.0	44.9	49.5	43.0	53.5	44.2	71.0
62	Feb. 27	39-4326	6	47.4	46.3	51.2	45.0	55.5	46.3	73.3
63	Feb. 27	39-4451	7	50.7	48.5	55.8	47.0	60.0	44.0	86.3
64	Feb. 27	39-4501	8	45.0	42.7	46.6	41.2	52.3	41.3	70.3
65	Feb. 27	39-4616	9	54.6	51.0	59.5	44.8	61.2	41.0	72.0
66	Feb. 27	39-4806	10	45.0	43.6	48.7	42.0	52.8	42.7	70.0
67	Feb. 27	39-5009	11	46.5	45.2	50.3	43.0	53.6	44.0	69.8
68	Feb. 27	39-5217	12	58.8	53.6	62.8	48.0	65.4	44.2	75.4
69	Feb. 27	39-5336	13	43.7	43.4	46.2	42.6	43.5	43.8	84.0
70	Feb. 27	39-5351	14	47.5	45.5	50.5	44.8	54.8	46.0	72.0
71	Feb. 27	39-5466	15	53.9	49.0	48.5	43.2	60.5	40.0	71.0
72	Feb. 27	39-5538	16	45.5	44.5	49.0	43.0	52.8	44.3	70.3
73	Feb. 27	39-5855	17	43.5	42.5	47.5	42.0	52.5	42.5	67.5

TABLE 10 (Continued)

Event No.	Date	Tape Footage	ID	Geophone Arrival Times (Ms) N-1	N-2	N-3	N-4	N-5	N-6	N-7
74	Mar. 6	01-0056	1	50.8	49.0	51.0	46.5	44.3	53.0	47.0
75	Mar. 6	01-0391	2	53.5	49.0	52.4	43.6	43.8	55.5	42.3
76	Mar. 6	01-0469	3	48.2	45.7	48.0	43.2	41.0	49.6	43.5
77	Mar. 6	01-0656	4	54.5	50.8	53.5	44.9	45.8	56.8	43.2
78	Mar. 6	01-0818	5	48.4	45.8	48.2	43.3	41.2	50.4	43.3
79	Mar. 6	01-1176	6	52.4	48.3	52.4	42.6	44.2	60.4	41.8
80	Mar. 6	01-1402	7	52.0	48.3	52.3	42.7	43.8	55.7	40.8
81	Mar. 6	01-1676	8	54.3	49.8	53.8	43.7	45.0	56.5	41.5
82	Mar. 6	01-1814	9	53.2	50.4	52.8	47.2	45.0	55.0	47.3
83	Mar. 6	01-1860	10	54.2	48.8	54.2	43.4	44.5	0.0	41.4
84	Mar. 6	01-2040	11	56.0	50.8	55.8	44.8	45.6	57.2	42.4
85	Mar. 6	01-2104	12	49.9	47.4	49.4	45.0	42.4	50.9	45.4
86	Mar. 6	01-2395	13	51.6	48.9	51.0	46.5	44.3	54.2	46.3

				N-1	N-2	N-3	N-4	N-6	N-7	N-15
87	Mar. 6	01-4663	1	56.6	52.0	57.0	46.3	60.4	43.6	69.9
88	Mar. 6	01-5062	2	46.0	43.4	46.1	40.5	47.2	40.2	63.8
89	Mar. 6	01-5656	3	46.9	44.2	47.0	41.0	49.5	40.5	64.5
90A	Mar. 6	01-5934A	4	54.9	53.5	58.5	47.5	60.8	45.0	71.5
90B	Mar. 6	01-5934B	5	55.0	50.5	55.3	43.6	57.6	41.0	67.6
91	Mar. 6	01-6086	6	45.4	42.8	45.2	39.8	47.5	39.8	60.8

				N-1	N-2	N-3	N-4	N-6	N-7
92	Mar. 13	101-0344	1	51.0	47.0	50.0	42.0	52.0	40.0

TABLE 10 (Continued)

Event No.	Date	Tape Footage	ID	Geophone Arrival Times (Ms)					
				N-3	N-7	N-9	N-10	N-11	N-14
93	May 3	43-3701	1	60.2	61.0	44.6	48.5	50.0	49.4
94	May 3	43-3772	2	58.0	60.0	43.0	49.0	50.0	51.0
				N-3	N-7	N-9	N-10	N-14	
95	May 3	43-6705	1	40.0	60.0	43.0	46.0	58.0	
96	May 3	43-6746	2	52.0	43.0	45.0	49.0	49.0	
				N-3	N-7	N-9	N-10	N-11	N-14
97	May 3	44-340	1	54.0	64.0	47.0	44.0	54.0	57.0
98	May 3	44-341	2	53.0	63.0	46.0	51.0	52.0	57.0
99	May 3	44-350	3	48.0	56.0	45.0	58.0	59.0	63.0
100	May 3	44-717	4	53.0	60.0	45.0	50.0	51.0	52.0
101	May 3	44-807	5	46.0	55.0	50.0	56.0	47.0	60.0
102	May 3	44-1226	6	57.0	51.0	47.0	55.0	41.0	49.0
103	May 10	44-1537	1	46.0	52.0	45.0	49.0	58.0	60.0
104	May 10	44-3054A	2	71.0	76.0	52.0	43.0	55.0	42.0
105	May 10	44-3054B	3	59.0	59.0	54.0	54.0	55.0	47.0
106	May 10	44-3888	4	61.0	51.0	52.0	54.0	40.0	49.0
				N-1	N-7	N-9D	N-9SH	N-9SF	N-12
107	May 10	44-5730	1	77.0	62.0	47.0	49.0	51.0	45.0
108	May 10	44-6319	2	79.0	60.0	48.0	49.0	45.0	52.0
109	May 10	44-6620	3	78.0	66.0	48.0	49.0	44.0	53.0

TABLE 10 (Continued)

Event No.	Date	Tape Footage	ID	Geophone Arrival Times (Ms) N-1	N-9D	N-9SH	N-9SF	N-11	N-14
110	May 30	46-335	1	79.2	52.7	54.0	58.2	42.2	46.8
111	May 30	46-606	2	82.2	55.8	56.7	61.3	44.8	49.5
112	May 30	46-735	3	73.2	42.0	47.0	51.5	55.8	60.8
113	May 30	46-888	4	73.5	44.0	47.5	50.5	49.5	53.2
114	May 30	46-900	5	74.0	44.8	47.0	50.3	51.5	55.5
115	May 30	46-1033	6	76.5	46.5	48.7	51.8	48.7	53.0
116	May 30	46-1153	7	85.3	47.7	49.5	55.3	46.0	49.2
117	May 30	46-1156	8	77.8	43.7	45.5	48.7	42.2	46.5
118	May 30	46-1158A	9	75.0	45.0	47.2	50.7	45.2	50.3
119	May 30	46-1158B	10	76.3	43.7	44.5	49.0	45.5	48.3
120	May 30	46-1184	11	79.8	51.2	52.5	54.2	43.2	48.3
121	May 30	46-1650	12	75.0	41.7	43.0	44.8	36.2	36.5
122	May 30	46-1651	13	80.5	49.2	50.7	53.2	42.2	46.0
123	May 30	46-2149	14	71.5	44.5	46.3	47.2	52.3	54.5

				N-1	N-7	N-9	N-10	N-11	N-13	N-14
124	May 30	46-2637	1	65.5	54.2	47.7	53.8	45.5	60.2	54.2
125	May 30	46-2788	2	86.0	65.0	56.5	62.5	62.0	47.2	54.7
126	May 30	46-2918	3	41.3	71.3	46.5	43.0	55.3	65.2	67.7
127	May 30	46-3268	4	46.0	74.2	46.8	44.3	55.5	67.5	69.0
128	May 30	46-3388	5	77.5	65.5	44.0	47.5	49.5	45.7	52.5
129	May 30	46-3415	6	47.2	83.2	49.2	44.3	56.7	67.0	81.3
130	May 30	46-5191	7	57.0	81.7	51.8	46.3	43.5	69.0	56.0
131	May 30	46-5195	8	57.3	72.7	52.0	46.3	57.5	71.7	73.2
132	May 30	46-5204	9	57.5	79.8	51.8	47.0	56.2	71.7	73.2
133	May 30	46-5266	10	81.3	61.8	47.5	52.5	45.3	53.8	50.3
134	May 30	46-5378	11	47.0	78.0	47.2	43.2	52.5	66.7	66.3

TABLE 10 (Continued)

Event No.	Date	Tape Footage	ID	Geophone Arrival Times (Ms) N-1	N-7	N-9	N-10	N-11	N-13	N-14
135	May 30	46-5672	12	48.5	85.5	50.0	44.8	56.5	68.8	55.5
136	May 30	46-5801	13	79.2	98.5	47.2	49.2	56.5	70.7	57.8
137	July 12	49-789	1	86.3	77.3	47.5	50.0	56.0	50.0	56.0
138	July 12	49-1150	2	61.0	85.0	47.5	41.5	69.0	49.2	66.7
139	July 12	49-2656	3	46.8	43.0	51.2	54.0	53.5	69.0	59.7
140	July 12	49-2717	4	85.5	75.0	44.3	50.5	55.8	52.7	53.2
141	July 19	49-5716	1	117.7	89.3	51.8	47.0	68.8	45.2	55.0
142	July 19	49-5856	2	92.2	76.7	59.3	53.2	44.0	43.5	44.0
143	July 19	49-5975	3	103.0	83.2	47.5	44.5	64.8	41.3	48.3
144	July 19	49-6027	4	56.5	75.3	47.7	42.8	68.5	52.3	68.3
145	July 24	53-1148	1	56.5	78.5	49.5	44.0	77.8	55.5	77.5
146	July 24	53-1436	2	110.2	85.3	63.8	60.8	67.3	52.0	44.3
147	July 24	53-1820	3	104.3	83.2	58.0	53.0	61.5	46.3	45.0
148	July 24	53-2437	4	100.5	78.5	49.0	51.8	59.5	78.5	55.3
149	July 24	53-2866	5	62.0	85.5	49.0	42.8	71.0	53.2	65.5
150	July 24	53-2935	6	104.5	69.5	61.3	58.2	52.5	47.5	41.7
151	July 24	53-3211	7	99.7	69.5	65.2	59.3	55.5	48.7	41.0

APPENDIX E

SOURCE LOCATIONS OF EVENTS: ISOTROPIC VELOCITY

Contained in Table 11 is a listing of the source locations of all events investigated. An isotropic velocity model was employed to obtain these results with the velocity ranging from 8,000 to 12,000 fps in 200 fps increments. A total of 21 source location solutions were obtained for each event, and the mean of these 21 solutions has been listed in the "x," "y," and "z" columns under "Source Location." The standard statistical deviations for the three source location components were computed and are listed under "Deviation" as "σ_x," "σ_y," and "σ_z." The time occurrence of each event was calculated to the nearest 5 s on a 24 hour clock, and the hour, minute, and second for each event are listed under "hh," "mm," and "ss," respectively. A total of nine different geophone array configurations were utilized during these studies and these are identified by the letters "A" through "I." Table 9 in Appendix C identifies the geophones utilized in each array.

TABLE 11

Source Locations of Events: Isotropic Velocity Case

Event No.	Tape-Footage	Date	Time of Event hh	mm	ss	Source Location x	y	z	Deviation σ_x	σ_y	σ_z	Array
1	36-0244	Feb. 18	13	34	35	2925	2887	1135	22.5	3.4	154	A
2	36-0387	Feb. 18	13	42	15	3038	2903	1801	18.1	7.9	97	A
3	36-1000A	Feb. 18	14	14	55	2976	2881	1290	14.9	4.2	117	A
4	36-1000B	Feb. 18	14	14	56	2909	2907	1076	19.3	0.6	150	A
5	36-1072	Feb. 18	14	18	45	3071	2912	1861	9.9	7.0	138	A
6	36-1489	Feb. 18	14	41	00	3098	2999	1813	6.5	6.8	124	A
7	36-3797	Feb. 18	17	43	30	3551	2839	1431	3.2	15.9	345	I
8	36-4207	Feb. 18	18	05	20	3304	2910	1486	9.4	6.4	87	I
9	36-4241	Feb. 18	18	07	10	3423	2846	1633	18.3	7.3	150	I
10	37-6412	Feb. 23	13	56	40	2508	3738	120	8.4	10.0	48	B
11	38-0807	Feb. 26	14	49	30	3052	2902	1256	5.4	5.0	37	B
12	38-1070	Feb. 26	15	03	30	3095	2916	1634	5.4	3.7	27	B
13	38-1100	Feb. 26	15	05	10	2762	2857	469	8.9	8.2	131	B
14	38-1196	Feb. 26	15	10	15	3175	3014	1707	7.8	5.3	235	B
15	38-1993	Feb. 26	15	52	45	3097	2981	1719	2.9	1.4	68	B
16	38-3170	Feb. 26	16	20	20	_(a)	_(a)	_(a)	-	-	-	B
17	38-3171	Feb. 26	16	20	25	2784	3159	195	5.3	0.4	107	B
18	38-3175B	Feb. 26	16	20	40	3113	3027	1469	3.2	4.1	63	B
19	38-3310	Feb. 26	16	27	50	3246	3021	1971	4.1	2.0	67	B
20	38-3560	Feb. 26	16	41	10	3033	2782	1193	2.7	5.7	67	B
21	38-3812	Feb. 26	16	54	35	3195	2972	2193	3.1	2.1	89	B
22	38-3817	Feb. 26	16	54	50	3174	2952	1689	9.0	9.2	304	B
23	38-3854A	Feb. 26	16	56	50	3229	2845	1847	13.7	24.9	172	B
24	38-3854B	Feb. 26	16	56	51	3066	3190	1238	3.4	3.0	85	B
25	38-4001	Feb. 26	17	04	40	3183	3054	1505	17.8	36.1	363	B

TABLE 11 (Continued)

Event No.	Tape-Footage	Date	Time of Event hh	mm	ss	Source Location x	y	z	Deviation σ_x	σ_y	σ_z	Array
26	38-4063	Feb. 26	17	08	00	2934	3185	602	5.1	5.8	154	B
27	38-4101	Feb. 26	17	10	00	3003	3018	899	1.4	1.9	85	B
28	38-4131	Feb. 26	17	11	35	2839	3173	253	10.3	4.2	119	B
29	38-4134	Feb. 26	17	11	45	3192	2961	1197	127.0	24.0	122	B
30	38-4280	Feb. 26	17	19	35	2990	2645	1088	0.4	1.9	103	B
31	38-4387	Feb. 26	17	25	15	2951	2782	969	3.0	0.7	116	B
32	38-4448	Feb. 26	17	28	30	2976	2976	950	13.4	4.9	153	B
33	38-4501	Feb. 26	17	31	20	3024	2965	1213	0.1	2.2	69	B
34	38-4650	Feb. 26	17	39	20	2948	2763	852	4.7	8.9	93	B
35	38-4652	Feb. 26	17	39	25	3081	2895	1624	7.7	4.8	23	B
36	38-4655	Feb. 26	17	39	35	2913	2771	760	1.0	4.0	128	B
37	38-4824	Feb. 26	17	48	35	3085	3209	766	3.2	2.0	123	B
38	38-4862	Feb. 26	17	50	35	3054	2862	1368	3.9	4.2	45	B
39	38-4894	Feb. 26	17	52	20	3124	3031	1520	1.6	0.9	56	B
40	38-4897	Feb. 26	17	52	30	3184	3040	1710	13.8	26.6	202	B
41	38-4939	Feb. 26	17	54	45	2974	2963	1049	2.8	3.1	98	B
42	38-4957	Feb. 26	17	55	40	3078	2941	1410	3.4	1.1	72	B
43	38-4919	Feb. 26	17	56	50	3256	2988	1518	0.6	3.3	66	B
44	38-4999	Feb. 26	17	57	55	3140	3070	1595	2.2	6.7	36	B
45	38-5313	Feb. 26	18	14	40	3134	2932	1651	26.1	52.3	275	B
46	38-5325	Feb. 26	18	15	20	3261	2862	1949	0.7	0.5	67	B
47	38-5327	Feb. 26	18	15	25	3087	3043	1243	6.0	7.1	100	B
48	38-5329	Feb. 26	18	15	30	3085	2890	1494	4.0	3.9	32	B
49	38-5377	Feb. 26	18	18	05	3225	2967	2400	0.8	3.1	69	B
50	39-0456	Feb. 27	13	34	45	2931	2691	822	4.7	10.2	103	B
51	39-0470	Feb. 27	13	35	30	3024	3343	622	8.6	14.9	186	B
52	39-0867	Feb. 27	13	56	40	3063	3255	847	7.1	13.1	154	B
53	39-1024	Feb. 27	14	05	05	3058	2827	1258	2.5	5.1	56	B
54	39-1243	Feb. 27	14	16	45	3137	3035	1386	11.3	20.4	283	B

TABLE 11 (Continued)

Event No.	Tape-Footage	Date	Time of Event hh	mm	ss	Source Location x	y	z	Deviation σ_x	σ_y	σ_z	Array
55	39-2176	Feb. 27	15	06	30	3010	2986	521	1.5	4.2	131	B
56	39-2177	Feb. 27	15	06	35	3246	2979	2066	1.0	2.4	46	B
57	39-2939	Feb. 27	16	08	05	2950	3125	523	12.0	10.8	207	C
58	39-3070	Feb. 27	16	15	00	3368	2557	1738	8.9	14.8	404	C
59	39-3079	Feb. 27	16	15	30	3095	3071	1299	10.8	17.3	138	C
60	39-3977	Feb. 27	17	03	25	2951	2909	735	11.1	1.2	174	C
61	39-4193	Feb. 27	17	14	55	2995	2882	884	9.2	1.1	151	C
62	39-4326	Feb. 27	17	22	00	2977	2897	850	10.4	0.7	159	C
63	39-4451	Feb. 27	17	28	40	3070	2872	1405	11.4	11.2	117	C
64	39-4501	Feb. 27	17	31	20	3017	2872	999	8.1	2.6	137	C
65	39-4616	Feb. 27	17	37	30	3018	2615	1074	3.3	6.3	122	C
66	39-4806	Feb. 27	17	47	35	2984	2869	869	9.7	1.6	154	C
67	39-5009	Feb. 27	17	58	25	2994	2854	845	8.3	1.6	152	C
68	39-5217	Feb. 27	18	09	30	2998	2586	1046	3.1	5.8	127	C
69	39-5336	Feb. 27	18	15	55	3167	2947	1679	9.2	9.9	339	C
70	39-5351	Feb. 27	18	16	40	2986	2895	837	8.9	0.6	155	C
71	39-5466	Feb. 27	18	22	50	3005	2600	1062	3.1	5.9	125	C
72	39-5538	Feb. 27	18	26	40	2993	2897	851	9.4	0.6	156	C
73	39-5855	Feb. 27	18	43	35	2892	2885	528	12.7	1.4	201	C
74	01-0056	Mar. 6	13	08	25	3117	2892	1159	3.7	0.7	98	A
75	01-0391	Mar. 6	13	26	20	3118	2791	1272	3.3	4.0	92	A
76	01-0469	Mar. 6	13	30	30	3124	2879	1164	3.4	0.6	95	A
77	01-0656	Mar. 6	13	40	25	3112	2771	1209	4.0	5.8	104	A
78	01-0818	Mar. 6	13	49	05	3117	2872	1164	3.6	0.1	98	A
79	01-1176	Mar. 6	14	08	10	3084	2841	1436	2.9	5.5	77	A
80	01-1402	Mar. 6	14	20	15	3098	2775	1241	4.3	7.2	103	A
81	01-1676	Mar. 6	14	34	50	3111	2748	1235	4.1	7.8	105	A
82	01-1814	Mar. 6	14	42	15	3124	2868	1238	3.0	0.1	86	A
83	01-1860	Mar. 6	14	44	40	3087	2840	1507	2.9	4.4	67	A
84	01-2040	Mar. 6	14	54	15	3123	2755	1297	3.5	7.2	97	A

TABLE 11 (Continued)

Event No.	Tape-Footage	Date	Time of Event hh	mm	ss	Source Location x	y	z	Deviation σ_x	σ_y	σ_z	Array
85	01-2104	Mar. 6	14	57	40	3129	2886	1174	3.2	0.9	93	A
86	01-2395	Mar. 6	15	13	10	3113	2873	1174	3.6	0.1	97	A
87	01-4663	Mar. 6	17	34	05	3058	2650	1022	3.4	3.9	123	C
88	01-5062	Mar. 6	17	55	20	3113	2847	1067	3.8	1.7	115	C
89	01-5656	Mar. 6	18	27	00	3087	2822	999	4.3	2.1	123	C
90A	01-5934A	Mar. 6	18	41	50	3035	2675	950	4.5	4.4	132	C
90B	01-5934B	Mar. 6	18	41	51	3086	2659	1099	2.9	4.3	113	C
91	01-6086	Mar. 6	18	49	55	3087	2824	866	4.2	0.8	132	C
92	101-0344	Mar. 13	13	47	50	3105	2687	990	3.7	3.0	149	B
93	43-3701	May 3	13	19	25	3470	2842	1371	3.4	5.5	89	G
94	43-3772	May 3	13	23	10	3440	2868	1410	3.9	4.6	77	G
95	43-6705	May 3	15	56	50	3379	3129	1306	3.2	5.7	124	H
96	43-6746	May 3	15	59	00	3336	2819	1835	3.2	10.8	225	H
97	44-340	May 3	16	53	05	3461	2994	1339	0.8	5.0	102	G
98	44-341	May 3	16	53	10	3416	2962	1325	1.2	4.8	104	G
99	44-350	May 3	16	53	40	3304	2971	1726	4.1	4.6	190	G
100	44-717	May 3	17	13	15	3442	2932	1181	1.5	4.9	116	G
101	44-807	May 3	17	18	00	3339	2924	1823	2.4	21.9	296	G
102	44-1226	May 3	17	40	25	3355	2769	1358	1.0	5.0	89	G
103	44-1537	May 10	12	14	05	3325	2978	1966	2.5	16.5	143	G
104	44-3054A	May 10	13	35	00	3971	2695	1073	218.1	53.2	493	C
105	44-3054B	May 10	13	35	01	3409	2804	2004	30.5	26.6	71	G
106	44-3888	May 10	14	19	30	3366	2752	1906	1.3	2.9	45	G
107	44-5730	May 10	17	15	25	3394	2815	1381	12.7	5.1	117	D
108	44-6319	May 10	17	46	50	3297	2841	1719	8.9	15.1	145	D
109	44-6620	May 10	18	02	50	3325	2900	1655	6.4	12.0	52	D
110	46-335	May 30	13	14	45	3334	2653	1417	8.2	5.8	91	F
111	46-606	May 30	13	31	05	3332	2652	1430	8.7	5.9	90	F

TABLE 11 (Continued)

Event No.	Tape-Footage	Date	Time of Event hh	mm	ss	Source Location x	y	z	Deviation σ_x	σ_y	σ_z	Array
112	46-735	May 30	13	38	00	3367	2951	1471	0.5	11.2	61	F
113	46-888	May 30	13	46	10	3385	2870	1370	0.6	9.7	76	F
114	46-900	May 30	13	46	50	3395	2902	1371	0.9	11.3	75	F
115	46-1033	May 30	13	53	55	3386	2834	1385	1.5	8.0	78	F
116	46-1153	May 30	14	00	20	3391	2764	1538	6.9	3.8	90	F
117	46-1156	May 30	14	00	25	3392	2780	1464	4.5	4.5	82	F
118	46-1158A	May 30	14	00	35	3371	2808	1411	3.2	6.2	76	F
119	46-1158B	May 30	14	00	36	3404	2817	1413	1.5	8.0	81	F
120	46-1184	May 30	14	01	55	3366	2707	1401	7.1	2.0	86	F
121	46-1650	May 30	14	26	45	3429	2699	1385	0.5	6.3	111	F
122	46-1651	May 30	14	26	50	3383	2709	1429	6.4	3.1	91	F
123	46-2149	May 30	14	53	25	3445	2957	1258	3.7	13.8	90	F
124	46-2637	May 30	16	00	05	3319	2899	1435	2.0	4.8	76	E
125	46-2788	May 30	16	08	10	3370	2887	1632	15.2	15.3	252	E
126	46-2918	May 30	16	15	05	3307	3075	1845	7.9	28.7	510	E
127	46-3268	May 30	16	33	45	3305	3088	1499	5.9	22.3	407	E
128	46-3388	May 30	16	40	10	3477	2909	1383	1.5	10.9	89	E
129	46-3415	May 30	16	41	35	3317	3089	1767	4.1	22.7	272	E
130	46-5191	May 30	18	16	20	3318	3007	1602	7.6	48.5	512	E
131	46-5195	May 30	18	16	30	3306	3071	1854	7.0	27.0	551	E
132	46-5204	May 30	18	17	00	3314	3069	1660	6.0	21.4	419	E
133	46-5266	May 30	18	20	20	3423	2821	1534	6.1	12.2	143	E
134	46-5378	May 30	18	26	15	3314	3042	1643	4.7	17.7	323	E
135	46-5672	May 30	18	42	00	3315	2968	1833	7.0	23.0	450	E
136	46-5801	May 30	18	48	50	3358	3006	1754	4.3	12.4	252	E
137	49-789	July 12	16	56	35	3515	2923	1447	1.9	13.1	91	E
138	49-1150	July 12	17	15	50	3385	3133	1678	25.8	55.5	320	E
139	49-2656	July 12	18	36	05	3231	2975	1984	11.0	12.5	278	E

TABLE 11 (Continued)

Event No.	Tape-Footage	Date	Time of Event hh	mm	ss	Source Location x	y	z	Deviation σ_x	σ_y	σ_z	Array
140	49-2717	July 12	18	39	20	3485	2906	1506	6.7	13.1	78	E
141	49-5716	July 19	18	22	20	3436	2796	1750	45.1	27.5	293	E
142	49-5856	July 19	18	29	45	3439	2847	1757	20.0	23.6	482	E
143	49-5975	July 19	18	36	10	3559	2834	1698	31.3	21.7	126	E
144	49-6027	July 19	18	38	55	3549	3682	1205	5.3	7.2	252	E
145	53-1148	July 24	16	50	40	3484	3682	1659	11.6	24.4	485	E
146	53-1436	July 24	17	06	05	3700	2618	1948	22.6	19.2	158	E
147	53-1820	July 24	17	26	30	3781	2664	1369	42.5	16.1	321	E
148	53-2437	July 24	17	59	25	3390	2847	1926	8.8	25.5	285	E
149	53-2866	July 24	18	22	20	3362	3071	1898	13.1	37.2	341	E
150	53-2935	July 24	18	26	00	3325	2937	1763	143.0	203.0	191	E
151	53-3211	July 24	18	47	45	2735	3791	2159	86.5	137.0	364	E

(a) Source location solution was outside the defined boundaries

APPENDIX F

SOURCE LOCATIONS OF EVENTS: UNIQUE VELOCITY

This appendix lists the location of all events for which it was possible to utilize unique velocity data for source location. The unique velocities were obtained by utilizing the subroutine VLDT which requires a blast to occur at a known location and accurate arrival times for all geophone stations. The blast considered was that one identified as 38-4280 which occurred on February 26, 1974. Only the "Location Source" for each event was computed. Table 12 presents source location data obtained using the six-geophone array (N-1, N-2, N-3, N-4, N-6, and N-7).

TABLE 12

Source Locations of Events: Unique Velocity Case

Event No.	Tape-Footage	Date	Time of Event hh	mm	ss	Source Location x	y	z
1	36-0244	Feb. 18	13	34	35	2889	2887	1377
2	36-0387	Feb. 18	13	42	15	2811	2838	1443
3	36-1000A	Feb. 18	14	14	55	2867	2864	1365
4	36-1000B	Feb. 18	14	14	56	2974	2919	1475
5	36-1072	Feb. 18	14	18	45	2763	2835	1280
6	36-1489	Feb. 18	14	41	00	2827	3032	1252
10	37-6412	Feb. 23	13	56	40	2193	3073	1329
11	38-0807	Feb. 26	14	49	30	2899	2866	1256
12	38-1070	Feb. 26	15	03	30	2866	2842	1303
13	38-1100	Feb. 26	15	05	10	2909	2895	1346
14	38-1196	Feb. 26	15	10	15	2804	2667	1221
15	38-1993	Feb. 26	15	52	45	3000	2981	1479
16	38-3170	Feb. 26	16	20	20	2899	2978	1289
17	38-3171	Feb. 26	16	20	25	2931	2976	1289
18	38-3175B	Feb. 26	16	20	40	2931	3026	1226
19	38-3310	Feb. 26	16	27	50	2912	2849	1302
20	38-3560	Feb. 26	16	41	10	2938	2803	1340
21	38-3812	Feb. 26	16	54	35	2947	2894	1145
22	38-3817	Feb. 26	16	54	50	2933	2959	1183
23	38-3854A	Feb. 26	16	56	50	2902	3128	1271
24	38-3854B	Feb. 26	16	56	51	2965	3108	1293
25	38-4001	Feb. 26	17	04	40	2825	2685	1287
26	38-4063	Feb. 26	17	08	00	2972	3008	1321
27	38-4101	Feb. 26	17	10	00	2898	2949	1211
28	34-4131	Feb. 26	17	11	35	2934	2985	1278
29	38-4134	Feb. 26	17	11	45	2866	2947	1233
30	38-4280	Feb. 26	17	19	35	2881	2720	1326
31	38-4387	Feb. 26	17	25	15	2962	2858	1400
32	38-4448	Feb. 26	17	28	30	2922	2934	1292
33	38-4501	Feb. 26	17	31	20	3000	2943	1426
34	38-4650	Feb. 26	17	39	20	2923	2835	1319
35	38-4652	Feb. 26	17	39	25	2815	2784	1315
36	38-4655	Feb. 26	17	39	35	2933	2853	1341
37	38-4824	Feb. 26	17	48	35	3031	3034	1308
38	38-4862	Feb. 26	17	50	35	2881	2313	1295
39	38-4894	Feb. 26	17	52	20	3043	3024	1402
40	38-4897	Feb. 26	17	52	30	2830	2683	1288
41	38-4939	Feb. 26	17	54	45	2964	2936	1378
42	38-4957	Feb. 26	17	55	40	3014	2928	1440
43	38-4919	Feb. 26	17	56	50	2661	2833	1170
44	38-4999	Feb. 26	17	57	55	3058	3094	1425
45	38-5313	Feb. 26	18	14	40	2837	2695	1295
46	38-5325	Feb. 26	18	15	20	2720	3043	1091

TABLE 12 (Continued)

Event No.	Tape-Footage	Date	Time of Event hh	mm	ss	Source Location x	y	z
47	38-5327	Feb. 26	18	15	25	2986	2998	1301
48	38-5329	Feb. 26	18	15	30	2863	2807	1264
49	38-5377	Feb. 26	18	18	05	2815	2864	1004
50	39-0456	Feb. 27	13	34	45	2940	2820	1357
51	39-0470	Feb. 27	13	35	30	2996	3071	1286
52	39-0867	Feb. 27	13	56	40	3000	3067	1281
53	39-1024	Feb. 27	14	05	05	2896	2794	1264
54	39-1243	Feb. 27	14	16	45	2980	3071	1247
55	39-2176	Feb. 27	15	06	30	2990	2936	1287
56	39-2177	Feb. 27	15	06	35	2781	2853	1103
57	39-2939	Feb. 27	16	08	05	2978	2985	1310
58	39-3070	Feb. 27	16	15	00	3190	2831	1585
59	39-3079	Feb. 27	16	15	30	3007	3026	1329
60	39-3977	Feb. 27	17	03	25	2947	2905	1308
61	39-4193	Feb. 27	17	14	55	2937	2883	1283
62	39-4326	Feb. 27	17	22	00	2935	2893	1289
63	39-4451	Feb. 27	17	28	40	2905	2817	1304
64	39-4501	Feb. 27	17	31	20	2991	3890	1367
65	39-4616	Feb. 27	17	37	30	2871	2684	1293
66	39-4806	Feb. 27	17	47	35	2934	2877	1287
67	39-5009	FEb. 27	17	58	25	2924	2867	1263
68	39-5217	Feb. 27	18	09	30	2918	2718	1352
69	39-5336	Feb. 27	18	15	55	2906	2889	1056
70	39-5351	Feb. 27	18	16	40	2956	2897	1308
71	39-5466	Feb. 27	18	22	50	2898	2706	1329
72	39-5538	Feb. 27	18	26	40	2935	2890	1272
73	39-5855	Feb. 27	18	43	35	2936	2898	1305
74	01-0056	Mar. 6	13	08	25	2988	2874	1252
75	01-0391	Mar. 6	13	26	20	3026	2815	1371
76	01-0469	Mar. 6	13	30	30	2997	2865	1259
77	01-0656	Mar. 6	13	40	25	3023	2812	1366
78	01-0801	Mar. 6	13	49	05	2999	2864	1277
79	01-1176	Mar. 6	14	08	10	3035	2861	1506
80	01-1402	Mar. 6	14	20	15	3000	2802	1357
81	01-1676	Mar. 6	14	35	50	3012	2787	1362
82	01-1814	Mar. 6	14	42	15	3005	2856	1289
83	01-1860	Mar. 6	14	44	40	3071	2902	1588
84	01-2040	Mar. 6	14	54	15	3002	2762	1337
85	01-2104	Mar. 6	14	57	40	3003	2870	1259
86	01-2395	Mar. 6	15	13	10	3012	2872	1312
87	01-4663	Mar. 6	17	34	05	2999	2787	1375
88	01-5062	Mar. 6	17	55	20	2986	2843	1241
89	01-5656	Mar. 6	18	27	00	2994	2847	1289

TABLE 12 (Continued)

Event No.	Tape-Footage	Date	Time of Event hh	mm	ss	Source Location x	y	z
90A	01-5934A	Mar. 6	18	41	50	2909	2753	1262
90B	01-5934B	Mar. 6	18	41	51	2996	2761	1355
91	01-6086	Mar. 6	18	49	55	3000	2858	1284
92	101-0344	Mar. 13	13	47	50	3014	2800	1321

APPENDIX G

BRIEF DAILY LONGWALL REPORTS

This appendix contains a condensation of all pertinent information contained in the three daily longwall shift reports associated with the B-4 East Longwall at the Greenwich, North Mine during the period January 1, 1974 to July 25, 1974. Miner's expressions and terms were copied verbatum to minimize errors in transferring information from the shift reports to this appendix. It should be noted that the support chocks are numbered 1-100 starting at the headgate end of the face.

TABLE 13

Brief Daily Longwall Report--January 1974

Date	Comments
01	No report
02	Bottom soft; chocks pull hard; shot and broke rock on pan line; rock falling from #18 to #30; shoot rock fallen from #18 to #30; bad rock falling #20 to #45; cutting sandrock; breaking rock in panline
03	Clay vein at #33 and #34 chock; bottom soft
04	Cutting slow due to sandrock; hard cutting sandrock from tailgate to #30 chock
05	Belt maintenance and rock dusting
06	No report
07	Low coal and sandrock; slow cutting due to sandrock
08	Cutting slow due to sandrock length of face; low coal
09	Shearer maintenance
10	Hard cutting sandrock
11	Hard cutting sandrock
12	Shearer maintenance
13	No report
14	Hard cutting sandrock; cutting one way; some rock falling from #80 chock to tailgate
15	Rock falling from #65 to tailgate; breaking rock in panline
16	Rock falling from #63 to tailgate; pull chocks and clean rock off canopies
17	Bad face from #60 to tailgate; smash rock in panline; bottom soft; pulling and cleaning chocks
18	Had trouble getting shearer to tailgate from #61 to #73; had to drop rock off to clear; shearer down a lot due to breaking rock in panline; pulled chocks; shot and broke rock
19	Roof bolted face from #40 to #70 chocks; dropped rocks off chocks from #60 to #75
20	No report
21	Face caved in from #65 to #74; couldn't run panline; shooting and smashing rock; pulling chocks and breaking rock in panline
22	Cut 40 chocks; pulling and cleaning chocks; breaking rock in panline; bad face from #65 to #80; roof bolting #65 to #75

TABLE 13 (Continued)

Date	Comments
23	Shot rock over chocks; broke rock in panline; rock in panline up to roof for a distance of 7 chocks
24	Shot rock over chocks to make clearance for shearer; shooting off face from tailgate towards #72 chock
25	Shot rock over chocks to make clearance for shearer; pulled chock and cribbed over chock
26	Shot rock; pulled chocks; broke rock on panline; dropped rock off canopies; cribbed over same; roof bolted face
27	No report
28	No report
29	Good cutting
30	Rock falling out from #33 to #55; shooting same; shooting rock in panline; shooting rock in hopper
31	Some rock falling from #30 to #40; shot rock in panline

TABLE 14

Brief Daily Longwall Report--February 1974

Date	Comments
01	Some rock falling from #20 to #30; smash rock in panline
02	Maintenance
03	No report
04	Breaking rock in panline
05	Good cutting
06	Good cutting; smash rock in panline
07	Rock down in panline; good cutting
08	Good cutting; shooting rock in panline
09	Maintenance
10	No report
11	Good cutting; shot and broke shot in panline; rock down from #40 to #44
12	Good cutting; rock falling at midface; shoot rock in panline; bad curve from #40 to #70; rock falling

TABLE 14 (Continued)

Date	Comments
13	Good cutting; smashing rock in panline; roof sagging from #25 to #60
14	Good cutting; smash rock in panline
15	Good cutting; smash rock in panline; shot out #57 chock trapped in gob; shot rock in panline
16	Maintenance
17	No report
18	Good cutting; smash rock in panline
19	Smash rock in panline; rock down in panline from #37 to #50
20	Bad roof from #30 to #50; dropped rock off chocks #30 to #35; shot rock at chocks #30 to #36; bad roof from #45 to #60
21	Shot and broke rock in panline; chocks were low from #20 to #55
22	Face bad from #20 to #60; lost face from #44 to #49; shooting rock
23	No report
24	No report
25	Broke rock on panline
26	Shot rock in panline; rock falling from #45 to #58
27	Shot and broke rock in panline; face bad midway; dropped and shot rock off canopies from #60 to #65
28	Bad face from #39 to #56; #71 to #77 one foot of rock falling; chocks low; lot of rock falling; shot rock

TABLE 15

Brief Daily Longwall Report--March 1974

Date	Comments
01	Timbered face from #20 to #80; pulled chocks; shot one chock out; shot rock in panline; set posts under chocks from #30 to #60 chocks
02	No report
03	No report
04	Pulled chocks; set timbers; smashed rock in panline

TABLE 15 (Continued)

Date	Comments
05	Bad face from #37 to #54; chocks too low for passage of shearer from #45 to #74; shot off one cut from #45 to #57; timbered chocks; shot face
06	Shot off coal; pulled chocks; shot off second cut
07	Shot coal off face; pulled chocks; dropped rock off chocks beginning at #48 chock and shot same; shot bottom; only 28" high from panline to roof
08	Shot coal off face from #48 to #64 chock; chocks too low for shearer to clear; face caved in
09	Pulled chocks from #50 to #60; chock squeezed down solid; shot bottom under legs to bring chocks in
10	Shot rock on face; shot bottom under chocks to pull chocks; unloaded tops of chocks to make height
11	Shot bottom in chock line; shot face off; got rock off top of chocks; cribbing and timbering; chocks too low for shearer to clear from #51 to #78
12	Dropped toprock over chocks in #65 to #75 chock to make height for passage of shearer; timbered face; took bottom in chock line
13	No report
14	No report
15	No report
16	No report
17	No report
18	Shot two chocks
19	Rock falling in panline; broke rock; had hard time getting chocks in as a lot of weight was on back ends; shot out chocks; cleaned rock off chock
20	Broke rock in panline; drilled and shot out chocks stuck in gob; installed 14 resin bolts in area of #44 to #58 chocks; cribbed over chocks at midface
21	Face caved in; breaking rock; shot out 8 chocks left in gob; shot and dropped rock over chocks from #48 to #54 and from #62 through #66 to get height from passage of shearer
22	Rock down on shearer; shearer won't clear 2 chocks; shot rock off drum of shearer; shot rock off chocks directly over shearer; rock settled on canopies; canopies down tight on shearer
23	No report
24	No report

TABLE 15 (Continued)

Date	Comments
25	Shot rock over chocks from height for passage of shearer; shot rock off face to gain access to drum; installed 8 resin bolts from #30 to #38
26	Rock caved in on shearer; smashing rock over top of chocks directly over shearer; approximately 8 feet of rock coming down; installed 18 resin bolts along face from #40 to #58
27	Timbered along face; cribbed chocks directly over shearer using 32 crib blocks over each chock; installed 14 resin bolts in face
28	Dropped rock off chocks; shot same; cribbed over chocks; installed 10 resin bolts from #70 to #80
29	Roof bolted face; cribbed chocks
30	Dropped rock off chocks to make height for passage of shearer
31	No report

TABLE 16

Brief Daily Longwall Report--April 1974

Date	Comments
01	No report
02	Dropped rock off chocks #60-63 to make height for passage of shearer; shot off rock on #59 and #60
03	Dropped rock off chocks #61-62; cleaned rock off #59-60
04	Cribbed on top of chocks in middle of panline; cleaned rock off chocks #61-63
05	Cleaned rock off chocks #47-49; cribbed #47-49
06	No report
07	No report
08	Slow cutting due to bad cave; cleaned rock behind shearer
09	Double cut face from #40-60; smashed rock in panline
10	Double cut face from #40-60; broke rock in panline; cleaned rock off chocks
11	Face bad from #45-52; rock falling out; double cutting face; smashed rock in panline
12	No report

TABLE 16 (Continued)

Date	Comments
13	No report
14	No report
15	Smash rock in panline
16	No report
17	No report
18	No report
19	No report
20	No report
21	No report
22	Rock fall out of face; double cutting face from #40-60
23	Face bad from #30-50; drop rock off chocks at midface and smash same; rock down from #32-54; drilled, shot, and smashed same; face bad from #23-57; 8" to 10" of rock down; rock in panline from #25-55; cleaned up rock; chocks #48-49 stuck; had to shoot out chocks
24	Shot and smashed rock in panline; drilled and shot rock; cribbed chocks
25	Cribbed over chock; smashed rock in panline; double cutting from #40-60
26	Shot out 2 chocks; shot top rock off chocks at midpoint to gain height; 4 chocks stuck; had to shoot out #49,50,52,53
27	Posted canopies in panline from #30-70
28	No report
29	Shot chock #45,52,53 out; chocks #54,55 stuck; shot out chocks; shot bottom under chocks at midface and also over chocks to gain height for passage of shearer
30	Breaking rock in panline; got #48-51 chocks in; shot out #55 chock

TABLE 17

Brief Daily Longwall Report--May 1974

Date	Comments
01	Double cut face from #40-60; good cutting
02	Rock falling in panline; double cut face from #40-60; 4" slate falling from #60-75; shot #48 chock; smashed rock in panline
03	Bad face broke from #18-77; broke rock in panline; shot #45 chock out; shot down top for height on chocks; 5 chocks stuck at halfway point; had to shoot out
04	No report
05	No report
06	Shot rock on face; broke rock in panline; got height on chocks
07	Chocks #36-38 too low for shearer to clear; had to clean rock off and crib; shot out #52 chock; smashed rock in panline; face caved in from #47-52
08	Rock down at face from #39-55 chock; drilled and shot rock off chocks to make height for passage of shearer; broke rock in panline
09	Drilled and shot rock; cleaned rock off chocks to make height for passage of shearer; timbered between chocks; roof bolted face with 10, 6' pins
10	Roof bolted face; shot rock; cribbed chocks; face bad but improving; smashed rock in panline; pulled and shot out chocks; timbered under chocks from #25-76; shot rock; bad face as middle caved in where pinning was stopped--middle caved in when chocks were released
11	No report
12	No report
13	Roof bolted 18 resin bolts from #35-53; dropped rock off chocks #58-60 to make height for passage of shearer; face caved from #40-60; pinned face; cribbed chocks; got height on 4 chocks; cleaned rock out of chocks
14	Dropped rock off chocks #47-50 to make height for passage of shearer; shearer wedged under chocks; cleaned rock off tops of chocks; drilled and shot to free shearer
15	Shearer at #42 chock going to tailgate; dropped and shot rock to make height; cleaned rock over top of chocks; pinned face
16	Shot rock over chocks; cleaned rock off top of chocks; roof bolted face with resin bolts

TABLE 17 (Continued)

Date	Comments
17	Shot and dropped rock off chocks to make height for passage of shearer; cleaned and cribbed 3 chocks; shot rock off 2 chocks; set 6x6 post under canopy of chocks; cribbed on top of #44; cleaned rock out along side of shearer; cribbed over #39-44
18	Dropped rock off #39-40 chock and cribbed over same; installed 10 resin bolts in face from #35-40; set post under canopies #35-40
19	No report
20	Pinned face with steel pins in front of shearer; cleaned rock off of #46 chock; pulling chocks; face bad but improving; no rock came out of face all last shift; pulled, cleaned, and shot chock #52-58; reset posts under canopies
21	Face broke from #43-63; roof sagged from #48-58; had hard time getting chocks in from #43-57; set timber under chocks; face bad from #48-56; drilled and shot rock off chocks #49, 53-56; set posts under chocks from #30-70 chocks; made height on #47-48, 54-56; cribbed over #54-56; double posted all canopies as height was made; rock still needed to be dropped and height made over chocks #49-53
22	No report
23	Cleaned rock off tops of chocks #49, 51-53; roof bolted face from #50 toward headgate; face was bad as roof broke from #47-58; cleaned and cribbed chocks to make height; dropped and shot rock over #57-59 for height; face bad but improving; shot and pulled chocks from #40-60; reset double posts under canopies from #40-70 as chocks were advanced; #52 and 58 were still partway back
24	Got #52 and 58 pulled; got height on #47,50,53,57; had hard time getting chocks from #40-60 in; timbered same; chocks #49 and 52 stuck; shot out same; double posted canopies from #40-60; cleaned canopies
25	No report
26	No report
27	No report
28	Rock fell from #30-40; had to drill and shoot; chocks #51 and 52 stuck; posted between chocks; double posted all canopies from #40-60 as chocks were pulled; shot out #50 chock
29	Set timber between and under chocks; put extension on #40 and 42 chock; installed leg extension on chocks #35-47, 57,58; timbered between chocks from #55-75; timbered under chocks; face had 46" height from #55-60 and 44" from #60-75

TABLE 17 (Continued)

Date	Comments
30	Put extensions on #58,59; timbered under chocks; installed extensions on #59-63, 70-75; face broke from #36-62; roof broke up; timbered under chocks; shot rock in panline from #36-40
31	No report

TABLE 18

Daily Brief Longwall Report--June 1974

Date	Comments
01	No report
02	No report
03	Roof breaking up midface; shot under chocks with no leg showing at midface; shot under chocks; chocks stuck from #45-54
04	Face broke up at middle; shot out chocks at face; chocks #48-52 and #54-55 stuck; got #53 chock in; 7 chocks stuck; 5 chocks shot out
05	Face bad; chocks pulled hard; shot roof over chocks; pulled same; rock fell in panline at midface; shot same; face bad from #48-54; rock down from #48-54; two chocks stuck -- #48 and 51
06	Face bad at midface; cleaned chocks at midface; pulled same; removed rear leg extensions from #50-51, 53,49; face bad at #48,55,61-62 chocks back; got #48,62 chocks in; face bad from #46-56; chocks #54,56 stuck; shot out chocks; cleaned rock from chocks to make height
07	Made height on #46-47, 55-56; cribbed over chocks 45-52; timbered panline; face bad from #47-60; cleaned rock off chocks #48, 56-58
08	No report
09	No report
10	Shot rock in panline; got chocks in from #40-60; face bad from #45-65; cribbed chocks #54-58; cleaned rock off chocks #60-65; cribbed over chocks #58-60; shot and dropped rock over #44-46
11	Face caving from #45-59; rock in panline #63-69; got height on #44,49,50,53; roof broke from #21-75; shot and pulled #45-46
12	Face bad from #34-68; shot out on top of #59,60; pulled in chocks from #40-60; timbered chocks from #30-60; cleaned rock off #41-42 for height; cribbed over chocks #41-42; set timber under canopies #40-60; removed leg extension from rear leg of #49 chock

TABLE 18 (Continued)

Date	Comments
13	Dropped and shot rock to make height; cribbed over chocks #39-42
14	Got height on #57,58,60,67,37,38,39,51,52 chocks; cleaned off chocks for height #32-36, 41-42
15	Made height on one chock; resin bolted face with twenty bolts from #40-60 chocks
16	No report
17	Cleaned rock off panline; face bad at midface; shot out and pulled chocks; got 6 chocks in; got height on 8 chocks; broke rock in panline
18	Chocks too low for shearer to clear from #50-60; chock #56 stuck; height on chocks at beginning of shift insufficient for passage of shearer from #49-61; made height on #58-61, 50-52; got #56 in; got height on #55-58; chocks #28,29,41,48,49,53,54 still too low
19	Cleaned off rock on chocks #53,54, 60-63; double posted chocks from head to tail; face bad but improving; made height on chocks; pulled chocks; shot rock in panline; got #53 in; couldn't get #46 in; got height from #46-53
20	Pulled and made height on #52; made 25" height on #47-49; #50 chock too low; face bad but improving; shot over chocks to make height for shearer; shot out and pulled #46 chock; installed 7 resin bolts from #53-60; got chocks in; shot off rock; pushed panline from #60-70 and got chocks in again; chock #48 still back
21	Face bad but improving; chocks pulling in slowly due to bad roof; shot off face; shot out chocks at midface; timbered face from #22-80
22	No report
23	No report
24	No report
25	No report
26	No report
27	No report
28	No report
29	No report
30	No report

TABLE 19

Daily Brief Longwall Report--July 1974

Date	Comments
01	No report
02	No report
03	No report
04	No report
05	No report
06	No report
07	No report
08	Maintenance
09	Pulling chocks; maintenance
10	Maintenance; roof broke from #20-65 chock
11	Face bad from #35-75; got height on chocks; got chocks in; chocks #52-53 stuck
12	Face bad; chocks #36-38 and #41-42 solid; shot out chocks; got chocks in; chocks #51-53 stuck
13	No report
14	No report
15	Good cutting
16	Face bad; chocks too low #36-58; shot #55 chock out; broke rock in panline; roof broke from #30-78 chock; #52-53 chock stuck; shot chocks out; face bad but improving; pulled chocks
17	Face bad; got #52-53, 56-57 chocks in and got height; chocks were low from #40-60; good cutting for 1st and 2nd shifts
18	Face caved in and made chocks too low; got chocks in; roof broke from #70-78 chock; chocks #49,52,53,58,59 stuck; chocks from #40-60 brought in; rock cleaned off chocks; good cutting 2nd shift
19	Good cutting; maintenance
20	No report
21	No report
22	Good cutting; rock falling in panline 2nd shift
23	Roof broke from #30-80 chocks; 4" of rock coming down along face; face bad, but improving -- no rock falling on last cut of 1st shift; dropped rock off canopies to make height for passage of shearer; shot out and pulled chocks; cleaned chocks off

TABLE 19 (Continued)

Date	Comments
24	Double cut face; #59 chock stuck; shot out #40 chock stuck in gob; double cut all passes headgate to tailgate -- on last cut small hole went through in doghole cut from the line rooms toward face
25	Short cutting face from #40 to tailgate; also double cutting; timbered face from #60-80 chock; timbered entire length of face in front end of chocks and timbered between chocks from #50-80 and #0-30; shot rock fallen in front of chocks from #40-60 approximately 2 feet back; shot and drilled rock in panline; timbered face between chocks; longwall completed.

APPENDIX H

SELECTED DETAILED LONGWALL REPORTS

This appendix presents selected detailed longwall reports for each day that microseismic monitoring was undertaken over the B-4 East longwall at the Greenwich North Mine. It includes all delays mentioned in the associated longwall shift report during the monitoring period, and lists the date, the time interval that a particular delay occurred, and a brief description of the reason(s) for the delay. It should be noted that the support chocks are numbered 1-100 starting at the headgate end of the face.

TABLE 20

Selected Detailed Longwall Reports

Ref	Date	Time	Operation--Delays
1	18 Feb 74	14:30-17:45	Conveyor belt down; shift change
2	22 Feb 74	...	Mine not working
3	23 Feb 74	...	Mine not working
4	26 Feb 74	15:20-16:35	Shift change
5	27 Feb 74	15:30-16:35	Shift change
		16:35-19:50	Midface bad; rock in panline from chock #40-#75; shot rock in panline
6	06 Mar 74	08:30-15:30	Completed shooting off first cut of face; pushed panline; pulled chocks and began shooting off second cut
		15:30-16:30	Shift change
		16:30-23:30	Drilled and shot face all shift
7	13 Mar 74	...	Mine not working
8	17 Apr 74	...	Mine not working
9	03 May 74	10:00-14:15	Bad face; 5 chocks stuck at midface; shot out chocks
		15:00-15:30	Serviced shearer
		15:30-16:35	Shift change
		17:10-17:30	Replaced hoses at chock #45; bad face
10	10 May 74	12:30-15:30	Pulled and shot out chocks; smashed rock in panline; bad face
		15:30-16:30	Shift change
		16:30-23:30	Pushed panline; brought four chocks in; shot rock all shift; midface caved in
11	30 May 74	13:15-13:45	Conveyor belt down
		15:30-16:45	Shift change
		17:45-19:00	Bad face broke from chock #36-#62; shot rock in panline
12	12 July 74	16:30-18:00	Chocks low on first pass
		18:00-19:00	Chocks #51-#53 stuck

TABLE 20 (Continued)

Ref	Date	Time	Operation--Delays
13	19 July 74	15:30-16:35	Shift change
		16:35-17:15	Conveyor belt down
14	24 July 74	15:25-16:30	Shift change
		17:30-17:50	Conveyor belt down
		18:30-18:45	Replaced slippage switch for belt
15	02 Aug 74	...	Longwall completed
16	21 Aug 74	...	Longwall completed

APPENDIX I

DETAILED UNDERGROUND OBSERVATIONS

This appendix presents information on detailed underground observations made by project personnel during a number of periods when microseismic monitoring was also underway.

On six occasions during the study, personnel were stationed at the headgate of the East B-4 longwall at the Greenwich North Mine to observe the mining operations and to record the times that each operation began and ended. These observations were then compiled in tabular form. Certain common operations such as the running of the shearer, conveyors, and pumps, and coal cutting are listed individually. A tape footage log was also incorporated to provide correlation between the underground observations and the tape recorded microseismic data obtained during the period of the detailed underground observations. The associated tape reel numbers are listed in Appendix J.

In order to obtain correlation between underground and tape footage on surface, the following procedure was employed. The watch which was to be taken underground was syncronized just before leaving the surface field site with the watch remaining on surface (to within an accuracy of 30 seconds). The watch on surface was used for referencing tape footages with surface times. The watch underground was used for referencing observed events underground with underground times. Errors which could occur at these points are:

(1) one watch runs faster than the other--over a four hour period the error should be less than one minute, also the error would increase with time,

(2) tape footage counter slippage,

(3) tape footage counter wheel being too small or too large,

(4) capstan drive rotating too slow or too fast,

(5) error in reading footage counter at the beginning and end of the survey,

(6) underground events generally accurate to within ±30 seconds as person underground observes the event and selects the nearest 30 second interval.

To minimize such errors the starting tape footage was subtracted from the final tape footage to obtain the total footage during the underground survey. The starting time was subtracted from the stopping time to obtain the total time in minutes during the underground survey. The total footage divided by the total time resulted in the apparent tape speed expressed in feet per minute (FPM).

Next, a convenient initial time was found which would make calculations simple. An equivalent footage was obtained by subtracting the starting time from the initial time and multiplying this result by the tape speed (FPM) and adding this answer to the starting footage, thus obtaining an "initial" footage.

Calculated footages of events such as blasts and cavings were then correlated to the nearest observed footages. In most instances footages correlated to within 30 feet (approximately two minutes error) of each other and generally observed similar trends throughout each particular survey (e.g., if calculated footages were 15 feet more than the observed footages, this 15 foot error remained relatively constant during the entire survey).

TABLE 21

Detailed Underground Observations, Trip No. 1--February 26, 1974

Footage	Time hh mm ss	Shearer	Conveyor	Pump	Description
	16 02 00	...	...	...	Entered shaft
	16 24 00	...	...	...	Arrived at face
2930	16 42 30	ON	ON	ON	
2976	16 45 00	ON	ON	ON	Chock started to move
3069	16 50 00	ON	ON	ON	Big caving
3149	16 54 15	ON	ON	ON	Small caving
3329	17 04 00	ON	ON	ON	Small caving
3440	17 10 00	OFF	OFF	ON	
3442	17 10 05	ON	ON	ON	
3624	17 19 55	ON	ON	ON	Big caving
3680	17 22 55	OFF	OFF	ON	
3716	17 24 50	ON	ON	ON	
3788	17 28 45	ON	ON	ON	Mini caving
3794	17 29 05	ON	ON	ON	Mini caving
3801	17 29 25	ON	ON	ON	Mini caving
3889	17 34 10	ON	ON	ON	Shearer at headgate
3904	17 35 00	ON	ON	ON	Medium caving
3929	17 36 20	ON	ON	ON	Shearer left headgate
3954	17 37 40	ON	ON	ON	Big caving
3978	17 39 00	ON	ON	ON	Shot on coal face at tailgate
	17 42 00				
3997	17 40 00	ON	ON	ON	Big caving
4087	17 44 50	OFF	OFF	OFF	
4094	17 45 15	OFF	OFF	ON	
4098	17 45 25	ON	ON	ON	
4183	17 50 00	ON	ON	ON	Caving
4193	17 50 35	ON	ON	ON	Caving
4204	17 51 10	ON	ON	ON	Caving at chock #14
4275	17 55 00 17 57 00	ON	ON	ON	Shot on face at tailgate. One stick, 35 feet from point 1759
4436	18 03 40	OFF	OFF	ON	
4441	18 03 55	ON	ON	ON	
4449	18 04 20	OFF	OFF	ON	
4473	18 05 40	ON	ON	ON	
4558	18 10 15 18 10 30	OFF	OFF	ON	Sledge hammer striking 10 times on the roof of the headgate entry
4574	18 11 05	ON	ON	ON	
4660	18 15 45	ON	ON	ON	
4861	18 26 35	ON	ON	ON	Big caving
4869	18 27 00 18 30 00	ON	ON	ON	Shearer not cutting coal, shearer started to leave headgate
4943	18 31 00	ON	ON	ON	Observer left face

TABLE 22

Detailed Underground Observations, Trip No. 2--February 27, 1974

Footage	Time hh mm ss	Shearer	Conveyor	Pump	Coal Cutting	Description
...	16 03 00	...	...	...	...	Entered at shaft
3347	16 30 00	OFF	OFF	ON	OFF	Arrived at headgate; rock blocks fell from roof in the middle of longwall face during the night and day shift
3979	17 04 00	OFF	OFF	ON	OFF	Blasting in the middle of longwall
4109	17 11 00	OFF	ON	ON	OFF	
4146	17 13 00	OFF	ON	ON	OFF	
4183	17 15 00	OFF	OFF	ON	OFF	Blasting in longwall face
4313	17 22 00	OFF	OFF	ON	OFF	Blasting in longwall face
4369	17 25 00	OFF	OFF	...	OFF	Pump on 10 seconds; pump off 10 seconds
4387	17 26 00	OFF	...	ON	OFF	Belt conveyor on; belt conveyor off
4499	17 32 00	OFF	OFF	ON	OFF	Blasting
4592	17 37 00	OFF	OFF	OFF	OFF	All electrical power off
4796	17 48 00	OFF	OFF	OFF	OFF	Blasting
4815	17 49 00	OFF	OFF	ON	OFF	Power on
4908	17 54 00	OFF	...	ON	OFF	Belt conveyor on 20 seconds
4926	17 55 00	OFF	ON	ON	OFF	
4945	17 56 00	OFF	OFF	ON	OFF	
4964	17 57 00	OFF	ON	ON	OFF	
4982	17 58 00	OFF	OFF	ON	OFF	
5001	17 59 00	OFF	OFF	ON	OFF	Blasting in longwall face
5019	18 00 00	OFF	OFF	ON	OFF	Eleven hammer shocks on headgate roof at two second intervals
5075	18 03 00	OFF	ON	ON	OFF	Chain conveyor on for 30 seconds
5094	18 04 00	OFF	OFF	ON	OFF	
5112	18 05 00	OFF	OFF	ON	OFF	
5335	18 17 00	OFF	OFF	ON	OFF	Blasting in longwall face
5540	18 28 00	OFF	OFF	ON	OFF	Blasting in longwall face
5577	18 30 00	OFF	ON	ON	OFF	
5595	18 31 00	OFF	OFF	ON	OFF	
5837	18 44 00	OFF	OFF	ON	OFF	Blasting in longwall face
...	18 50 00	...	...	...	...	Observer left face

TABLE 23

Detailed Underground Observations, Trip No. 3--March 6, 1974

Footage	Time hh mm ss	Shearer	Conveyor	Pump	Coal Cutting	Description
...	16 30 00	...	...	...	...	Arrived at headgate
3569	16 36 00	OFF	OFF	OFF	OFF	Wagon passed; rock was falling from roof
3791	16 48 00	OFF	...	OFF	OFF	Conveyor on 10 seconds
3810	16 49 00	OFF	OFF	ON	OFF	
4070	17 03 00	OFF	OFF	ON	OFF	
4144	17 07 00	ON	ON	ON	OFF	
4172	17 08 30	OFF	OFF	ON	OFF	
4636	17 33 30	OFF	OFF	ON	OFF	Blasting--three holes, three sticks, 3/4 way from headgate
5036	17 55 00	OFF	OFF	ON	OFF	Blasting--two holes, two sticks
5221	18 05 00	OFF	OFF	OFF	OFF	
5249	18 06 30	OFF	OFF	OFF	OFF	Blasting--three holes, three sticks
5277	18 08 00	OFF	ON	ON	OFF	
5305	18 09 30	OFF	OFF	OFF	OFF	
5370	18 13 00	OFF	OFF	ON	OFF	
5630	18 27 00	OFF	OFF	ON	OFF	
...	18 30 00	...	...	...	...	Observer left headgate

TABLE 24

Detailed Underground Observations, Trip No. 4--May 3, 1974

Footage	Time hh mm ss	Shearer	Conveyor	Pump	Coal Cutting	Description
...	16 30 00	OFF	OFF	OFF	OFF	Shearer at headgate
35	16 37 00	ON	OFF	OFF	OFF	
71	16 39 00	OFF	OFF	OFF	OFF	
124	16 42 00	ON	ON	OFF	OFF	
141	16 43 00	ON	OFF	OFF	OFF	
186	16 45 30	OFF	OFF	OFF	OFF	Switch on shearer
195	16 46 00	ON	OFF	OFF	OFF	Switch off shearer
203	16 46 30	OFF	ON	ON	OFF	
212	16 47 00	ON	ON	ON	OFF	
230	16 48 00	ON	ON	ON	ON	Shearer at headgate
265	16 50 00	ON	ON	ON	ON	
575	17 07 30	OFF	ON	ON	OFF	
584	17 08 00	OFF	OFF	ON	OFF	
690	17 14 00	OFF	ON	ON	OFF	
707	17 15 00	ON	ON	ON	ON	
866	17 24 00	OFF	OFF	ON	OFF	
884	17 25 00	OFF	ON	ON	OFF	
893	17 25 30	ON	ON	ON	ON	
920	17 30 00	ON	ON	ON	ON	Blasting at tailgate; four sticks, two holes
973	17 33 00	OFF	OFF	ON	OFF	
990	17 34 00	ON	ON	ON	ON	300 feet outby point 1817
1450	18 00 00	...	...	...	...	Observer left headgate

TABLE 25

Detailed Underground Observations, Trip No. 5--May 30, 1974

Footage	Time hh mm ss	Shearer	Conveyors Chain	Conveyors Belt	Pump	Coal Cutting	Description
3577	16 51 00	...	...	...	...	...	Arrived at headgate; roof trouble in middle of longwall
3745	17 00 00	OFF	ON	ON	ON	OFF	
3762	17 01 00	ON	ON	ON	ON	ON	
3772	17 02 30	OFF	OFF	OFF	ON	OFF	
3790	17 02 30	ON	ON	ON	ON	ON	
3799	17 03 00	OFF	OFF	ON	ON	OFF	
3809	17 03 30	ON	ON	ON	ON	ON	
3818	17 04 00	OFF	OFF	ON	ON	OFF	
3827	17 04 30	ON	ON	ON	ON	ON	
3836	17 05 00	OFF	OFF	ON	ON	OFF	
3846	17 05 30	ON	ON	ON	ON	ON	
3892	17 08 00	OFF	OFF	ON	ON	OFF	
3901	17 08 30	ON	ON	ON	ON	ON	
3929	17 10 00	OFF	OFF	ON	ON	OFF	
3948	17 11 00	OFF	OFF	OFF	OFF	OFF	
3957	17 11 30	OFF	OFF	OFF	ON	OFF	
4022	17 15 00	OFF	OFF	OFF	OFF	OFF	
4031	17 15 30	OFF	OFF	OFF	ON	OFF	
4059	17 17 00	OFF	OFF	OFF	OFF	OFF	
4062	17 17 10	OFF	OFF	OFF	ON	OFF	
4114	17 20 00	ON	ON	ON	ON	ON	
4224	17 27 00	OFF	OFF	ON	ON	OFF	
4262	17 28 00	OFF	OFF	OFF	OFF	OFF	
4272	17 28 30	ON	ON	ON	ON	ON	
4300	17 30 00	OFF	OFF	ON	ON	OFF	
4429	17 37 00	OFF	OFF	OFF	ON	OFF	
4448	17 38 00	OFF	OFF	OFF	OFF	OFF	
4466	17 39 00	OFF	OFF	OFF	ON	OFF	
4485	17 40 00	OFF	OFF	ON	ON	OFF	
4488	17 40 10	OFF	OFF	OFF	ON	OFF	
4503	17 41 00	OFF	OFF	OFF	OFF	OFF	
4506	17 41 10	OFF	OFF	ON	ON	OFF	
4540	17 43 00	OFF	OFF	OFF	ON	OFF	Rock falls from roof; blasting, five sticks--60 chocks from headgate
4726	17 53 00	OFF	OFF	OFF	OFF	OFF	No pressure for pump
4744	17 54 00	OFF	OFF	OFF	ON	OFF	
4763	17 55 00	OFF	OFF	OFF	OFF	OFF	
4781	17 56 00	OFF	OFF	OFF	ON	OFF	
5435	18 20 30	OFF	OFF	OFF	ON	OFF	Blasting, five sticks--60 chocks from headgate
...	18 30 00	...	...	...	...	...	Observer left headgate

TABLE 26

Detailed Underground Observations, Trip No. 6--July 19, 1974

Footage	Time hh mm ss	Shearer	Conveyors Chain	Conveyors Belt	Pump	Coal Cutting	Description
4064	16 55 00	OFF	OFF	OFF	ON	OFF	
4137	16 59 00	OFF	ON	ON	ON	OFF	
4174	17 01 00	OFF	OFF	OFF	ON	OFF	
4285	17 07 00	OFF	OFF	OFF	ON	OFF	10 impacts on roof*
4304	17 08 00	OFF	OFF	OFF	OFF	OFF	
4322	17 09 00	OFF	OFF	OFF	OFF	OFF	10 impacts on roof**
4341	17 10 00	OFF	OFF	ON	OFF	OFF	
4433	17 15 00	OFF	ON	ON	ON	OFF	
4489	17 18 00	ON	ON	ON	ON	ON	Cleaned panline
4600	17 24 00	ON	ON	ON	ON	OFF	Going under low support
4618	17 25 00	ON	ON	ON	ON	ON	
4803	17 35 00	OFF	OFF	OFF	ON	OFF	Turn around for new pass
4932	17 42 00	ON	ON	ON	ON	ON	
5468	18 11 00	OFF	OFF	OFF	ON	OFF	
5764	18 27 00	ON	ON	ON	ON	ON	
...	18 30 00	...	...	...	...	...	Observer left headgate

* Ten impacts, the roof was struck with a hammer while the hydraulic pumps were operating.

** Ten impacts, a roof bolt was struck with a hammer while the pumps were turned off. There was no other equipment operating at this time in the section.

APPENDIX J

MONITORING SYSTEM OPERATING CONDITIONS

This appendix presents a description of the monitoring system operating conditions during field trips associated with the microseismic monitoring at the East B-4 longwall. The first column (#) represents the total number of field trips made to the particular site by the date given. The "date column" is the day that microseismic data was recorded, and the "tape reel number" identifies the reel of tape on which the data was recorded. "Geophones utilized" identifies which geophones were employed in obtaining data. The "period of recording" is divided into two parts, namely (1) the tape starting and stopping footages, denoted by the bracketed quantities, and (2) the starting and stopping times during which data was recorded. The "frequency" column specifies the lower-upper frequency limits for the recorded data. "System gain" represents the total gain in dB of the microseismic system at the tape recorder, which includes the preamplifier (40 dB), the post amplifier (-10 to 50 dB), and the filter (dB). The tape speed at which the microseismic data was recorded is given in the "tape speed" column in inches per second (ips). During all field trips, the monitoring equipment was powered by a motor generator. Any other pertinent information is presented in the remarks column and includes a weather column which summarizes briefly the weather conditions during the recording session.

TABLE 27

Monitoring System Operating Conditions

#	Date	Tape Reel #	Geophones	Period of Recording	Frequency Hz	System Gain dB	Tape Speed ips	Remarks	
								Weather	Other Details
1	28 Nov 73	33	1,2,3,4,5 7,8	[10-2200] 13:10-15:00	0-100 to 0-1000	50-80	3-3/4	Strong west wind	
2	10 Dec 73	33	6,9,10,11, 12,13,14	[2300-4000] 13:30-15:00	0-500	90	3-3/4	Snow	
3	04 Feb 74	33	1,2,3,4,5, 6,7	[4000-5050] 15:30-16:30	0-500	40-70	3-3/4	Snow flurries Cold	120 Hz problem with power supply--no data Longwall at 3287'
4	18 Feb 74	36	1,2,3,4,5, 6,7	[10-100] 13:20-13:25 [100-3200] 13:27-16:21	0-1000	90	3-3/4	No wind	Good cutting; long-wall at 3700'
			8,9,10,11, 12,13,15	[3210-3750] 17:06-17:36	0-1000	90			
			8,9,10,11, 12,13,14	[3750-4300] 17:41-18:11	0-1000	90			
5	22 Feb 74	37	1,2,3,4,5, 6,7	[0-110] 15:27-15:35 [111-3900] 15:37-19:01	0-1000	90	3-3/4	Windy Hail Thunder	Caving on panline; mine not working; longwall at 3785'
6	23 Feb 74	37	1,2,3,4,5, 6,7	[3900-3999] 11:35-11:41 [4000-6515] 11:48-13:58	0-1000	90	3-3/4	Strong wind	Mine not working; longwall at 3800'
7	26 Feb 74	38	1,2,3,4,5, 6,7	[10-2150] 14:07-16:00 [2160-5500] 16:01-19:01	0-1000	90	3-3/4	Little wind	Good cutting; long-wall at 3830'

TABLE 27 (Continued)

#	Date	Tape Reel #	Geophones	Period of Recording	Frequency Hz	System Gain dB	Tape Speed ips	Remarks	
								Weather	Other Details
8	27 Feb 74	39	1,2,3,4,5,6,7	[10-2900] 13:11-15:46	0-1000	90	3-3/4	Occasional wind	Roof bad at midface; longwall at 3840'
			1,2,3,4,6,7,15	[2910-6060] 16:06-18:56					
9	06 Mar 74	01	1,2,3,4,5,6,7	[10-2600] 13:06-15:25	0-1000	90	3-3/4	Slight wind	Poor roof conditions; blasting face free to relocate longwall; longwall at 3870'
			1,2,3,4,6,7,15	[2607-2900] 15:43-15:59					
			1,2,3,4,5,6,7,15	[2900-6500] 16:10-19:22					
10	13 Mar 74	101	1,2,3,4,6,7,8	[10-2800] 13:30-16:00	0-1000	90	3-3/4	Windy	Mine not working; longwall at 3880'
			9,10,11,12,13,14,15	[2815-3563] 17:40-18:20					
11	17 Apr 74	43	1,2,3,4,6,7,9	[10-1700] 12:18-13:49	0-1000	90	3-3/4	Mild	Mine not working; longwall at 4020'
			8,10,11,12,13,15,5	[1710-1900] 15:38-15:48					
			8,10,11,12,13,14,15	[1910-3530] 16:05-17:32					

TABLE 27 (Continued)

#	Date	Tape Reel #	Geophones	Period of Recording	Frequency Hz	System Gain dB	Tape Speed ips	Remarks	
								Weather	Other Details
12	03 May 74	43	3,7,9,10, 11,13,14	[3600-6765] 13:14-16:00	0-1000	90	3-3/4	Light rain 14:40-15:45	Bad face; longwall at 4160'
		44	3,7,9,10, 11,13,14	[0-1450] 16:35-18:00	0-1000	90	3-3/4	Thunder-storm 16:40	
13	10 May 74	44	3,7,9,10, 11,13,14	[1460-4050] 12:10-14:30	0-1000	90	3-3/4	Slight breeze	Bad face; longwall at 4180'
			3,7,9D,9SH, 9SF,11,13	[4060-5000] 15:15-16:05					
			1,7,9,10, 12,13,14	[5010-6700] 16:37-18:08					
14	30 May 74	46	1,9D,9SH, 9SF,9ACC, 11,14	[40-500] 12:59-13:26	0-1000	90 9ACC:40	3-3/4	Slight breeze	Roof starting to break at midface; longwall at 4220'
			1,9D,9SH, 9SF,9ACC, 11,14	[510-2400] 13:26-15:08					
			1,9D,7,10, 13,11,14	[2410-5800] 15:48-18:51					
15	12 July 74	49	1,3,7,9,10, 11,13,14	[10-3000] 16:15-17:00	0-1000	90	3-3/4	Breezy	Fair cutting; chocks becoming stuck; longwall at 4350'

TABLE 27 (Continued)

#	Date	Tape Reel #	Geophones	Period of Recording	Frequency Hz	System Gain dB	Tape Speed ips	Remarks	
								Weather	Other Details
16	19 July 74	49	1,7,9,10, 11,13,14	[3010-6300] 15:58-18:56	0-1000	90	3-3/4	Very windy	Good cutting; long-wall at 4470'
17	24 July 74	53	1,7,9,10, 11,13,14	[10-3000] 15:50-18:30	0-1000	90	3-3/4	Breezy	Fair cutting; long-wall at 4510'
			1,7,9,10, 11,13,14	[3010-3300] 18:37-18:52	0-100	100	3-3/4		
18	02 Aug 74	53	1,7,9,10, 11,13,14	[3311-6615] 11:28-14:35	0-1000	90	3-3/4	Thunder-storm 14:14 rain, high winds 14:25	
19	21 Aug 74	32	1,7,9,10, 12,13,14	[1430-4830] 11:59-15:02	0-1000	90	3-3/4	Slight breeze	